

UNCLASSIFIED

AD NUMBER

AD923424

LIMITATION CHANGES

TO:

Approved for public release; distribution is unlimited.

FROM:

Distribution authorized to U.S. Gov't. agencies only; Test and Evaluation; OCT 1974. Other requests shall be referred to Air Force Armament Laboratory, Attn: DLJC and Armament Development and Test Center, Attn: SDTT, Eglin AFB, FL 32542.

AUTHORITY

AFATL ltr 10 Feb 1977

THIS PAGE IS UNCLASSIFIED

NOV 7 1974

AUG 15 1985

AEDC-TR-74-103

AFATL-TR-74-164

cy.2



**FLOW-FIELD, AERODYNAMIC LOADS, AND SEPARATION
TRAJECTORY TESTS ON THE MK-84 AND SUU-54
SUPER HOBOS GUIDED WEAPONS WITH THE
F-4C AND A-7D PARENT AIRCRAFT
AT MACH NUMBERS 0.65 TO 1.60**

**J. B. Carman
ARO, Inc.**

**PROPULSION WIND TUNNEL FACILITY
ARNOLD ENGINEERING DEVELOPMENT CENTER
AIR FORCE SYSTEMS COMMAND
ARNOLD AIR FORCE STATION, TENNESSEE 37389**

October 1974

Final Report for Period March 15, 1974 - June 29, 1974

Distribution limited to U.S. Government agencies only; this report contains information on test and evaluation of military hardware; October 1974; other request for this document must be referred to Air Force Armament Laboratory (AFATL/DLJC) and Armament Development and Test Center (ADTC/SDTT), Eglin AFB, FL 32542.

**TECHNICAL REPORTS
FILE COPY**

Prepared for

**AIR FORCE ARMAMENT LABORATORY (AFATL/DLJC),
AND
ARMAMENT DEVELOPMENT AND TEST CENTER (ADTC/SDTT)
AIR FORCE SYSTEMS COMMAND
EGLIN AIR FORCE BASE, FLORIDA 32542**

NOV 11 1974
F40300-75-0-0001

NOTICES

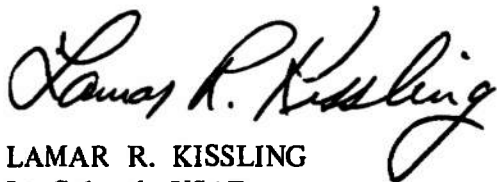
When U. S. Government drawings specifications, or other data are used for any purpose other than a definitely related Government procurement operation, the Government thereby incurs no responsibility nor any obligation whatsoever, and the fact that the Government may have formulated, furnished, or in any way supplied the said drawings, specifications, or other data, is not to be regarded by implication or otherwise, or in any manner licensing the holder or any other person or corporation, or conveying any rights or permission to manufacture, use, or sell any patented invention that may in any way be related thereto.

Qualified users may obtain copies of this report from the Defense Documentation Center.

References to named commercial products in this report are not to be considered in any sense as an endorsement of the product by the United States Air Force or the Government.

APPROVAL STATEMENT

This technical report has been reviewed and is approved.



LAMAR R. KISSLING
Lt Colonel, USAF
Chief Air Force Test Director, PWT
Directorate of Test



FRANK J. PASSARELLO
Colonel, USAF
Director of Test

UNCLASSIFIED

REPORT DOCUMENTATION PAGE		READ INSTRUCTIONS BEFORE COMPLETING FORM
1. REPORT NUMBER AEDC-TR-74-103 AFATL-TR-74-164	2. GOVT ACCESSION NO.	3. RECIPIENT'S CATALOG NUMBER
4. TITLE (and Subtitle) FLOW-FIELD, AERODYNAMIC LOADS, AND SEPARATION TRAJECTORY TESTS ON THE MK-84 AND SUU-54 SUPER HOBOS GUIDED WEAPONS WITH THE F-4C AND A-7D PARENT AIRCRAFT AT MACH NUMBERS 0.65 TO 1.60		5. TYPE OF REPORT & PERIOD COVERED Final Report, March 15 - June 29, 1974
7. AUTHOR(s) J. B. Carman, ARO, Inc.		6. PERFORMING ORG. REPORT NUMBER
9. PERFORMING ORGANIZATION NAME AND ADDRESS Arnold Engineering Development Center (XO) Arnold Air Force Station, TN 37389		8. CONTRACT OR GRANT NUMBER(s)
11. CONTROLLING OFFICE NAME AND ADDRESS Air Force Armament Laboratory (AFATL/DLJC) and Armament Development and Test Center (ADTC/SDTT), Eglin AFB, FL 32542		10. PROGRAM ELEMENT, PROJECT, TASK AREA & WORK UNIT NUMBERS Program Element 64733F Project 2076
14. MONITORING AGENCY NAME & ADDRESS (if different from Controlling Office)		12. REPORT DATE October 1974
		13. NUMBER OF PAGES 138
		15. SECURITY CLASS. (of this report) UNCLASSIFIED
		15a. DECLASSIFICATION/DOWNGRADING SCHEDULE N/A
16. DISTRIBUTION STATEMENT (of this Report) Distribution limited to U.S. Government agencies only; this report contains information on test and evaluation of military hardware; October 1974; other requests for this document must be referred to Air Force Armament Laboratory (DLJC) and Armament Development and Test Center (SDTT), Eglin AFB, FL 32542.		
17. DISTRIBUTION STATEMENT (of the abstract entered in Block 20, if different from Report)		
18. SUPPLEMENTARY NOTES Available in DDC		
19. KEY WORDS (Continue on reverse side if necessary and identify by block number) <div style="display: flex; justify-content: space-between;"> <div> MK-84 Super HOBOS SUU-54 Super HOBOS F-4C aircraft A-7D aircraft flow fields </div> <div> external stores separation trajectories aerodynamic loading transonic flow </div> <div> wind tunnel tests </div> </div>		
20. ABSTRACT (Continue on reverse side if necessary and identify by block number) Wind tunnel tests were conducted with 0.05-scale models of the F-4C and A-7D aircraft and Super HOBOS stores to study parent-aircraft flow-field, store aerodynamic loading, and store separation characteristics. Free-stream aerodynamic characteristics were determined for both the MK-84 and SUU-54 Super HOBOS with fin tips retracted and extended at angles of attack up to 44 deg. Additional free-stream data were obtained on the MK-84 store with only one fin tip extended. Flow angularity measurements were made		

UNCLASSIFIED

UNCLASSIFIED

20, Continued

under the left- and right-wing inboard pylons and centerline of the F-4C and under the left- and right-wing center pylons of the A-7D up to 20 ft away from the pylons for aircraft angles of attack up to 16 deg and sideslip angles of 0 and 9 deg. Aerodynamic loads data were obtained on the MK-84 store with fin tips retracted and extended at the same positions in the aircraft flow fields where flow angularity measurements were made. Separation trajectories for the MK-84 and SUU-54 Super HOBOS with tips retracted were initiated from the F-4C inboard wing pylons and A-7D center and outboard wing pylons at simulated altitudes from sea level to 40,000 ft for dive angles from 0 to 60 deg and at Mach numbers from 0.65 to 1.6. Aircraft angle of attack ranged from -1 to 10 deg. Trajectories for the extended-tip configurations of the Super HOBOS were initiated at a point 3.5 ft below the pylons, using initial positions and velocities as determined from the corresponding separation trajectories for the retracted-tip configurations.

UNCLASSIFIED

PREFACE

The work reported herein was done by the Arnold Engineering Development Center (AEDC) for Rockwell International, Missile Systems Division and sponsored by the Air Force Armament Laboratory (AFATL/DLJC) and Armament Development and Test Center (ADTC/SDTT), Air Force Systems Command (AFSC), under Program Element 64733F/2076.

The test results presented were obtained by ARO, Inc. (a subsidiary of Sverdrup & Parcel and Associates, Inc.), contract operator of the AEDC, AFSC, Arnold Air Force Station, Tennessee. The tests were conducted from March 15 through June 29, 1974, under ARO Project No. PA468. The manuscript (ARO Control No. ARO-PWT-TR-74-76) was submitted for publication on August 30, 1974.

This report may also be identified as ADTC-TR-74-96.

CONTENTS

	<u>Page</u>
1.0 INTRODUCTION	7
2.0 APPARATUS	
2.1 Test Facility	7
2.2 Test Articles	8
2.3 Instrumentation	9
3.0 TEST DESCRIPTION	
3.1 Test Conditions	9
3.2 Data Acquisition	9
3.3 Corrections	11
3.4 Precision of Data	12
4.0 RESULTS AND DISCUSSION	
4.1 Basic Flow-Field Data	13
4.2 Free-Stream Aerodynamic Data	14
4.3 Aerodynamic Data in the Aircraft Flow Fields	14
4.4 Separation Trajectories	15
5.0 CONCLUDING REMARKS	17
REFERENCES	17

ILLUSTRATIONS

Figure

1. Isometric Drawing of a Typical Store Separation Installation and a Block Diagram of the Computer Control Loop	19
2. Schematic of the Tunnel Test Section Showing Model Locations	20
3. Sketch of the Parent-Aircraft Models	22
4. Details of the F-4C Pylon Models	24
5. Details of the A-7D Pylon Models	25
6. Details of the F-4C Fuel Tank Models	26
7. Details of the A-7D 300-gal Fuel Tank Model	28
8. Details of the ALQ-131 Terminal-Threat Pod Model	29
9. Details of the Data Link Pod Model	30
10. Details of the Super HOBOS Models	31
11. Details of the 40-deg Conical Probe	34
12. Tunnel Installation Photographs Showing Parent Aircraft, Probe, Store, and CTS	35
13. Axis System Defining Directions and Angles for Flow-Field Measurements	36

<u>Figure</u>	<u>Page</u>
14. Flow-Field Measurements Beneath the F-4C Left-Wing Inboard Pylon, Configuration 43	38
15. Flow-Field Measurements Beneath the A-7D Right-Wing Center Pylon, Configuration 54	50
16. Free-Stream Aerodynamic Characteristics of the Super HOBOS/MK-84 Store with Tips Retracted and Extended	56
17. Variation of the Super HOBOS Longitudinal Stability Derivatives and Axial-Force Coefficients with Mach Number, $\alpha_s = 0$	63
18. Carriage Position Characteristics of the MK-84 Store for the F-4C Inboard Pylons	64
19. Aerodynamic Characteristics of the MK-84 store in the F-4C Flow Field, $Y_p = 0, \beta = 0$	70
20. Aerodynamic Characteristics of the MK-84 Store in the A-7D Flow Field, $Y_p = 0, \beta = 0$	82
21. Separation Characteristics of the MK-84 Store from the F-4C Left-Wing Inboard Pylon with No Adjacent Stores	88
22. MK-84 Trajectory Comparisons for the F-4C with and without the 370-gal Fuel Tank, Launch Configurations 1 and 2	96
23. MK-84 Trajectory Comparisons for the F-4C with and without the Data Link Pod, Launch Configurations 1 and 4	98
24. MK-84 Trajectory Comparisons for the F-4C with 370- and 600-gal Fuel Tanks, Launch Configurations 2 and 3	104
25. MK-84 Trajectory Comparisons for the F-4C with and without the ALQ-131 ECM Pod, Launch Configurations 2 and 5	108
26. Comparison of the Separation Characteristics of the MK-84 and SUU-54 Stores from the F-4C, Launch Configurations 1 and 6	114
27. Separation Characteristics of the MK-84 Store from the A-7D Left-Wing Center Pylon with No Adjacent Stores	118
28. Separation Characteristics of the MK-84 Store from the A-7D Right-Wing Outboard Pylon, Launch Configuration 21	121

TABLES

1. Wind Tunnel Test Conditions	124
2. Test Summary	125
3. F-4C Load Configurations	129

<u>Tables</u>	<u>Page</u>
4. A-7D Load Configurations	131
5. Full-Scale Store Parameters Used in Trajectory Calculations	132
6. Adjustments to the Pitching-Moment and Yawing-Moment Coefficients for Trajectory Calculations	133
NOMENCLATURE	134

1.0 INTRODUCTION

A wind tunnel investigation, consisting of flow-angularity measurements in the F-4C and A-7D aircraft flow fields, aerodynamic loads on the Super HOBOS weapons in the free stream and in the parent-aircraft flow fields, and separation trajectories of the stores from both parent aircraft, was conducted using a six-degree-of-freedom captive trajectory store separation system (CTS). The data were obtained at Mach numbers 0.65 to 1.6 in the Aerodynamic Wind Tunnel (4T) of the Propulsion Wind Tunnel Facility (PWT) using 0.05-scale models of the parent aircraft and stores. The flow-angularity data were recorded under the left- and right-wing inboard pylons and centerline of the F-4C aircraft and under the left- and right-wing center pylons of the A-7D aircraft at selected axial and vertical positions. Parent aircraft angle of attack varied from -2 to 16 deg for sideslip angles of 0 and 9 deg. The free-stream aerodynamic characteristics of the MK-84 and SUU-54 Super HOBOS with fin tips retracted and extended were measured at angles of attack from -4 to 44 deg for roll angles of 0 and 22.5 deg. Additional free-stream data were obtained on the MK-84 configuration with one tip extended (a simulated failure condition) at angles of attack from -44 to 44 deg. Carriage-loads aerodynamic data for the MK-84 Super HOBOS were obtained at the inboard pylons for the F-4C parent aircraft at angles of attack from -2 to 16 deg at sideslip angles of 0, 4, and 9 deg. Additional aerodynamic data for the MK-84 Super HOBOS with fin tips retracted and extended were measured in the plane of the F-4C left- and right-wing inboard pylons and the A-7D right-wing center pylon at distances up to 20 ft (full scale) away from the pylons. Parent aircraft angle of attack varied from 0 to 8 deg at zero sideslip. Separation trajectories for the MK-84 and SUU-54 Super HOBOS (tips retracted) were initiated from the F-4C left- and right-wing inboard pylon, the A-7D left- and right-wing center pylons, and the A-7D right-wing outboard pylons using simulated full-scale store weights, center-of-gravity (cg) locations, dive angles, and altitudes. At a point on the store flight path approximately 3.5 ft away from the pylons, continuation trajectories were initiated for the MK-84 and SUU-54 stores with fin tips extended, using initial positions and velocities as determined from the corresponding separation trajectories for the retracted-tip configurations. Parent aircraft angle of attack ranged from -1 to 10 deg at zero sideslip.

2.0 APPARATUS

2.1 TEST FACILITY

The Aerodynamic Wind Tunnel (4T) is a closed-loop, continuous flow, variable-density tunnel in which the Mach number can be varied from 0.1 to 1.3 and can be set at 1.6 and 2.0 by placing nozzle inserts over the permanent sonic nozzle. At all Mach numbers, the stagnation pressure can be varied from 300 to 3700 psfa. The test section is 4 ft

square and 12.5 ft long with perforated, variable porosity (0.5- to 10-percent open) walls. It is completely enclosed in a plenum chamber from which the air can be evacuated, allowing part of the tunnel airflow to be removed through the perforated walls of the test section.

Two separate and independent support systems were used to support the models. The parent aircraft model was inverted in the test section and supported by an offset sting attached to the main pitch sector. The store model (or flow-field survey probe) was supported by the CTS which extends down from the tunnel top wall and provides store (or probe) movement (six degrees of freedom) independent of the parent-aircraft model. An isometric drawing of a typical installation is shown in Fig. 1.

Also shown in Fig. 1 is a block diagram of the computer control loop used during testing. The analog system and the digital computer work as an integrated unit and, utilizing required input information, control the store (or probe) movement. Positioning is accomplished by use of six individual direct-current (d-c) electric motors. Maximum translational travel of the CTS is ± 15 in. from the tunnel centerline in the lateral and vertical directions and 36 in. in the axial direction. Maximum angular displacements are ± 45 deg in pitch and yaw and ± 360 deg in roll. A more complete description of the test facility can be found in Ref. 1. A schematic showing the test section details and the location of the models in the tunnel is shown in Fig. 2.

2.2 TEST ARTICLES

The basic details of the 0.05-scale F-4C and A-7D parent models are presented in Fig. 3. The parent models are geometrically similar to the full-scale airplanes except that the F-4C tail section and A-7D horizontal tails are removed to minimize interference with CTS support movement. Details of the F-4 and A-7 pylons are shown in Figs. 4 and 5, respectively. Details of the store models are given as follows: F-4, 370-gal fuel tank (Fig. 6a), F-4, 600-gal fuel tank (Fig. 6b), A-7, 300-gal fuel tank (Fig. 7), ALQ-131 terminal-threat pod (Fig. 8), data link pod (Fig. 9), and Super HOBOS (Fig. 10). During the first test phase, the MK-84 Super HOBOS model with the wedge-shaped leading- and trailing-edge fins and strakes was used (Fig. 10a). For the second test phase, the fins and strakes for the MK-84 were modified (Fig. 10b) to match more closely those of the full-scale weapon. For both the MK-84 and SUU-54 models, interchangeable afterbody configurations were fabricated, each with a full set of retracted or extended fin tips. An additional afterbody configuration with one tip extended was also provided for the MK-84 model. The normal orientation of this configuration ($\phi = 0$) was with the extended tip on the lower right fin as shown in Fig. 10a. Data at $\phi = 0$ and 22.5 deg were obtained by rolling the support sting. Data at $\phi = 90$ and 112.5 deg were obtained with the store

model rolled 90 deg with respect to the balance. The Super HOBOS and data link pod store models were furnished by Rockwell International, Missile Systems Division, and all other test articles were obtained from the AEDC-PWT inventory.

The probe used to obtain flow-field measurements was attached directly to the CTS and consisted of a single cone-cylinder with a 40-deg included tip angle (Fig. 11). There were four equally spaced static pressure orifices on the cone surface and a total pressure orifice at the cone apex. Typical tunnel installation photographs showing parent aircraft, probe, store, and CTS are shown in Fig. 12.

2.3 INSTRUMENTATION

Static and total pressures on the cone probe were measured with 5-psid transducers. A six-component internal strain-gage balance was used to obtain store aerodynamic force and moment data. Translational and angular positions of the store were obtained from CTS analog inputs during separation trajectories and from digital computer commands during aerodynamic and flow-field testing. The parent-model angle of attack was determined using an internal, gravimetric angular position indicator. The pylons contained a touch-wire system which enabled the store and probe to be accurately positioned initially with respect to the parent aircraft. The system was also wired to automatically stop the CTS motion and give visual indication should the store, probe, or sting support make contact with any surface other than the touch wire.

3.0 TEST DESCRIPTION

3.1 TEST CONDITIONS

A complete test summary and the wind tunnel test conditions are given in Tables 1 through 6. Aerodynamic, flow-field, and separation trajectory data were obtained at Mach numbers from 0.65 to 1.6. Tunnel conditions were held constant at the desired Mach number while the data were obtained. The trajectories were terminated when the store or sting contacted the parent-aircraft model or when a CTS limit was reached.

3.2 DATA ACQUISITION

3.2.1 Flow-Field Survey Data

All flow-field measurements were obtained in the pylon-axis system. Definitions of the positive directions of the flow-field velocity vectors, flow angles, and probe displacements are given in Fig.-13. During testing, tunnel conditions were established and the probe tip was positioned at a known coordinate point relative to the parent aircraft.

At this position, initial-point data were obtained which oriented the computer program controlling CTS movement (see block diagram, Fig. 1). After the initial data were recorded, the computer automatically positioned the probe at preselected locations (see Table 2) where tunnel conditions and probe tip pressures were recorded. Using predetermined probe calibration data, the probe pressure measurements were reduced to flow-angularity data, and these were tabulated point-by-point with the same digital computer which controlled the CTS movement.

3.2.2 Aerodynamic Loads Data

Store aerodynamic data in the free stream and in the parent aircraft flow field were obtained in the following manner. After tunnel conditions were established and the aircraft model angle of attack was set (when applicable), the store was manually set at $\alpha_s = 0$ (free-stream data) or at the carriage position ($X_p = Y_p = Z_p = 0$) (flow-field data). Operational control of the CTS was then switched to the digital computer, which controlled the store movement through commands to the CTS (see block diagram, Fig. 1). The preselected orientations and cg positions of the store programmed into the computer are given in Table 2. At each position set, the wind tunnel operating conditions and the store model forces and moments were measured and recorded. The model aerodynamic loads were then reduced to coefficient form and tabulated point by point by the digital computer.

3.2.3 Trajectory Data

To obtain a trajectory, test conditions were established in the tunnel and the parent model was positioned at the desired angle of attack. Operational control of the CTS was then switched to the digital computer which automatically oriented the store model at a position corresponding to the carriage location and then controlled the store movement during the trajectory through commands to the CTS analog system (see block diagram, Fig. 1). Data from the wind tunnel, consisting of measured model forces and moments, wind tunnel operating conditions, and CTS rig positions, were input to the digital computer for use in the full-scale trajectory calculations.

The digital computer was programmed to solve the six-degree-of-freedom equations to calculate the angular and linear displacements of the store relative to the parent aircraft pylon (Ref. 2). In general, the program involves using the last two successive measured values of each static aerodynamic coefficient to predict the magnitude of the coefficients over the next time interval of the trajectory. These predicted values are used to calculate the new position and attitude of the store at the end of the time interval. The CTS is then commanded to move the store model to this new position and the aerodynamic

loads are measured. If these new measurements agree with the predicted values, the process is continued over another time interval of the same magnitude. If the measured and predicted values do not agree within the desired precision, the calculation is repeated over a time interval one-half the previous value. This process is repeated until a complete trajectory has been obtained.

In applying the wind tunnel data to the calculations of the full-scale store trajectories, the measured forces and moments are reduced to coefficient form and then applied with proper full-scale store dimensions and flight dynamic pressure. Dynamic pressure was calculated using a flight velocity equal to the free-stream velocity component plus the components of store velocity relative to the aircraft, and a density corresponding to the simulated altitude.

The initial portion of each launch trajectory incorporated simulated ejector forces in addition to the measured aerodynamic forces acting on the store. The ejector force was considered to act perpendicular to the pylon mounting surface. The ejector forces and locations along with other full-scale store parameters used in the trajectory calculations are listed in Table 5.

3.3 CORRECTIONS

Probe free-stream calibration data were used to obtain corrections to account for any minor misalignment in the probe pitch or yaw orientation. However, no attempt was made to correct the measured flow angles for deflections attributable to aerodynamic loading on the probe.

Balance, sting, and support deflections caused by the aerodynamic loads on the store models were accounted for in the data reduction program to calculate the true store-model angles. Corrections were also made for model weight tares to calculate the net aerodynamic forces on the store model.

In applying the aerodynamic data from the 0.05-scale model to the calculation of full-scale missile trajectories, minor corrections were made to the pitching-moment and yawing-moment coefficient data. Differences between the free-stream data from the present test and those in Refs. 3 and 4 were used to correct the 0.05-scale model data. Changes in the pitching-moment coefficient derivative (C_{m_α}) were accomplished by shifting the apparent cg of the 0.05-scale model (in the pitch plane only), whereas the zero-angle-of-attack intercepts (C_{m_0} and C_{n_0}) were adjusted by adding an incremental coefficient. These corrections (ΔX_{cg} , C_{m_0} , and C_{n_0}) are listed in Table 6 for each Mach number at which trajectory data were obtained.

3.4 PRECISION OF DATA

Uncertainties in the basic tunnel parameters, total pressure (p_t), total temperature (T_t), and Mach number (M_∞), were estimated from repeat calibrations of the instrumentation and from repeatability and uniformity of the test section flow during tunnel calibration. These uncertainties were then used to estimate the uncertainties in other free-stream properties, using the Taylor series method of error propagation (Ref. 5).

Free-Stream Mach Number	Uncertainty, percent						
	ΔM_∞	Δp_t	ΔT_t	Δq_∞	Δp_∞	ΔV_∞	ΔRe_∞
0.65	± 0.3	± 0.1	± 0.4	± 0.5	± 0.2	± 0.4	± 0.6
0.80	± 0.3	± 0.1	± 0.4	± 0.4	± 0.3	± 0.3	± 0.5
0.90	± 0.3	± 0.1	± 0.4	± 0.3	± 0.3	± 0.3	± 0.5
0.95	± 0.3	± 0.1	± 0.4	± 0.3	± 0.4	± 0.4	± 0.5
1.05	± 0.5	± 0.1	± 0.4	± 0.4	± 0.6	± 0.4	± 0.5
1.20	± 0.8	± 0.1	± 0.4	± 0.4	± 2.0	± 0.6	± 0.5
1.60	± 0.5	± 0.1	± 0.4	± 0.2	± 1.2	± 0.4	± 0.6

The balance uncertainties, based on a 95-percent confidence level, were combined with the uncertainties in the tunnel parameters, assuming a Taylor series error propagation, to estimate the precision of the aerodynamic coefficients. The maximum estimated uncertainties are given as follows:

Free-Stream Mach Number	Uncertainty					
	ΔC_N	ΔC_m	ΔC_Y	ΔC_n	ΔC_l	ΔC_A
0.65	± 0.11	± 0.06	± 0.11	± 0.05	± 0.03	± 0.03
0.80	± 0.09	± 0.05	± 0.08	± 0.04	± 0.02	± 0.02
0.90	± 0.08	± 0.04	± 0.07	± 0.04	± 0.02	± 0.02
0.95	± 0.08	± 0.04	± 0.07	± 0.03	± 0.02	± 0.02
1.05	± 0.07	± 0.03	± 0.06	± 0.03	± 0.02	± 0.02
1.20	± 0.06	± 0.03	± 0.06	± 0.03	± 0.02	± 0.02
1.60	± 0.04	± 0.04	± 0.03	± 0.03	± 0.01	± 0.02

The estimated uncertainties in store model and probe positioning from the ability of the CTS to set on a specified value were ± 0.08 ft (full-scale equivalent) in X, Y, and Z, ± 0.15 deg in pitch and yaw, and ± 1.0 deg in roll. The estimated uncertainties

in parent-aircraft angles of attack and sideslip are ± 0.1 and ± 0.2 , deg, respectively. From repeatability of measurement, the estimated uncertainties in α_{XY} and α_{XZ} are ± 0.4 deg at all Mach numbers.

The trajectory data are subject to error from several sources including tunnel conditions, balance measurements, extrapolation tolerances allowed in the predicted coefficients, computer inputs, and CTS positioning control. Extrapolation tolerances were ± 0.10 for the aerodynamic coefficients. The maximum uncertainties in the full-scale position data caused by the balance inaccuracies are given below:

Free-Stream Mach Number		Uncertainty						
		t	ΔX	ΔY	ΔZ	$\Delta \theta$	$\Delta \psi$	$\Delta \phi$
0.65	1	0.4	± 0.1	± 0.1	± 0.1	± 0.4	± 0.4	± 2.2
0.80		0.4	± 0.1	± 0.1	± 0.1	± 0.5	± 0.5	± 3.3
0.90		0.4	± 0.1	± 0.1	± 0.1	± 0.6	± 0.6	± 3.8
0.95		0.4	± 0.1	± 0.1	± 0.1	± 0.7	± 0.6	± 4.1
1.05		0.4	± 0.1	± 0.1	± 0.1	± 0.4	± 0.4	± 2.2
1.20		0.4	± 0.1	± 0.1	± 0.1	± 0.7	± 0.7	± 4.4
1.60		0.4	± 0.1	± 0.1	± 0.1	± 0.5	± 0.5	± 3.0

4.0 RESULTS AND DISCUSSION

Data obtained during the test consisted of basic flow angularity measurements in the F-4C and A-7D flow fields, aerodynamic loads on the Super HOBOS stores in the free stream and in the flow fields of the parent aircraft, and separation trajectories of the stores launched from both parent aircraft. Summaries of the test conditions and data obtained are given in Tables 1 and 2, and test configurations are listed in Tables 3 and 4. Because of the large volume of data obtained, only representative data are presented herein.

4.1 BASIC FLOW-FIELD DATA

Flow-field measurements beneath the F-4C left-wing inboard pylon and the A-7D right-wing center pylon are presented in Figs. 14 and 15, respectively, for the clean aircraft (no adjacent stores). The upwash and sidewash angles are measured with respect to a line parallel to the pylon lower surface in the aircraft plane of symmetry. The two axial stations where measurements were obtained represented the estimated center-of-pressure locations for the strakes ($X_P = 0$) and fins ($X_P = -8.333$ ft) of the MK-84 store in the carriage position.

3 For both parent aircraft, deviations of the flow angles at $Z_p = 0$ (carriage position) from the free-stream values were quite sensitive to parent-aircraft angle of attack, with the larger deviations generally occurring at the higher α 's. Also, differences in the flow angles between the two axial positions were in many cases several degrees. As would be expected, the flow angles tended to return to free-stream values as distance from the parent aircraft increased. At a distance of 20 ft away, deviations from the free-stream flow angles were generally less than 1 deg.

4.2 FREE-STREAM AERODYNAMIC DATA

The variation of the free-stream aerodynamic coefficients with angle of attack are shown in Fig. 16 for the MK-84 Super HOBOS store with fin tips retracted and extended (rounded leading-edge fins and strakes). At $\alpha_s = 0$ the store was statically unstable with tips retracted and statically stable with tips extended at all Mach numbers. For the store with tips retracted, the pitching-moment variations were highly nonlinear at the higher angles of attack and trim conditions were obtained near $\alpha_s = 30$ deg at the higher Mach numbers. The longitudinal stability and axial-force characteristics at $\alpha_s = 0$ of all the Super HOBOS models are presented in Fig. 17 along with the 0.25-scale model data of Refs. 3 and 4. Comparison of the stability derivatives for the MK-84 stores with the different fin and strake configurations showed significant differences only in C_{m_α} for the tips retracted models. Axial-force coefficients were consistently higher for the store with wedge-shaped fins with both retracted and extended tips. For clarity, the stability derivatives for the 0.25-scale model are shown only where measureable differences between the two different scale models occurred. As may be seen, there were essentially no differences in the normal-force derivatives, and the small differences in the pitching-moment derivatives for the two different scale models can probably be attributed to the inability to accurately reproduce the true external shape at such a small scale (e.g., fin and strake leading edges and profile).

4.3 AERODYNAMIC DATA IN THE AIRCRAFT FLOW FIELDS

The aerodynamic characteristics of the MK-84 Super HOBOS, with tips retracted and extended, in the flow fields of both the F-4C and A-7D aircraft are presented in Figs. 18 through 20. The carriage loads data were obtained with the sting-mounted store at the carriage position. The data of the store with rounded-leading-edge fins and strakes (Fig. 18) show that variations in the angle of attack or sideslip angle of the F-4C aircraft influenced all the coefficients. For the $\beta = 0$ case (Fig. 18a), trends in the carriage loads data can be explained by an examination of the flow-angularity data (Fig. 14) and free-stream aerodynamic data (Fig. 16). As parent-aircraft angle of attack was increased, the flow angles in the pitch plane at the center of pressure of the strakes generally remained

equal to or became slightly larger than the free-stream flow angles, whereas those at the center of pressure of the fins decreased substantially. Therefore, when compared with the free-stream data at the same angle of attack, the carriage loads data should show a reduction in the normal-force coefficient and an increase in the pitching-moment coefficient, which was the case. Correspondingly, as parent angle of attack increased, outboard crossflow increased. This would result in the increased negative side force indicated by the carriage loads data. Since the free-stream data show a basically unstable store, the large negative side force would be expected to produce a large negative yawing moment. However, further examination of the crossflow angles show that angularities were larger at the center of pressure of the fins than at the center of pressure of the strakes, thus creating a restoring moment in the yaw plane. Therefore, for the same angle of attack, the store should be less unstable in yaw at the carriage position than at free-stream conditions, which the carriage loads data indicated. The increase in rolling-moment coefficient with parent angle of attack can be attributed to a crossflow shielding effect by the pylon on the two fins nearest the aircraft wing.

The lateral coefficients were more significantly affected by changes in parent-aircraft sideslip angle (Fig. 18f) for constant angle of attack as would be expected. It should be noted that the data for the store model on the aircraft left wing at positive aircraft sideslip angles can be considered equivalent to data for the store on the right wing at negative sideslip angles by reversing the signs of C_Y , C_n , and C_l .

The aerodynamic loads data up to 20 ft away from the F-4C pylons for the store with the wedge-leading-edge fins and strakes are presented in Fig. 19 for fin tips, both retracted and extended. Similar data for the A-7D aircraft are shown in Fig. 20. Comparison of the aerodynamic loads at the F-4C carriage position ($Z_p = 0$) for the rounded-leading-edge fins (Fig. 18) and the wedge-leading-edge fins (Fig. 19) indicated some minor variations in the magnitudes of the coefficients. However, this was to be expected since similar discrepancies were noted in the free-stream data. The trends in the aerodynamic loads as distance between the store and aircraft increased could generally be predicted by an examination of the variations in the flow angle measurements.

4.4 SEPARATION TRAJECTORIES

The ejector-separated trajectories simulated release from the wing inboard pylons of the F-4C and the wing center and outboard pylons of the A-7D. Data showing the linear displacements of the store relative to the carriage position and the angular displacements relative to the flight-axis system are presented as functions of full-scale trajectory time. Positive X, Y, and Z displacements (as seen by the pilot) are forward, to the right, and down, respectively. Positive changes in θ , ψ , and ϕ (as seen by the pilot) are nose up, nose to the right, and clockwise, respectively. The full-scale store parameters used in

trajectory calculations are listed in Table 5, and the pitching-moment and yawing-moment corrections (see Section 3.3) applied to the store model data are given in Table 6.

The separation characteristics of the MK-84 Super HOBOS (rounded-leading-edge fins and strakes) from the F-4C left wing inboard pylon with no adjacent stores are presented in Fig. 21. Initial trends in the trajectories could generally be predicted from a consideration of the carriage loads data (Fig. 18) and ejector forces. Only small deviations in the nose-left yaw rates were noted with variations in either parent-aircraft angle of attack or Mach number as supported by the carriage loads yawing-moment data, whereas the increased pitch-up characteristics with increasing parent angle of attack are clearly indicated by the pitching-moment data. As shown, there was little tendency for the unstable store (tips retracted) to recover in either pitch or yaw. However, when the tips were extended (about 3.5 ft away from the aircraft), the stable store began to seek its trimmed condition. In a few instances, the stable store attempted to fly back toward the aircraft. At $\alpha = 1$ deg, an increase in the free-stream Mach number (Fig. 21h) resulted in faster rates of aft and outboard store movement. The pitch data showed increased pitch-up at $M_\infty = 0.90$ but increased pitch-down at $M_\infty = 1.20$ when compared with the $M_\infty = 0.65$ data. The period of both the pitch and yaw motions seemed to decrease with increasing Mach number.

Typical trajectories initiated from the inboard pylons for different F-4C load configurations are compared in Figs. 22 through 25. For the purpose of direct comparison, the signs on Y , ψ , and ϕ have been reversed on the right-wing trajectories to make them equivalent to the left-wing data. Configuration numbers in the figure headings followed by the letter "A" designate this change. When compared with data for the empty aircraft, data for models with adjacent stores on the aircraft centerline show that outboard travel and nose-left yawing generally increased, whereas opposite effects were noted with the 370-gal fuel tanks on the outboard pylons at low angles of attack (Figs. 22 through 24). This would suggest increased crossflow with centerline store carriage and reduced crossflow for the outboard store carriage. Effects of the adjacent stores on the trajectory characteristics diminished as aircraft angle of attack increased, indicating that the aircraft flow field was becoming increasingly dominated by angle of attack. With the ECM pod in the missile well, effects on the trajectory data were similar to those of centerline store carriage (Fig. 25). Although the magnitudes of the pitch and yaw excursions for the MK-84 and SUU-54 trajectories were sometimes different, basic trends in the separation characteristics for the two stores were similar (Fig. 26).

Separation characteristics of the MK-84 store from the right-wing center and left-wing outboard pylons of the A-7D are presented in Figs. 27 and 28, respectively. At constant angle of attack, increasing the free-stream Mach number generally resulted in increased pitch-down and nose-outboard yaw of the store from both release positions.

5.0 CONCLUDING REMARKS

Flow-angularity measurements in the F-4C and A-7D flow fields, aerodynamic loads on the Super HOBOS stores in the free stream and flow fields of both parent aircraft, and store separation trajectories from both parent aircraft were obtained at Mach numbers from 0.65 to 1.60 using 0.05-scale models. Based on test results, the following comments can be made:

1. Crossflow at the F-4C and A-7D wing pylon carriage positions increased as parent-aircraft angle of attack increased.
2. At a distance of 20 ft from the pylons, the measured flow angles were very nearly equal to free-stream conditions.
3. Comparison of the free-stream aerodynamic characteristics for the 0.05-scale models of the present test and the 0.25-scale models of Refs. 3 and 4 showed reasonable agreement for both the MK-84 and SUU-54 Super HOBOS.
4. Trends in the aerodynamic loads at the carriage position could generally be predicted from the flow-field and free-stream aerodynamic data.
5. Initial trends in the separation trajectory data could generally be predicted from the carriage loads data.

REFERENCES

1. Test Facilities Handbook (Tenth Edition). "Propulsion Wind Tunnel Facility, Vol. 4." Arnold Engineering Development Center, May 1974.
2. Christopher, J. P. and Carleton, W. E. "Captive-Trajectory Store-Separation System of the AEDC-PWT 4-Foot Transonic Tunnel." AEDC-TR-68-200 (AD839743), September 1968.
3. Smith, D. K. "Static Stability and Control Effectiveness of the Super HOBOS/MK-84 (EOGB-II) Munition at Mach Numbers from 0.4 to 1.6." AEDC-TR-74-68, July 1974.
4. Heim, E. R. and Smith, D. K. "Aerodynamic Characteristics of the Super HOBOS/SUU-54 Munition at Mach Numbers from 0.4 to 1.6." AEDC-TR-74-81, September 1974.
5. Beers, Yardley. Introduction to the Theory of Error. Addison-Wesley Publishing Company, Inc., Reading, Massachusetts, 1957, pp. 26-36.

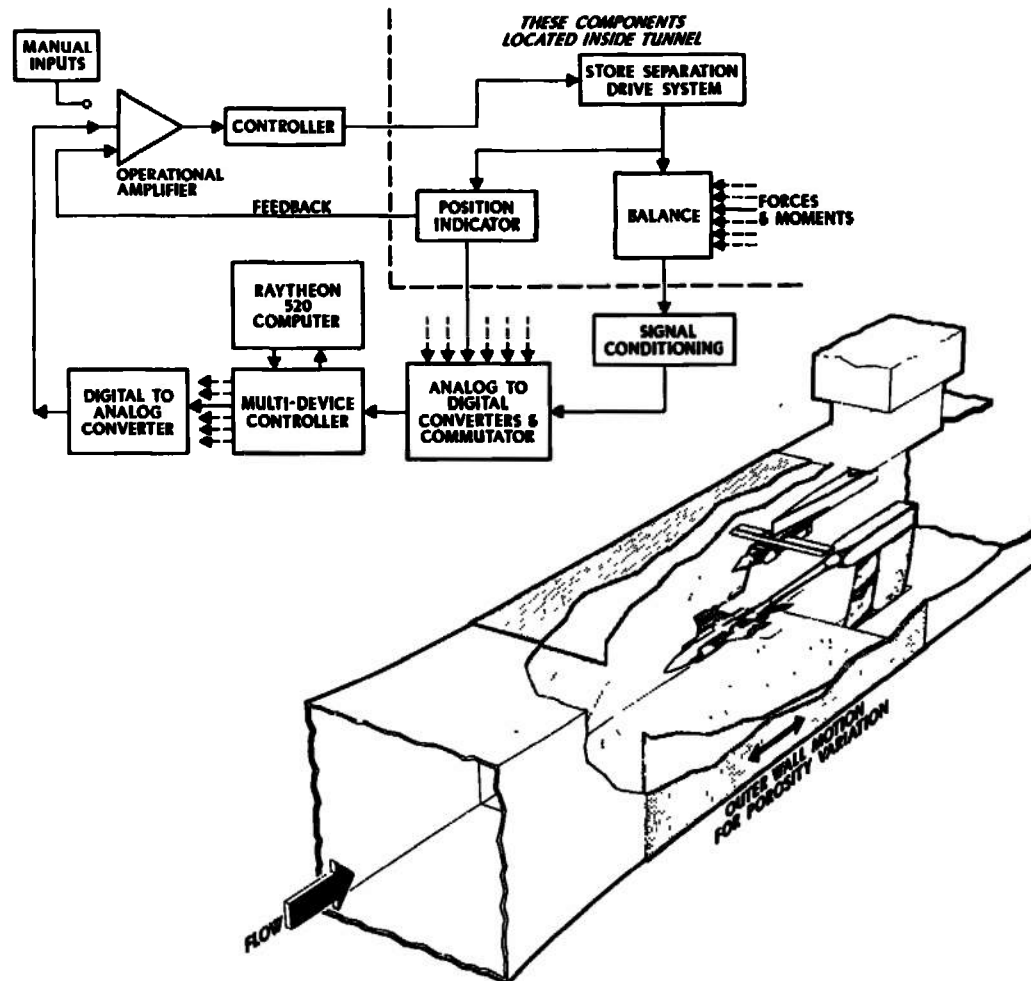
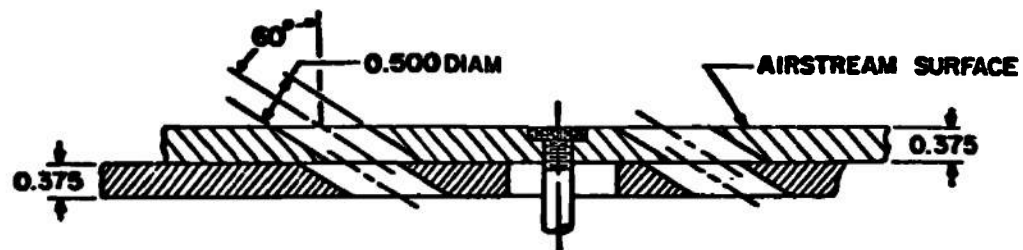
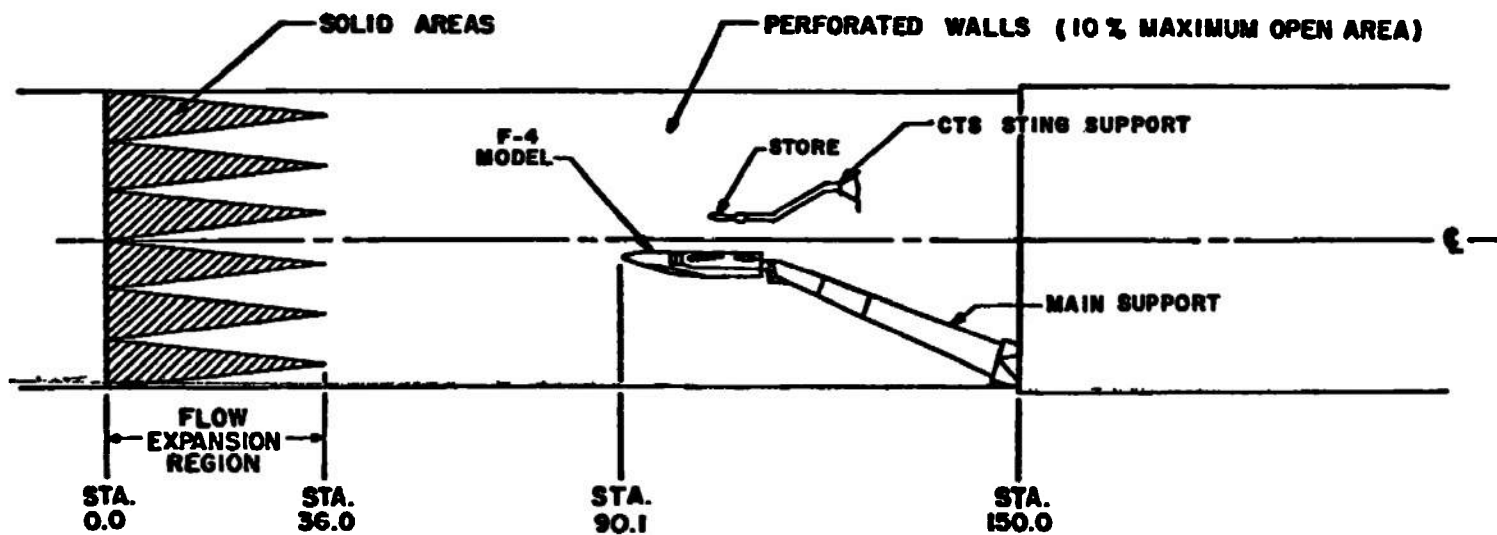


Figure 1. Isometric drawing of a typical store separation installation and a block diagram of the computer control loop.



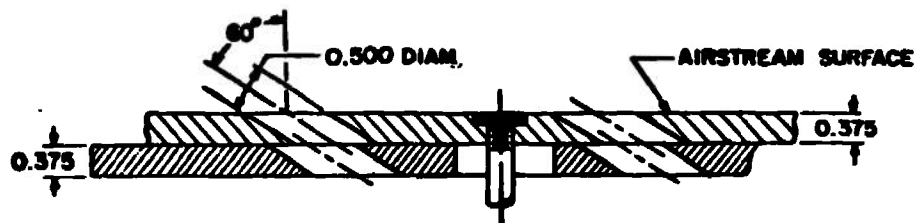
TYPICAL PERFORATED WALL CROSS SECTION

TUNNEL STATIONS AND DIMENSIONS
ARE IN INCHES



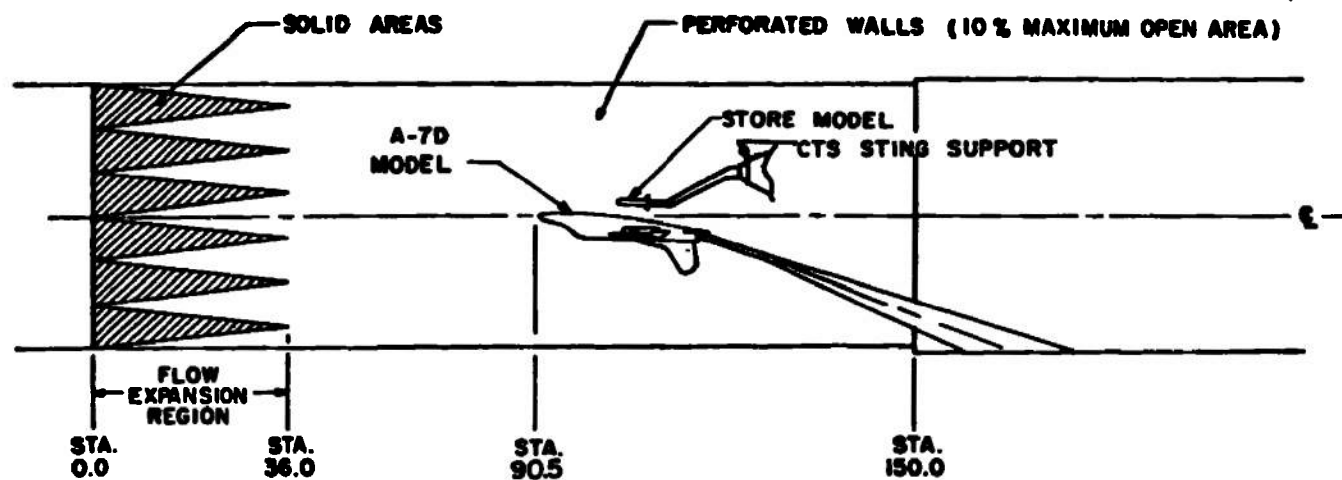
a. F-4C

Figure 2. Schematic of the tunnel test section showing model locations.

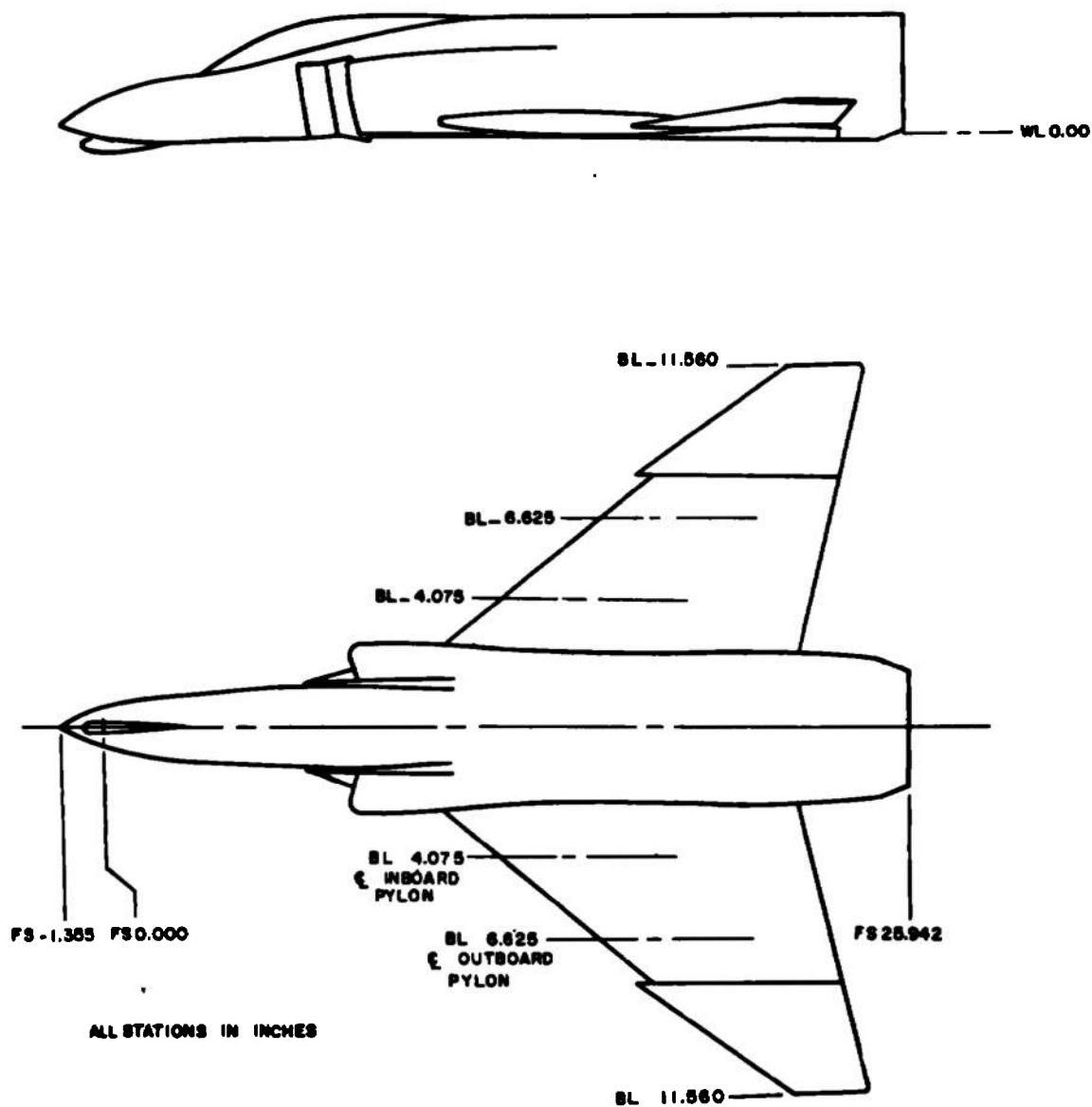


TYPICAL PERFORATED WALL CROSS SECTION

ALL DIMENSIONS AND TUNNEL STATIONS IN INCHES

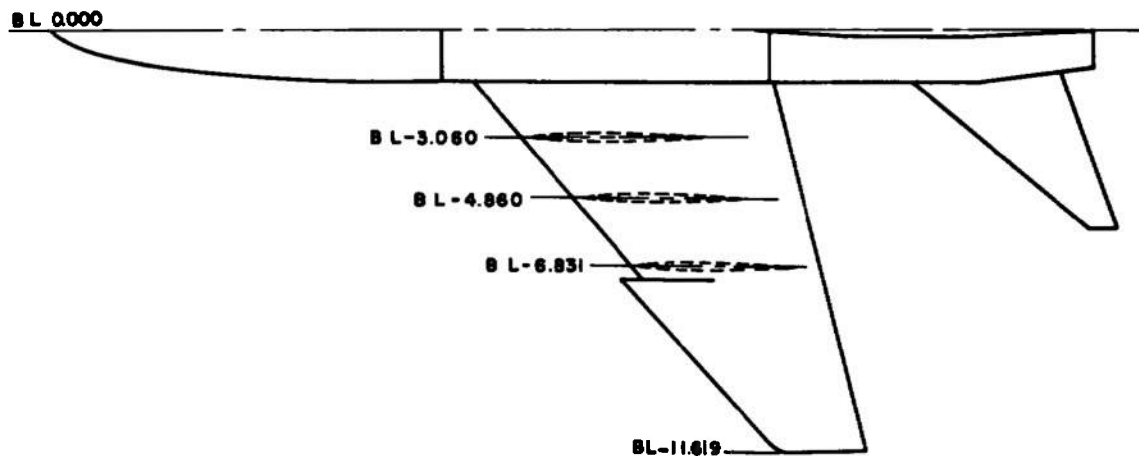


b. A-7D
Figure 2. Concluded.

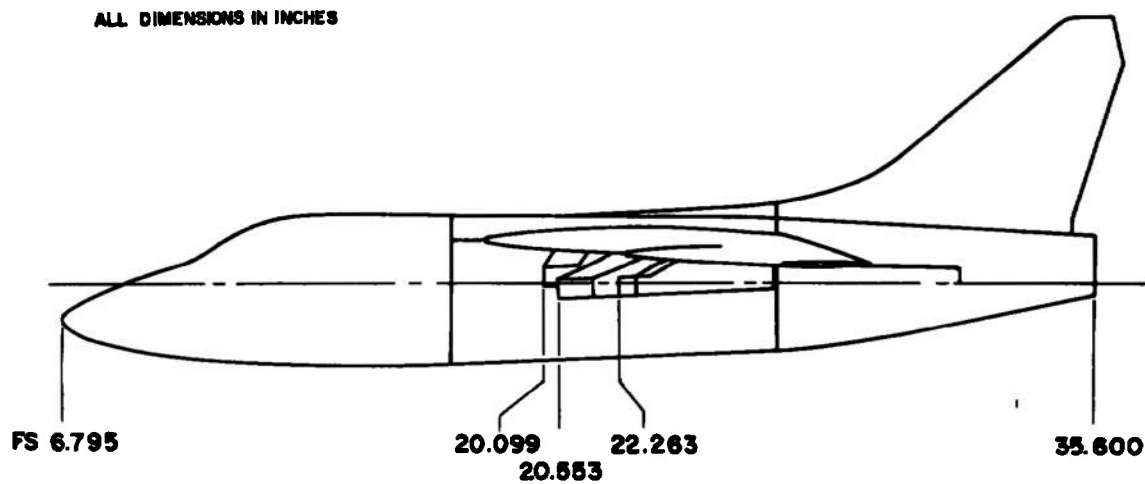


a. F-4C

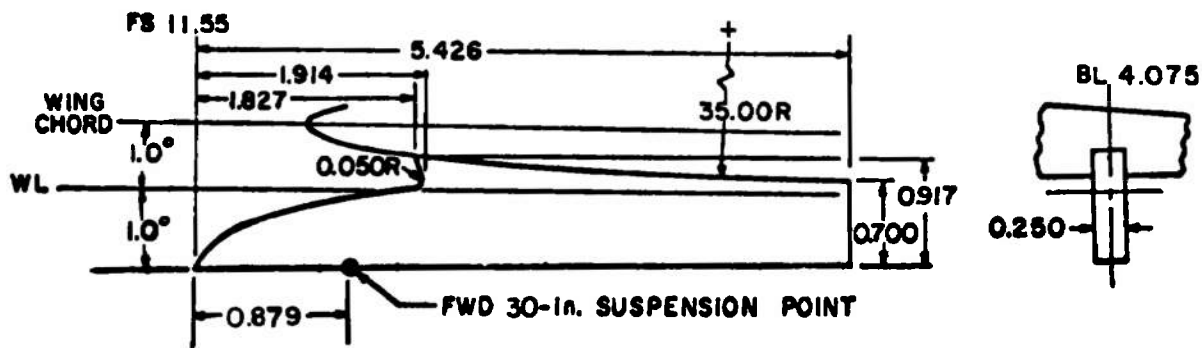
Figure 3. Sketch of the parent-aircraft models.



ALL DIMENSIONS IN INCHES

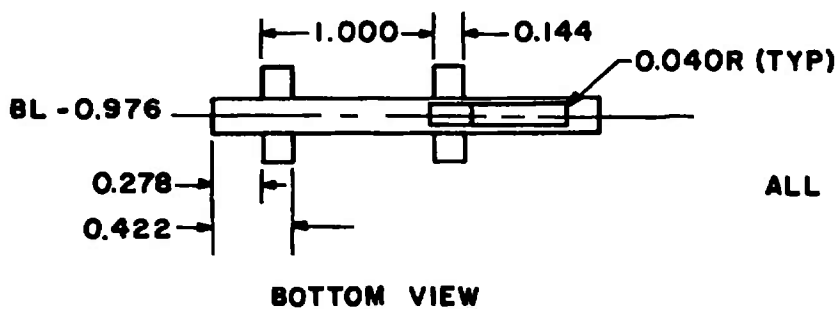
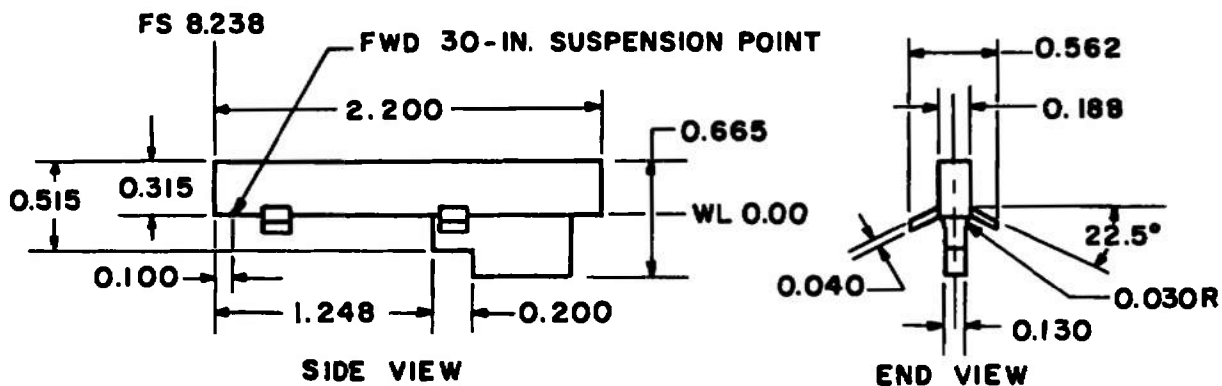


b. A-7D
Figure 3. Concluded.



ALL DIMENSIONS IN INCHES

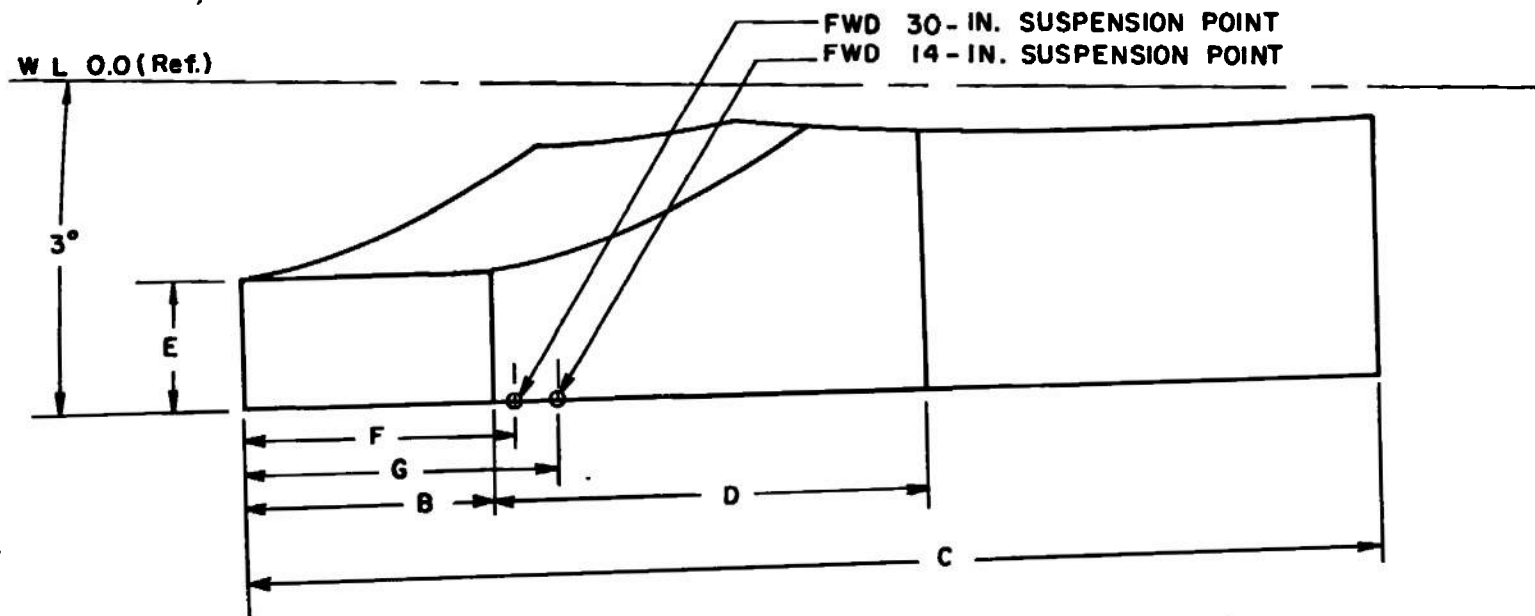
a. Inboard wing pylon



ALL DIMENSIONS IN INCHES

b. Station 4 missile well pylon

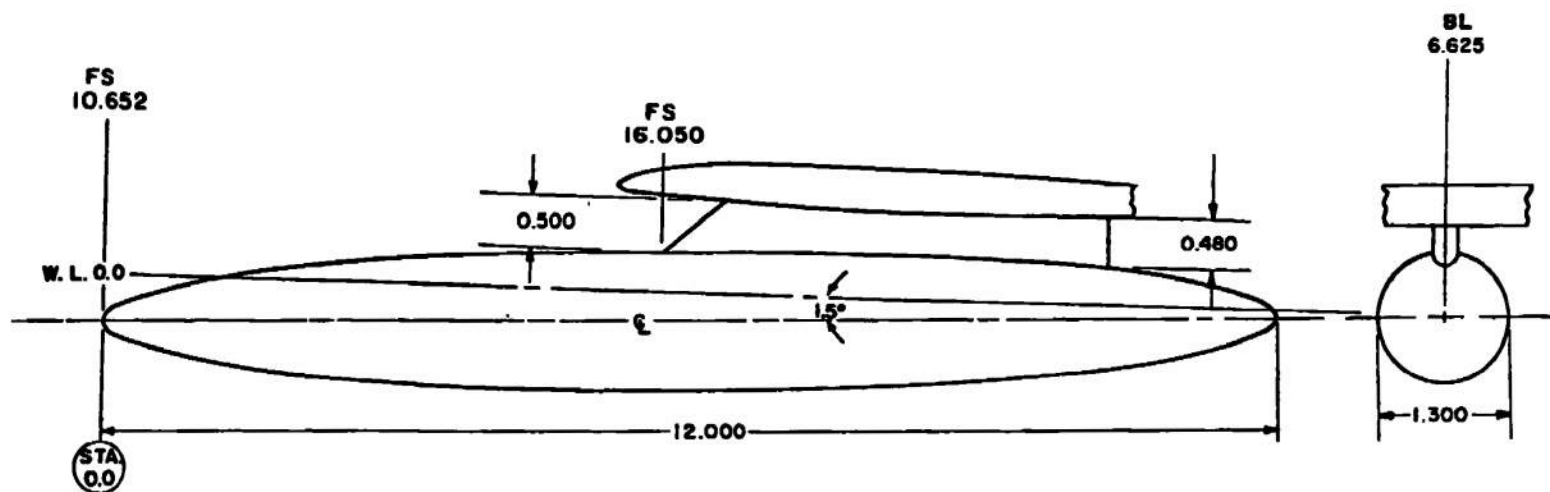
Figure 4. Details of the F-4C pylon models.



ALL DIMENSIONS IN INCHES

	INBOARD	CENTER	OUTBOARD
B	1.030	1.030	0.515
C	4.580	4.850	4.437
D	1.630	1.905	2.008
E	0.575	0.575	0.513
F	0.950	0.950	0.750
G	1.350	1.350	1.150

Figure 5. Details of the A-7D pylon models.



NOTE: MODEL STATIONS AND
DIMENSIONS IN INCHES

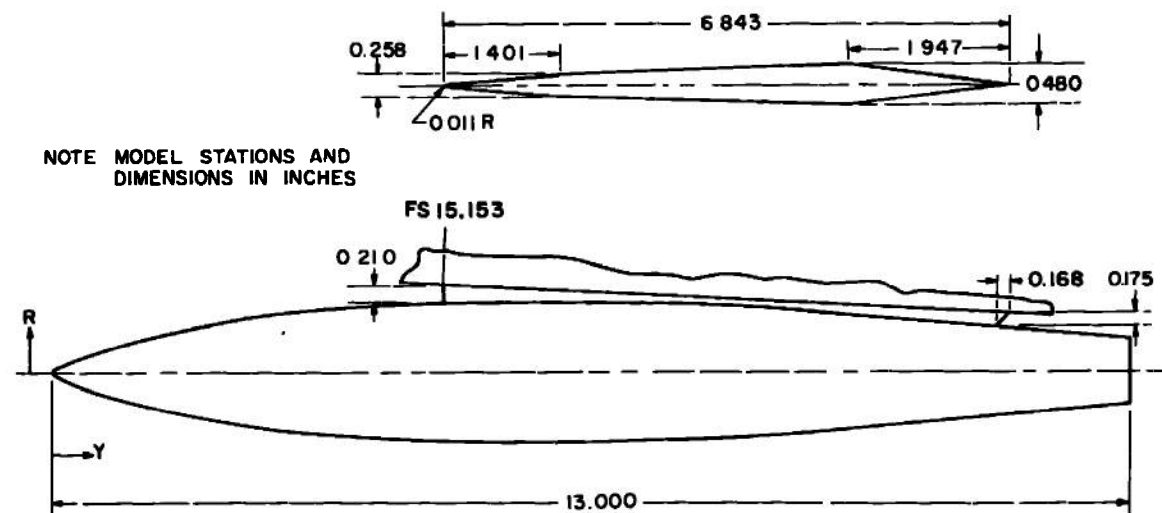
BODY CONTOUR, TYPICAL BOTH ENDS

STATION	BODY DIAM	STATION	BODY DIAM
0.000	0.000	2.500	1.116
0.025	0.100	2.750	1.156
0.050	0.144	3.000	1.190
0.150	0.258	3.250	1.218
0.250	0.340	3.500	1.242
0.500	0.498	3.750	1.260
0.750	0.622	4.000	1.274
1.000	0.724	4.250	1.286
1.250	0.812	4.500	1.294
1.500	0.890	4.750	1.298
1.750	0.958	5.000	1.300
2.000	1.016	6.000	1.300
2.250	1.070		

a. 370-gal

Figure 6. Details of the F-4C fuel tank models.

BODY CONTOUR			
Y	R	Y	R
0.000	0.000	4.250	0.827
0.050	0.049	4.500	0.838
0.100	0.077	4.750	0.847
0.150	0.101	5.000	0.854
0.200	0.122	5.250	0.859
0.250	0.143	5.500	0.860
0.500	0.232	6.250	0.860
0.750	0.308	6.500	0.859
1.000	0.376	6.750	0.856
1.250	0.438	7.000	0.852
1.500	0.494	7.250	0.846
1.750	0.546	7.500	0.839
2.000	0.593	7.750	0.830
2.250	0.637	8.000	0.820
2.500	0.679	8.250	0.809
2.750	0.713	8.500	0.796
3.000	0.740	8.750	0.781
3.250	0.762	9.000	0.765
3.500	0.782	9.250	0.745
3.750	0.799	3.000	0.400
4.000	0.814		



b. 600-gal
Figure 6. Concluded.

ORDINATES

MODEL STA "X"	RADIUS "R"	MODEL STA "X"	RADIUS "R"
0 000	0.0000	2 250	0 5531
0 060	0 0000	2 500	0 5777
0 100	0 0511	2.750	0 5989
0.150	0 0751		CONSTANT SLOPE
0.200	0 0981	3.450	0 6625
0 250	0 1203		CONSTANT DIAM
0.300	0.1415	6.638	0 6625
0.350	0 1619		CONSTANT SLOPE
0.400	0 1815	7.713	0.5680
0.450	0 2003	7.763	0 5637
0.500	0.2183	8.013	0 5409
0.550	0 2355	8.263	0 5162
0.600	0 2521	8.513	0 4899
0.650	0.2680	8.763	0 4620
0.700	0.2833	9.013	0 4327
0.750	0.2979	9.113	0.4206
0.800	0.3119		CONSTANT SLOPE
0.850	0.3253	10.900	0.1815
0.900	0.3383	10.950	0.1733
1.000	0 3628	11.000	0 1646
1.250	0.4153	11 100	0 1441
1 500	0.4587	11 200	0 1170
1.750	0.4950	11 300	0.0725
2.000	0.5260	11 350	0 0000

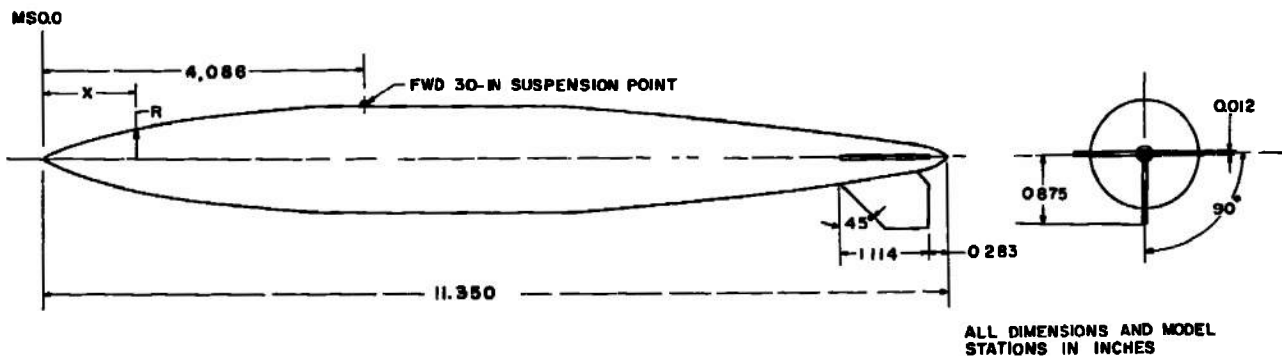
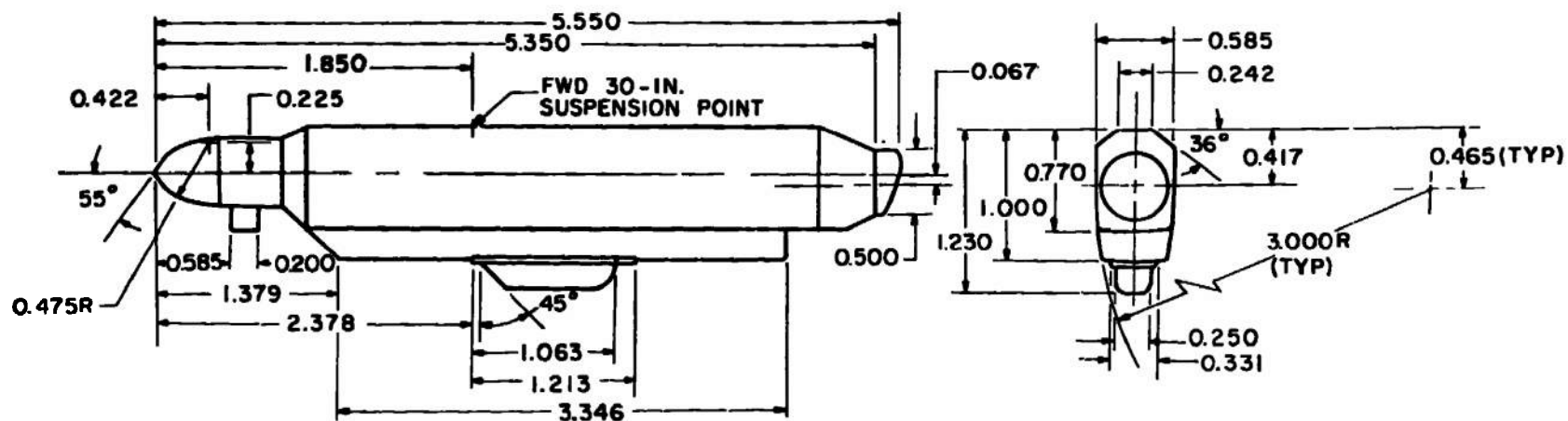


Figure 7. Details of the A-7D 300-gal fuel tank model.



ALL DIMENSIONS IN INCHES

Figure 8. Details of the ALQ-131 terminal-threat pod model.

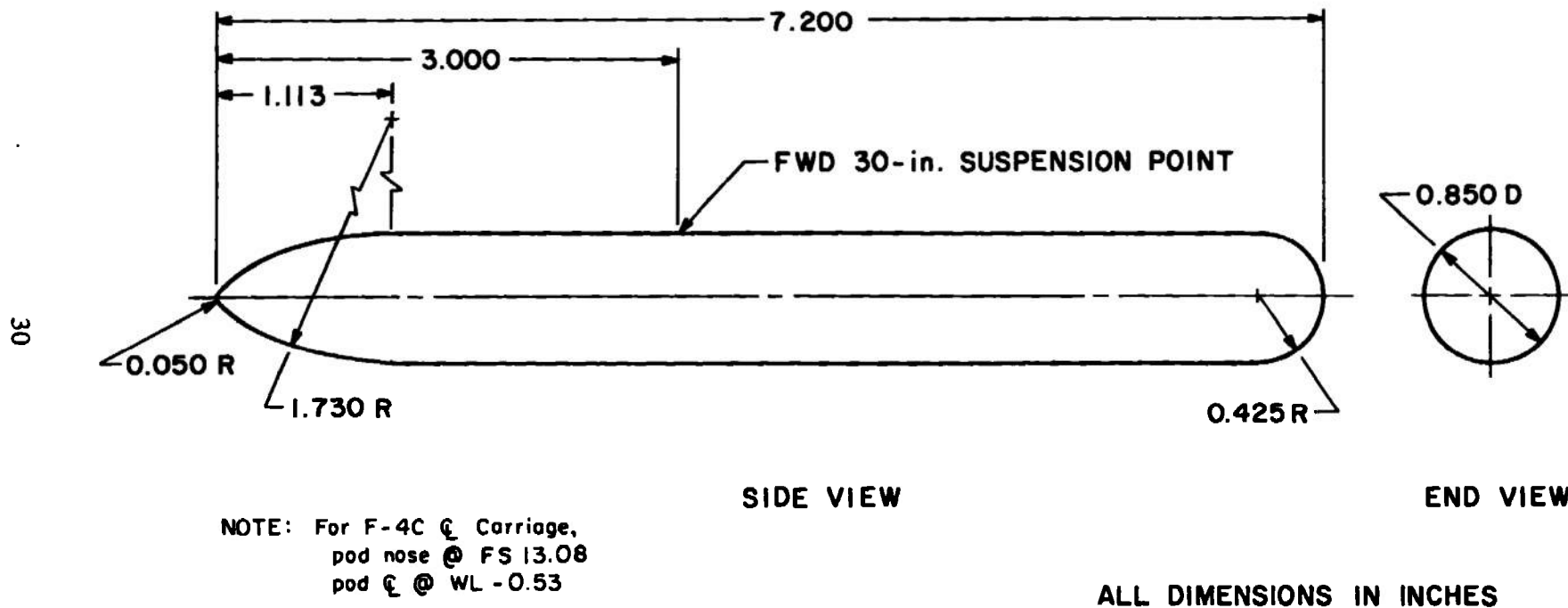
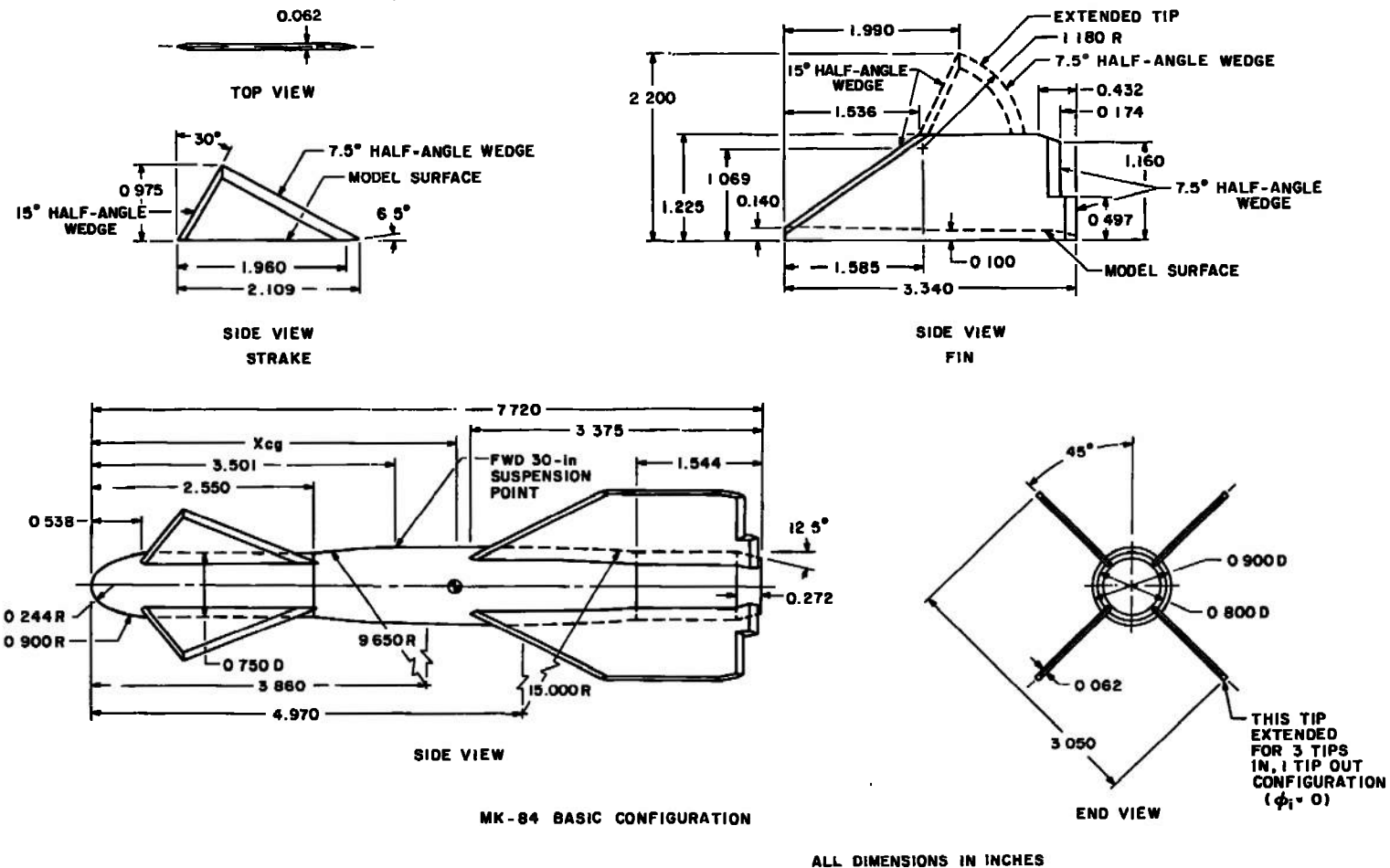
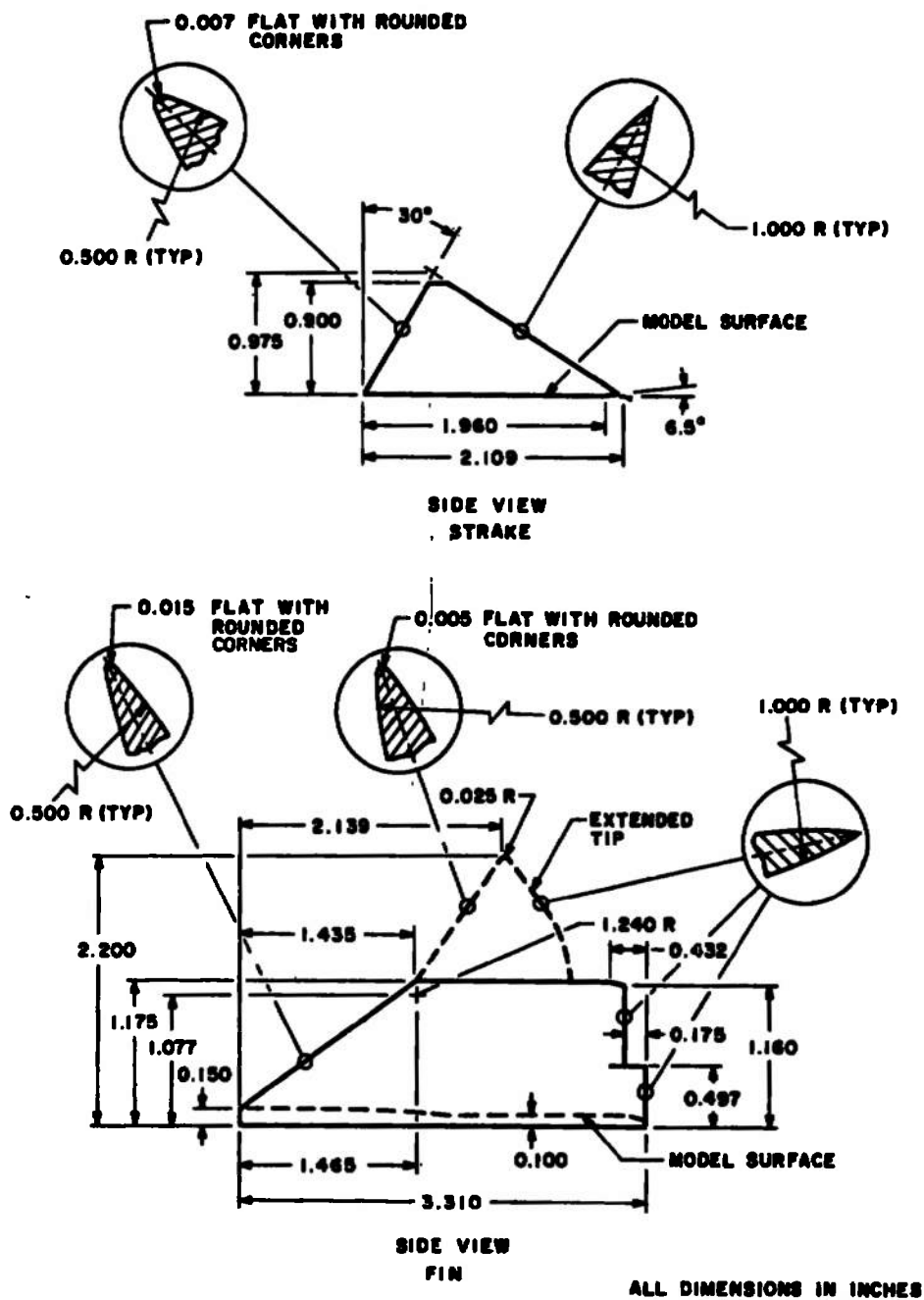


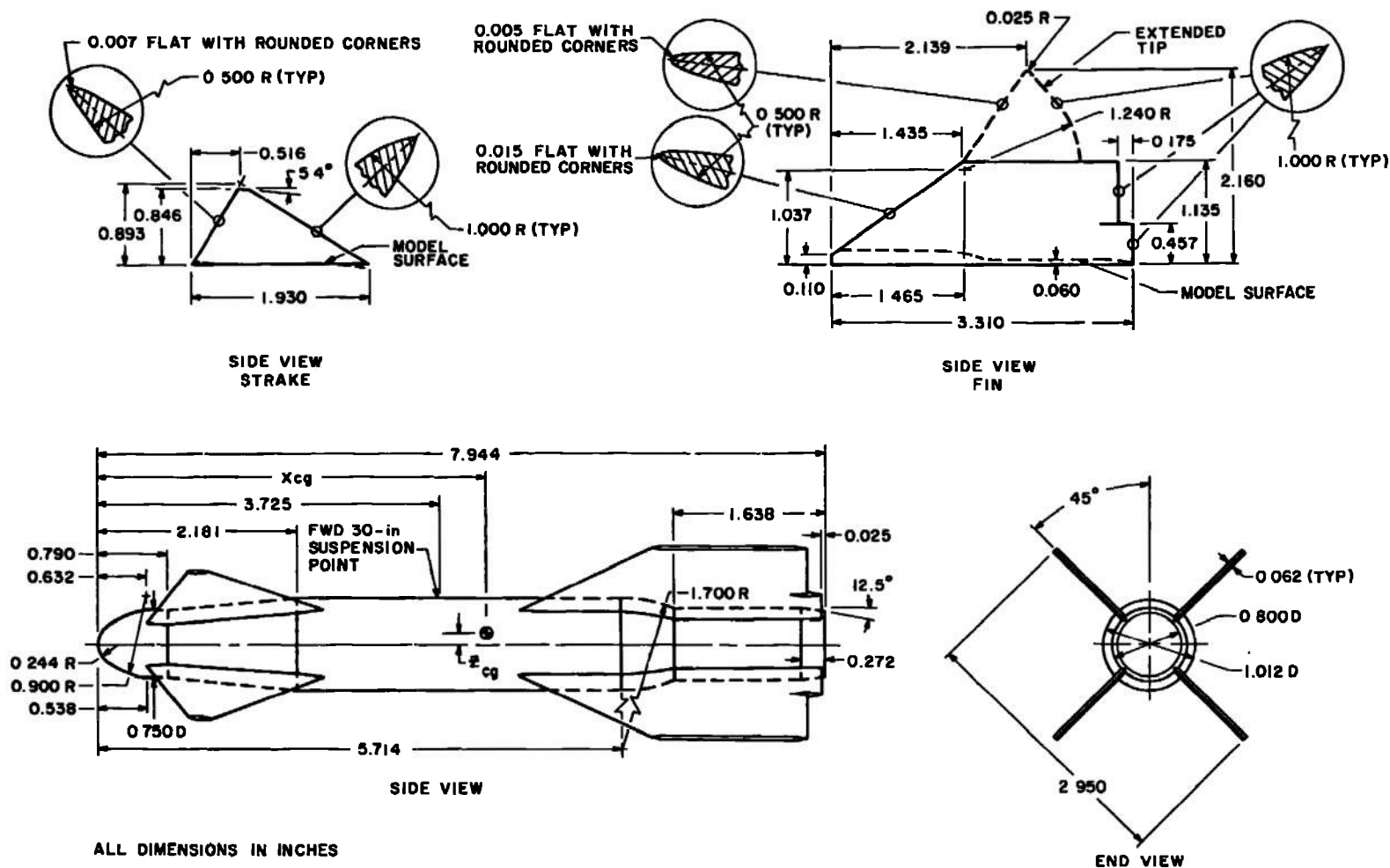
Figure 9. Details of the data link pod model.



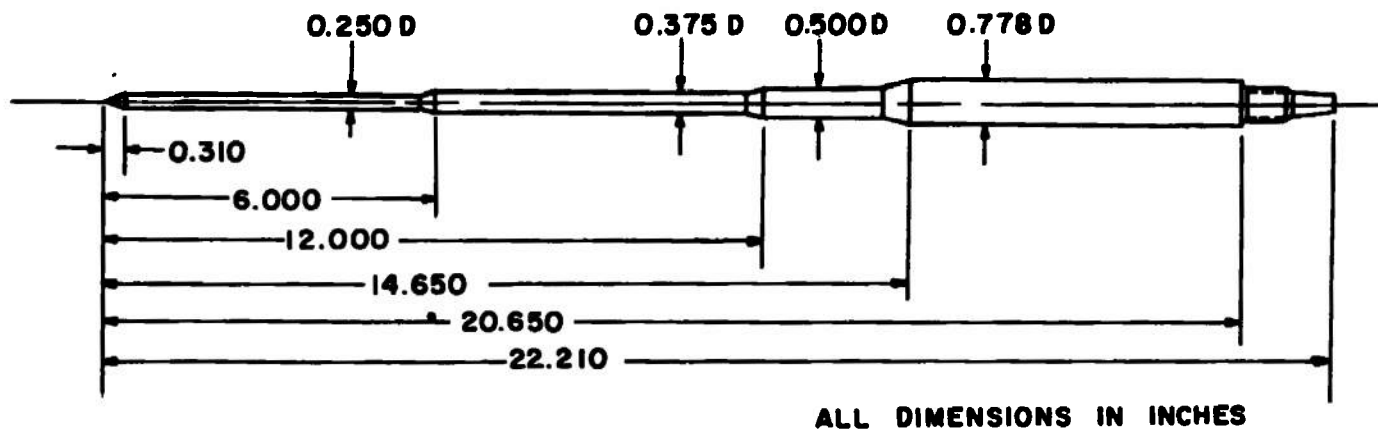
a. MK-84 basic configuration
 Figure 10. Details of the Super HOBOS models.



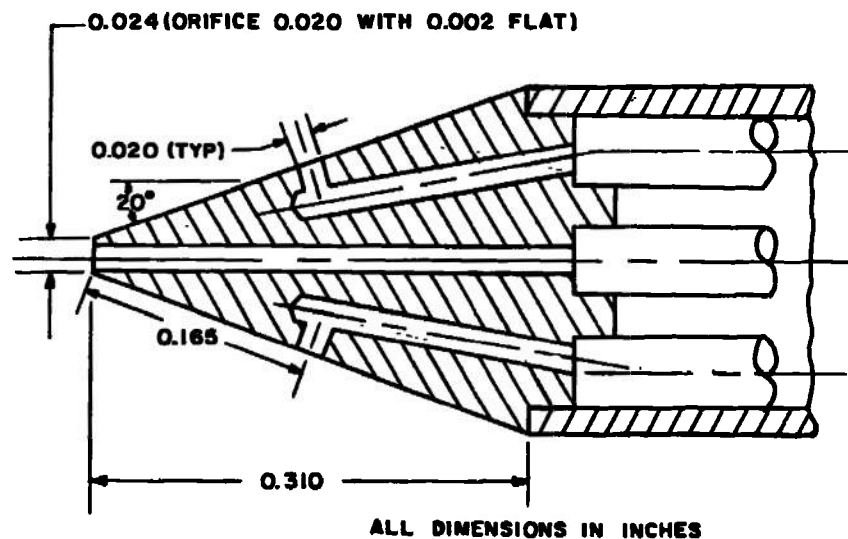
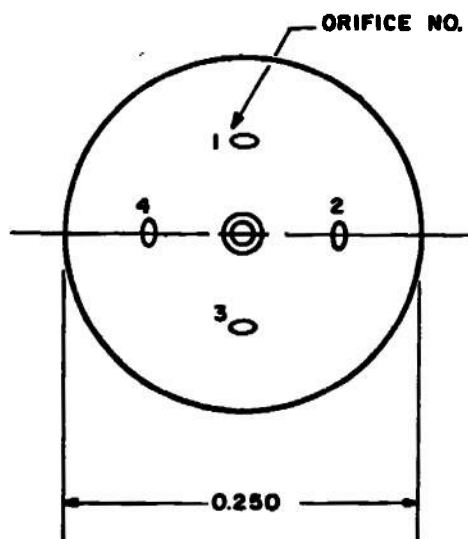
b. MK-84 modified fins and strakes
Figure 10. Continued.



c. SUU-54 basic configuration
Figure 10. Concluded.



a. Basic probe configuration



b. Probe tip

Figure 11. Details of the 40-deg conical probe.

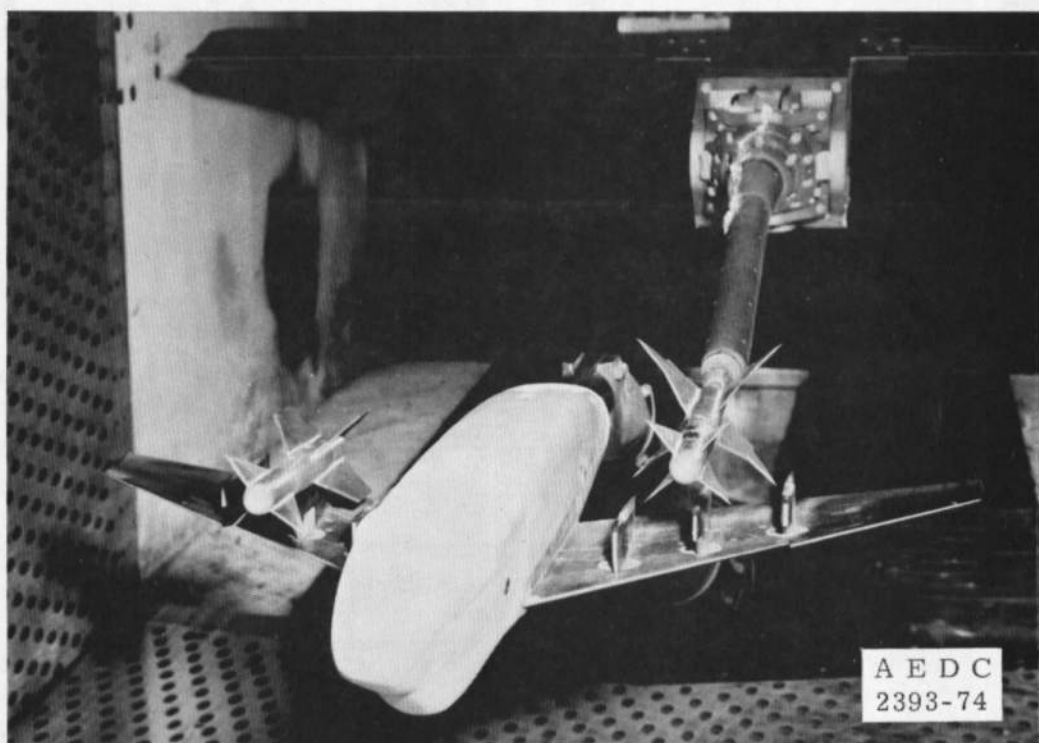
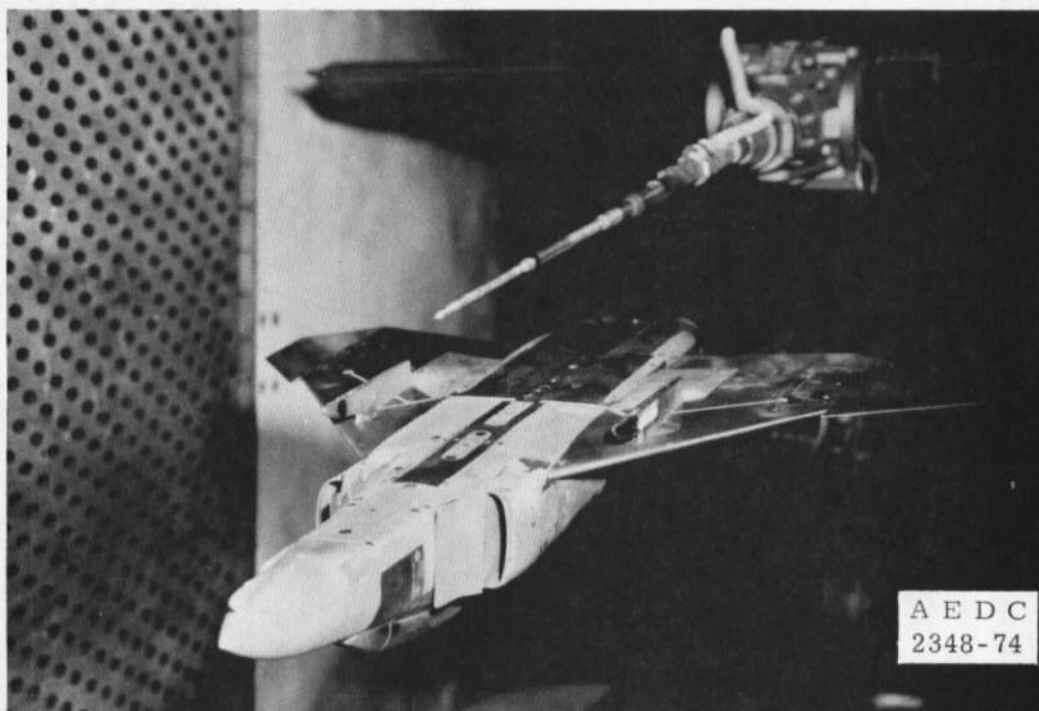
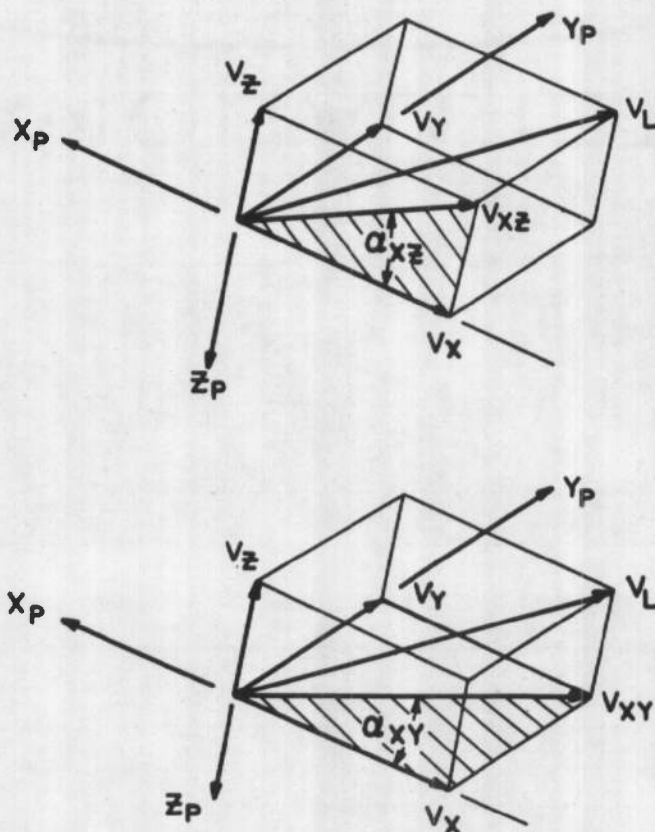


Figure 12. Tunnel installation photographs showing parent aircraft, probe, store, and CTS.

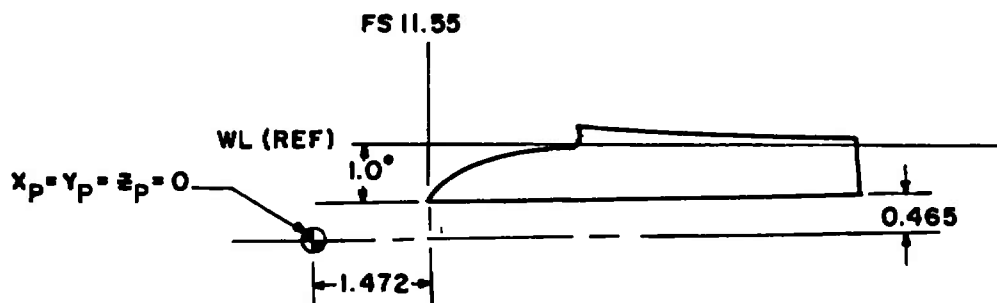
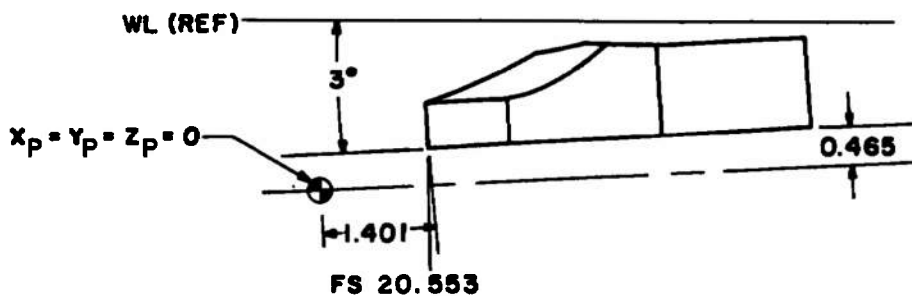


Note:

- 1) $+\alpha_{xz}$ indicates upwash with respect to probe longitudinal axis.
- 2) $+\alpha_{xy}$ indicates sidewash outboard on the right wing and inboard on the left wing with respect to the probe longitudinal axis.

a. Coordinate system

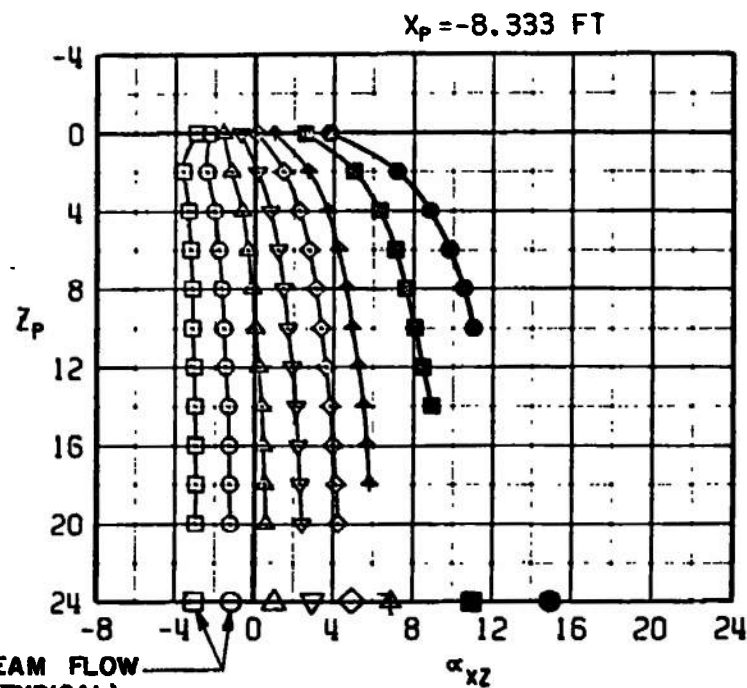
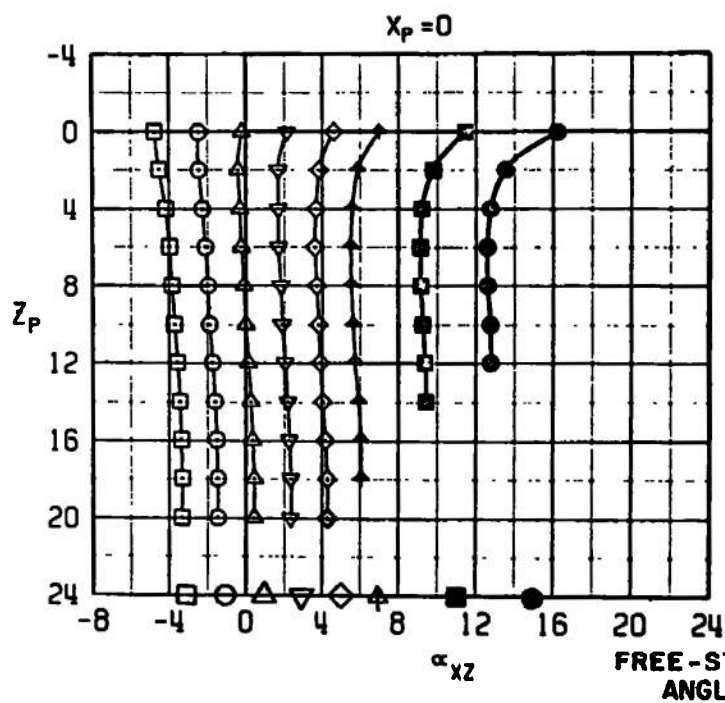
Figure 13. Axis system defining directions and angles for flow-field measurements.

**F-4 INBOARD PYLON****A-7 CENTER PYLON****ALL DIMENSIONS IN INCHES**

Note: For F-4 \mathcal{C} surveys, $x_p = y_p = z_p = 0$ at FS 13.08,
WL -0.53

b. Origins
Figure 13. Concluded.

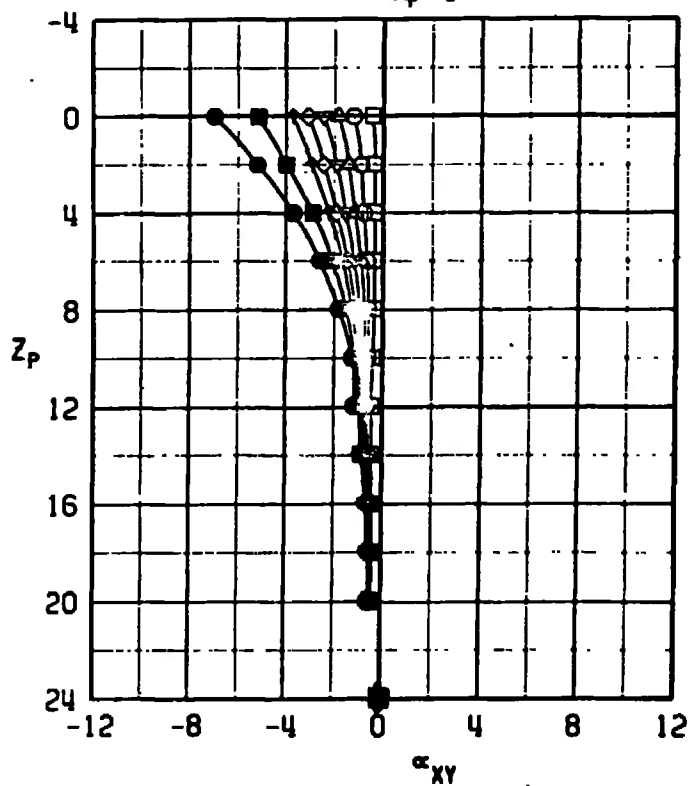
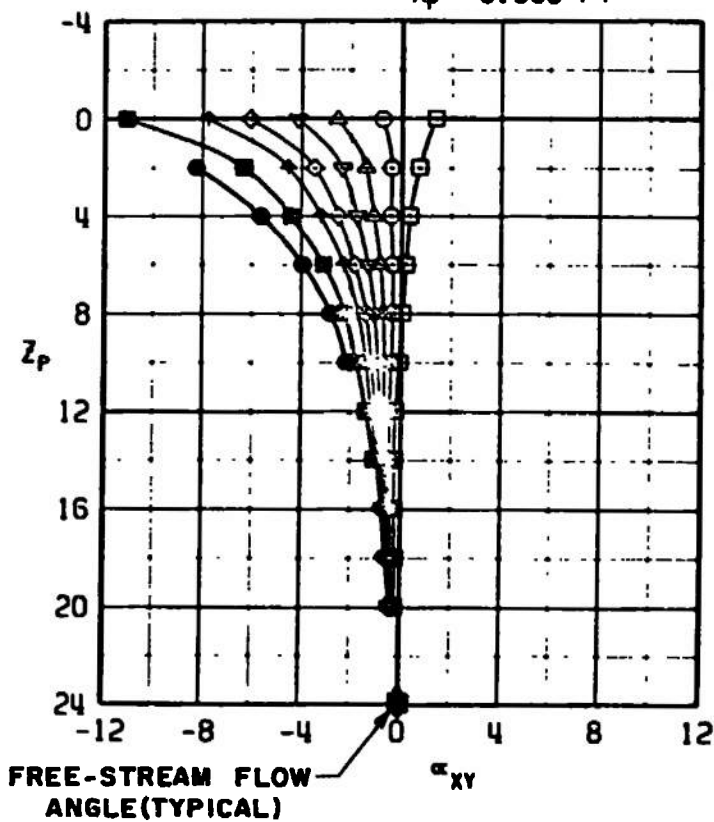
SYMBOL	α	β	M_∞	A/C	PYLON
□	-2	0	0.65	F-4C	LW INBD
○	0	0	0.65	F-4C	LW INBD
△	2	0	0.65	F-4C	LW INBD
▽	4	0	0.65	F-4C	LW INBD
◇	6	0	0.65	F-4C	LW INBD
↑	8	0	0.65	F-4C	LW INBD
■	12	0	0.65	F-4C	LW INBD
●	16	0	0.65	F-4C	LW INBD



a. $M_\infty = 0.65$, upwash

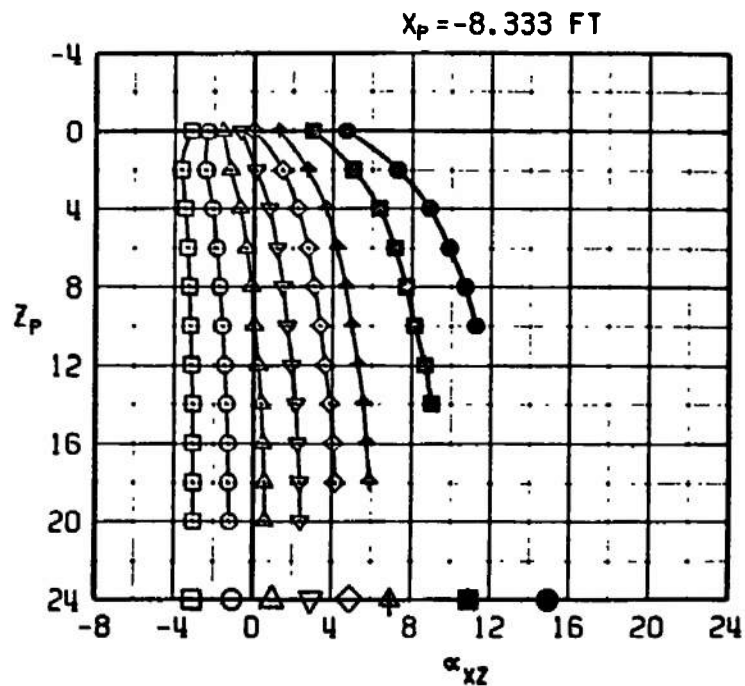
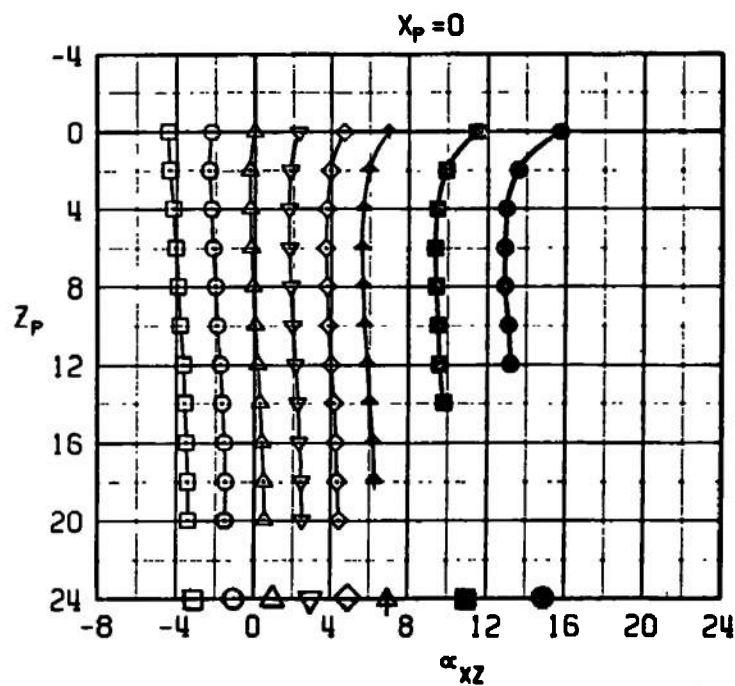
Figure 14. Flow-field measurements beneath the F-4C left-wing inboard pylon, configuration 43.

SYMBOL	α	β	M_∞	A/C	PYLON
□	-2	0	0.65	F-4C	LW INBD
○	0	0	0.65	F-4C	LW INBD
△	2	0	0.65	F-4C	LW INBD
▽	4	0	0.65	F-4C	LW INBD
◇	6	0	0.65	F-4C	LW INBD
+	8	0	0.65	F-4C	LW INBD
■	12	0	0.65	F-4C	LW INBD
●	16	0	0.65	F-4C	LW INBD

 $x_p = 0$  $x_p = -8.333$ FT

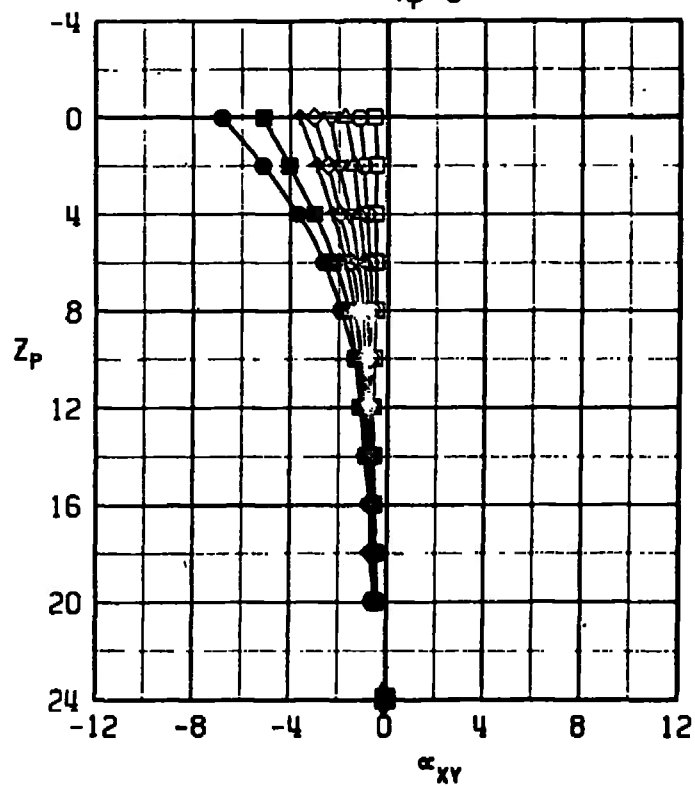
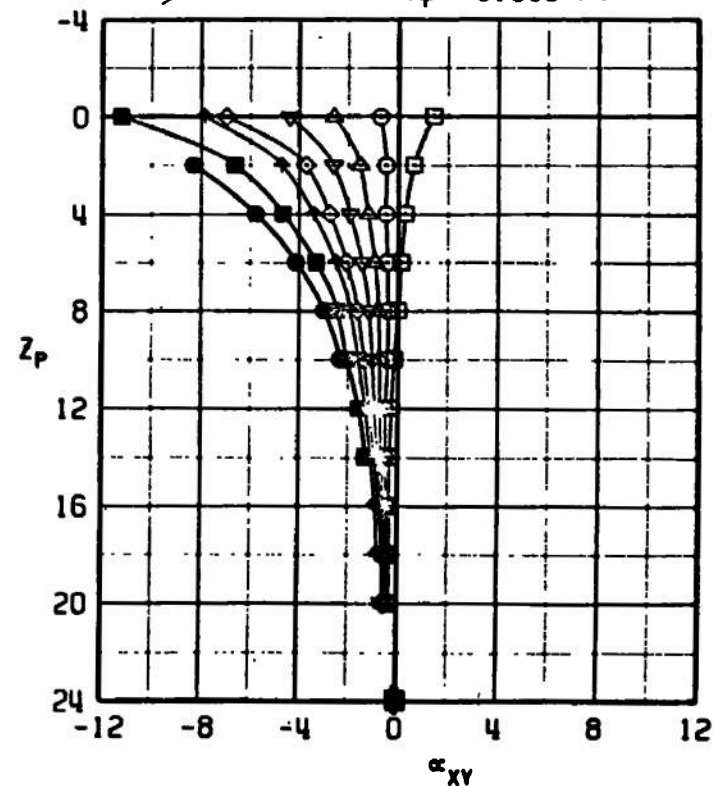
b. $M_\infty = 0.65$, sidewash
Figure 14. Continued.

SYMBOL	α	β	M_∞	R/C	PYLON
□	-2	0	0.80	F-4C	LW IN80
○	0	0	0.80	F-4C	LW IN80
△	2	0	0.80	F-4C	LW IN80
▽	4	0	0.80	F-4C	LW IN80
◇	6	0	0.80	F-4C	LW IN80
↑	8	0	0.80	F-4C	LW IN80
■	12	0	0.80	F-4C	LW IN80
●	16	0	0.80	F-4C	LW IN80



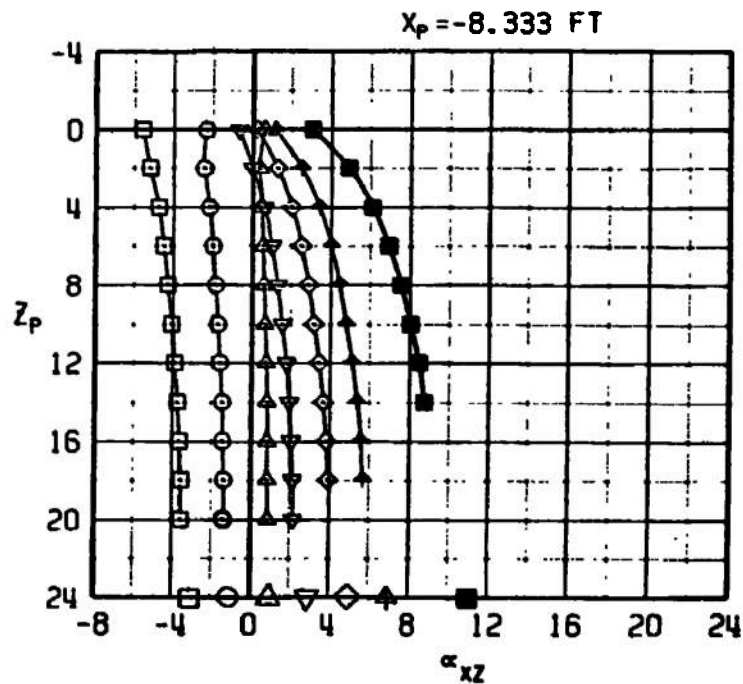
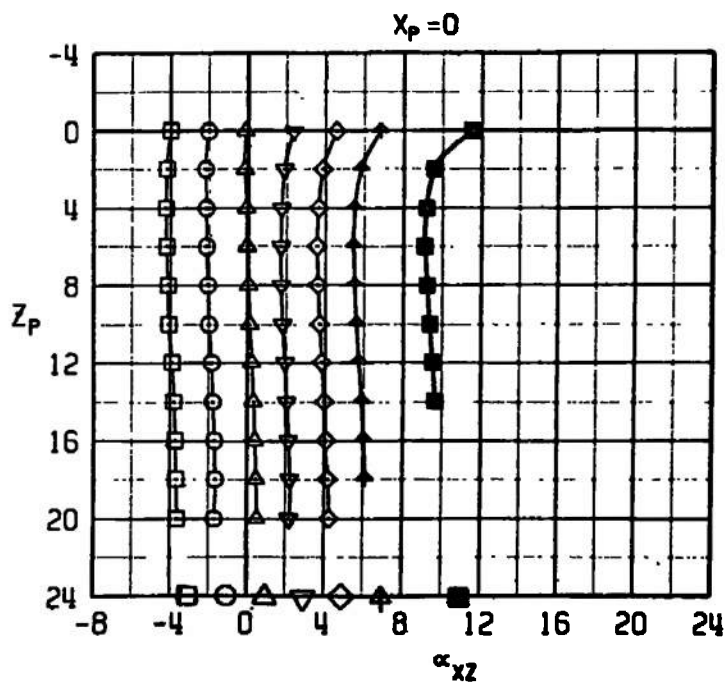
c. $M_\infty = 0.80$, upwash
Figure 14. Continued.

SYMBOL	α	β	M_{∞}	A/C	PYLON
□	-2	0	0.80	F-4C	LW INBD
○	0	0	0.80	F-4C	LW INBD
△	2	0	0.80	F-4C	LW INBD
▽	4	0	0.80	F-4C	LW INBD
◇	6	0	0.80	F-4C	LW INBD
+	8	0	0.80	F-4C	LW INBD
■	12	0	0.80	F-4C	LW INBD
●	16	0	0.80	F-4C	LW INBD

 $x_p = 0$  $x_p = -8.333 \text{ FT}$ 

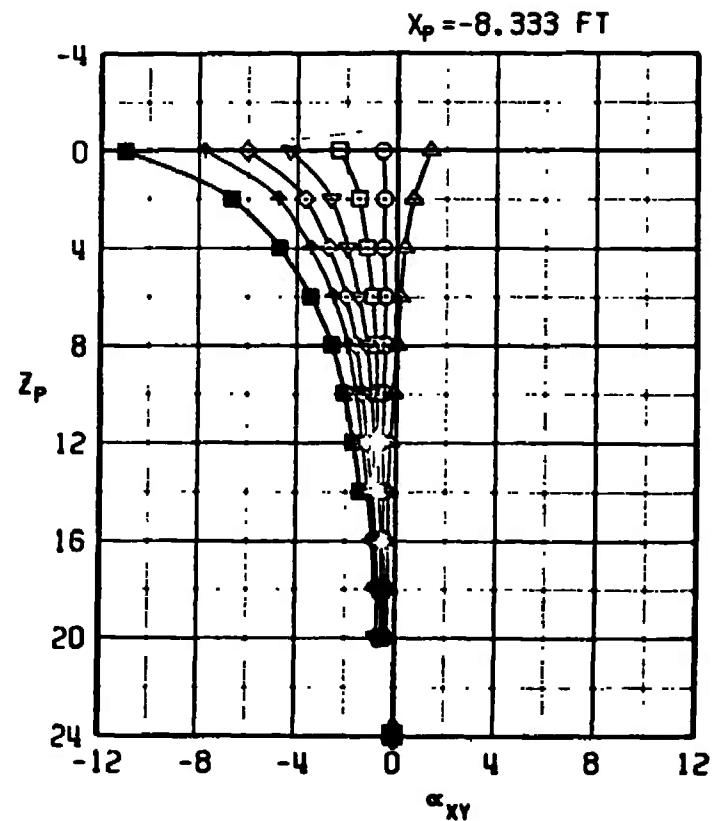
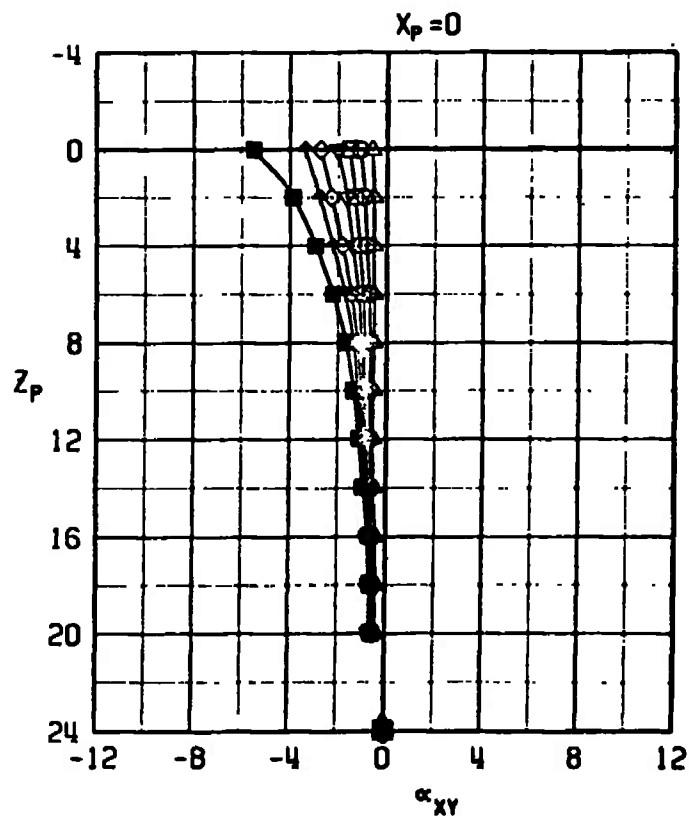
d. $M_{\infty} = 0.80$, sidewash
Figure 14. Continued.

SYMBOL	α	β	M_w	A/C	PYLON
□	-2	0	0.90	F-4C	LW INBD
○	0	0	0.90	F-4C	LW INBD
△	2	0	0.90	F-4C	LW INBD
▽	4	0	0.90	F-4C	LW INBD
◇	6	0	0.90	F-4C	LW INBD
+	8	0	0.90	F-4C	LW INBD
■	12	0	0.90	F-4C	LW INBD



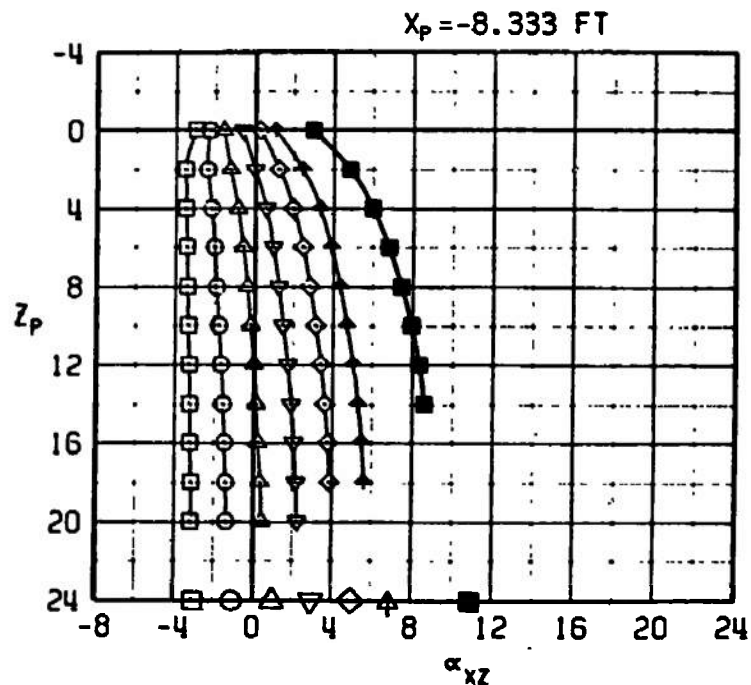
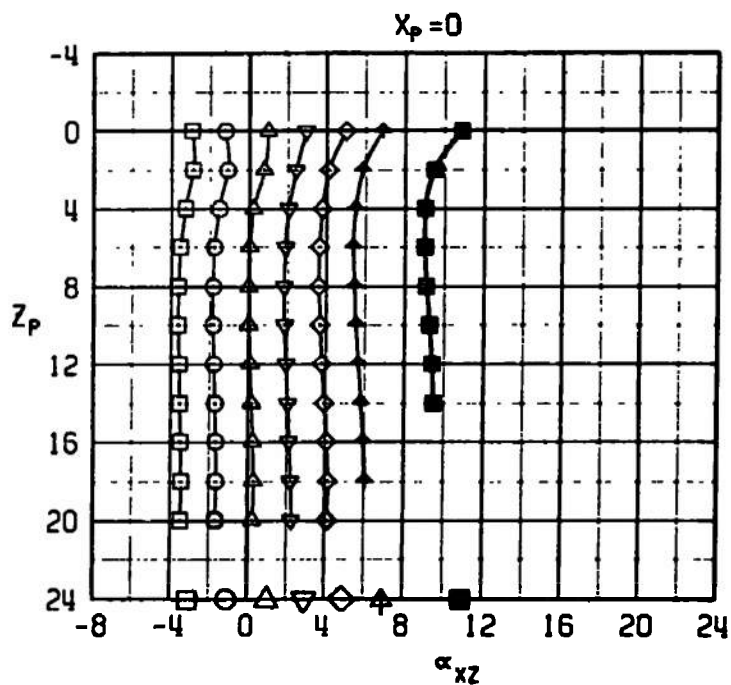
e. $M_w = 0.90$, upwash
Figure 14. Continued.

SYMBOL	α	β	M_u	A/C	PYLON
□	-2	0	0.90	F-4C	LW INBD
○	0	0	0.90	F-4C	LW INBD
△	2	0	0.90	F-4C	LW INBD
▽	4	0	0.90	F-4C	LW INBD
◇	6	0	0.90	F-4C	LW INBD
+	8	0	0.90	F-4C	LW INBD
■	12	0	0.90	F-4C	LW INBD



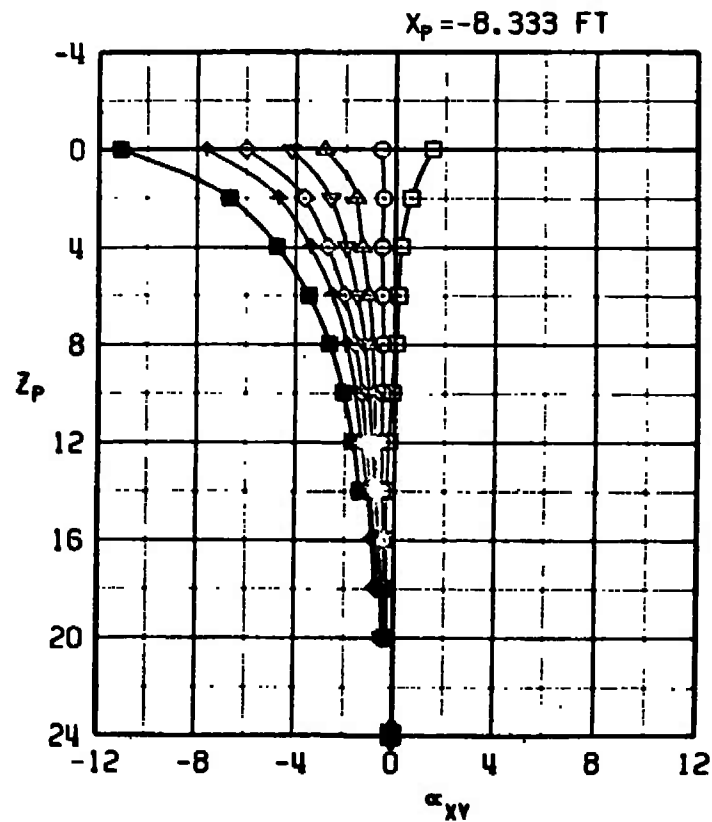
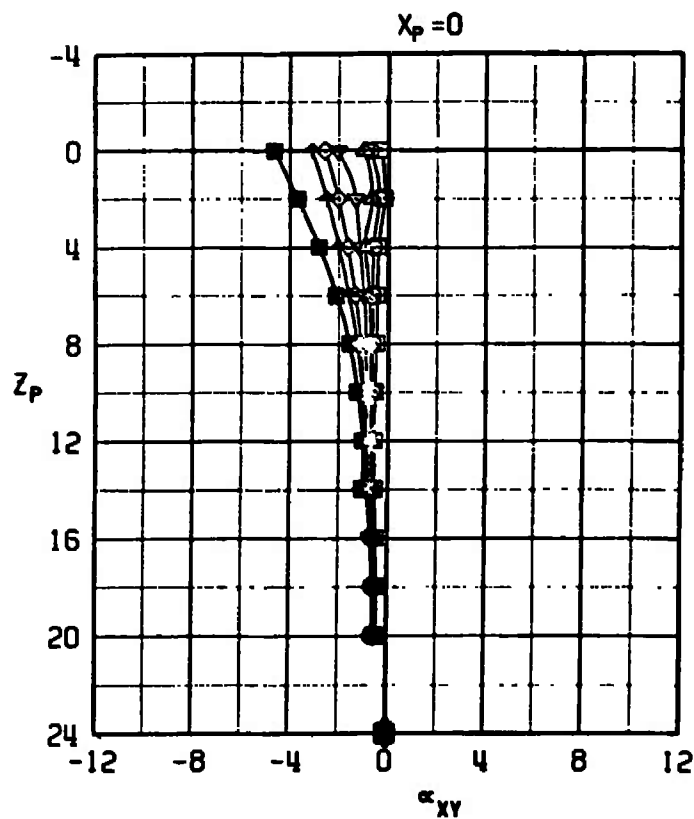
f. $M_u = 0.90$, sidewash
Figure 14. Continued.

SYMBOL	α	β	M_∞	A/C	PYLON
□	-2	0	0.95	F-4C	LW INBD
○	0	0	0.95	F-4C	LW INBD
△	2	0	0.95	F-4C	LW INBD
▽	4	0	0.95	F-4C	LW INBD
◇	6	0	0.95	F-4C	LW INBD
↑	8	0	0.95	F-4C	LW INBD
■	12	0	0.95	F-4C	LW INBD



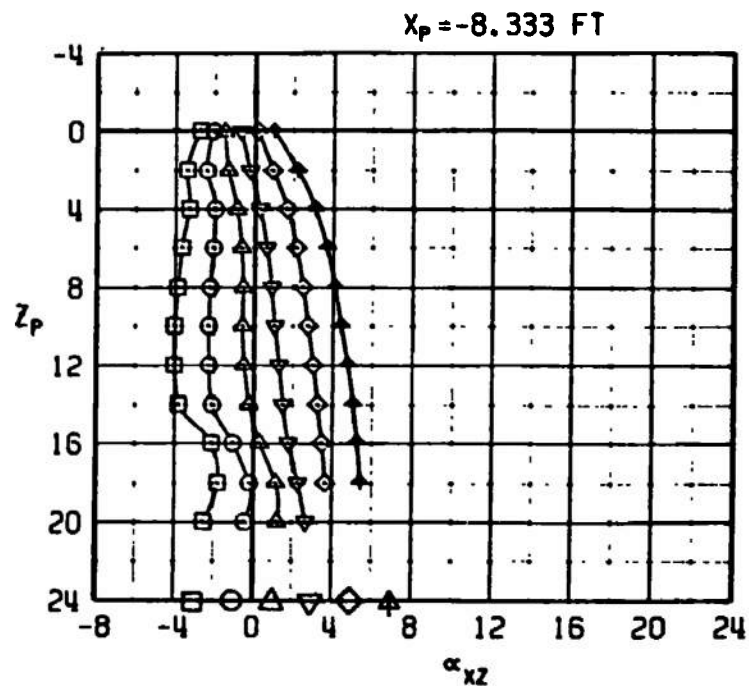
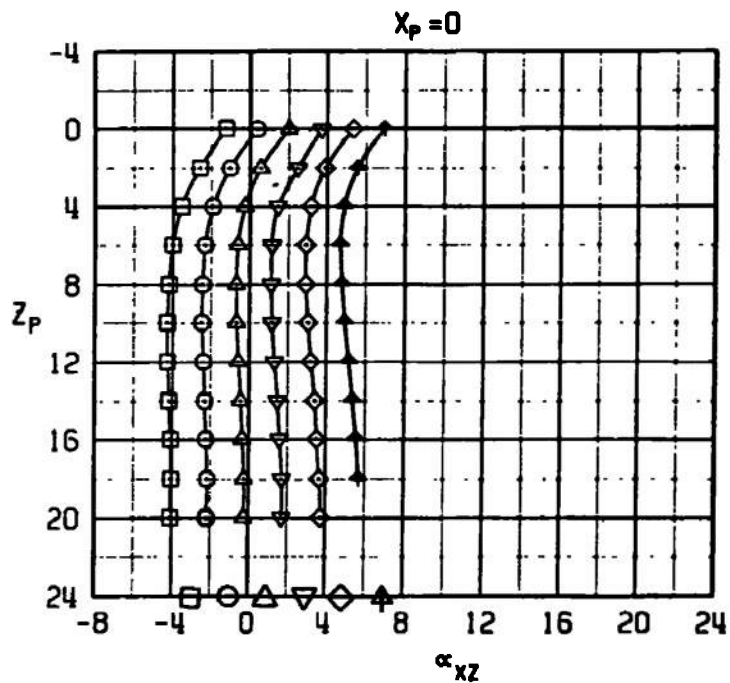
g. $M_\infty = 0.95$, upwash
Figure 14. Continued.

SYMBOL	α	β	M_{∞}	A/C	PYLON
□	-2	0	0.95	F-4C	LW INBD
○	0	0	0.95	F-4C	LW INBD
△	2	0	0.95	F-4C	LW INBD
▽	4	0	0.95	F-4C	LW INBD
◇	6	0	0.95	F-4C	LW INBD
+	8	0	0.95	F-4C	LW INBD
■	12	0	0.95	F-4C	LW INBD



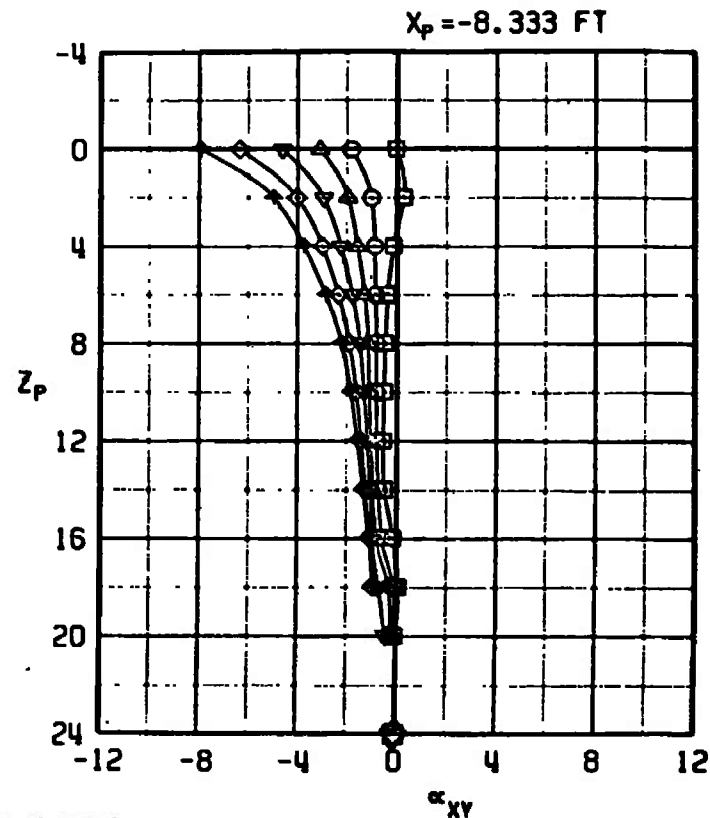
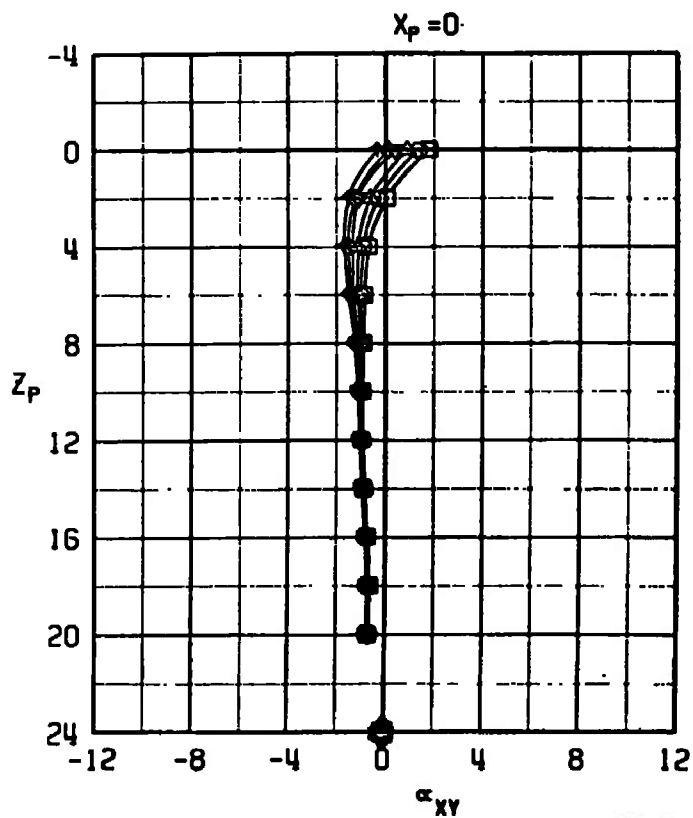
h. $M_{\infty} = 0.95$, sidewash
Figure 14. Continued.

SYMBOL	α	β	M_∞	A/C	PYLON
□	-2	0	1.05	F-4C	LW INBD
○	0	0	1.05	F-4C	LW INBD
△	2	0	1.05	F-4C	LW INBD
▽	4	0	1.05	F-4C	LW INBD
◇	6	0	1.05	F-4C	LW INBD
↑	8	0	1.05	F-4C	LW INBD



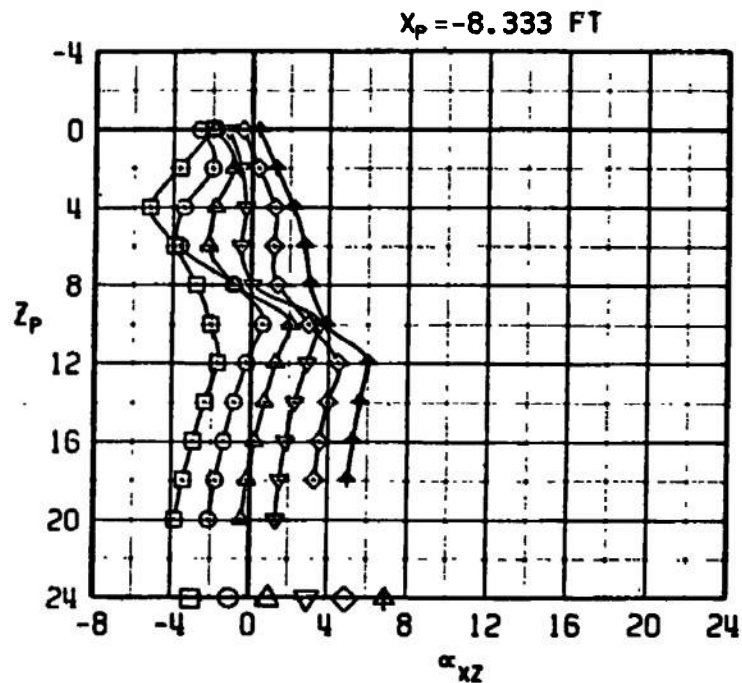
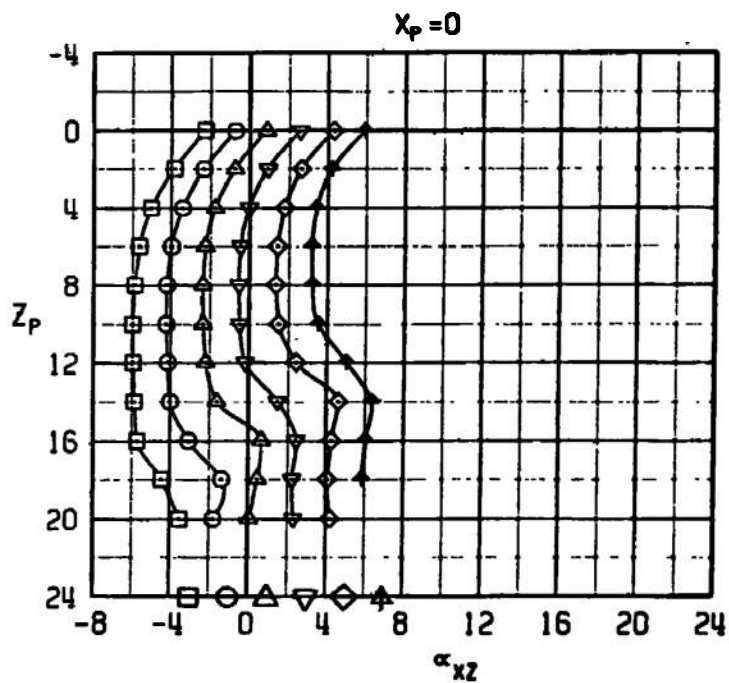
i. $M_\infty = 1.05$, upwash
Figure 14. Continued.

SYMBOL	α	β	M_∞	A/C	PYLON
□	-2	0	1.05	F-4C	LW INBD
○	0	0	1.05	F-4C	LW INBD
△	2	0	1.05	F-4C	LW INBD
▽	4	0	1.05	F-4C	LW INBD
◇	6	0	1.05	F-4C	LW INBD
+	8	0	1.05	F-4C	LW INBD



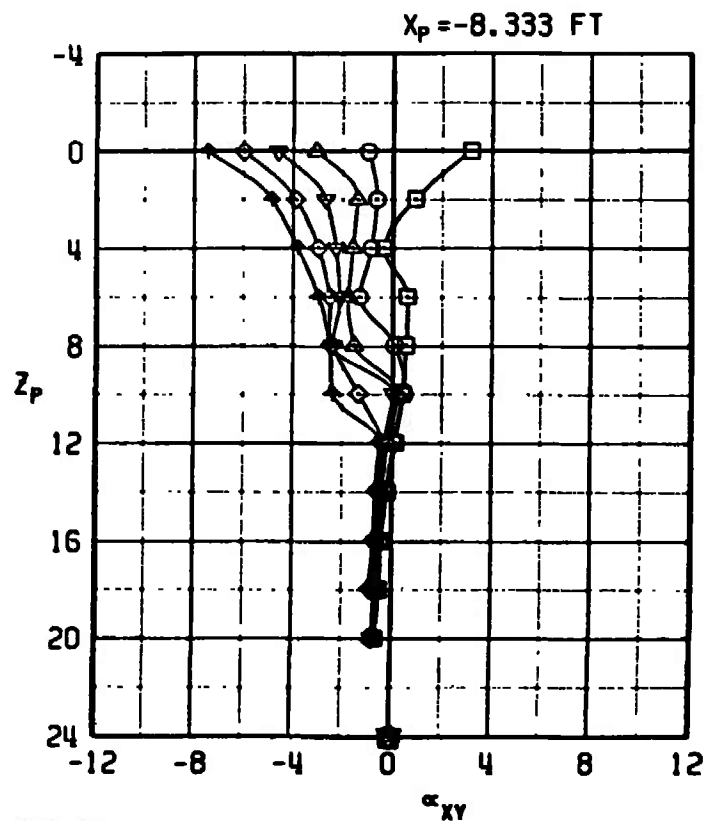
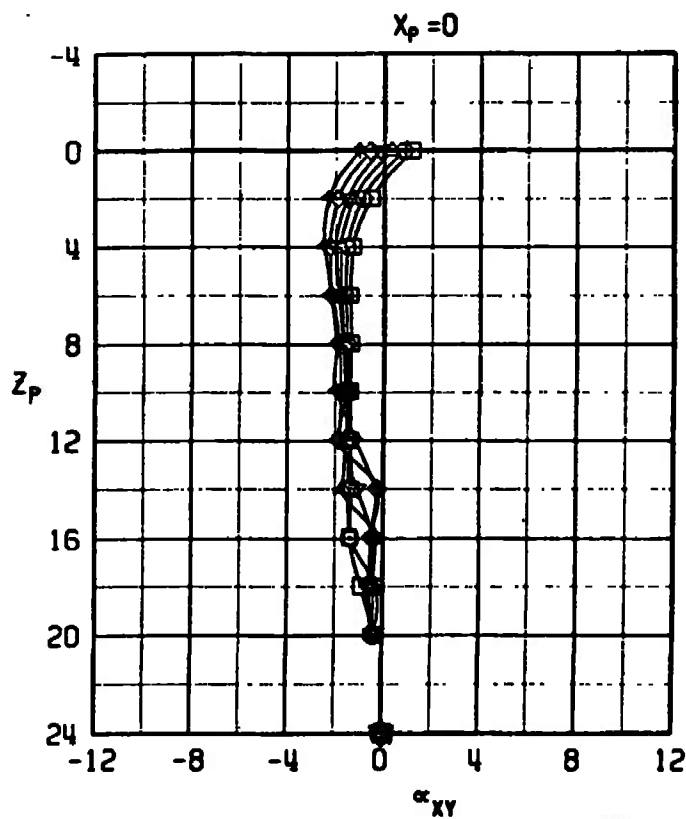
j. $M_\infty = 1.05$, sidewash
Figure 14. Continued.

SYMBOL	α	β	M_∞	R/C	PYLON
□	-2	0	1.20	F-4C	LW INBD
○	0	0	1.20	F-4C	LW INBD
△	2	0	1.20	F-4C	LW INBD
▽	4	0	1.20	F-4C	LW INBD
◇	6	0	1.20	F-4C	LW INBD
↑	8	0	1.20	F-4C	LW INBD



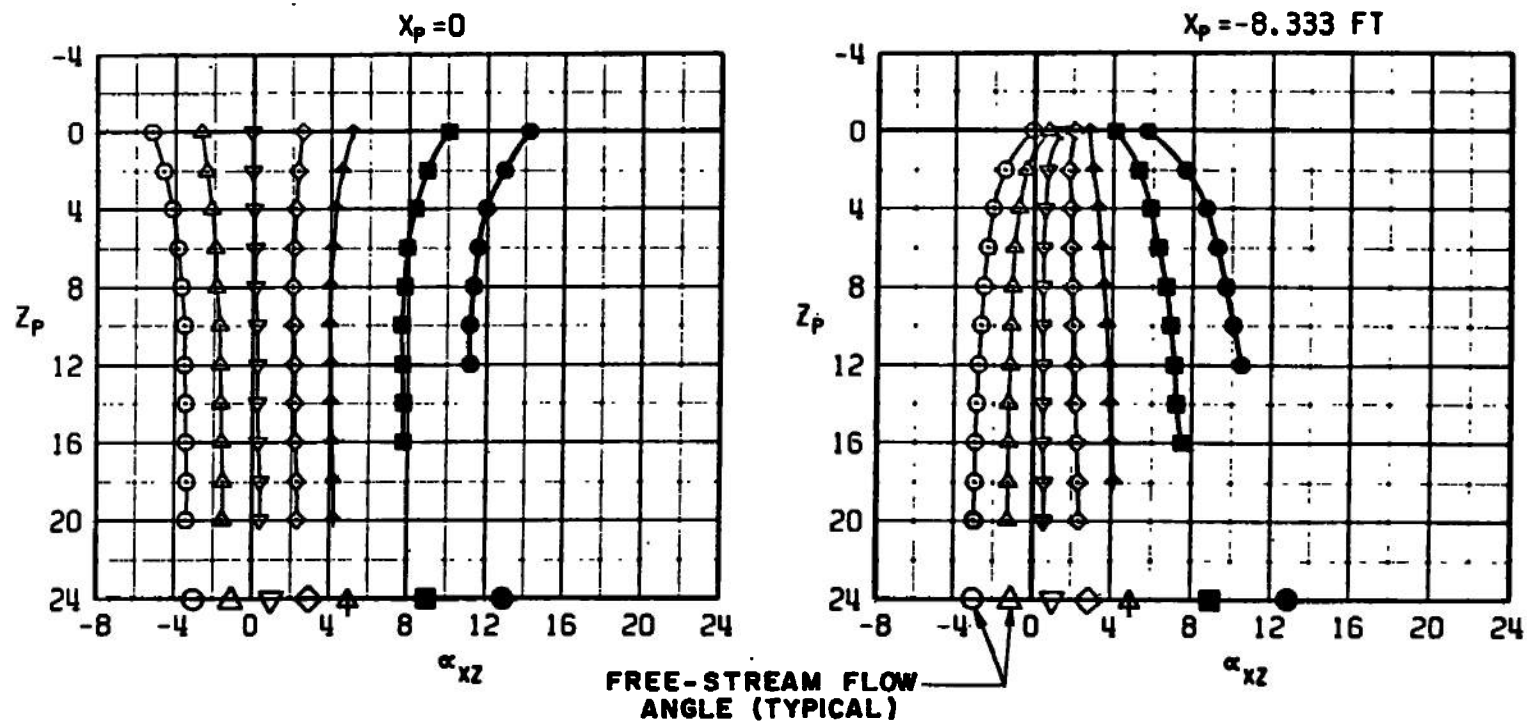
k. $M_\infty = 1.20$, upwash
Figure 14. Continued.

SYMBOL	α	β	M_{∞}	A/C	PYLON
□	-2	0	1.20	F-4C	LW INBD
○	0	0	1.20	F-4C	LW INBD
△	2	0	1.20	F-4C	LW INBD
▽	4	0	1.20	F-4C	LW INBD
◇	6	0	1.20	F-4C	LW INBD
↑	8	0	1.20	F-4C	LW INBD



I. $M_{\infty} = 1.20$, sidewash
Figure 14. Concluded.

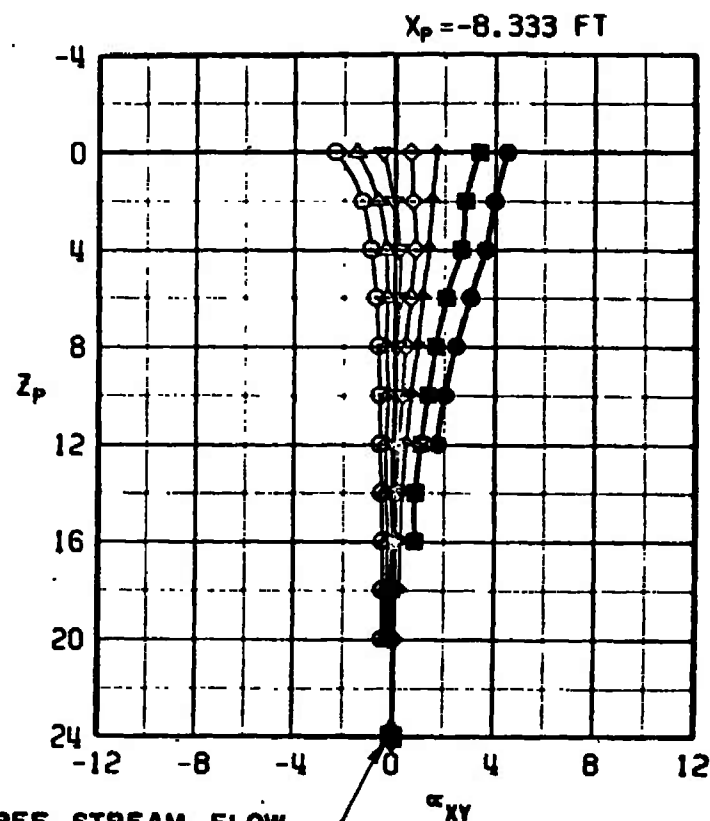
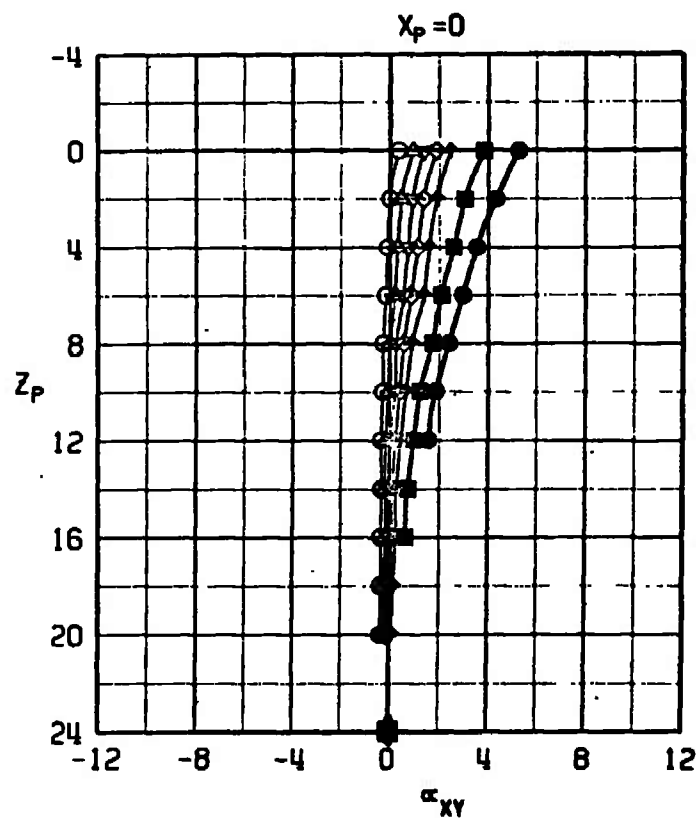
SYMBOL	α	β	M_∞	A/C	PYLON
○	0	0	0.65	A-7D	RW CNTR
△	2	0	0.65	A-7D	RW CNTR
▽	4	0	0.65	A-7D	RW CNTR
◇	6	0	0.65	A-7D	RW CNTR
+	8	0	0.65	A-7D	RW CNTR
■	12	0	0.65	A-7D	RW CNTR
●	16	0	0.65	A-7D	RW CNTR



a. $M_\infty = 0.65$, upwash

Figure 15. Flow-field measurements beneath the A-7D right-wing center pylon, configuration 54.

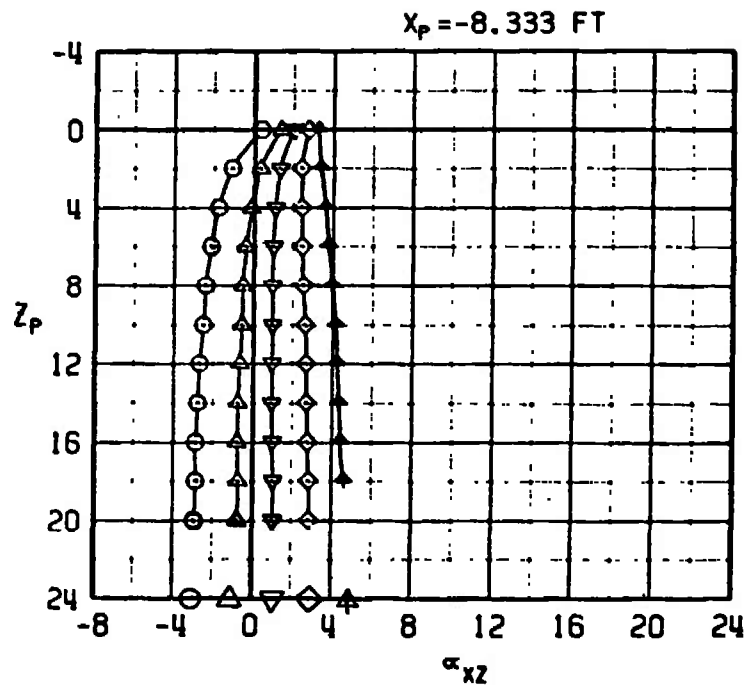
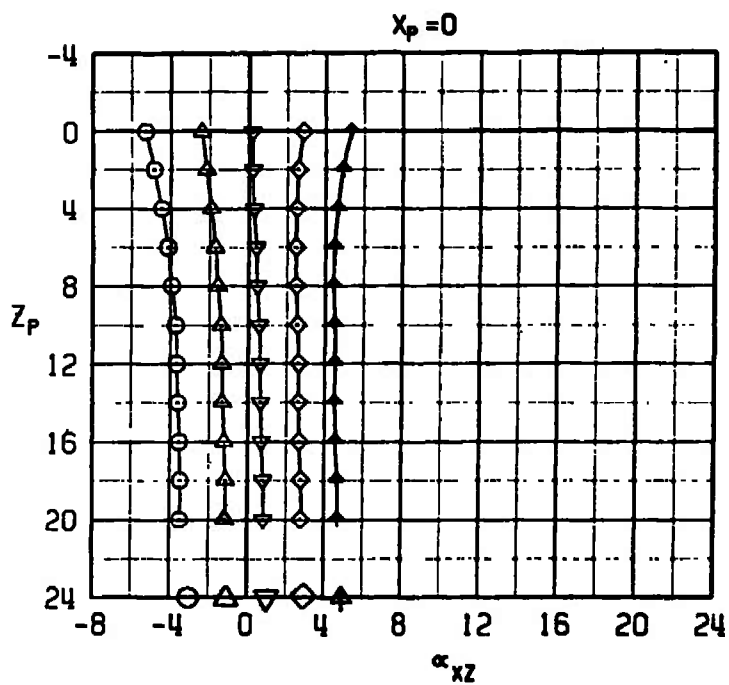
SYMBOL	α	β	M_∞	A/C	PYLON
○	0	0	0.65	A-70	RW CNTR
△	2	0	0.65	A-70	RW CNTR
▽	4	0	0.65	A-70	RW CNTR
◇	6	0	0.65	A-70	RW CNTR
↑	8	0	0.65	A-70	RW CNTR
■	12	0	0.65	A-70	RW CNTR
●	16	0	0.65	A-70	RW CNTR



FREE-STREAM FLOW
ANGLE (TYPICAL)

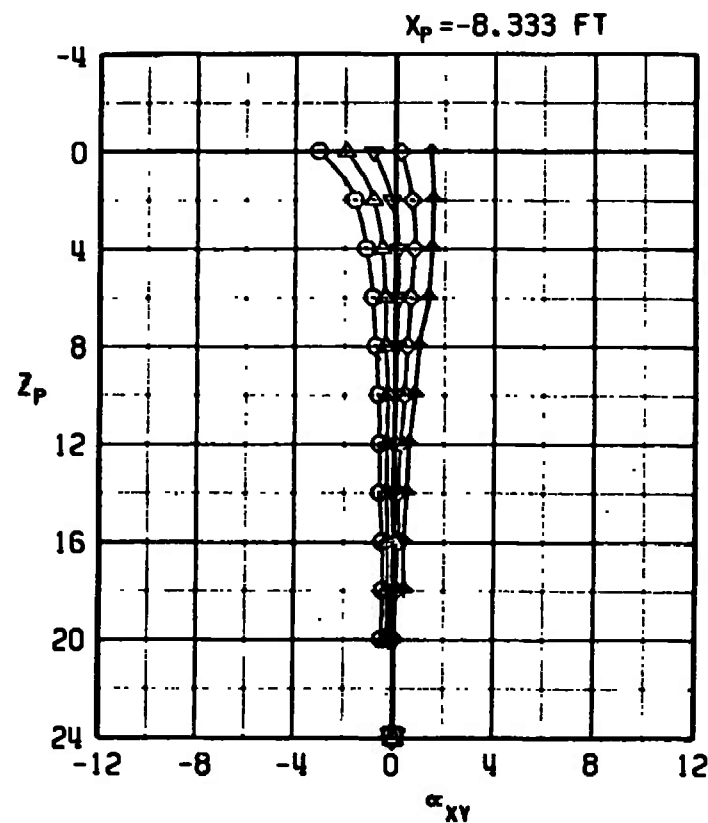
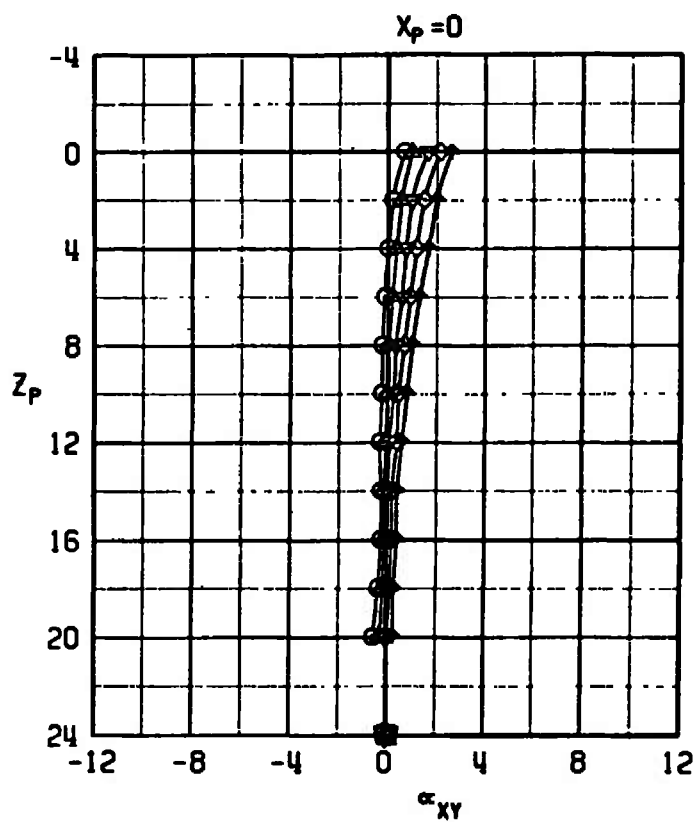
b. $M_\infty = 0.65$, sidewash
Figure 15. Continued.

SYMBOL	α	β	M_∞	A/C	PYLON
○	0	0	0.80	A-7D	RW CNTR
△	2	0	0.80	A-7D	RW CNTR
▽	4	0	0.80	A-7D	RW CNTR
◇	6	0	0.80	A-7D	RW CNTR
↑	8	0	0.80	A-7D	RW CNTR



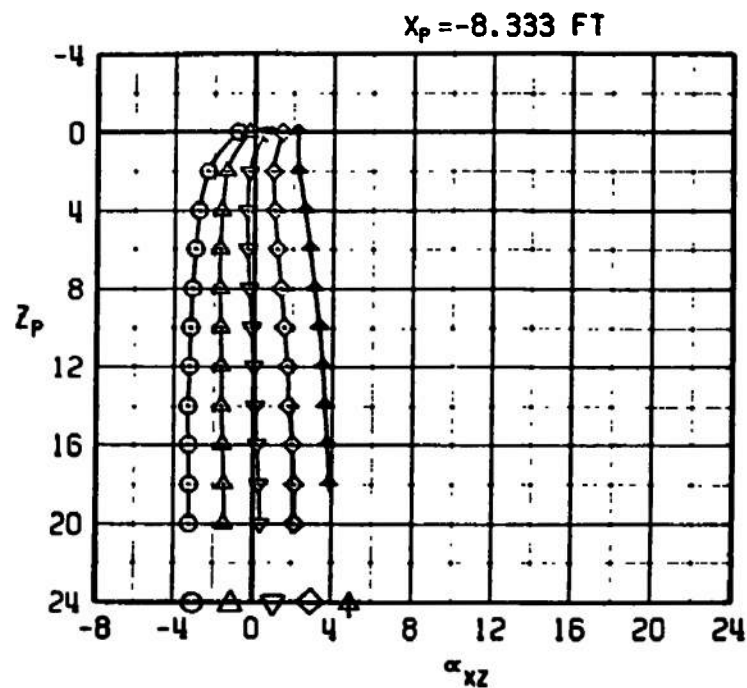
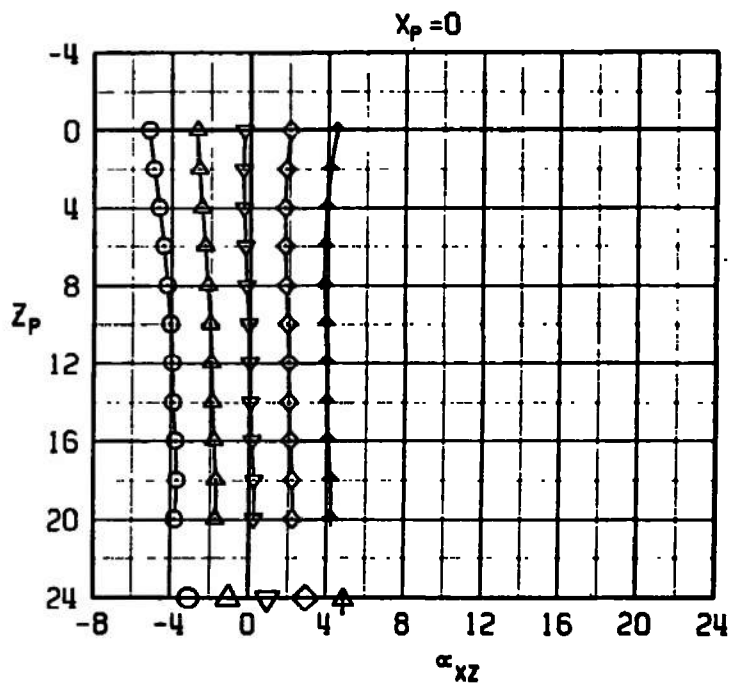
c. $M_\infty = 0.80$, upwash
Figure 15. Continued.

SYMBOL	α	β	M_{\perp}	A/C	PYLON
○	0	0	0.80	A-7D	RW CNTR
△	2	0	0.80	A-7D	RW CNTR
▽	4	0	0.80	A-7D	RW CNTR
◇	6	0	0.80	A-7D	RW CNTR
+	8	0	0.80	A-7D	RW CNTR



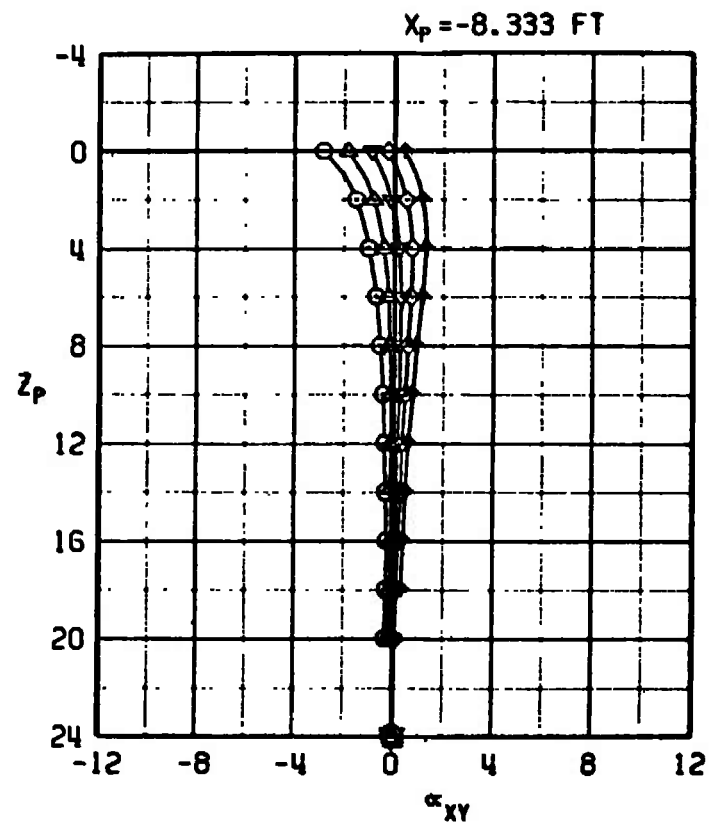
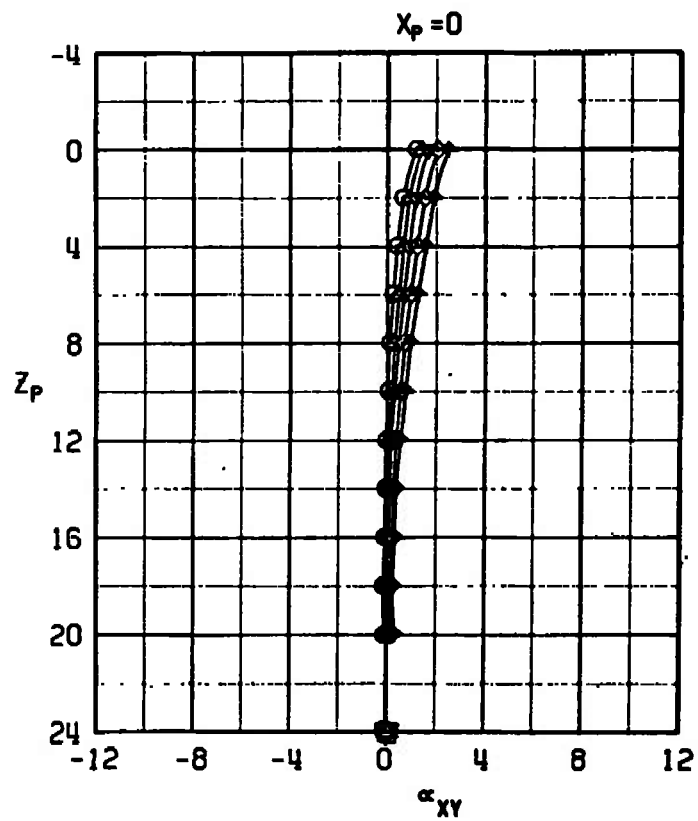
d. $M_{\perp} = 0.80$, sidewash
Figure 15. Continued.

SYMBOL	α	β	M_{∞}	A/C	PYLON
○	0	0	0.95	A-70	RW CNTR
△	2	0	0.95	A-70	RW CNTR
▽	4	0	0.95	A-70	RW CNTR
◇	6	0	0.95	A-70	RW CNTR
↑	8	0	0.95	A-70	RW CNTR



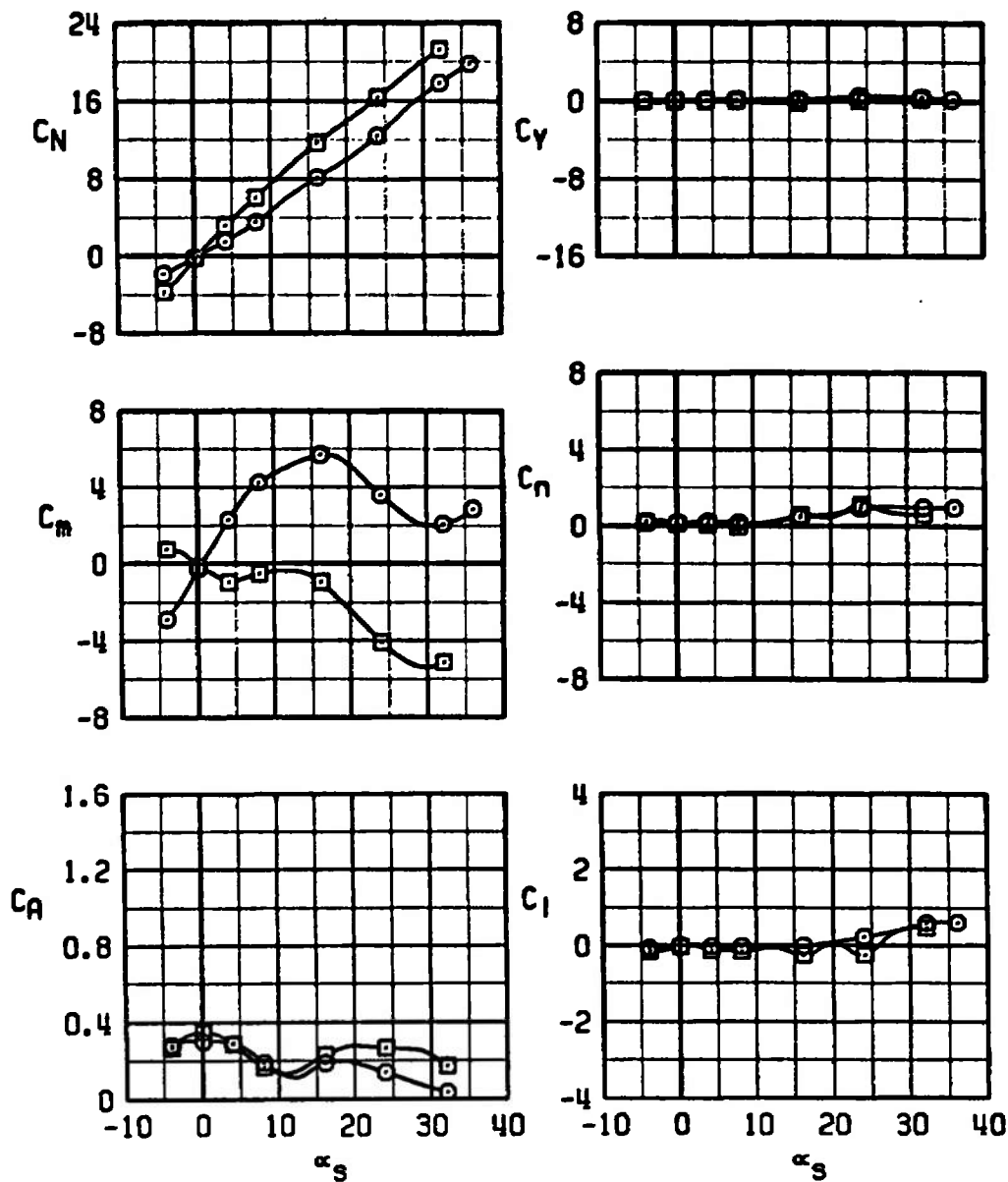
e. $M_{\infty} = 0.95$, upwash
Figure 15. Continued.

SYMBOL	α	β	M_u	A/C	PYLON
○	0	0	0.95	A-7D	RW CNTR
△	2	0	0.95	A-7D	RW CNTR
▽	4	0	0.95	A-7D	RW CNTR
◇	6	0	0.95	A-7D	RW CNTR
↑	8	0	0.95	A-7D	RW CNTR



f. $M_u = 0.95$, sidewash
Figure 15. Concluded.

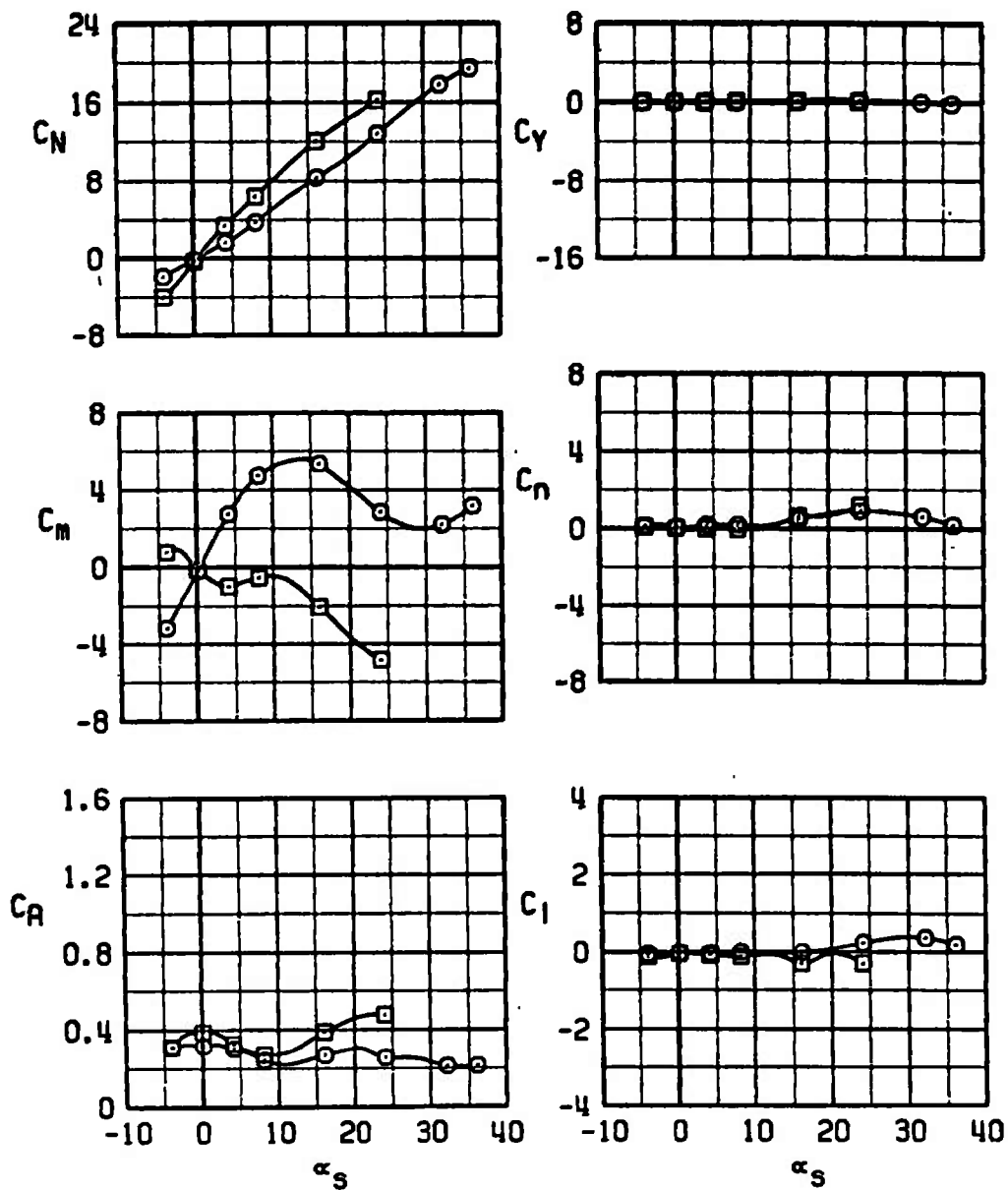
SYMBOL	M_∞	STORE	TIPS	●
○	0.65	MK-84	RETRACTED	0
□	0.65	MK-84	EXTENDED	0



a. $M_\infty = 0.65$

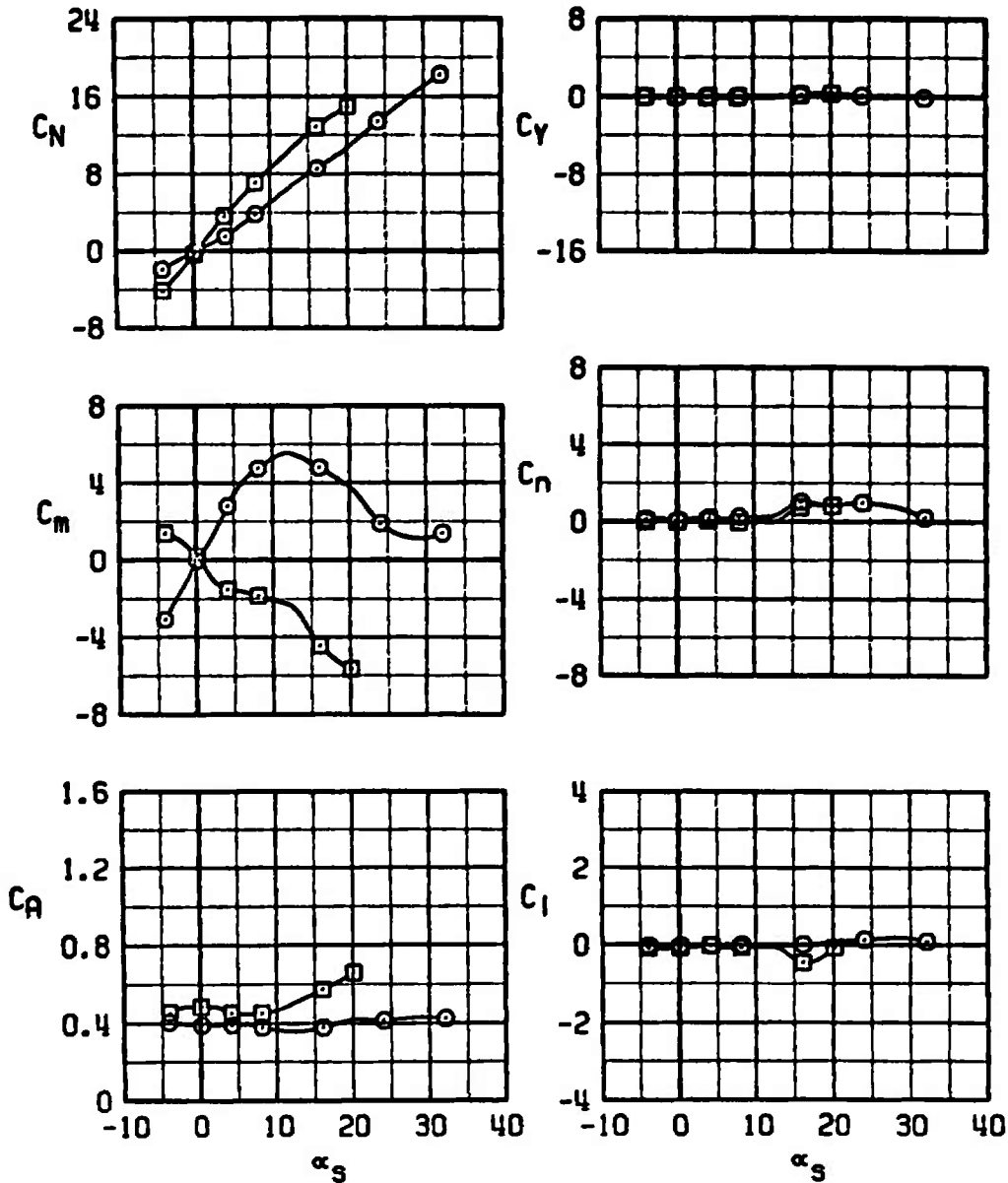
Figure 16. Free-stream aerodynamic characteristics of the Super HOBOS/MK-84 store with tips retracted and extended.

SYMBOL	M_∞	STORE	TIPS	δ
○	0.80	MK-84	RETRACTED	0
□	0.80	MK-84	EXTENDED	0



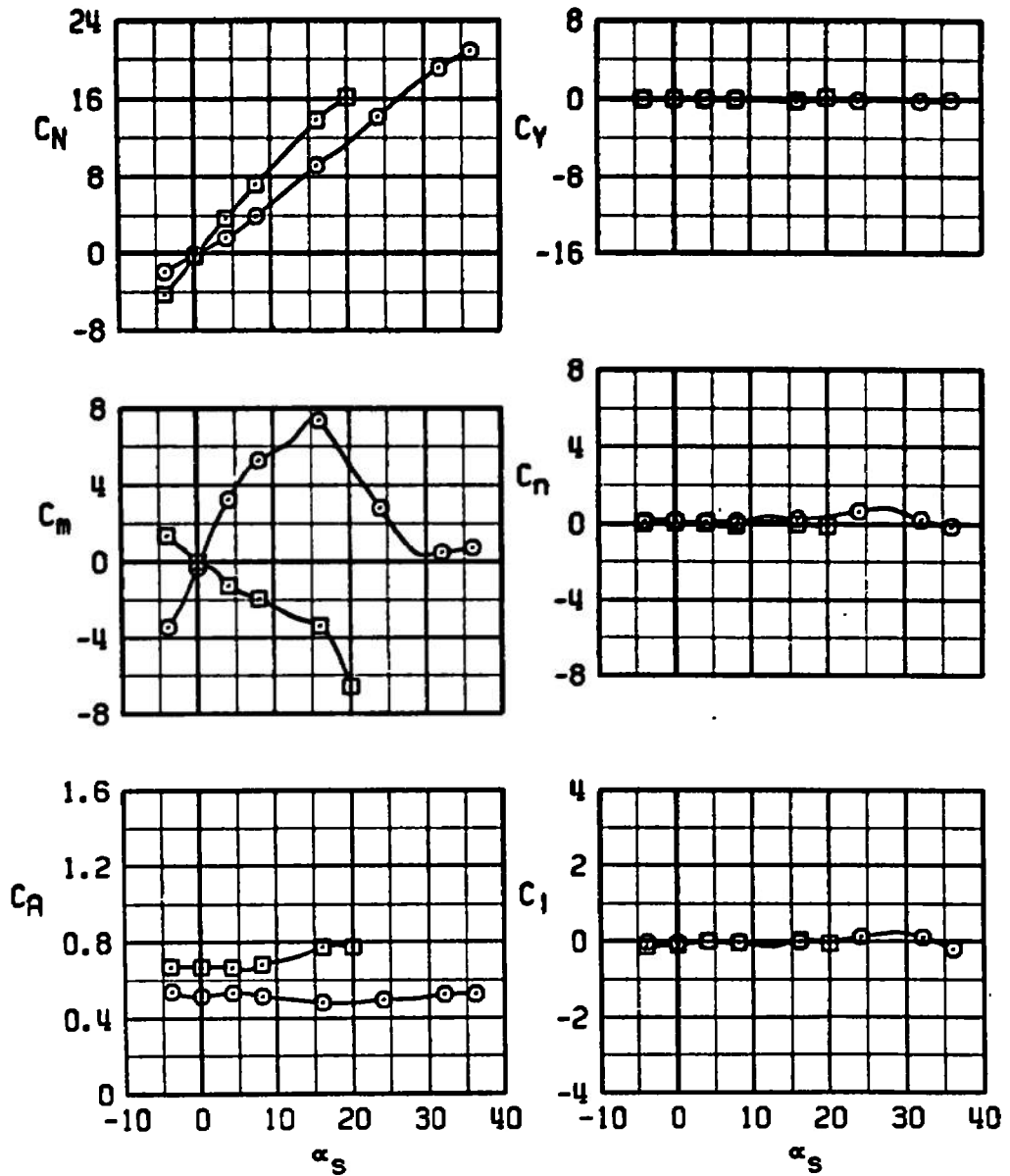
b. $M_\infty = 0.80$
Figure 16. Continued.

SYMBOL	M_∞	STORE	TIPS	•
○	0.90	MK-84	RETRACTED	0
□	0.90	MK-84	EXTENDED	0



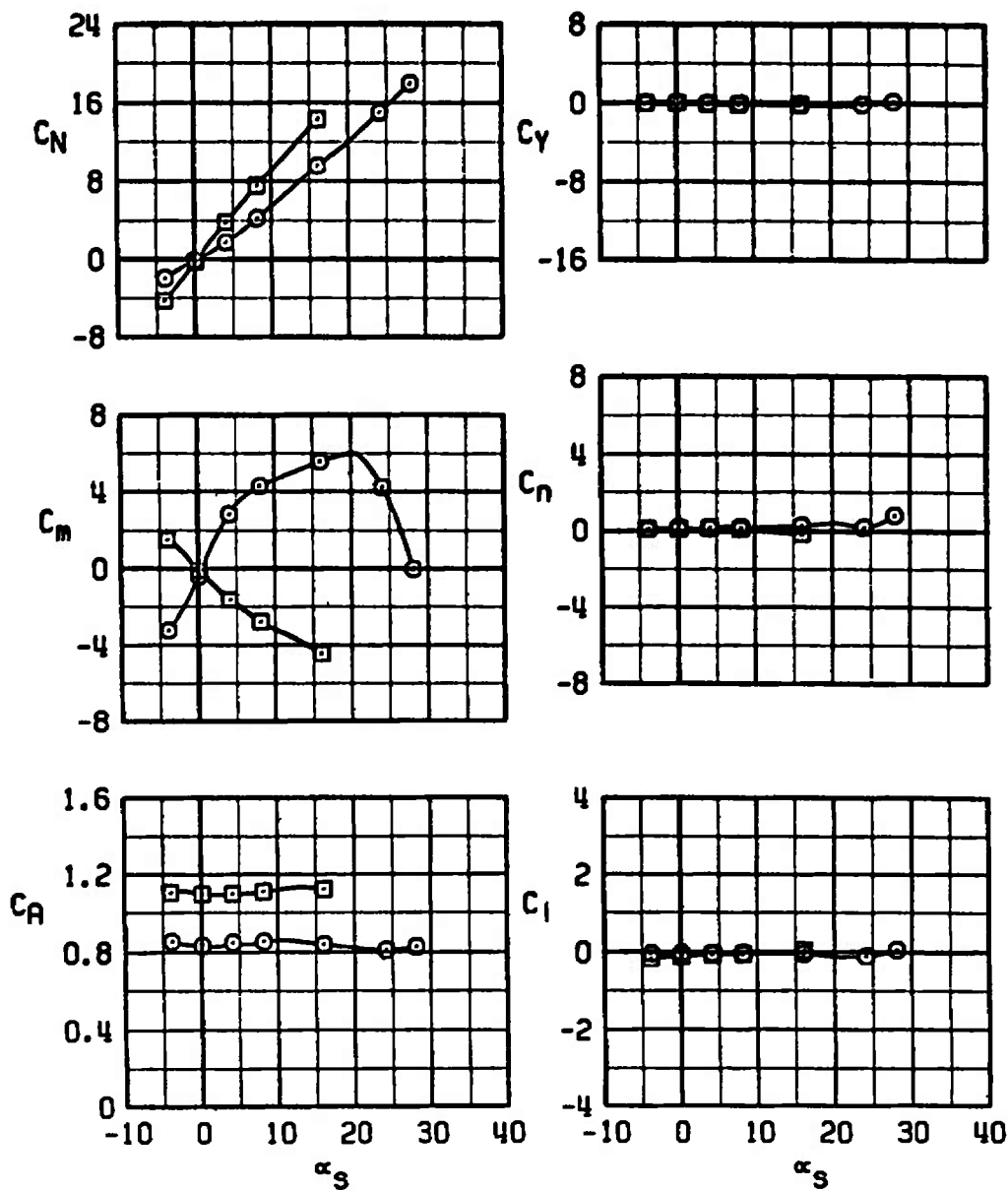
c. $M_\infty = 0.90$
Figure 16. Continued.

SYMBOL	M_∞	STORE	TIPS	α
\circ	0.95	MK-84	RETRACTED	0
\square	0.95	MK-84	EXTENDED	0



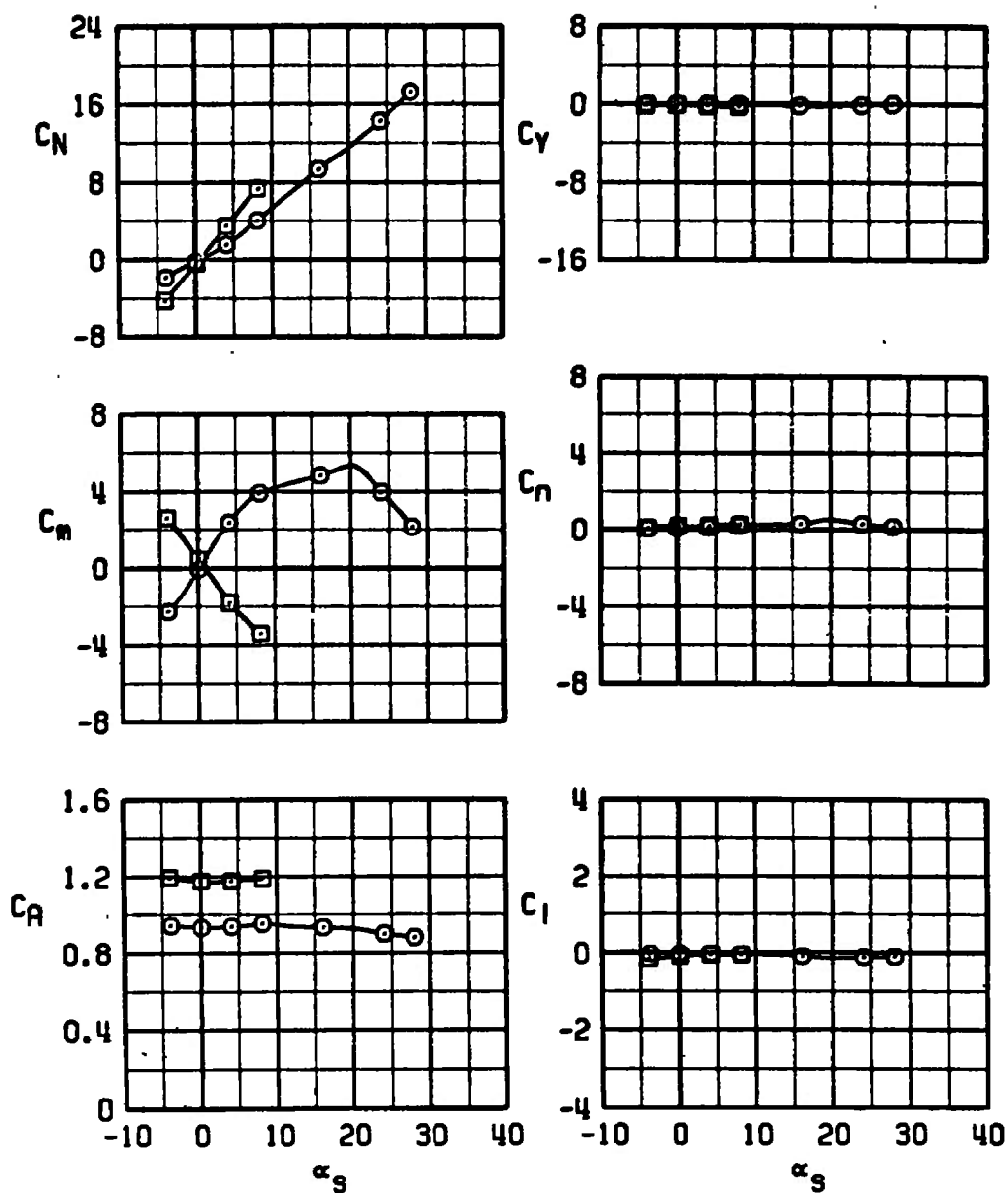
d. $M_\infty = 0.95$
Figure 16. Continued.

SYMBOL	M_∞	STORE	TIPS	δ
○	1.05	MK-84	RETRACTED	0
□	1.05	MK-84	EXTENDED	0



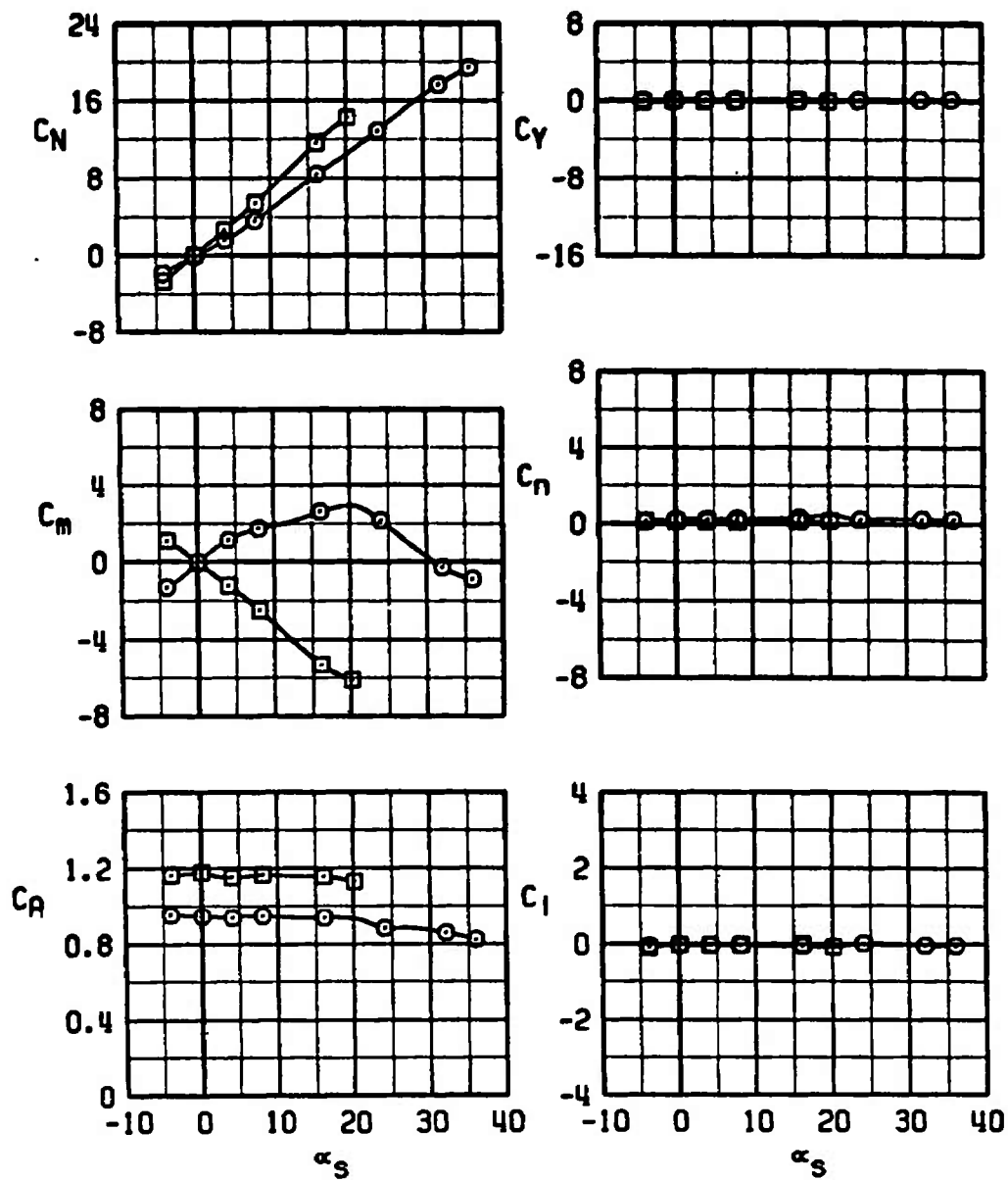
e. $M_\infty = 1.05$
Figure 16. Continued.

SYMBOL	M_∞	STORE	TIPS	●
○	1.20	MK-84	RETRACTED	0
□	1.20	MK-84	EXTENDED	0



f. $M_\infty = 1.20$
Figure 16. Continued.

SYMBOL	M_∞	STORE	TIPS	•
○	1.60	MK-84	RETRACTED	0
□	1.60	MK-84	EXTENDED	0



g. $M_\infty = 1.60$
Figure 16. Concluded.

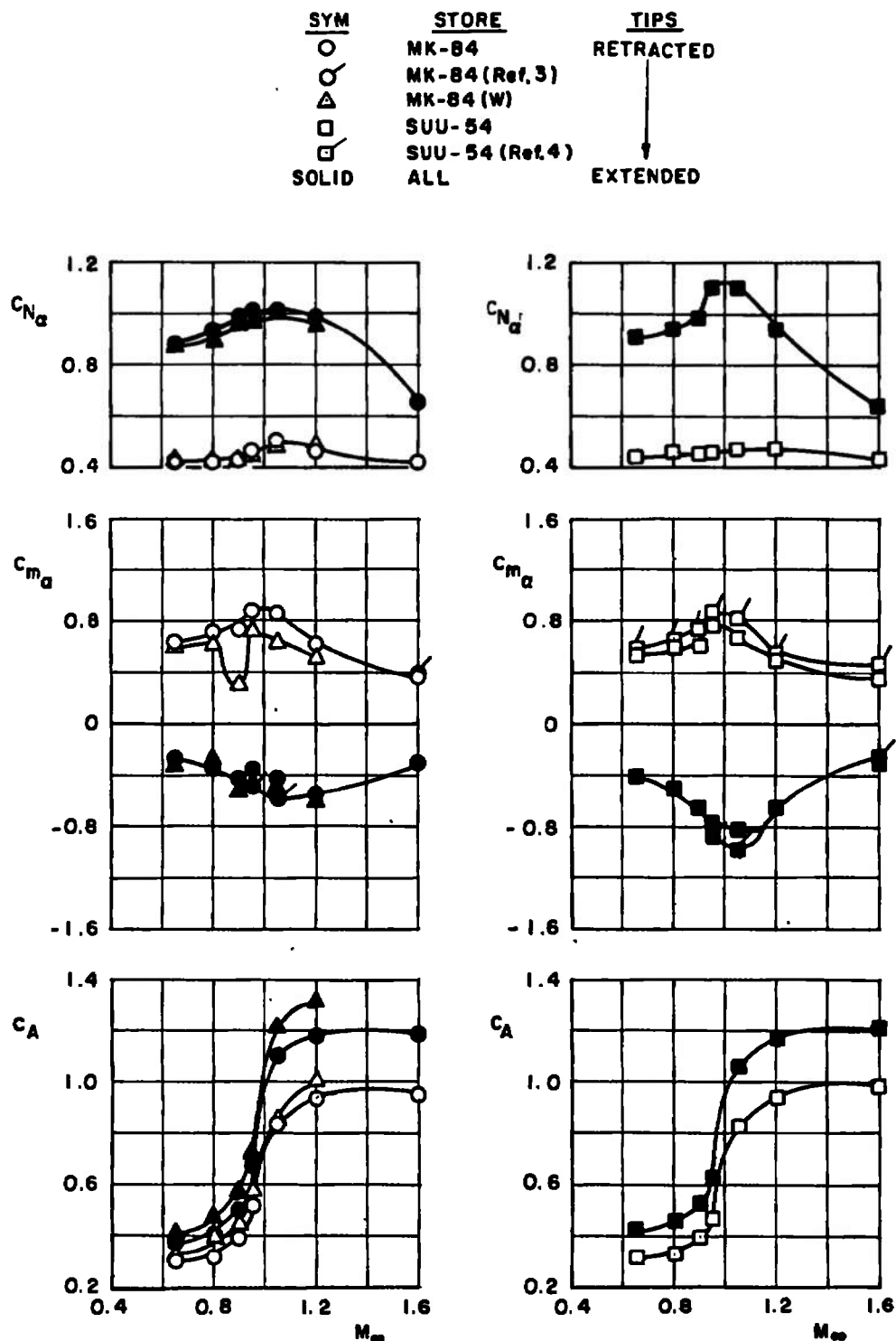
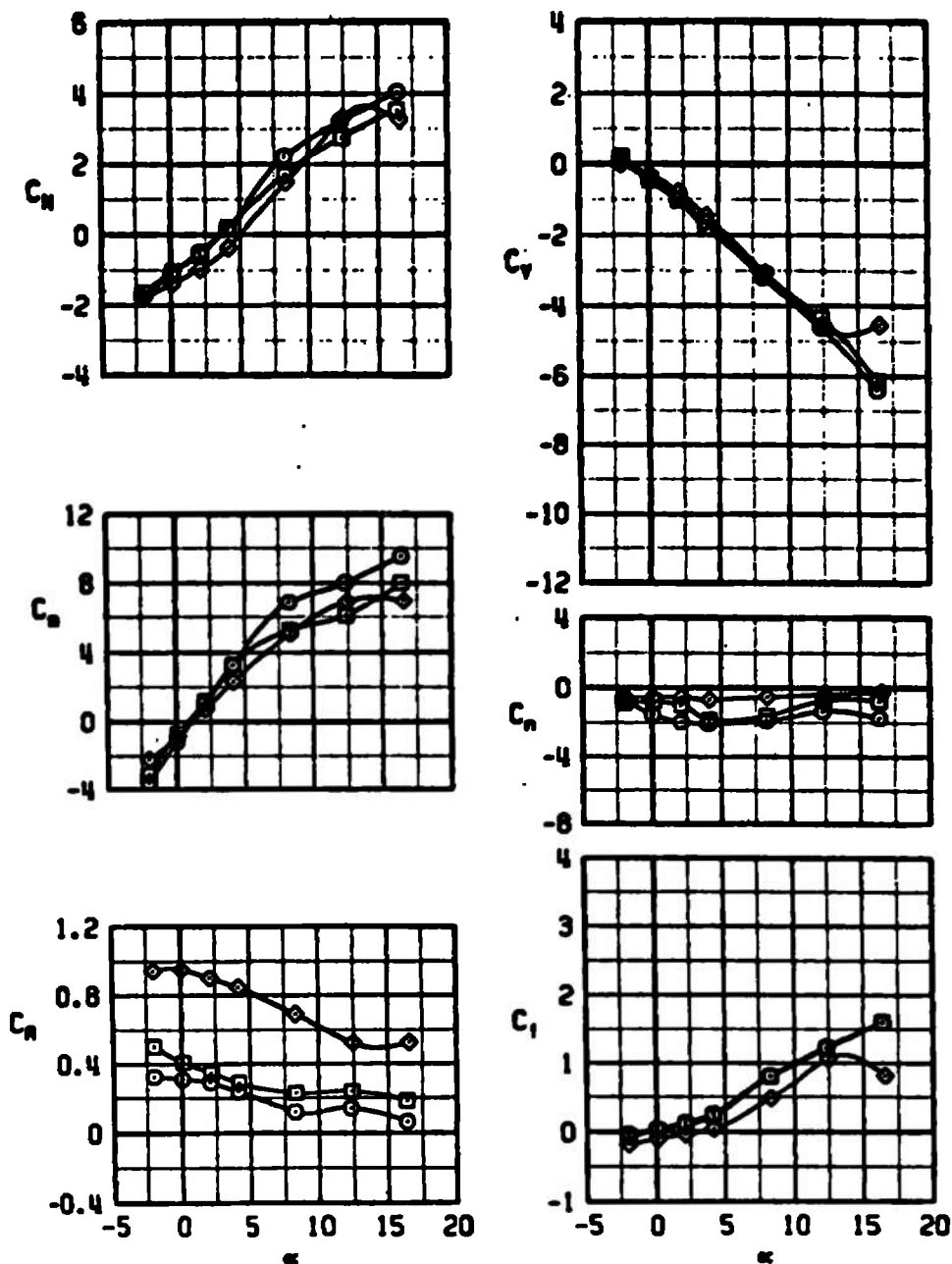


Figure 17. Variation of the Super HOBOS longitudinal stability derivatives and axial-force coefficients with Mach number, $\alpha_s = 0$.

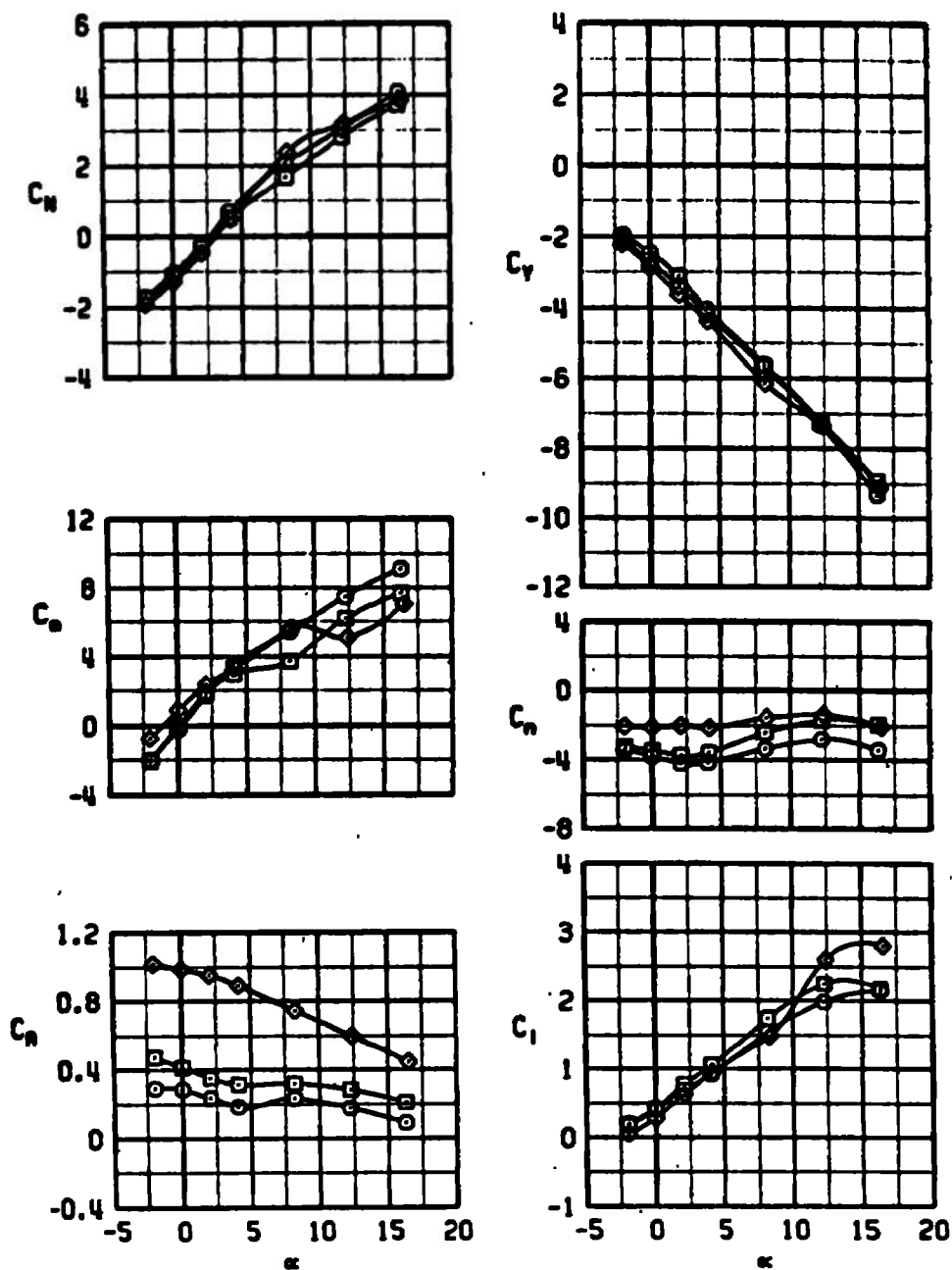
SYMBOL	M_∞	β	PYLON	CONFIG
○	0.65	0	LW INB'D	18
□	0.90	0	LW INB'D	18
◇	1.20	0	LW INB'D	18



a. Variation with α , LW INB'D, $\beta = 0$

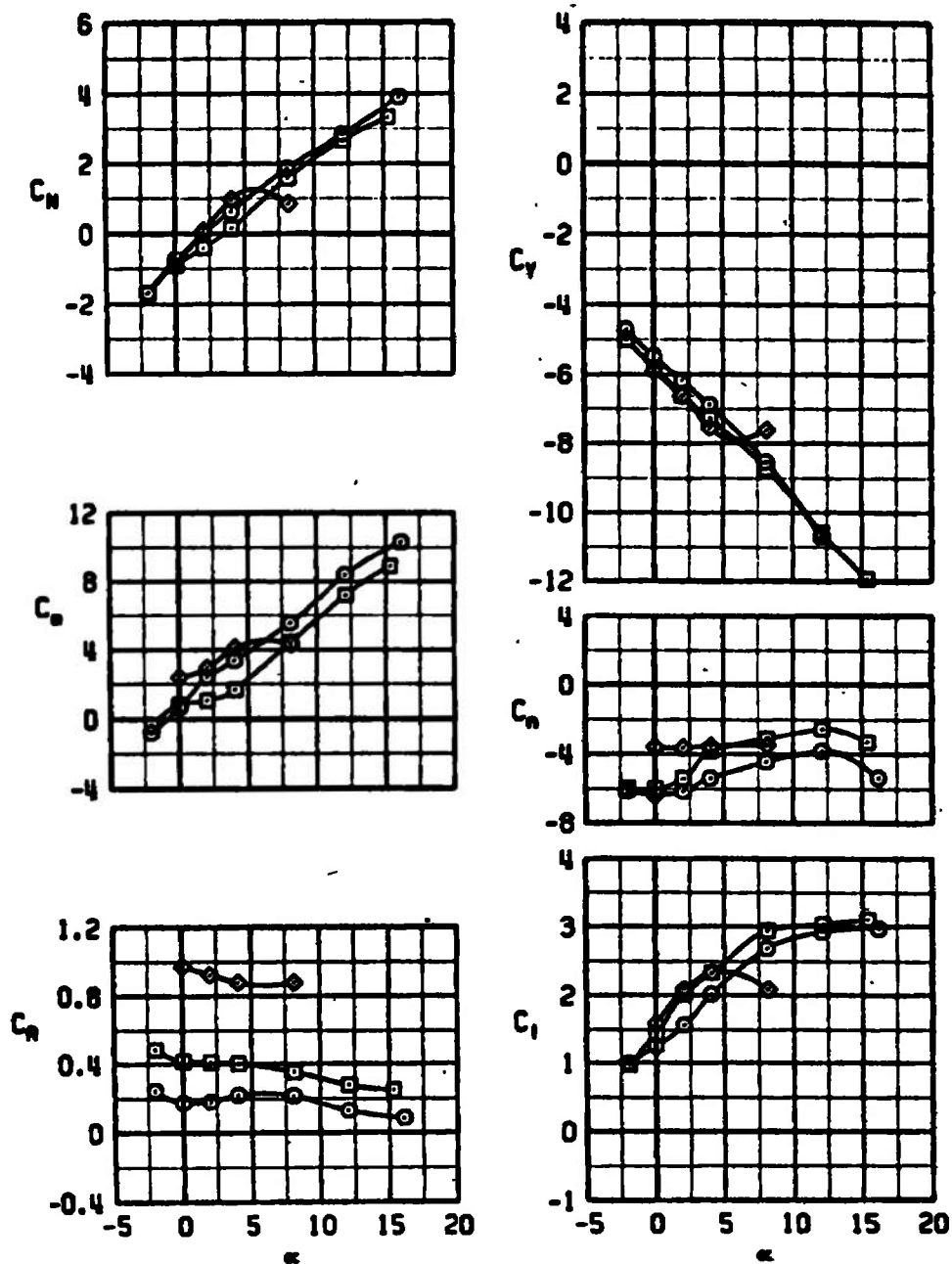
Figure 18. Carriage position characteristics of the MK-84 store for the F-4C inboard pylons.

SYMBOL	M_∞	β	PYLON	CONFIG
○	0.65	4	LW INB'D	18
□	0.90	4	LW INB'D	18
◇	1.20	4	LW INB'D	18



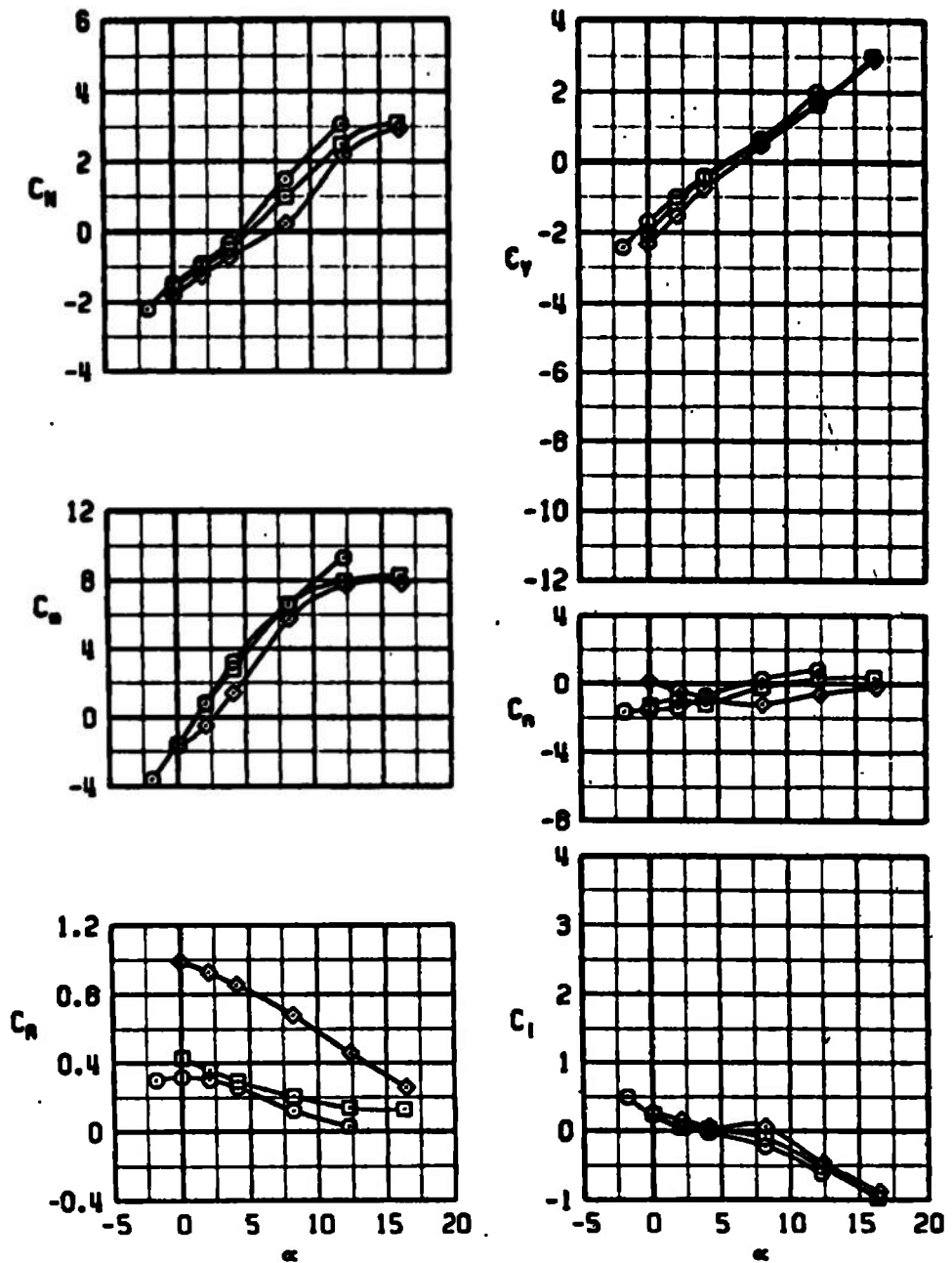
b. Variation with α , LW INB'D, $\beta = 4$ deg
Figure 18. Continued.

SYMBOL	M_∞	β	PYLON	CONFIG
○	0.65	9	LW INB'D	18
□	0.90	9	LW INB'D	18
◇	1.20	9	LW INB'D	18



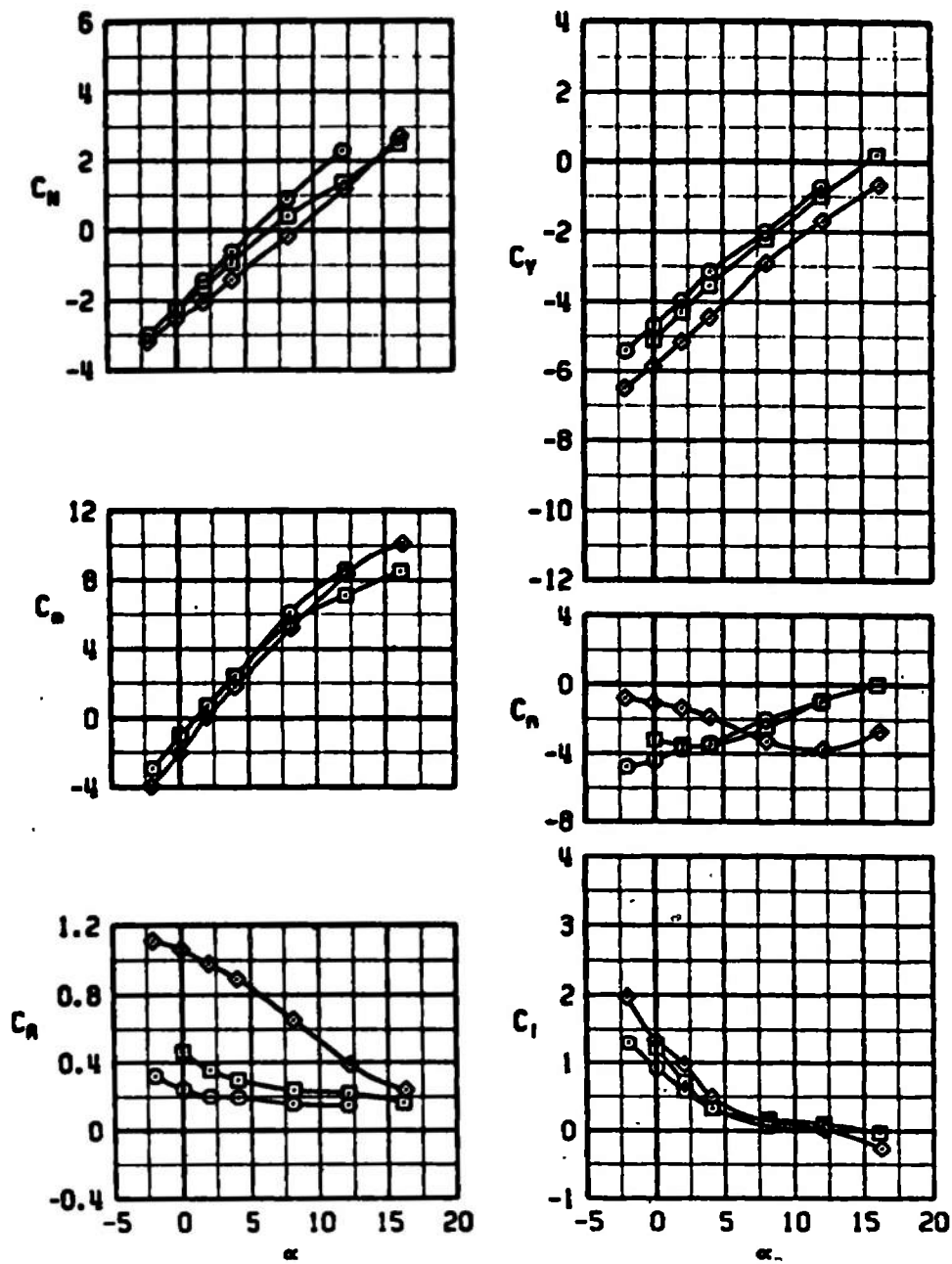
c. Variation with α , LW INB'D, $\beta = 9$ deg
Figure 18. Continued.

SYMBOL	M_∞	β	PYLON	CONFIG
○	0.65	4	RW INB'D	19
□	0.90	4	RW INB'D	19
◇	1.20	4	RW INB'D	19

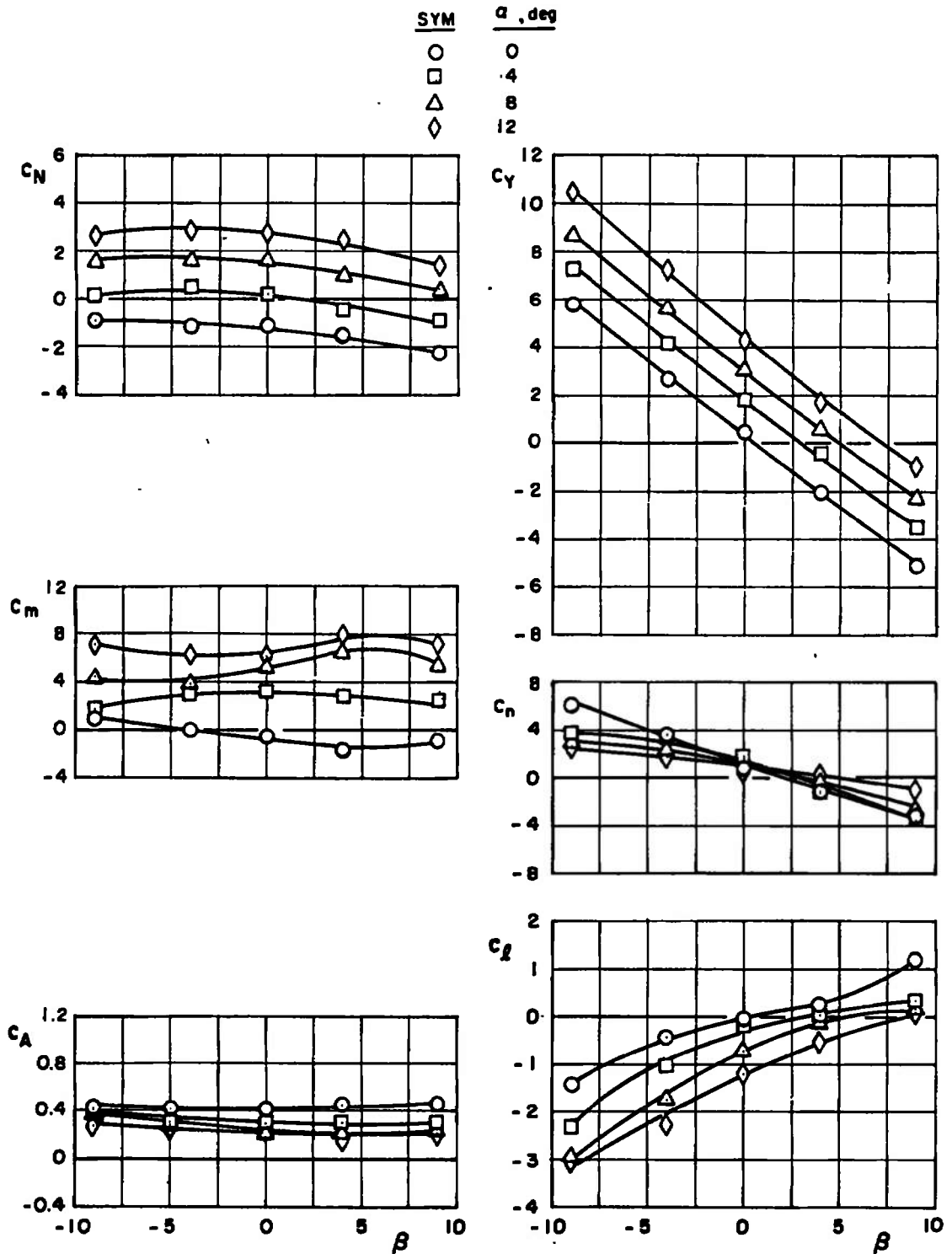


d. Variation with α , RW INB'D, $\beta = 4$ deg
Figure 18. Continued.

SYMBOL	M_∞	β	PYLON	CONFIG
○	0.65	9	RW INB'D	19
□	0.90	9	RW INB'D	19
◇	1.20	9	RW INB'D	19

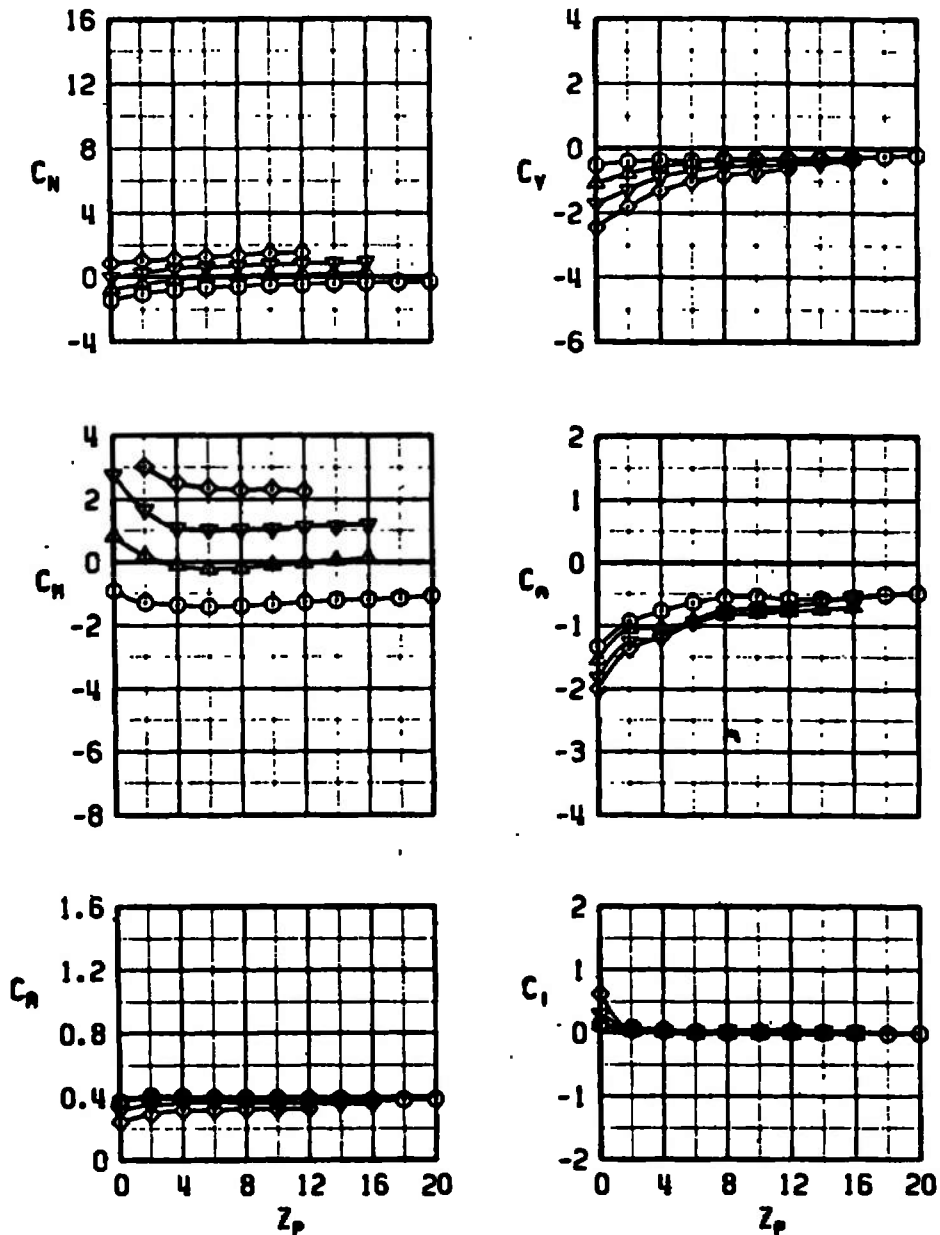


e. Variation with α , RW INB'D, $\beta = 9^\circ$
Figure 18. Continued.



f. Variation with β , RW INB'D, $M_\infty = 0.90$
 Figure 18. Concluded.

SYM	N	M _∞	A/C	PYLON	STORE
○	0	0.65	F-4C	LW INBD	MK-84 TIPS RETRACTED
△	2	0.65	F-4C	LW INBD	MK-84 TIPS RETRACTED
▽	4	0.65	F-4C	LW INBD	MK-84 TIPS RETRACTED
◇	6	0.65	F-4C	LW INBD	MK-84 TIPS RETRACTED

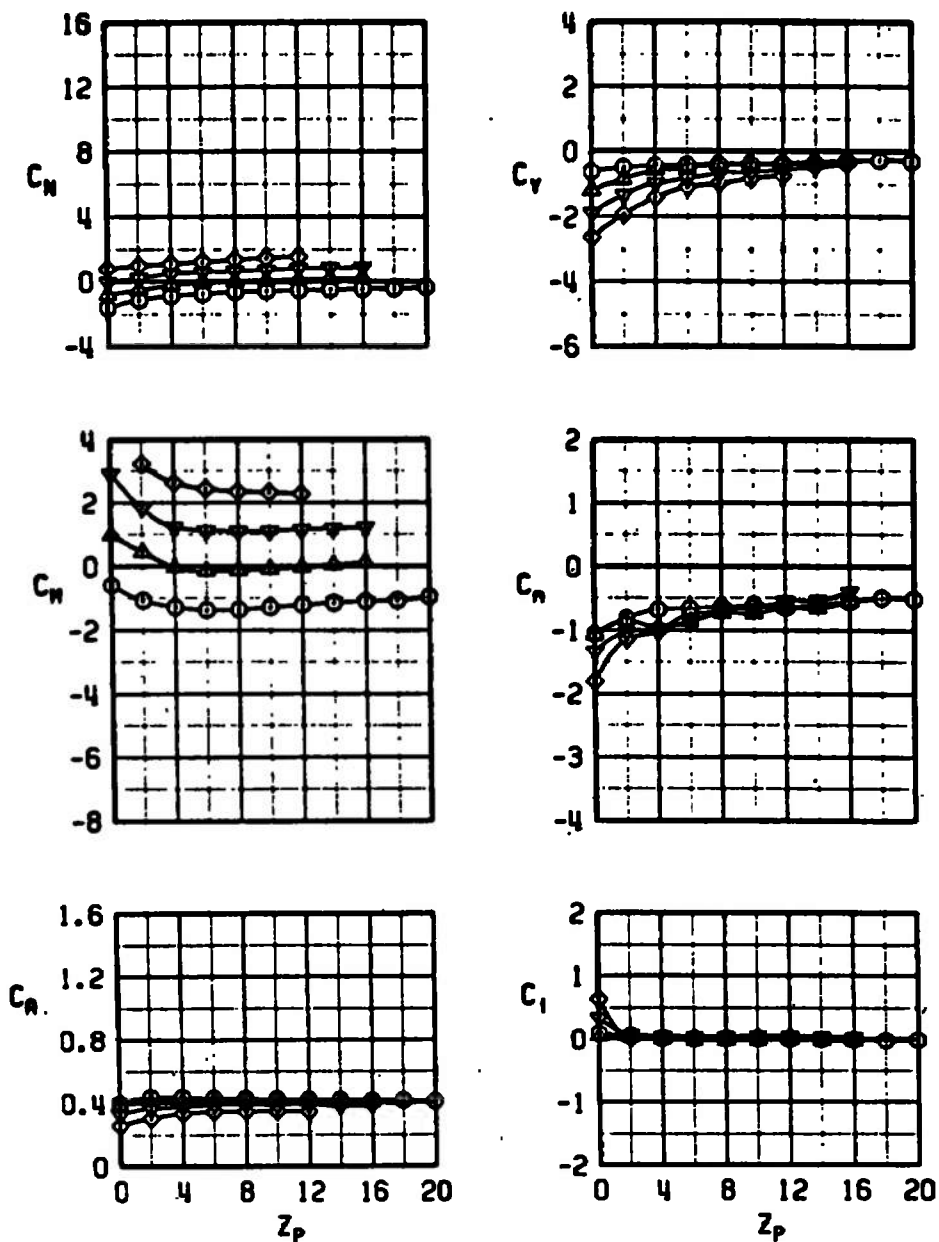


a. $M_\infty = 0.65$, tips retracted

Figure 19. Aerodynamic characteristics of the MK-84 store in the F-4C flow field, $Y_p = 0$, $\beta = 0$.

SYM	α	M_∞	A/C	PYLON
○	0	0.80	F-4C	LW INBD
▲	2	0.80	F-4C	LW INBD
▼	4	0.80	F-4C	LW INBD
◇	6	0.80	F-4C	LW INBD

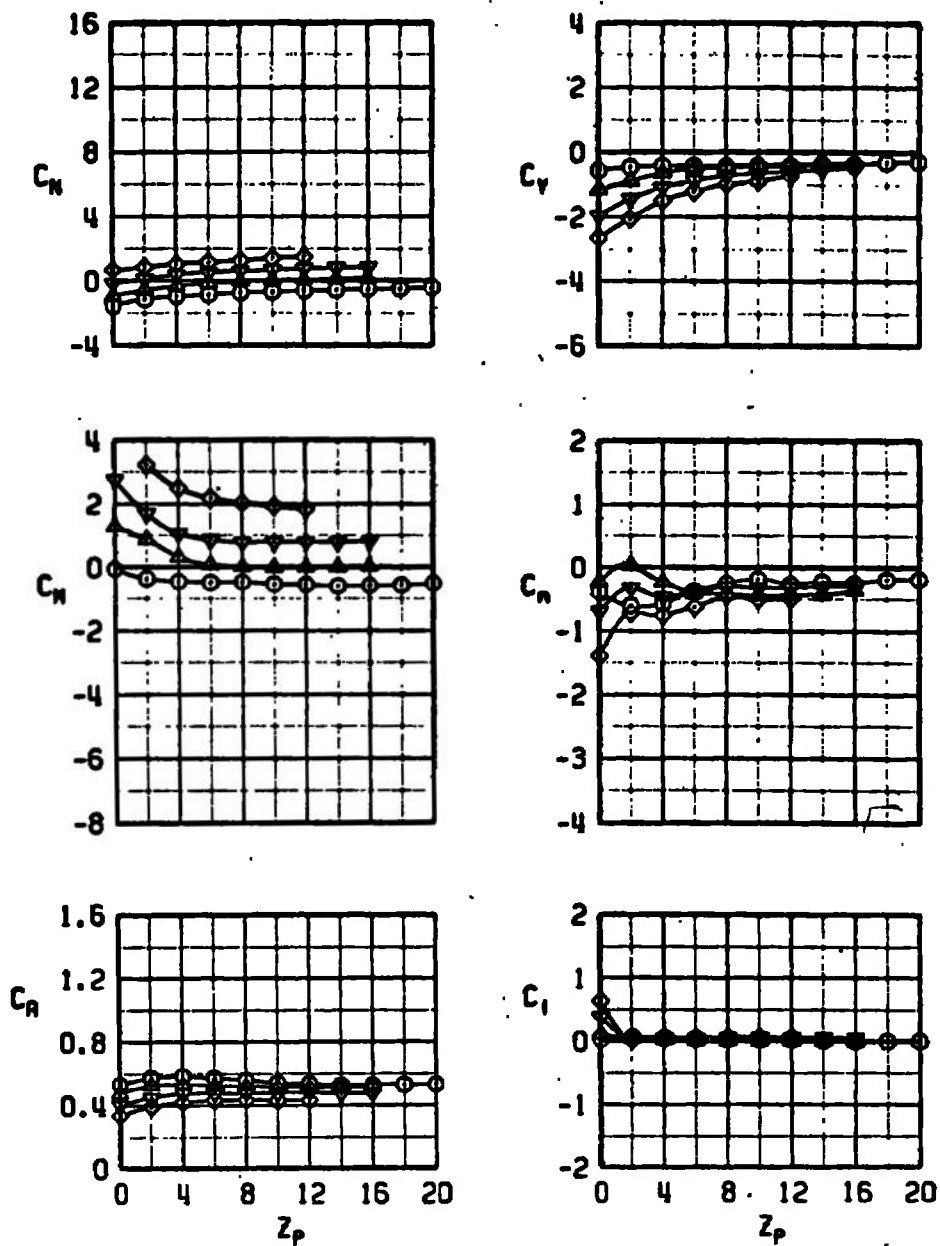
STORE
 MK-84 TIPS RETRACTED
 MK-84 TIPS RETRACTED
 MK-84 TIPS RETRACTED
 MK-84 TIPS RETRACTED



b. $M_\infty = 0.80$, tips retracted
 Figure 19. Continued.

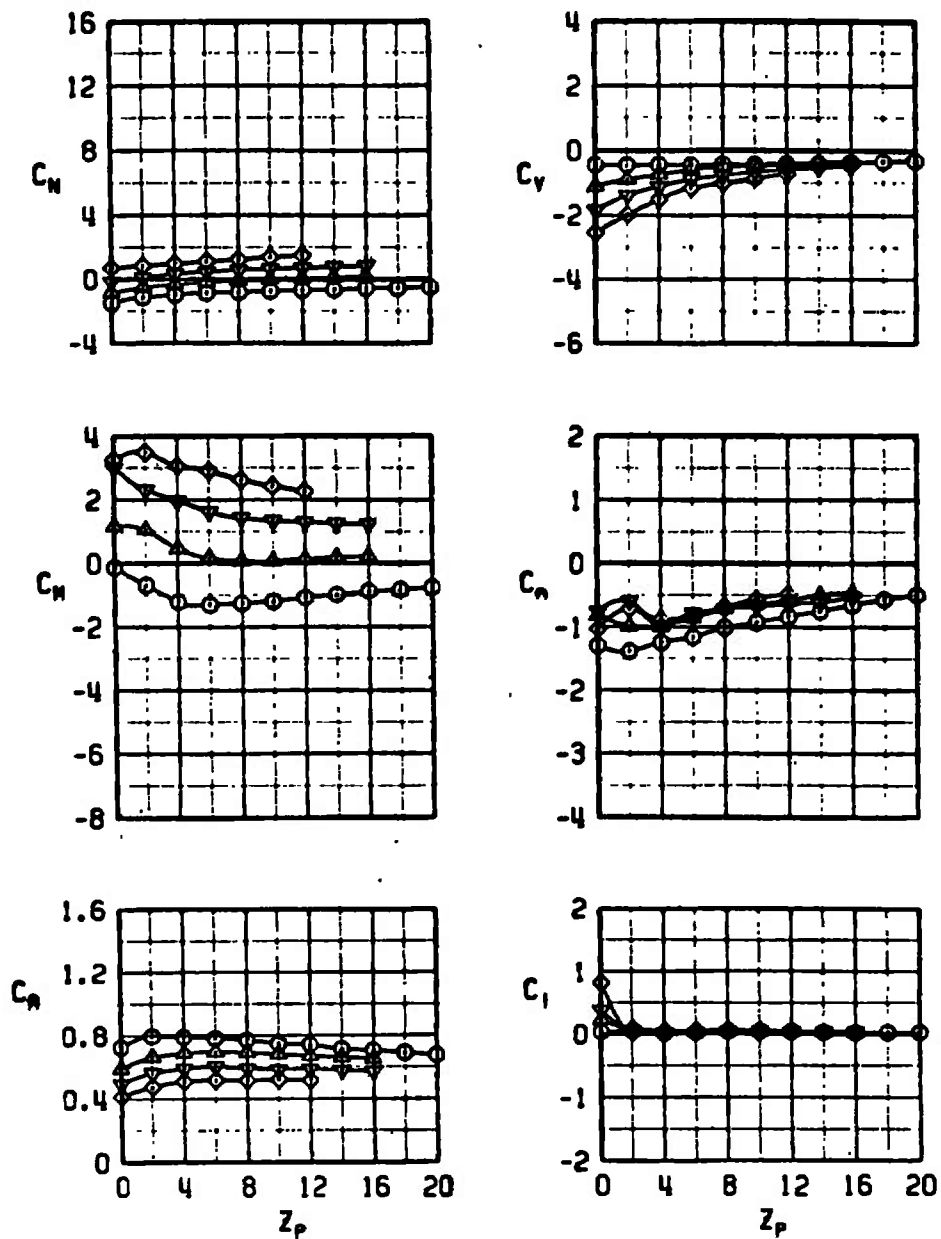
SYM	α	M_∞	A/C	PYLON
○	0	0.90	F-4C	LW INBD
△	2	0.90	F-4C	LW INBD
▽	4	0.90	F-4C	LW INBD
◇	6	0.90	F-4C	LW INBD

STORE
 MK-84 TIPS RETRACTED
 MK-84 TIPS RETRACTED
 MK-84 TIPS RETRACTED
 MK-84 TIPS RETRACTED



c. $M_\infty = 0.90$, tips retracted
 Figure 19. Continued.

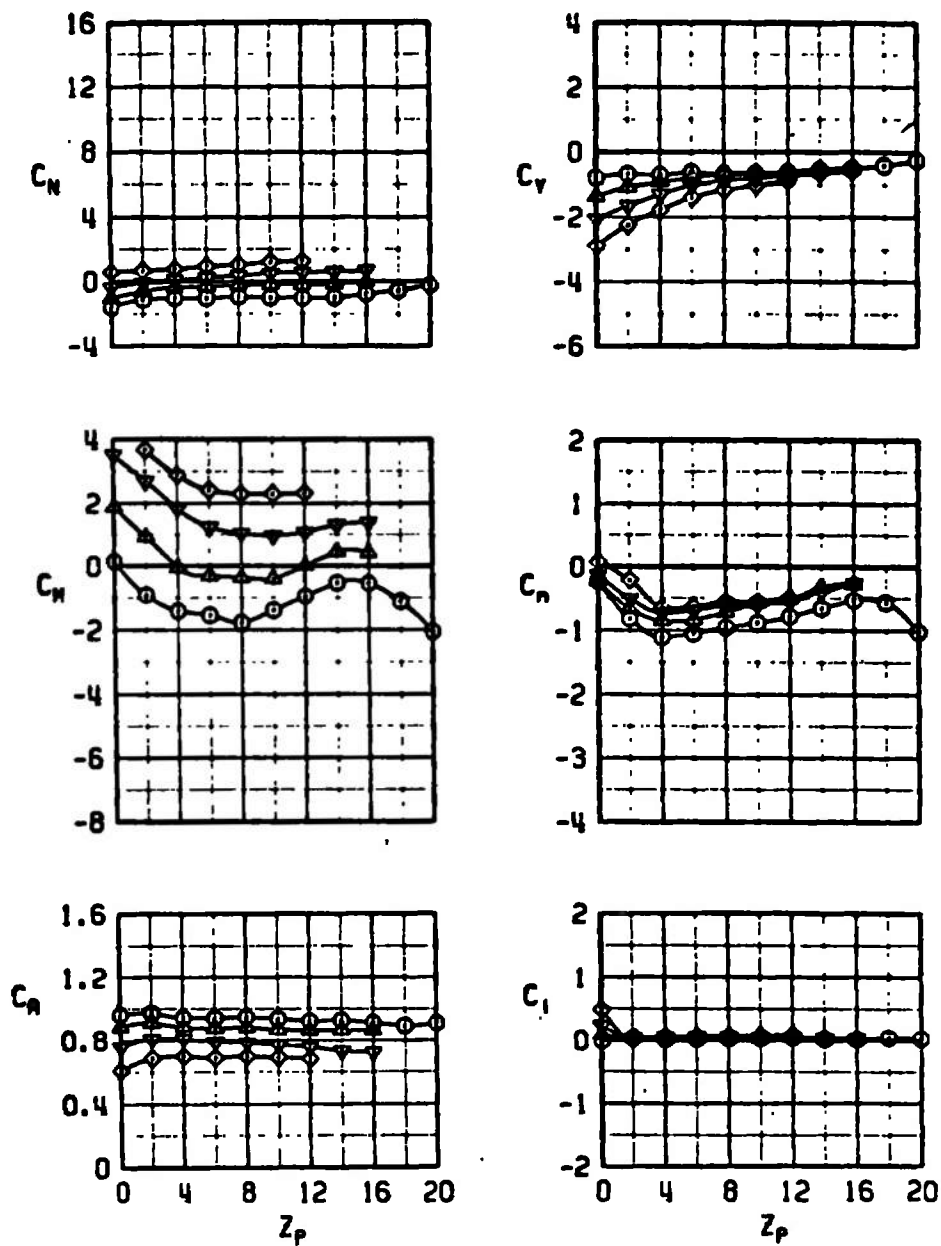
SYM	α	M_∞	A/C	PYLON	STORE
○	0	0.95	F-4C	LW INBD	MK-84 TIPS RETRACTED
▲	2	0.95	F-4C	LW INBD	MK-84 TIPS RETRACTED
▼	4	0.95	F-4C	LW INBD	MK-84 TIPS RETRACTED
◇	6	0.95	F-4C	LW INBD	MK-84 TIPS RETRACTED



d. $M_\infty = 0.95$, tips retracted
Figure 19. Continued.

SYM	a	M _∞	A/C	PYLON
○	0	1.05	F-4C	LW IN80
▲	2	1.05	F-4C	LW IN80
▼	4	1.05	F-4C	LW IN80
◇	6	1.05	F-4C	LW IN80

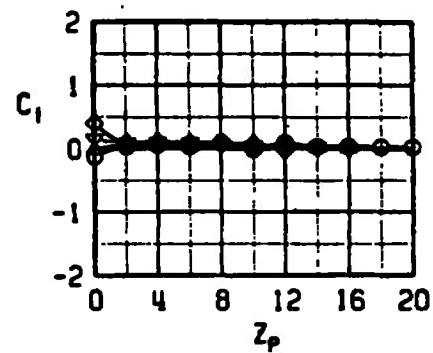
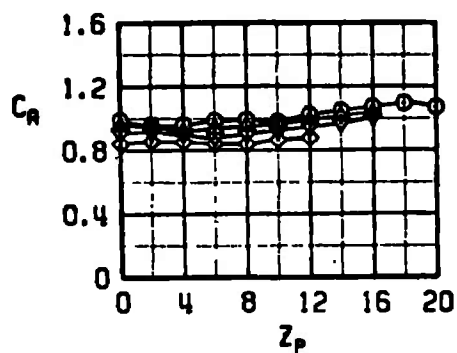
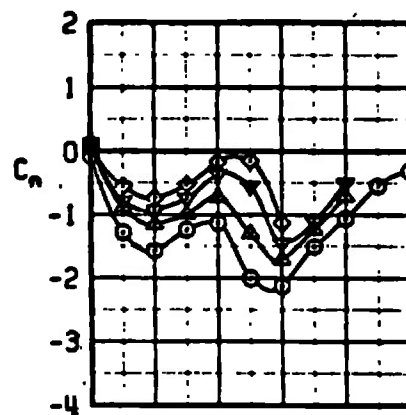
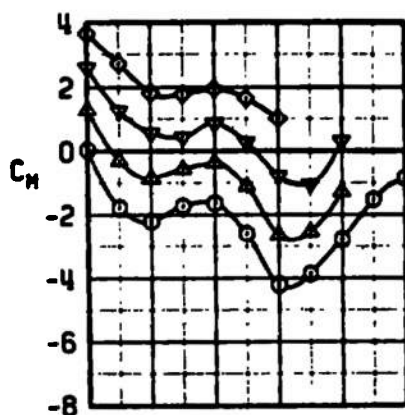
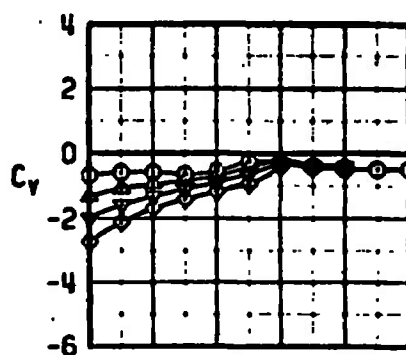
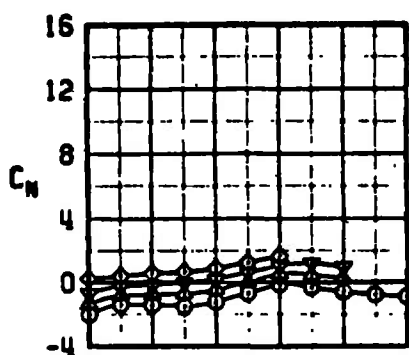
STORE
 MK-84 TIPS RETRACTED
 MK-84 TIPS RETRACTED
 MK-84 TIPS RETRACTED
 MK-84 TIPS RETRACTED



e. $M_\infty = 1.05$, tips retracted
 Figure 19. Continued.

SYM	a	M _∞	A/C	PYLON
○	0	1.20	F-4C	LW INBD
▲	2	1.20	F-4C	LW INBD
▼	4	1.20	F-4C	LW INBD
◇	6	1.20	F-4C	LW INBD

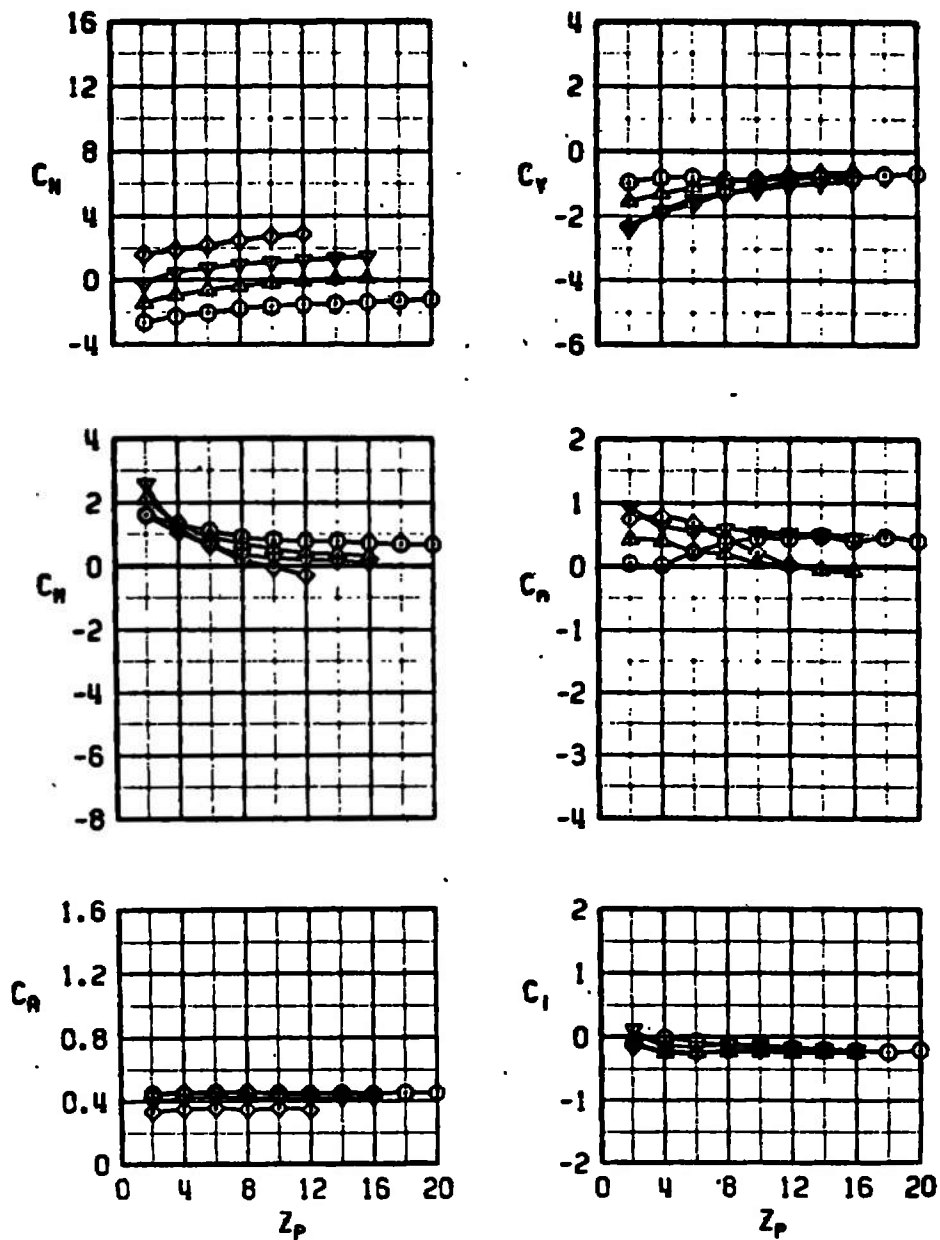
STORE
 MK-84 TIPS RETRACTED
 MK-84 TIPS RETRACTED
 MK-84 TIPS RETRACTED
 MK-84 TIPS RETRACTED



f. $M_{\infty} = 1.20$, tips retracted
 Figure 19. Continued.

SYM	n	M_u	A/C	PYLON
⊖	0	0.65	F-4C	LW INBD
▲	2	0.65	F-4C	LW INBD
▼	4	0.65	F-4C	LW INBD
◇	6	0.65	F-4C	LW INBD

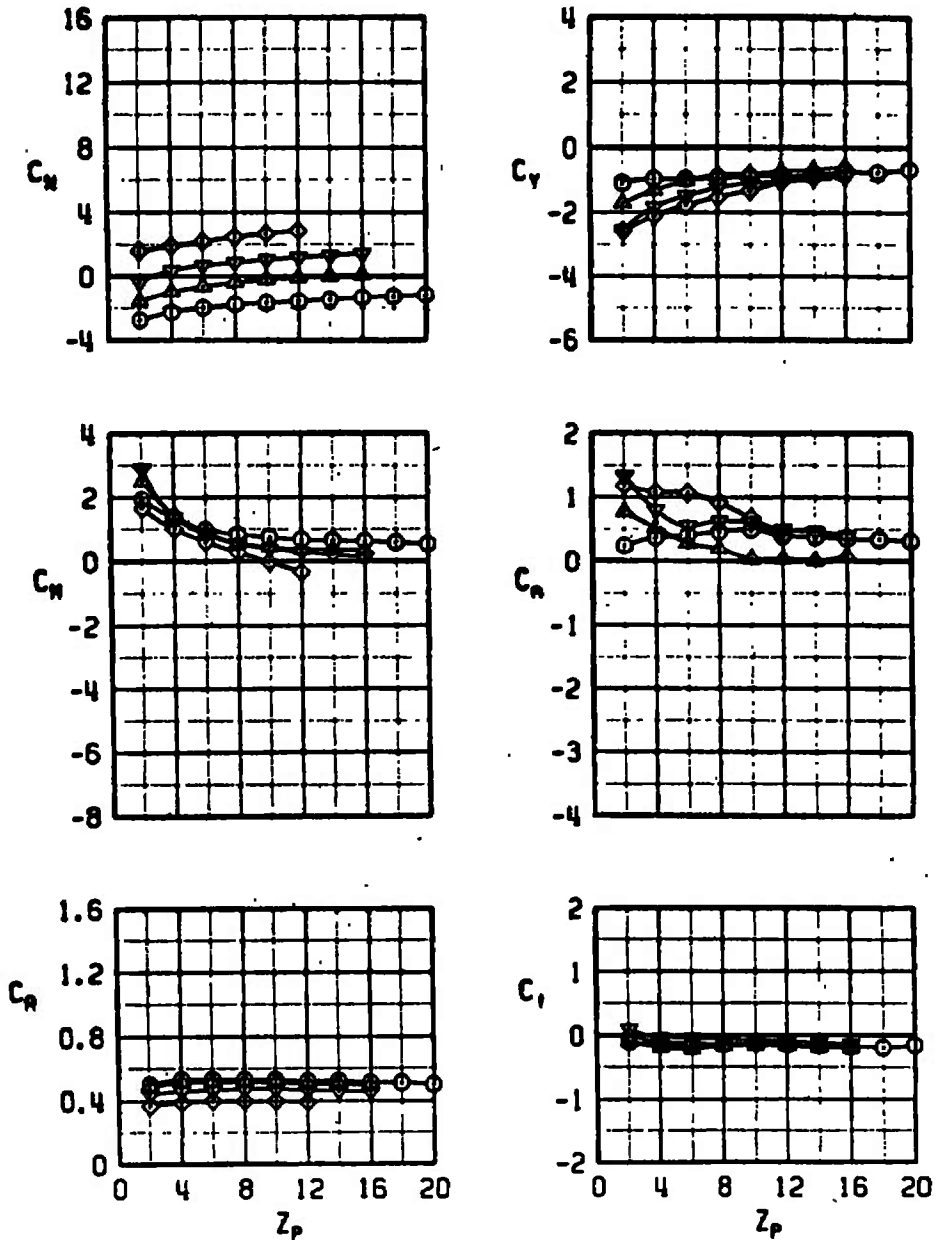
STORE
HK-04 TIPS EXTENDED
HK-04 TIPS EXTENDED
HK-04 TIPS EXTENDED
HK-04 TIPS EXTENDED



g. $M_u = 0.65$, tips extended
Figure 19. Continued.

SYM	α	M_∞	A/C	PYLON
○	0	0.80	F-4C	LW INBO
▲	2	0.80	F-4C	LW INBO
▼	4	0.80	F-4C	LW INBO
◇	6	0.80	F-4C	LW INBO

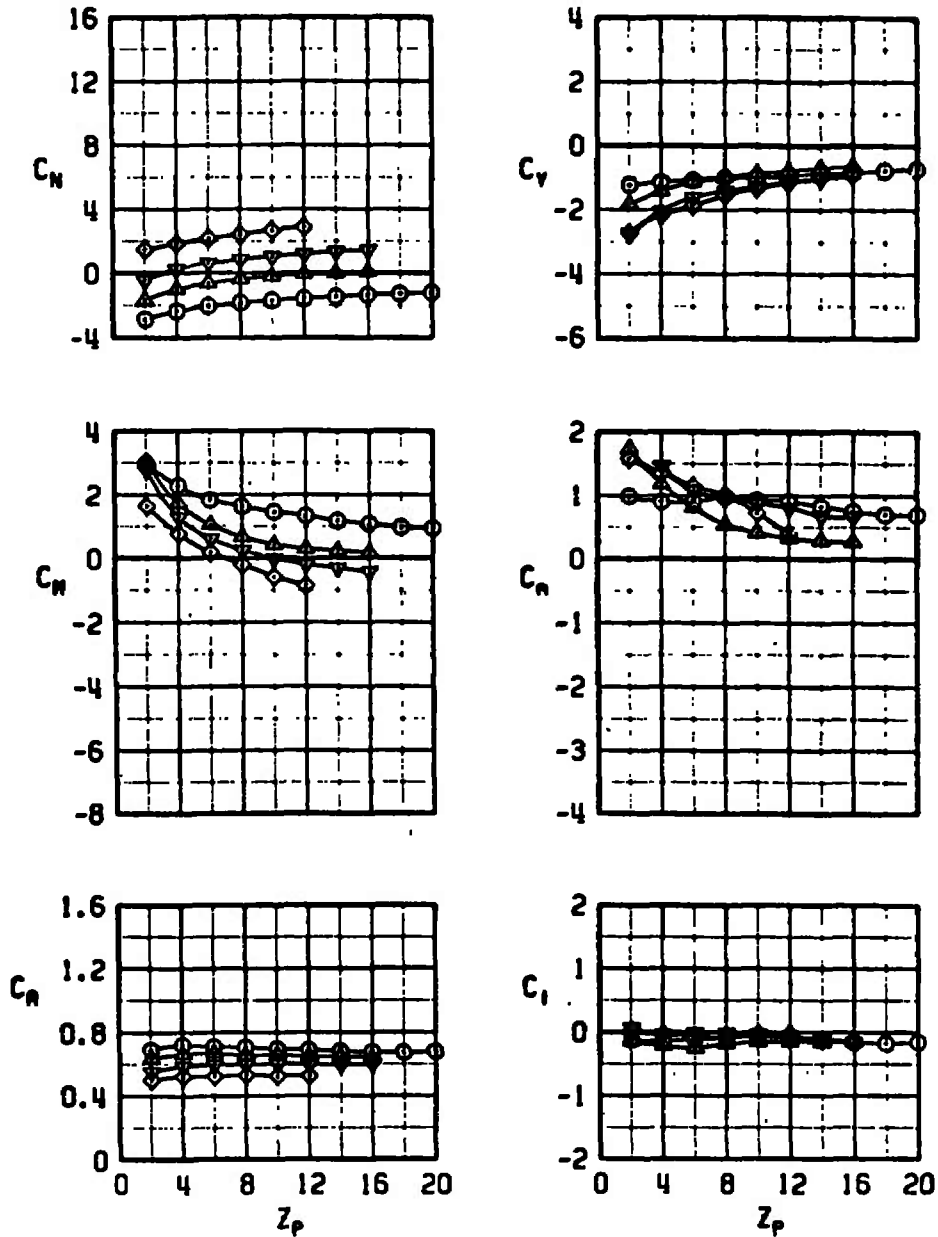
STORE
MK-84 TIPS EXTENDED
MK-84 TIPS EXTENDED
MK-84 TIPS EXTENDED
MK-84 TIPS EXTENDED



h. $M_\infty = 0.80$, tips extended
Figure 19. Continued.

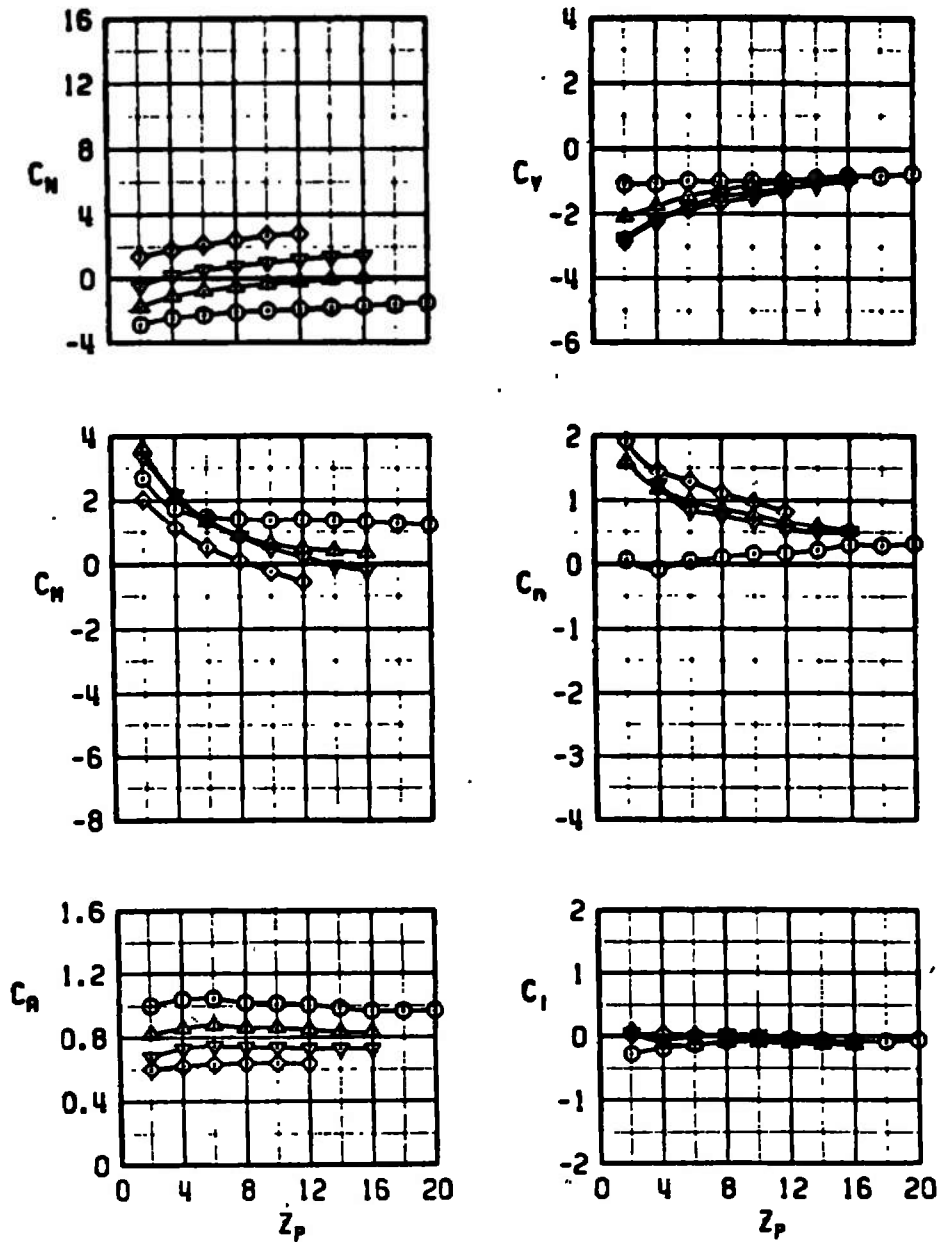
SYM	α	M_∞	A/C	PYLON
○	0	0.90	F-4C	LM INBD
△	2	0.90	F-4C	LM INBD
▽	4	0.90	F-4C	LM INBD
◇	6	0.90	F-4C	LM INBD

STORE
MK-84 TIPS EXTENDED
MK-84 TIPS EXTENDED
MK-84 TIPS EXTENDED
MK-84 TIPS EXTENDED



i. $M_\infty = 0.90$, tips extended
Figure 19. Continued.

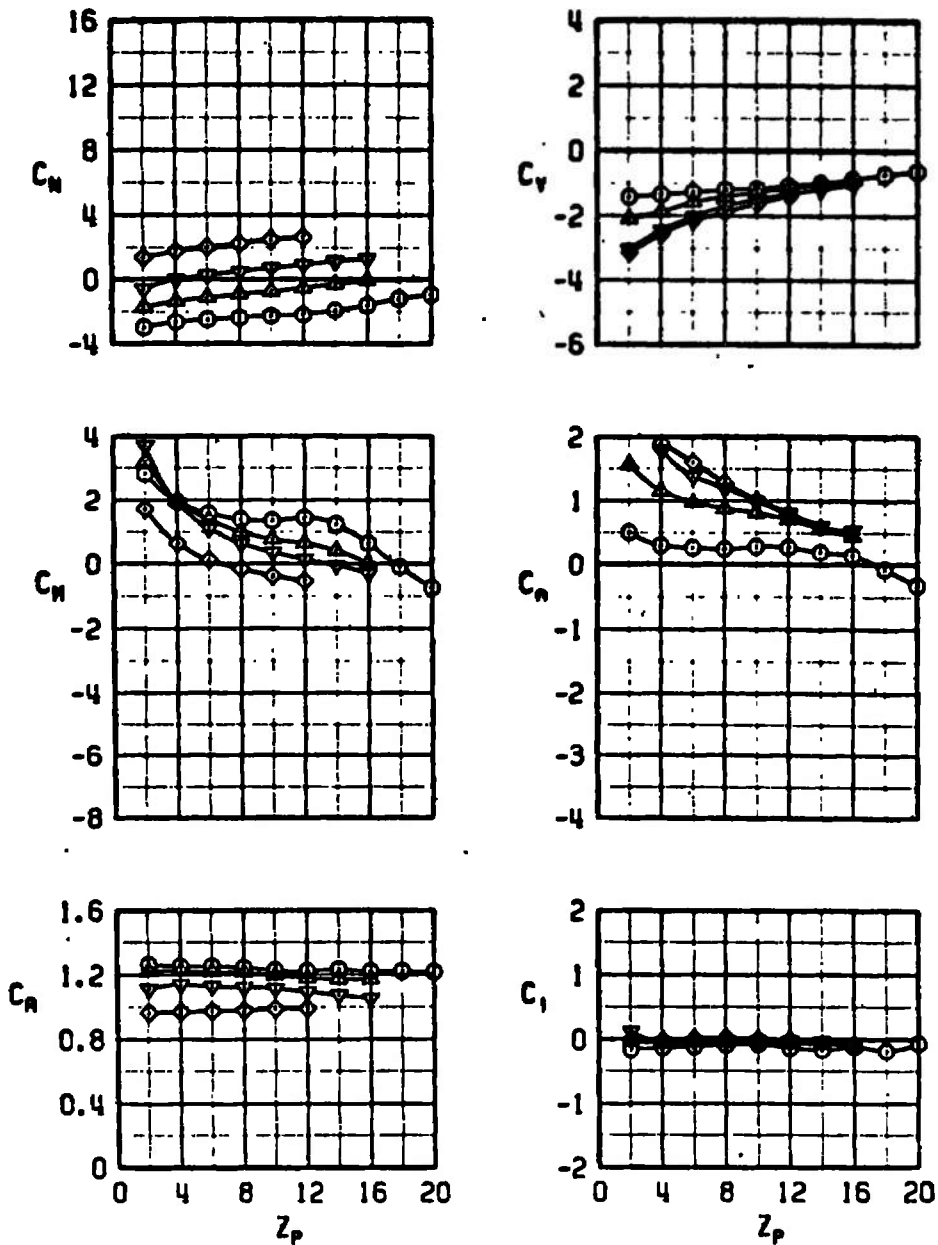
SYM	α	NL	M/C	PTLON	STORE
○	0	0.95	F-4C	LN INBD	MK-84 TIPS EXTENDED
▲	2	0.95	F-4C	LN INBD	MK-84 TIPS EXTENDED
▼	4	0.95	F-4C	LN INBD	MK-84 TIPS EXTENDED
◇	6	0.95	F-4C	LN INBD	MK-84 TIPS EXTENDED



j. $M_\infty = 0.95$, tips extended
Figure 19. Continued.

SYM	α	M_∞	A/C	PYLON
○	0	1.05	F-4C	LN IN80
△	2	1.05	F-4C	LN IN80
▽	4	1.05	F-4C	LN IN80
◇	6	1.05	F-4C	LN IN80

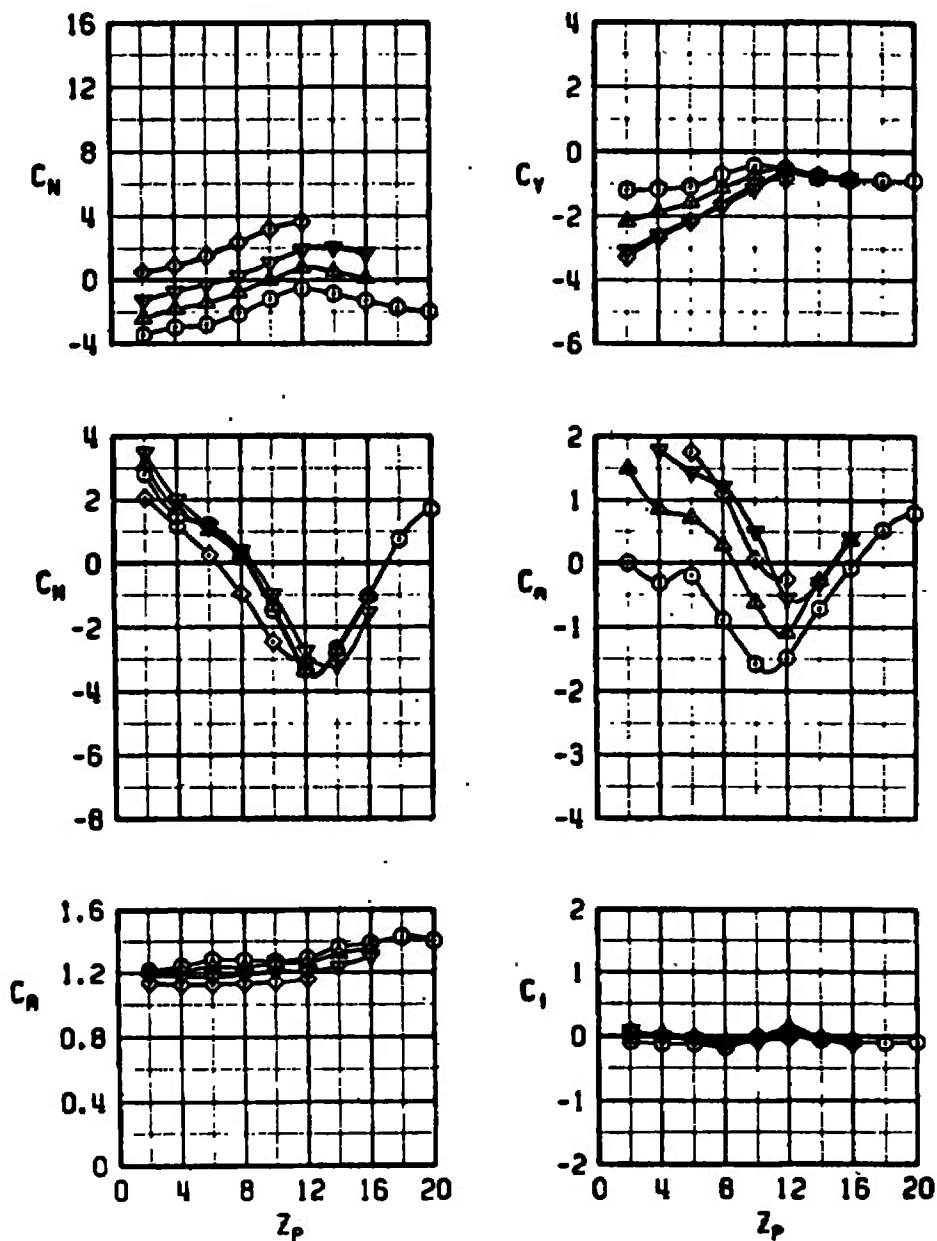
STORE
HK-84 TIPS EXTENDED
HK-84 TIPS EXTENDED
HK-84 TIPS EXTENDED
HK-84 TIPS EXTENDED



k. $M_\infty = 1.05$, tips extended
Figure 19. Continued.

SYM	α	M_∞	A/C	PYLON
○	0	1.20	F-4C	LW INBD
△	2	1.20	F-4C	LW INBD
▽	4	1.20	F-4C	LW INBD
◇	6	1.20	F-4C	LW INBD

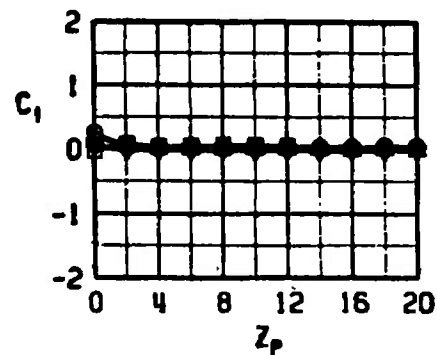
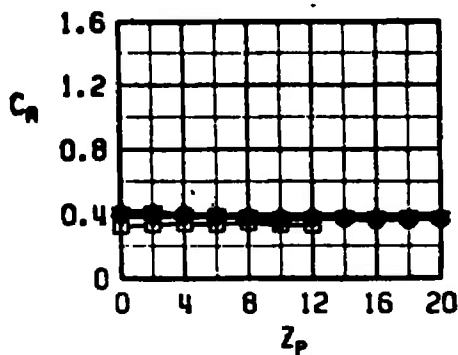
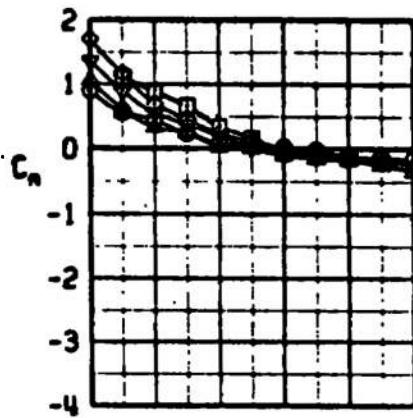
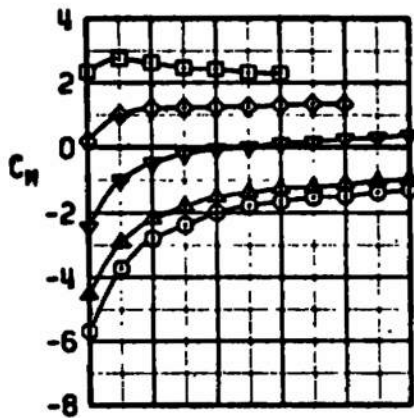
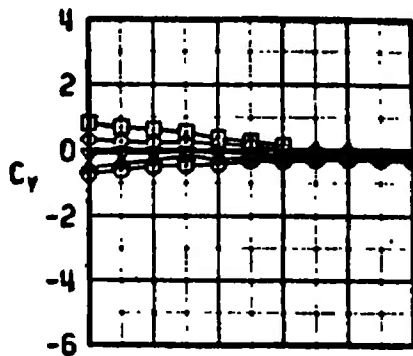
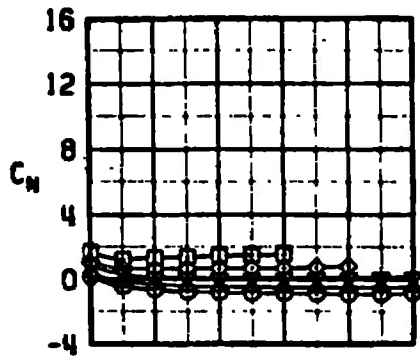
STORE
MK-84 TIPS EXTENDED
MK-84 TIPS EXTENDED
MK-84 TIPS EXTENDED
MK-84 TIPS EXTENDED



I. $M_\infty = 1.20$, tips extended
Figure 19. Concluded.

SYM	n	M _∞	A/C	PYLON
○	1	0.65	A-7D	RW CNTR
△	2	0.65	A-7D	RW CNTR
▽	4	0.65	A-7D	RW CNTR
◇	6	0.65	A-7D	RW CNTR
□	8	0.65	A-7D	RW CNTR

STORE
MK-84 TIPS RETRACTED
MK-84 TIPS RETRACTED
MK-84 TIPS RETRACTED
MK-84 TIPS RETRACTED
MK-84 TIPS RETRACTED

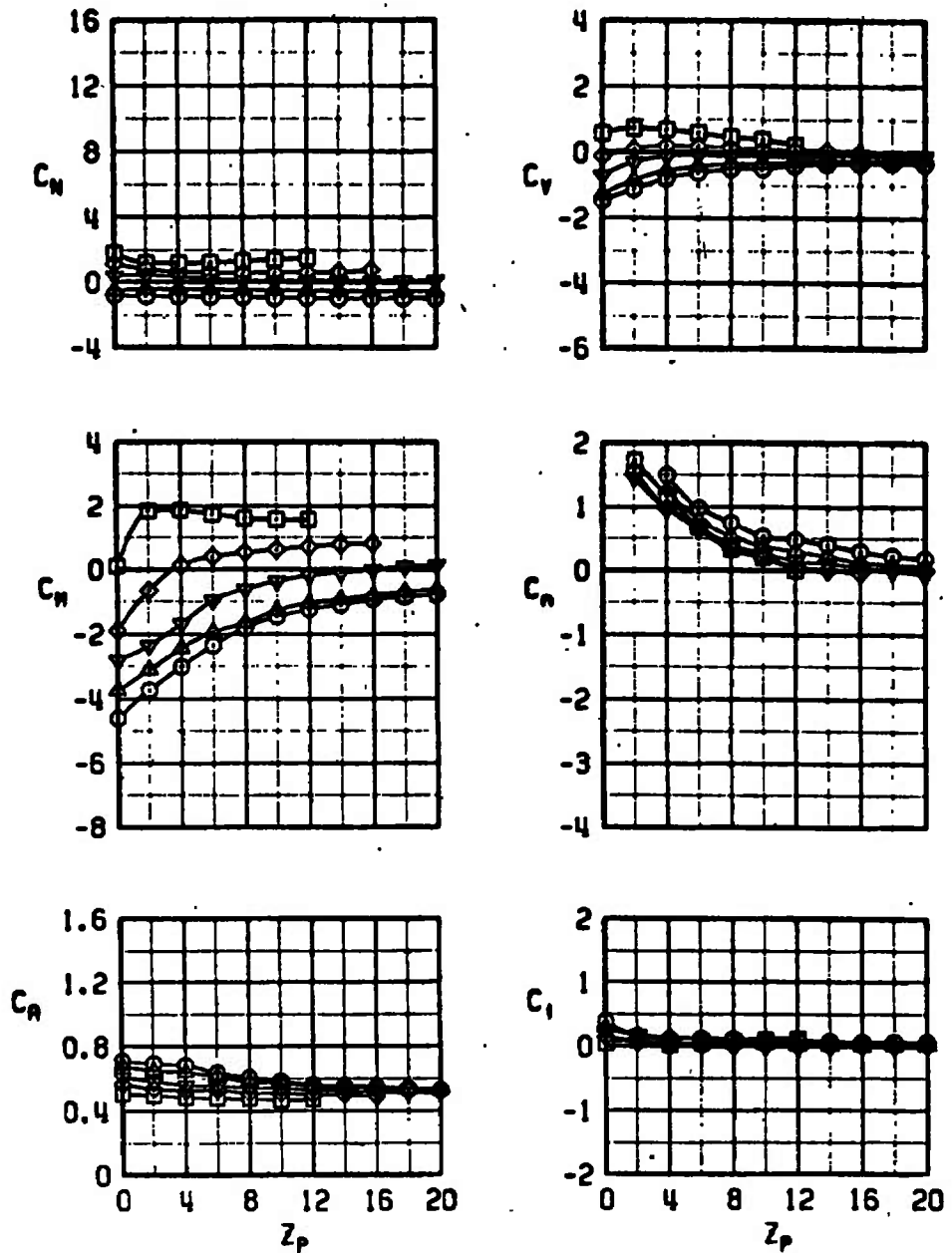


a. $M_{\infty} = 0.65$, tips retracted

Figure 20. Aerodynamic characteristics of the MK-84 store in the A-7D flow field, $Y_p = 0$, $\beta = 0$.

SYM	α	M_∞	A/C	PYLON
○	1	0.90	A-7D	RW CNTR
▲	2	0.90	A-7D	RW CNTR
▼	4	0.90	A-7D	RW CNTR
◇	6	0.90	A-7D	RW CNTR
□	8	0.90	A-7D	RW CNTR

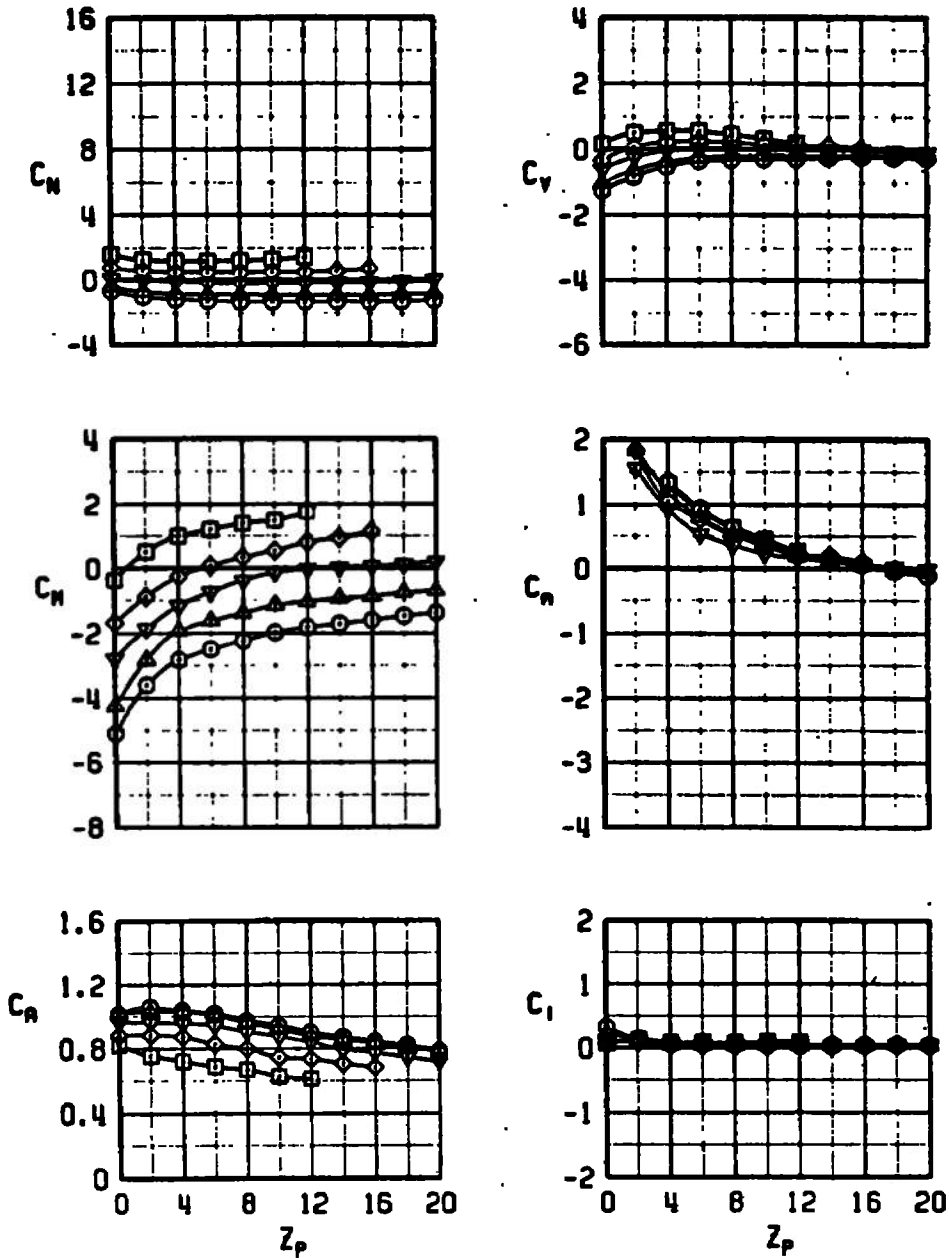
STORE
 MK-84 TIPS RETRACTED
 MK-84 TIPS RETRACTED
 MK-84 TIPS RETRACTED
 MK-84 TIPS RETRACTED
 MK-84 TIPS RETRACTED



b. $M_\infty = 0.90$, tips retracted
 Figure 20. Continued.

SYM	α	M_∞	A/C	PYLON
○	1	0.95	A-7D	RW CNTR
△	2	0.95	A-7D	RW CNTR
▽	4	0.95	A-7D	RW CNTR
◇	6	0.95	A-7D	RW CNTR
□	8	0.95	A-7D	RW CNTR

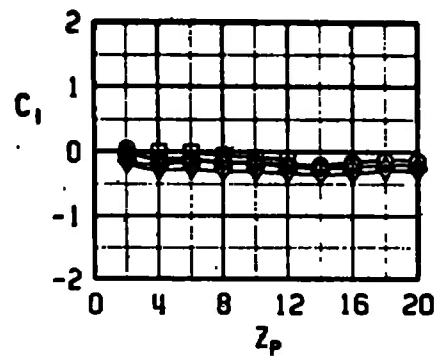
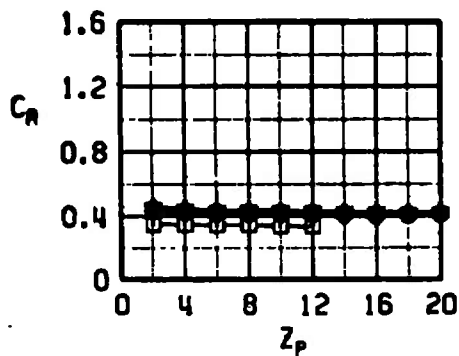
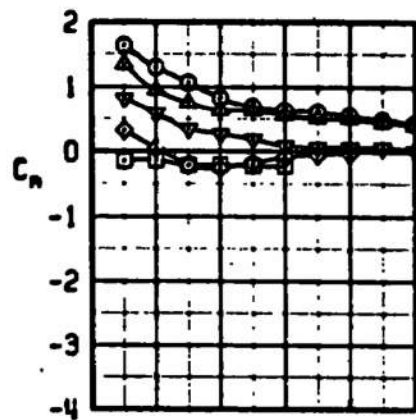
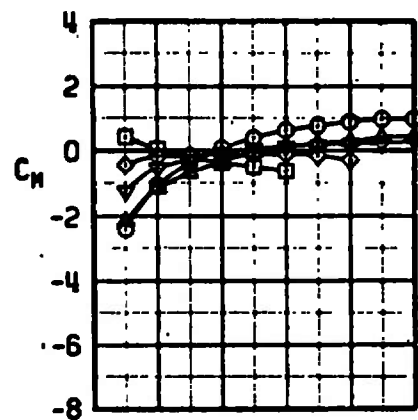
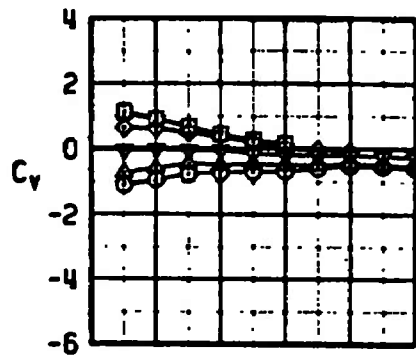
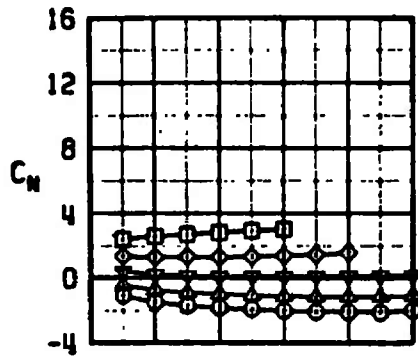
STORE
NK-04 TIPS RETRACTED
NK-04 TIPS RETRACTED
NK-04 TIPS RETRACTED
NK-04 TIPS RETRACTED
NK-04 TIPS RETRACTED



c. $M_\infty = 0.95$, tips retracted
Figure 20. Continued.

SYM	n	M_∞	A/C	PYLON
○	1	0.65	A-7D	RW CNTR
▲	2	0.65	A-7D	RW CNTR
▼	4	0.65	A-7D	RW CNTR
◇	6	0.65	A-7D	RW CNTR
□	8	0.65	A-7D	RW CNTR

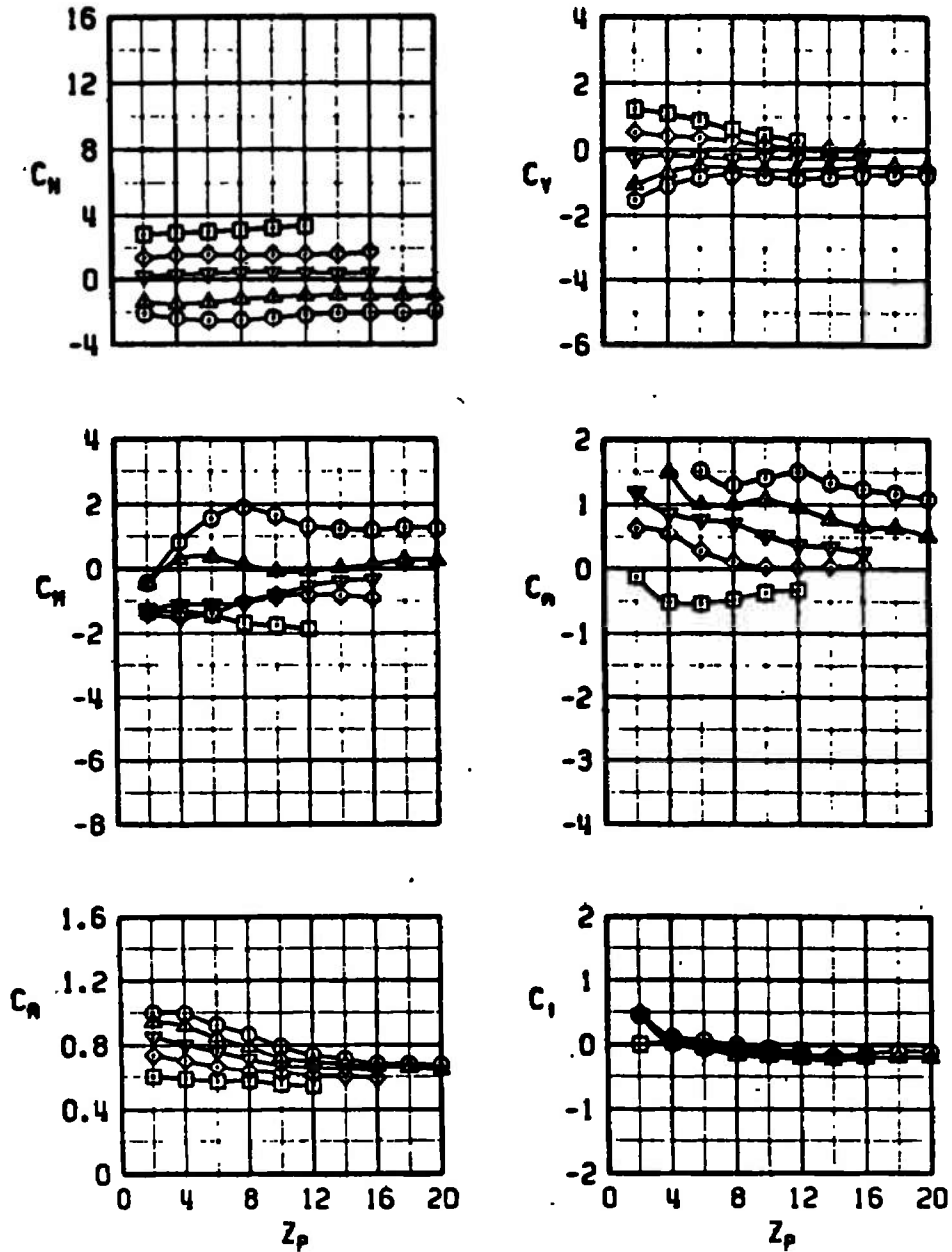
STORE
MK-84 TIPS EXTENDED
MK-84 TIPS EXTENDED
MK-84 TIPS EXTENDED
MK-84 TIPS EXTENDED
MK-84 TIPS EXTENDED



d. $M_\infty = 0.65$, tips extended
Figure 20. Continued.

SYM	α	M_∞	A/C	PYLON
○	1	0.90	A-7D	RW CNTR
△	2	0.90	A-7D	RW CNTR
▽	4	0.90	A-7D	RW CNTR
◇	6	0.90	A-7D	RW CNTR
□	8	0.90	A-7D	RW CNTR

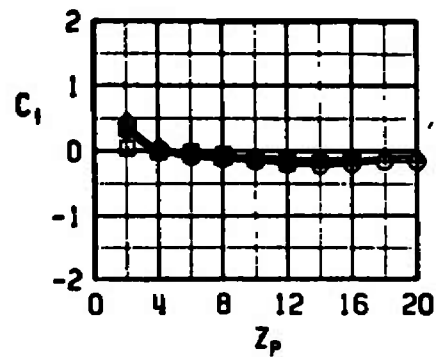
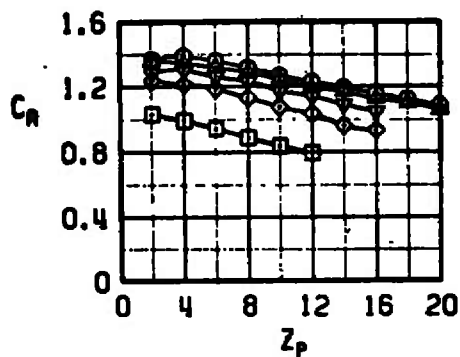
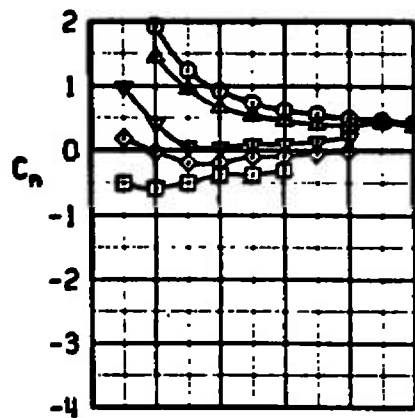
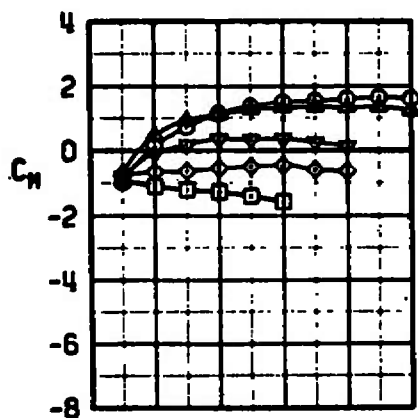
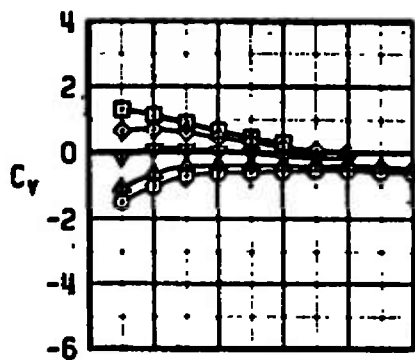
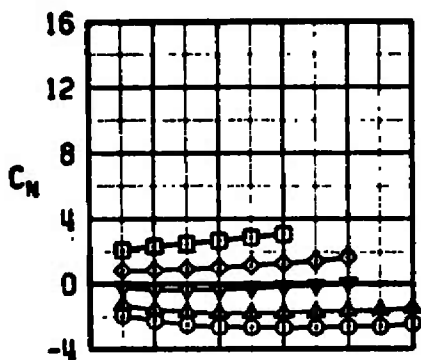
STORE
HK-84 TIPS EXTENDED
HK-84 TIPS EXTENDED
HK-84 TIPS EXTENDED
HK-84 TIPS EXTENDED
HK-84 TIPS EXTENDED



e. $M_\infty = 0.90$, tips extended
Figure 20. Continued.

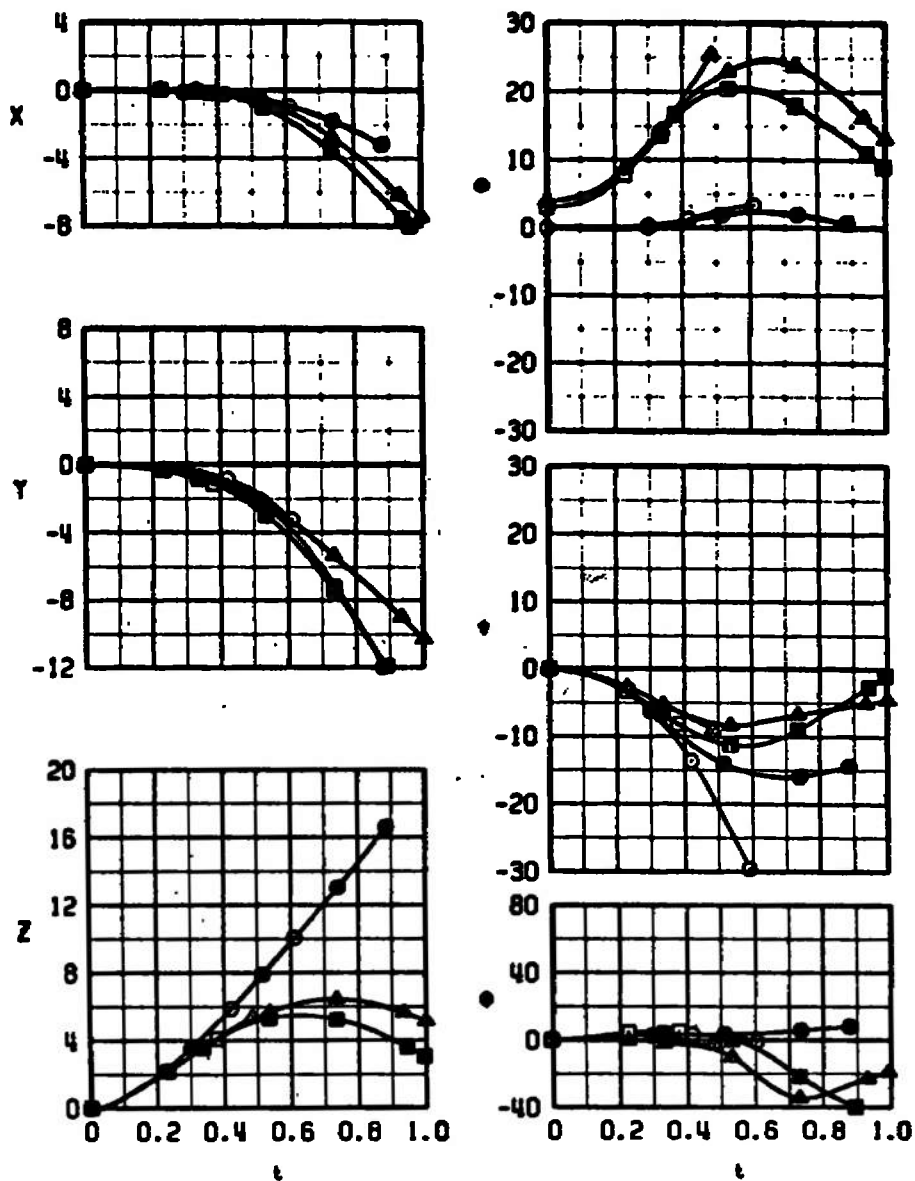
SYM	a	M_∞	A/C	PYLON
○	1	0.95	A-7D	PM CNTR
△	2	0.95	A-7D	PM CNTR
▽	4	0.95	A-7D	PM CNTR
◇	6	0.95	A-7D	PM CNTR
□	8	0.95	A-7D	PM CNTR

STORE
 MK-84 TIPS EXTENDED
 MK-84 TIPS EXTENDED
 MK-84 TIPS EXTENDED
 MK-84 TIPS EXTENDED
 MK-84 TIPS EXTENDED



f. $M_\infty = 0.95$, tips extended
 Figure 20. Concluded.

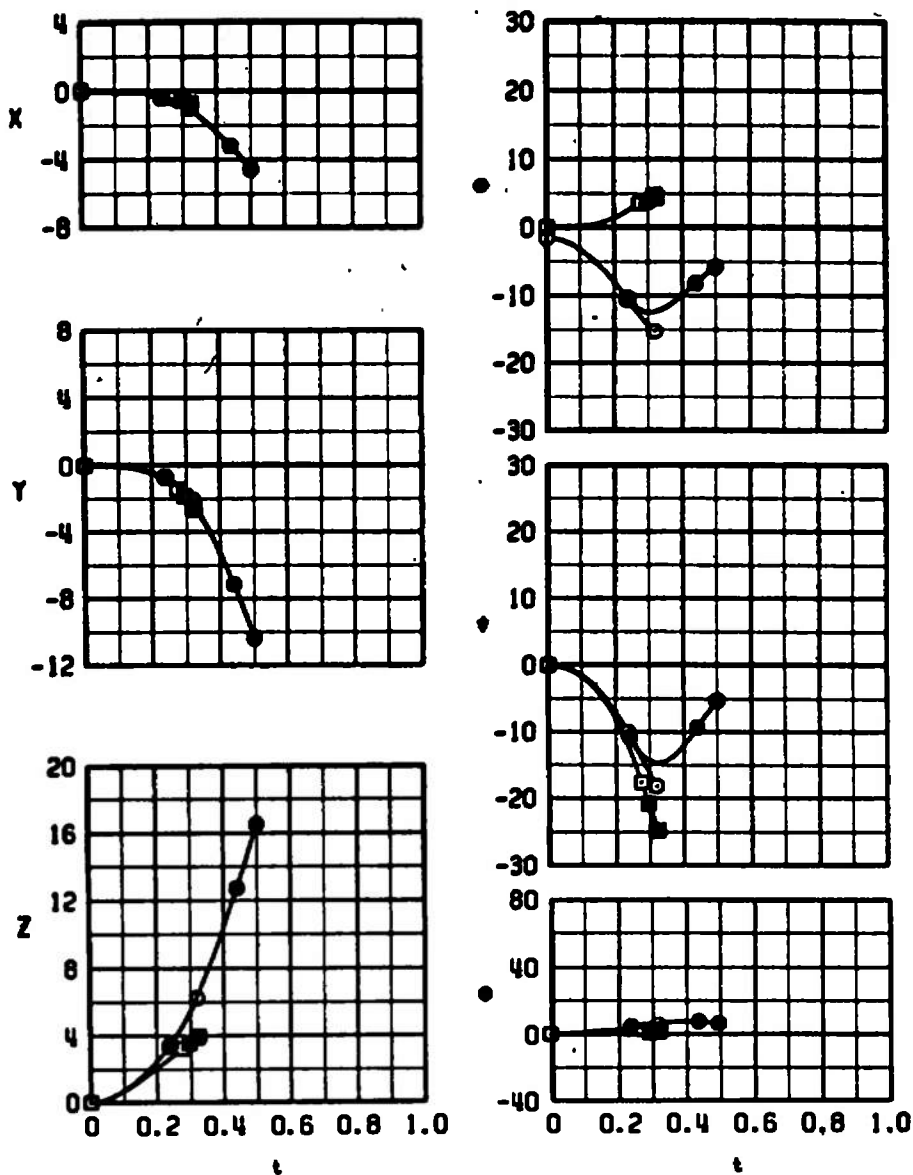
SYMBOL	M_∞	α	CONFIG	ALTITUDE	DIVE	TIPS
○	0.65	1.0	I	20K	0	RETRACTED
□	0.65	4.0	I	20K	0	RETRACTED
△	0.65	4.8	I	25K	0	RETRACTED
●	0.65	1.0	II	20K	0	EXTENDED
■	0.65	4.0	II	20K	0	EXTENDED
▲	0.65	4.8	II	25K	0	EXTENDED



a. Variation with α , $M_\infty = 0.65$

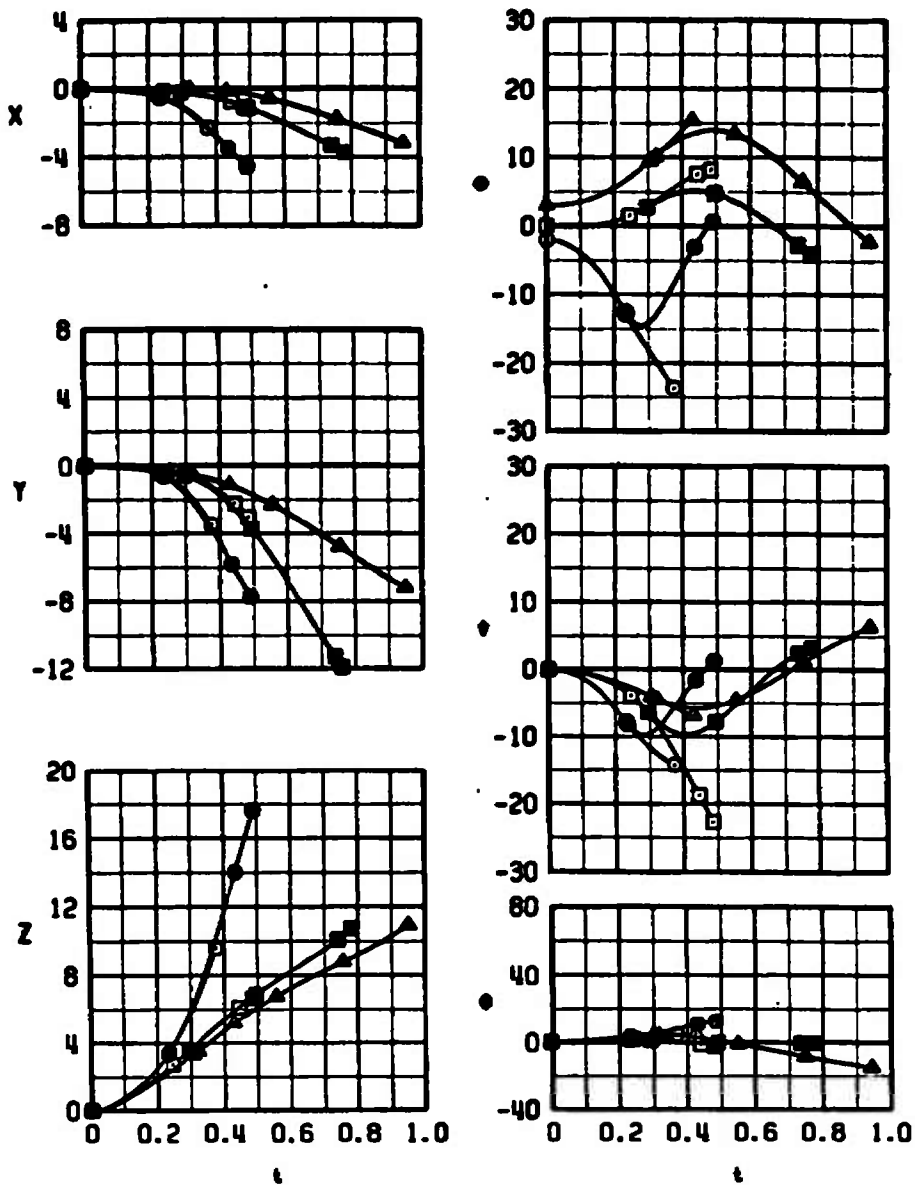
Figure 21. Separation characteristics of the MK-84 store from the F-4C left-wing inboard pylon with no adjacent stores.

SYMBOL	M_∞	α	CONFIG	ALTITUDE	DIVE	TIPS
○	0.80	-0.6	I	SL	0	RETRACTED
□	0.80	1.0	I	SL	0	RETRACTED
●	0.80	-0.6	II	SL	0	EXTENDED
■	0.80	1.0	II	SL	0	EXTENDED



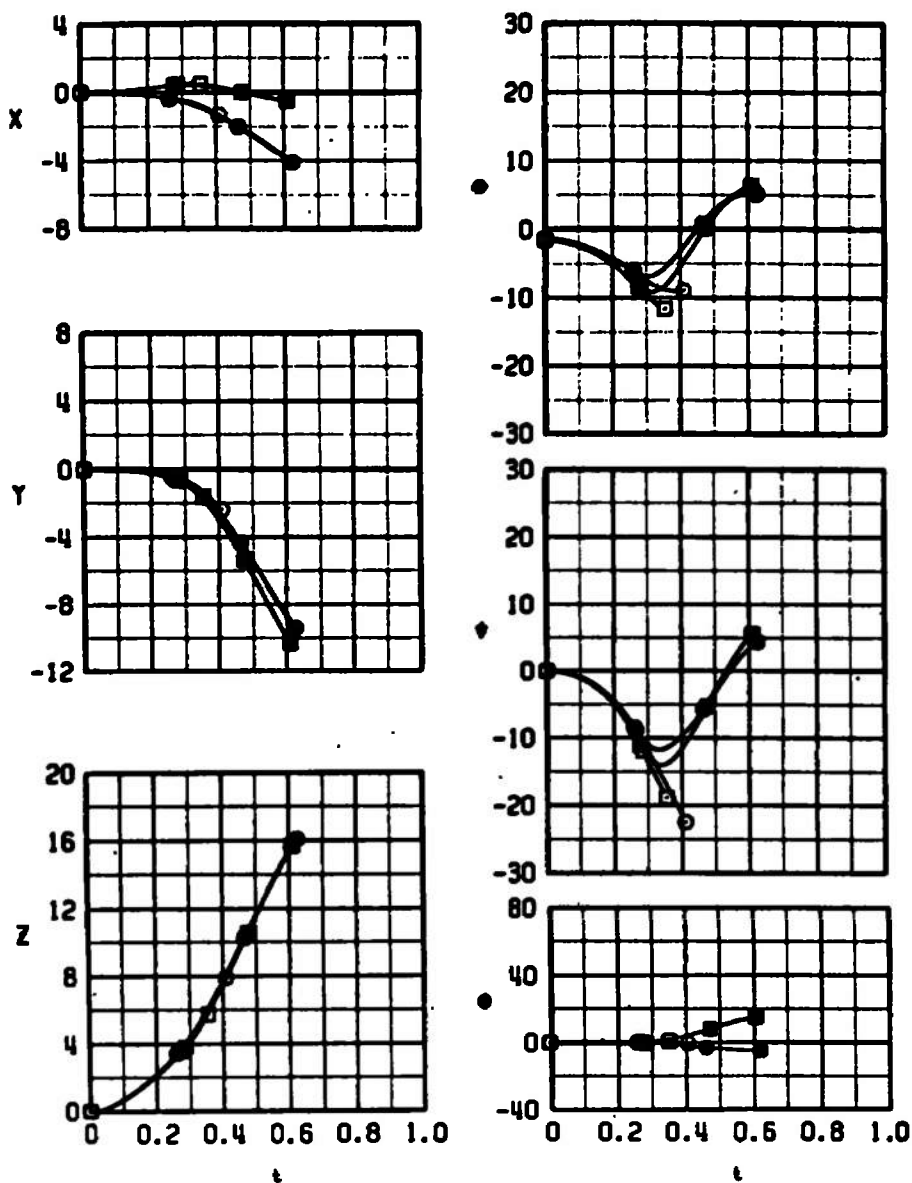
b. Variation with α , $M_\infty = 0.80$
Figure 21. Continued.

SYMBOL	M_∞	α	CONFIG	ALTITUDE	DIVE	TIPS
○	0.90	-1.0	1	5K	0	RETRACTED
□	0.90	1.0	1	20K	0	↓
△	0.90	4.0	1	40K	0	EXTENDED
●	0.90	-1.0	11	5K	0	↓
■	0.90	1.0	11	20K	0	EXTENDED
▲	0.90	4.0	11	40K	0	↓



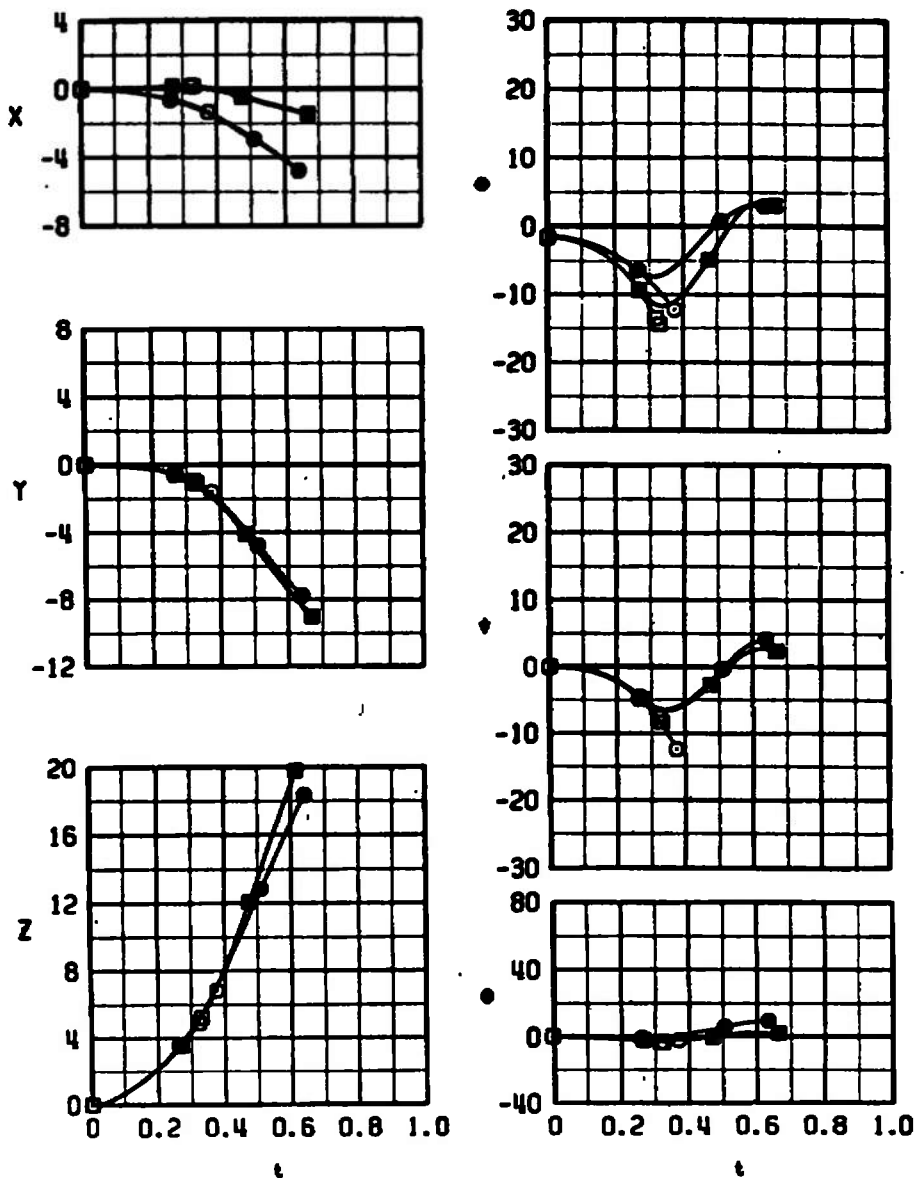
c. Variation with α , $M_\infty = 0.90$
Figure 21. Continued.

SYMBOL	M_∞	α	CONFIG	ALTITUDE	DIVE	TIPS
○	0.95	-0.4	I	20K	0	RETRACTED
□	0.95	-0.6	I	20K	45	↓
●	0.95	-0.4	II	20K	0	EXTENDED
■	0.95	-0.6	II	20K	45	↓



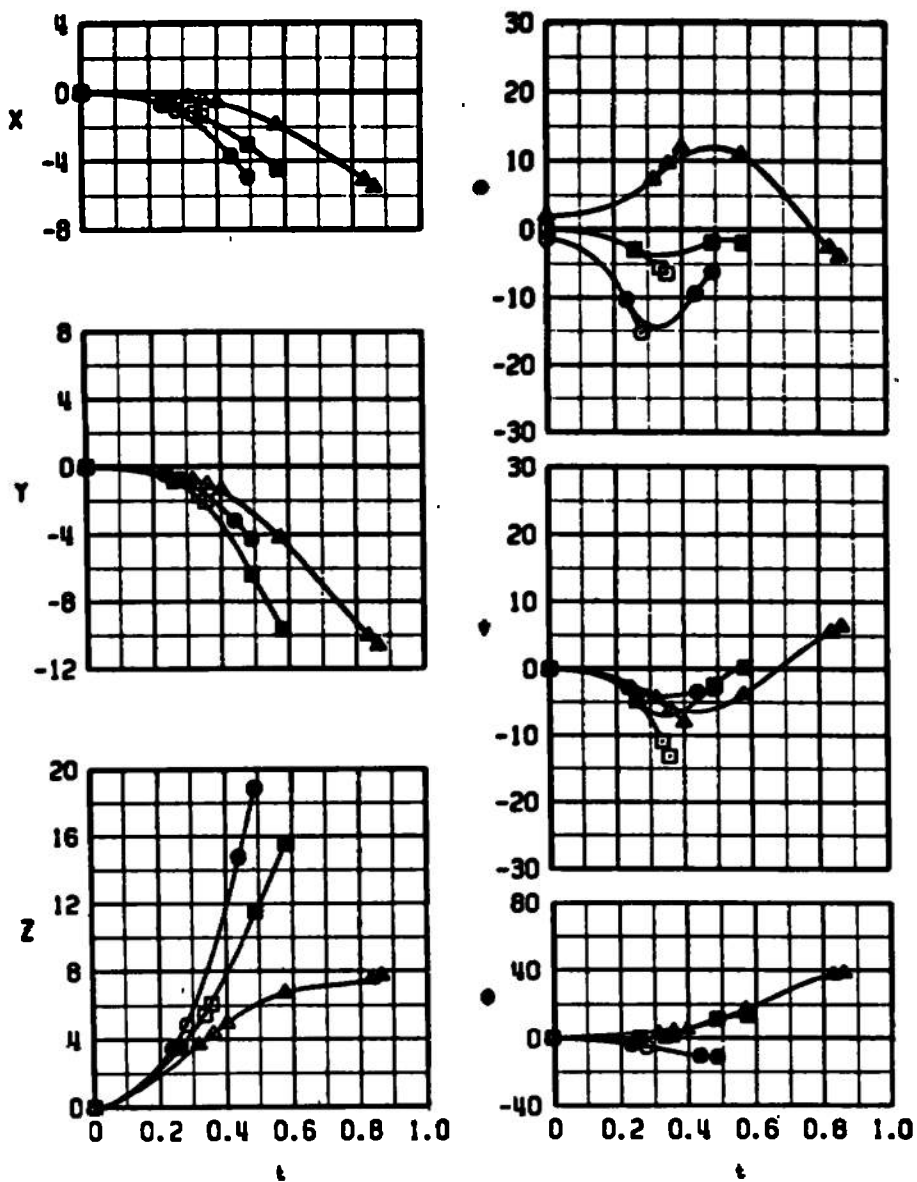
d. Variation with α , $M_\infty = 0.95$
Figure 21. Continued.

SYMBOL	M_∞	α	CONFIG	ALTITUDE	DIVE	TIPS
○	1.05	-0.4	I	20K	0	RETRACTED
□	1.05	-0.6	I	20K	45	↓
●	1.05	-0.4	II	20K	0	EXTENDED
■	1.05	-0.6	II	20K	45	↓



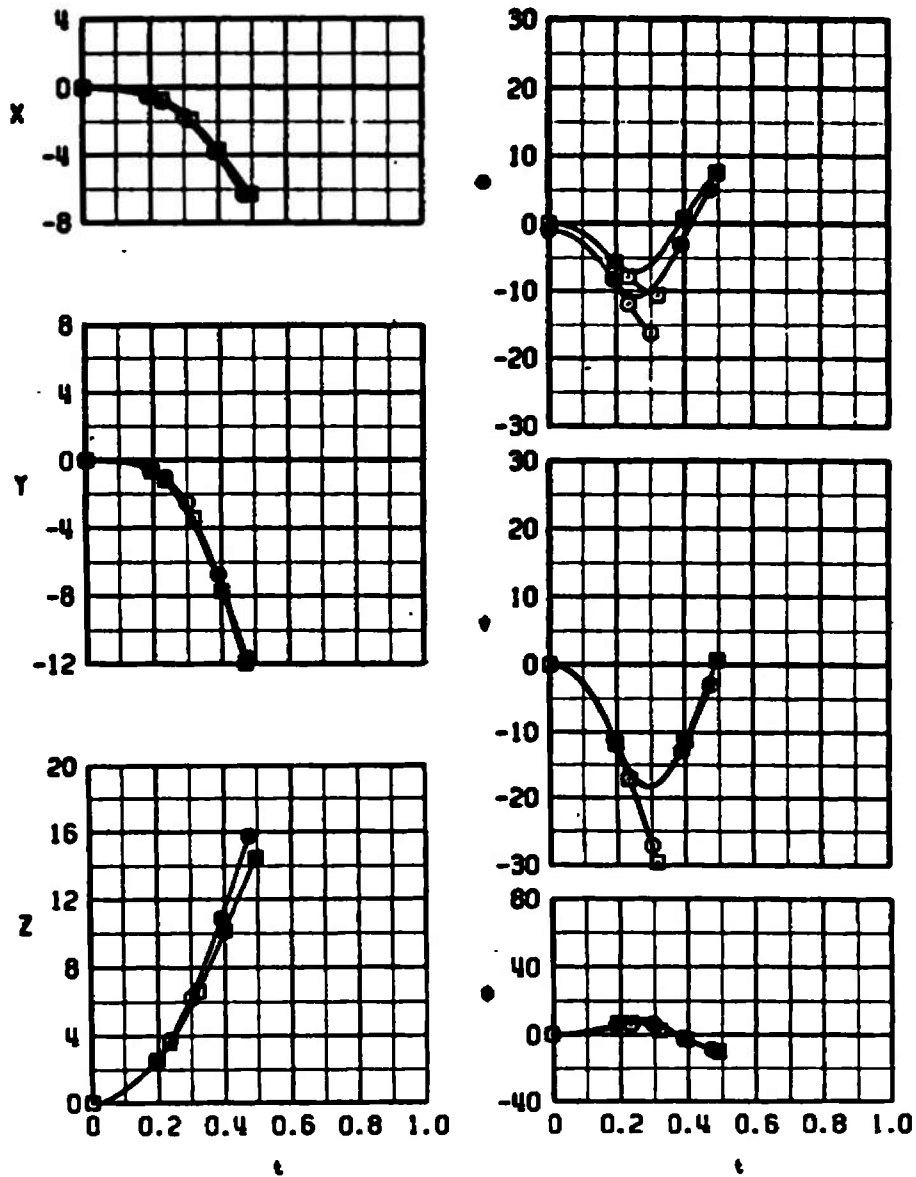
e. Variation with α , $M_\infty = 1.05$
Figure 21. Continued.

SYMBOL	M_∞	α	CONFIG	ALTITUDE	DIVE	TIPS
○	1.20	-0.4	I	20K	0	RETRACTED
□	1.20	1.0	I	20K	0	↓
△	1.20	3.0	I	40K	0	↓
●	1.20	-0.4	II	20K	0	EXTENDED
■	1.20	1.0	II	20K	0	↓
▲	1.20	3.0	II	40K	0	↓



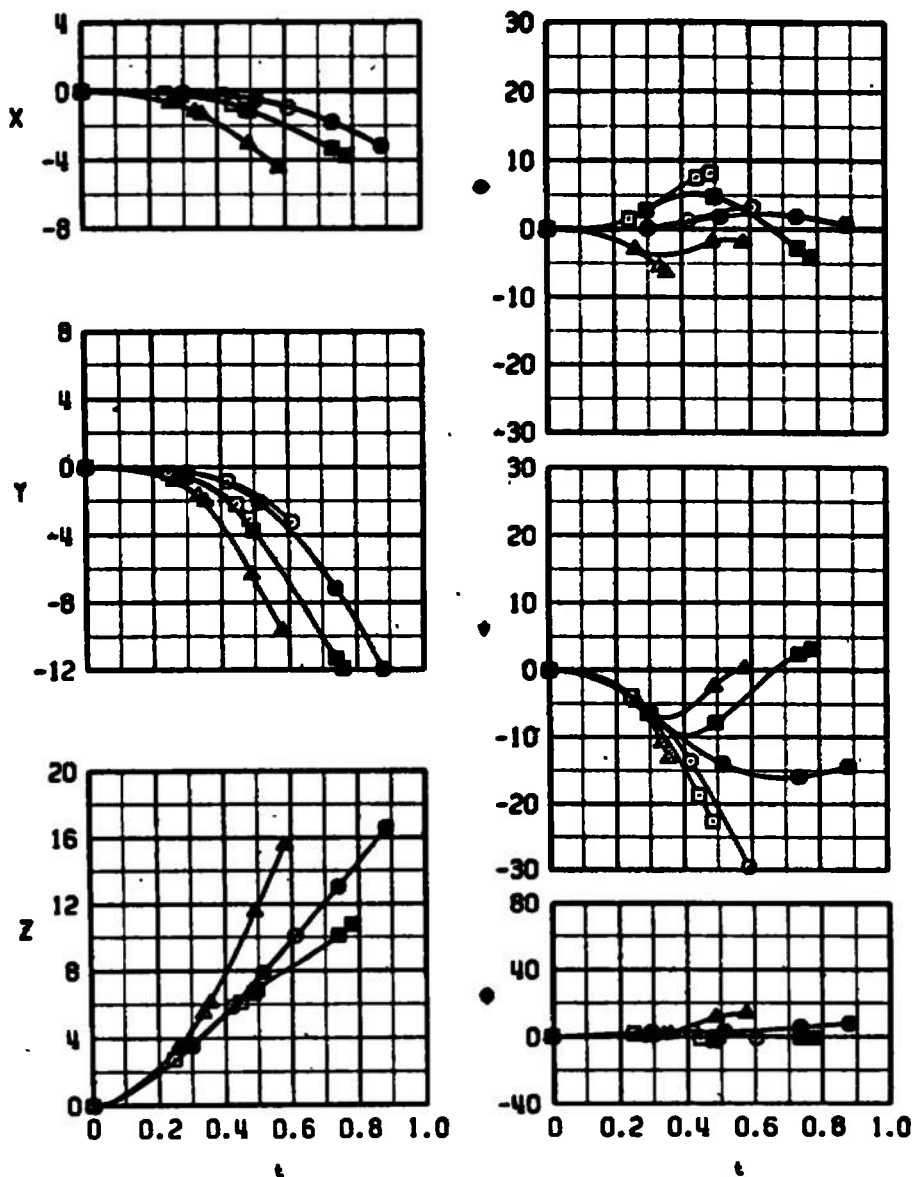
f. Variation with α , $M_\infty = 1.20$
Figure 21. Continued.

SYMBOL	M_∞	α	CONFIG	ALTITUDE	DIVE	TIPS
○	1.60	0.0	I	35K	0	RETRACTED
□	1.60	1.0	I	35K	0	↓
●	1.60	0.0	II	35K	0	EXTENDED
■	1.60	1.0	II	35K	0	↓



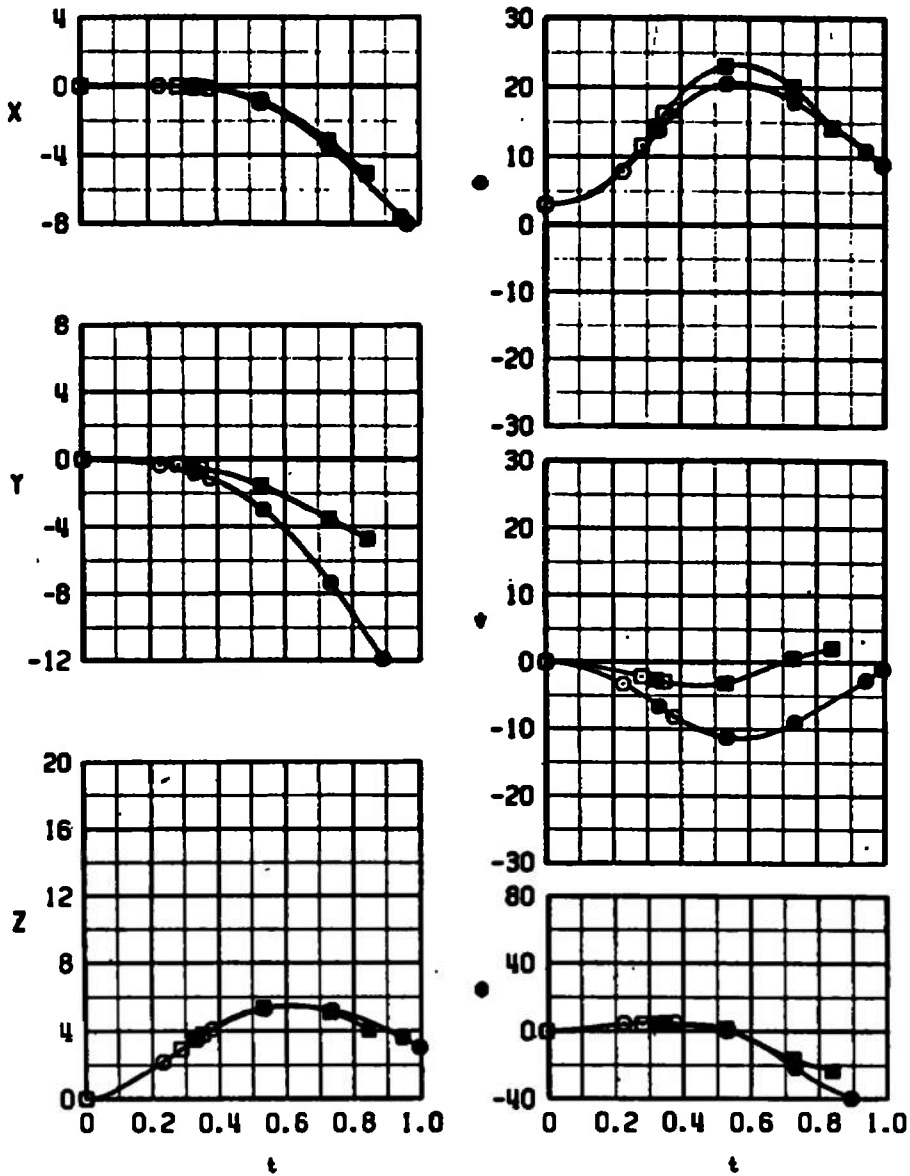
g. Variation with α , $M_\infty = 1.60$
Figure 21. Continued.

SYMBOL	M_∞	α	CONFIG	ALTITUDE	DIVE	TIPS
○	0.65	1.0	I	20K	0	RETRACTED
□	0.90	1.0	I	20K	0	↓
△	1.20	1.0	I	20K	0	↓
●	0.65	1.0	II	20K	0	EXTENDED
■	0.90	1.0	II	20K	0	↓
▲	1.20	1.0	II	20K	0	↓



h. Variation with M_∞ , $\alpha = 1$ deg
Figure 21. Concluded.

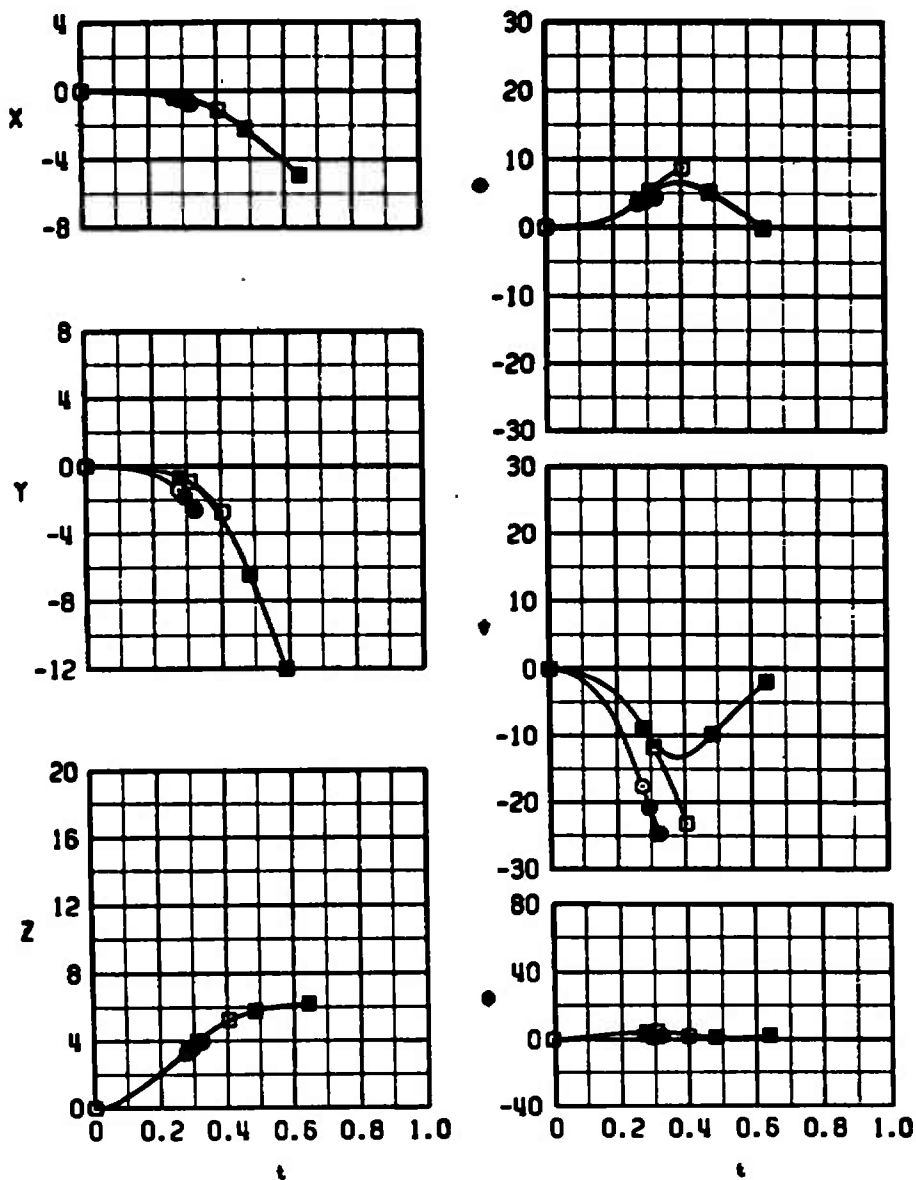
SYMBOL	M_∞	α	CONFIG	ALTITUDE	DIVE	TIPS	TANK
○	0.65	4.0	1	20K	0	RETRACTED	OFF
□	0.65	4.0	2A	20K	0	↓	ON
●	0.65	4.0	11	20K	0	EXTENDED	OFF
■	0.65	4.0	12A	20K	0	↓	ON



a. $M_\infty = 0.65$

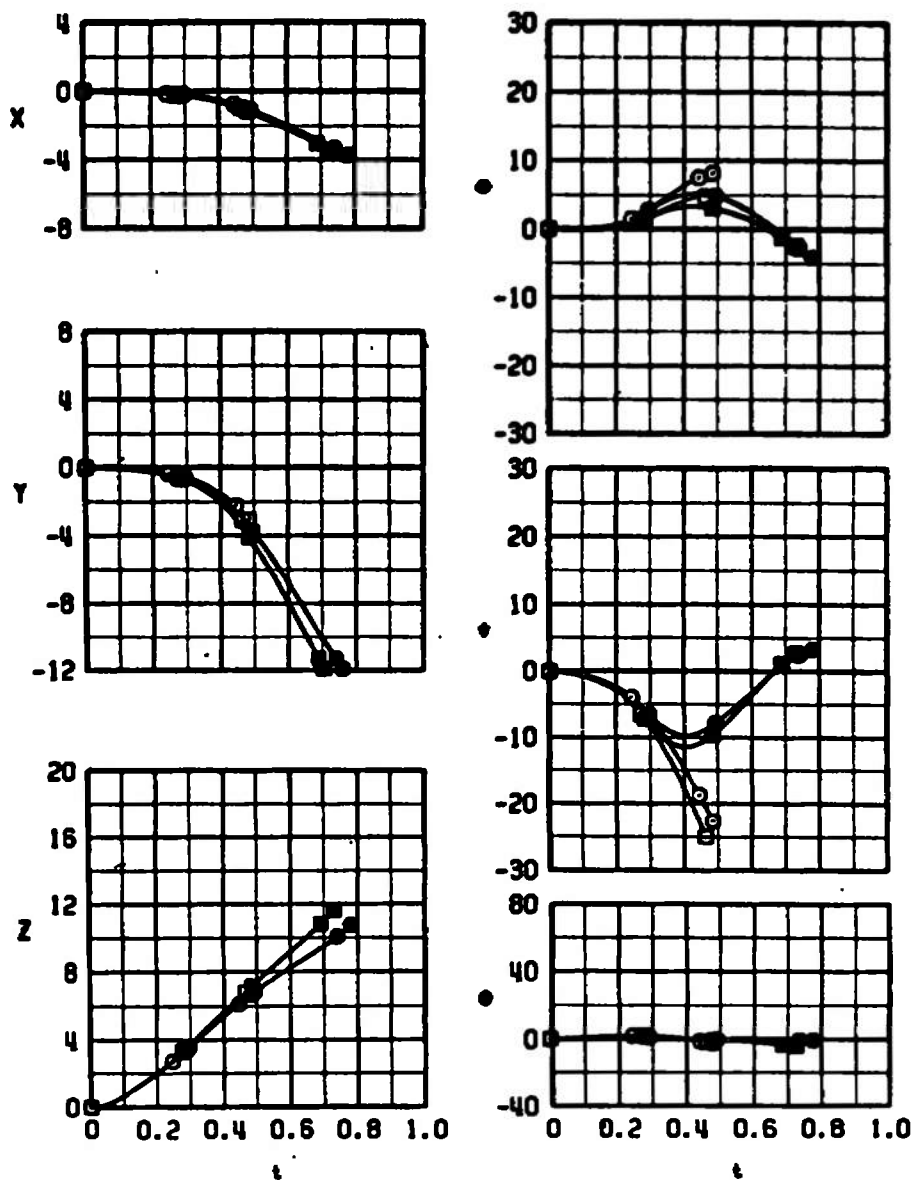
Figure 22. MK-84 trajectory comparisons for the F-4C with and without the 370-gal fuel tank, launch configurations 1 and 2.

SYMBOL	M_∞	α	CONFIG	ALTITUDE	DIVE	TIPS	TANK
○	0.80	1.0	I	SL	0	RETRACTED	OFF
□	0.80	1.0	2A	SL	0	↓	ON
●	0.80	1.0	11	SL	0	EXTENDED	OFF
■	0.80	1.0	12A	SL	0	↓	ON



b. $M_\infty = 0.80$
Figure 22. Concluded.

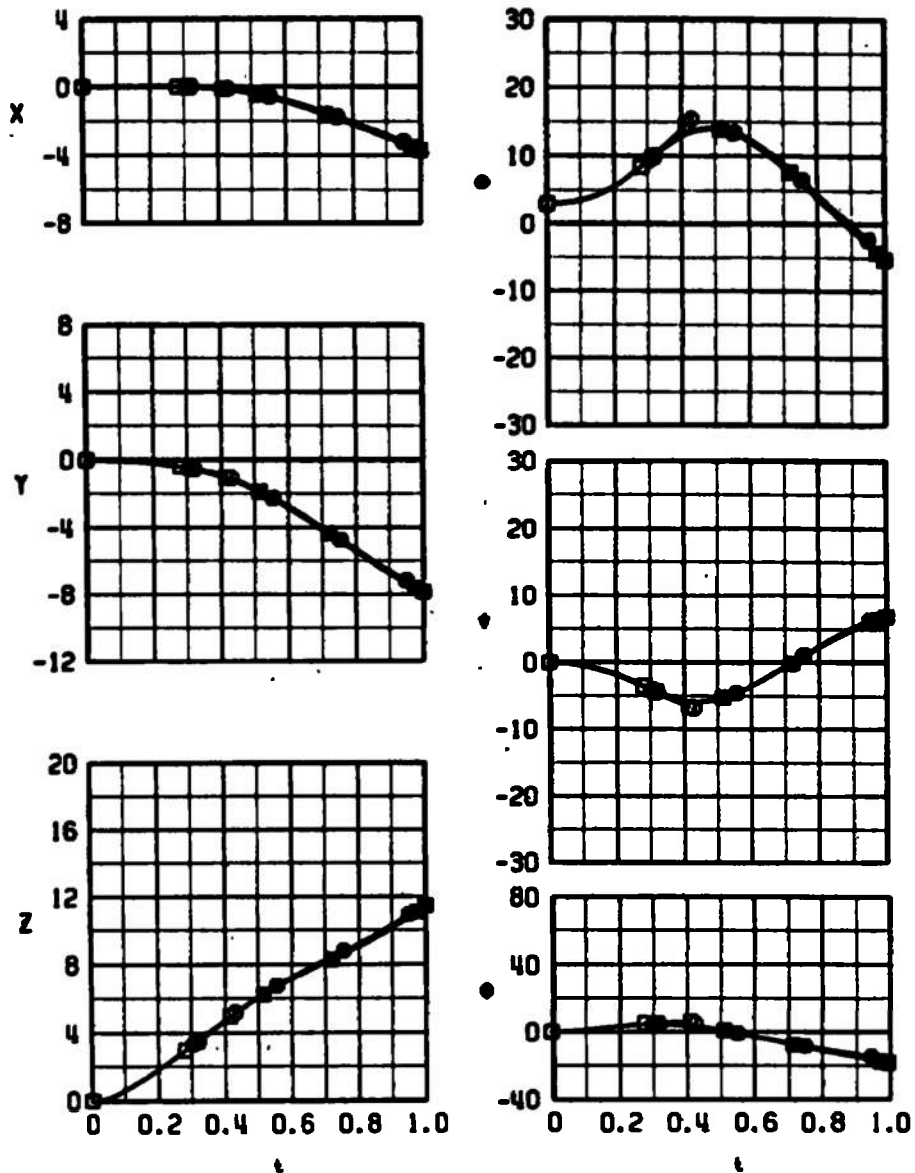
SYMBOL	M _∞	α	CONFIG	ALTITUDE	DIVE	TIPS	POD
○	0.90	1.0	1	20K	0	RETRACTED	OFF
◻	0.90	1.0	4	20K	0	↓	ON
●	0.90	1.0	11	20K	0	EXTENDED	OFF
■	0.90	1.0	14	20K	0	↓	ON



a. $M_{\infty} = 0.90$, $\alpha = 1$ deg

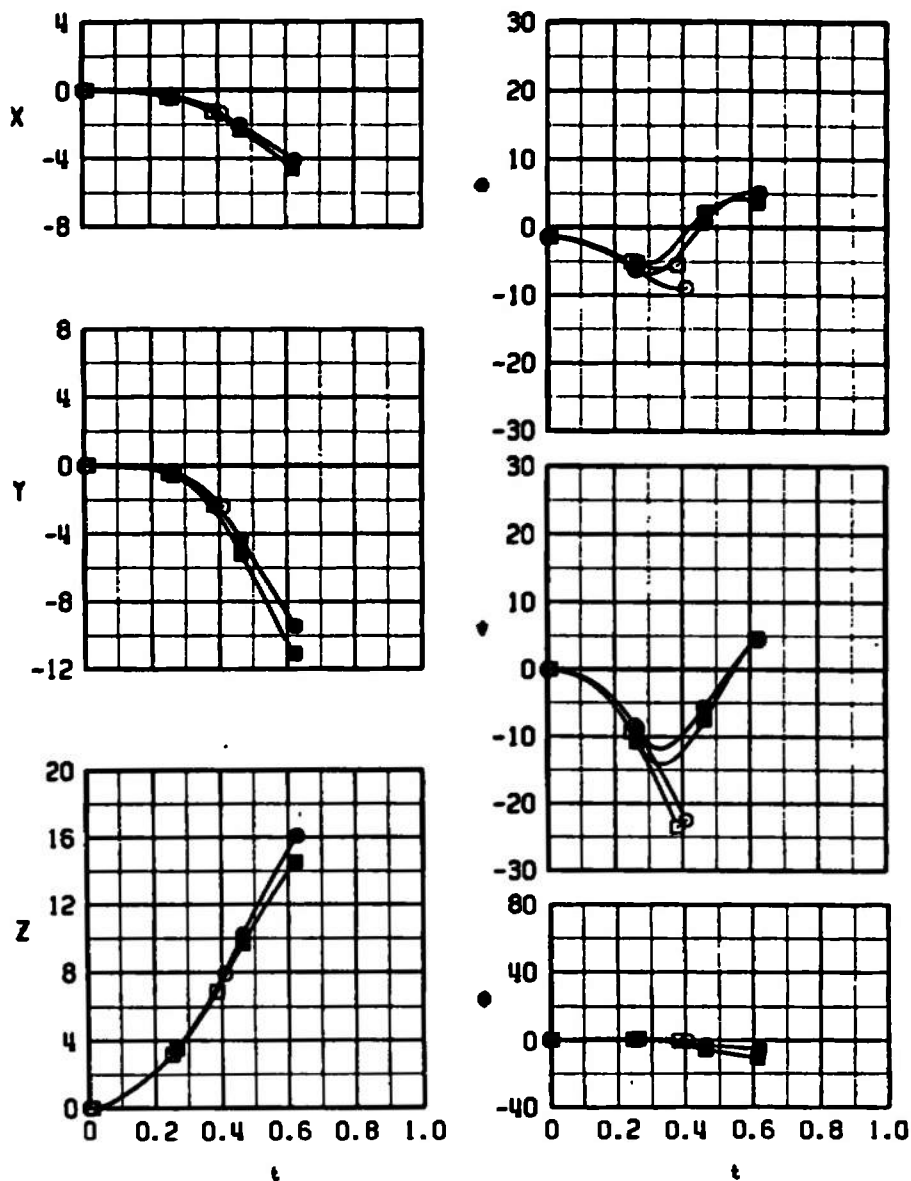
Figure 23. MK-84 trajectory comparisons for the F-4C with and without the data link pod, launch configurations 1 and 4.

SYMBOL	M_∞	α	CONFIG	ALTITUDE	DIVE	TIPS	POD
○	0.90	4.0	1	40K	0	RETRACTED	OFF
□	0.90	4.0	4	40K	0	↓	ON
●	0.90	4.0	11	40K	0	EXTENDED	OFF
■	0.90	4.0	14	40K	0	↓	ON



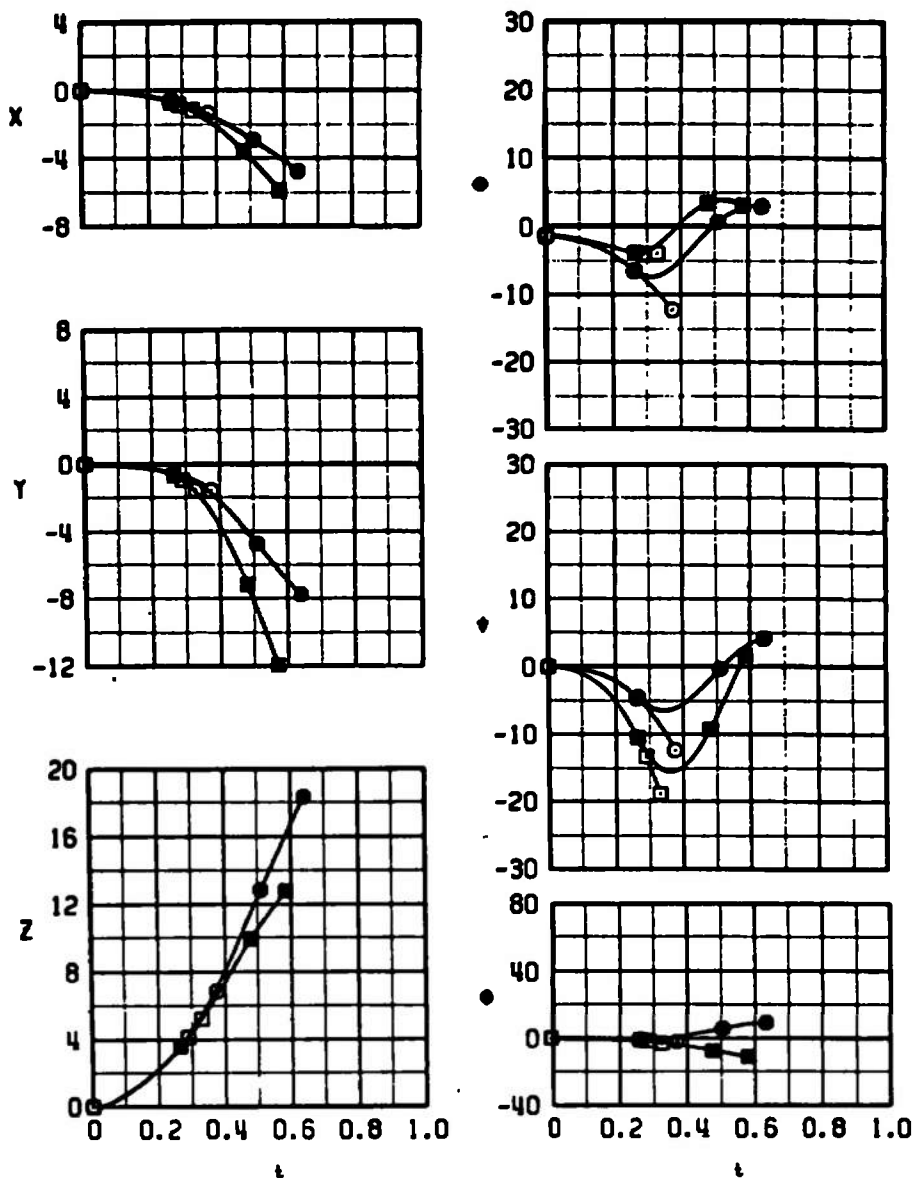
b. $M_\infty = 0.90$, $\alpha = 4$ deg
Figure 23. Continued.

SYMBOL	M_∞	α	CONFIG	ALTITUDE	DIVE	TIPS	POD
○	0.95	-0.4	1	20K	0	RETRACTED	OFF
□	0.95	-0.4	4	20K	0	↓	ON
●	0.95	-0.4	11	20K	0	EXTENDED	OFF
■	0.95	-0.4	14	20K	0	↓	ON



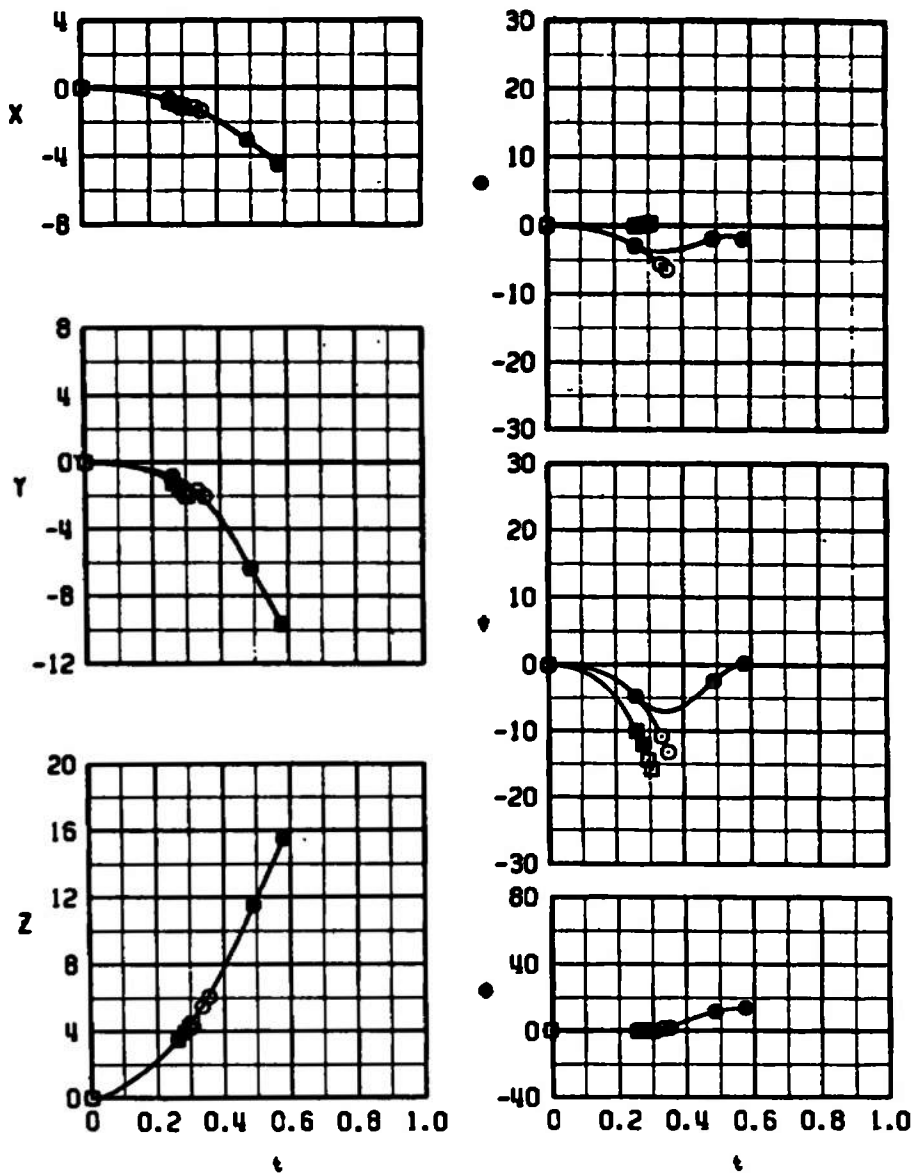
c. $M_\infty = 0.95$, $\alpha = -0.4$ deg
Figure 23. Continued.

SYMBOL	M_∞	α	CONFIG	ALTITUDE	DIVE	TIPS	POD
○	1.05	-0.4	1	20K	0	RETRACTED	OFF
□	1.05	-0.4	4	20K	0	↓	ON
●	1.05	-0.4	11	20K	0	EXTENDED	OFF
■	1.05	-0.4	14	20K	0	↓	ON



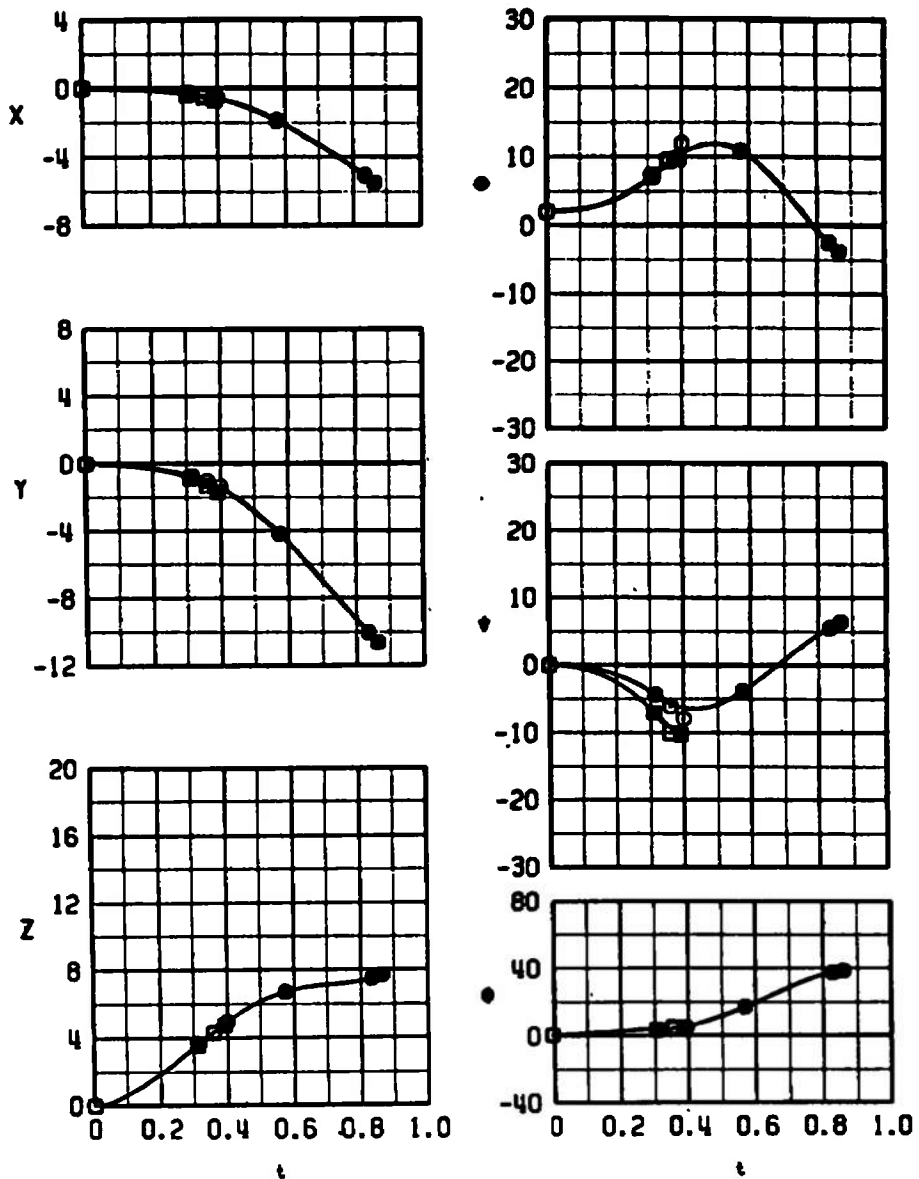
d. $M_\infty = 1.05$, $\alpha = -0.4$ deg
Figure 23. Continued.

SYMBOL	M_∞	α	CONFIG	ALTITUDE	DIVE	TIPS	POD
○	1.20	1.0	1	20K	0	RETRACTED	OFF
□	1.20	1.0	4	20K	0	↓	ON
●	1.20	1.0	11	20K	0	EXTENDED	OFF
■	1.20	1.0	14	20K	0	↓	ON



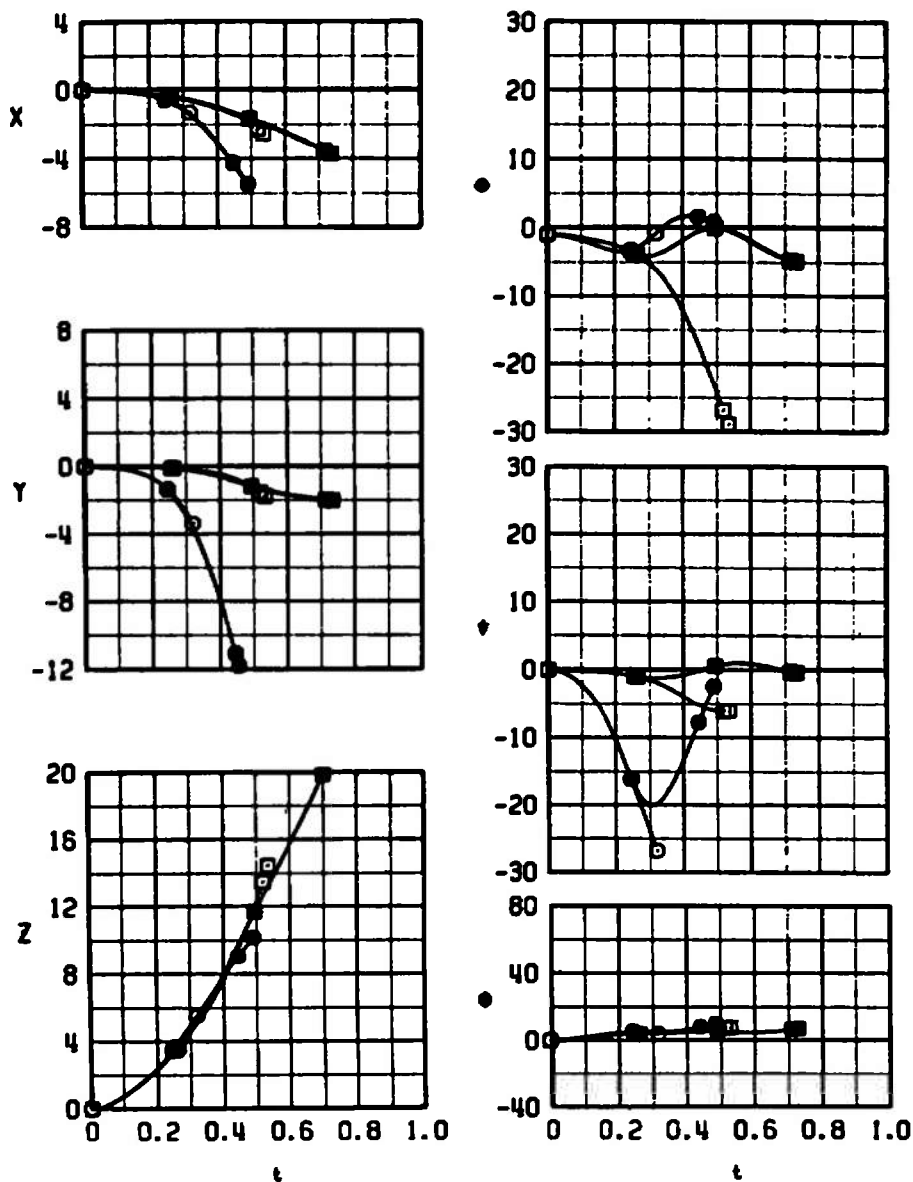
e. $M_\infty = 1.20$, $\alpha = 1$ deg
Figure 23. Continued.

SYMBOL	M_∞	α	CONFIG	ALTITUDE	DIVE	TIPS	POD
○	1.20	3.0	1	40K	0	RETRACTED	OFF
□	1.20	3.0	4	40K	0	↓	ON
●	1.20	3.0	11	40K	0	EXTENDED	OFF
■	1.20	3.0	14	40K	0	↓	ON



f. $M_\infty = 1.20$, $\alpha = 3$ deg
Figure 23. Concluded.

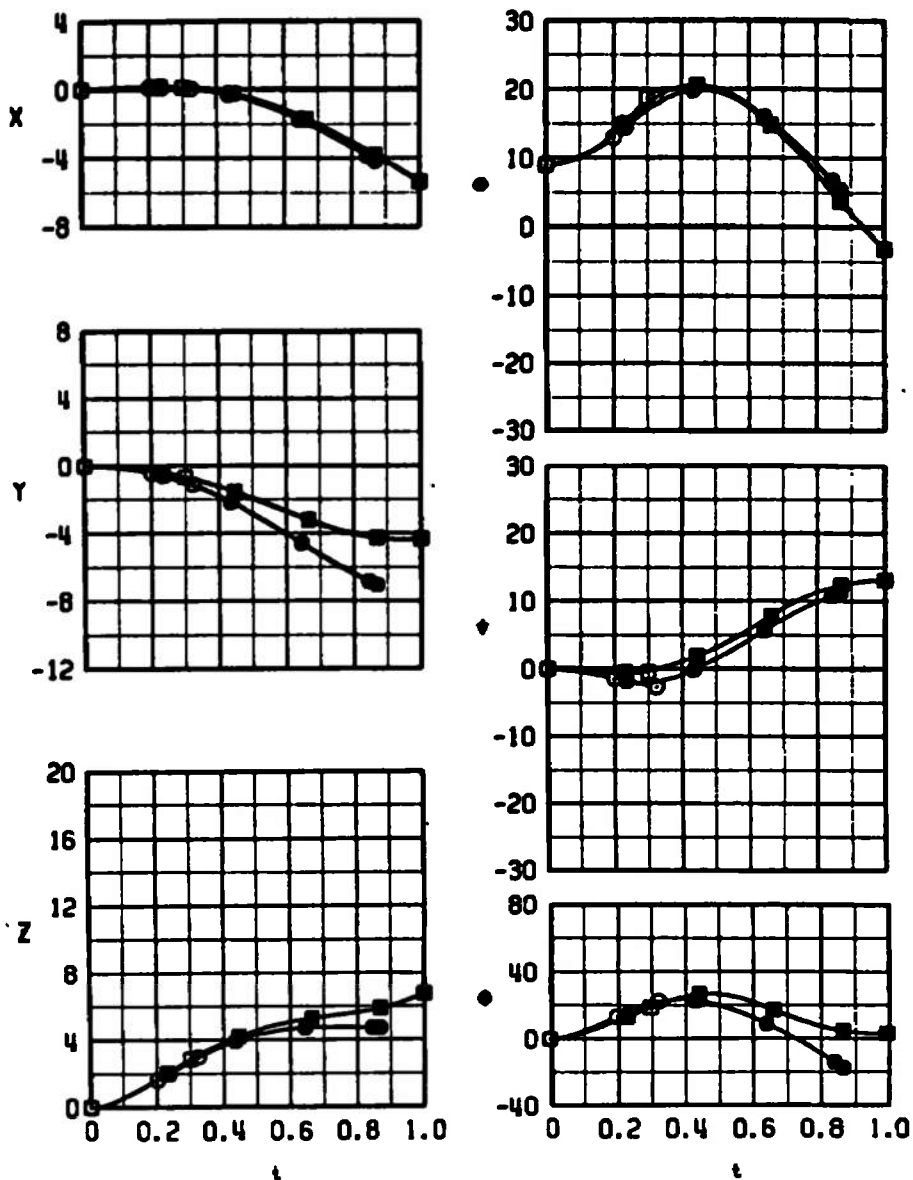
SYMBOL	M_∞	α	CONFIG	ALTITUDE	DIVE	TIPS	TANK
○	0.90	0.0	3	5K	0	RETRACTED	600
□	0.90	0.0	2A	5K	0	↓	370
●	0.90	0.0	13	5K	0	EXTENDED	600
■	0.90	0.0	12A	5K	0	↓	370



a. $M_\infty = 0.90$, $\alpha = 0$

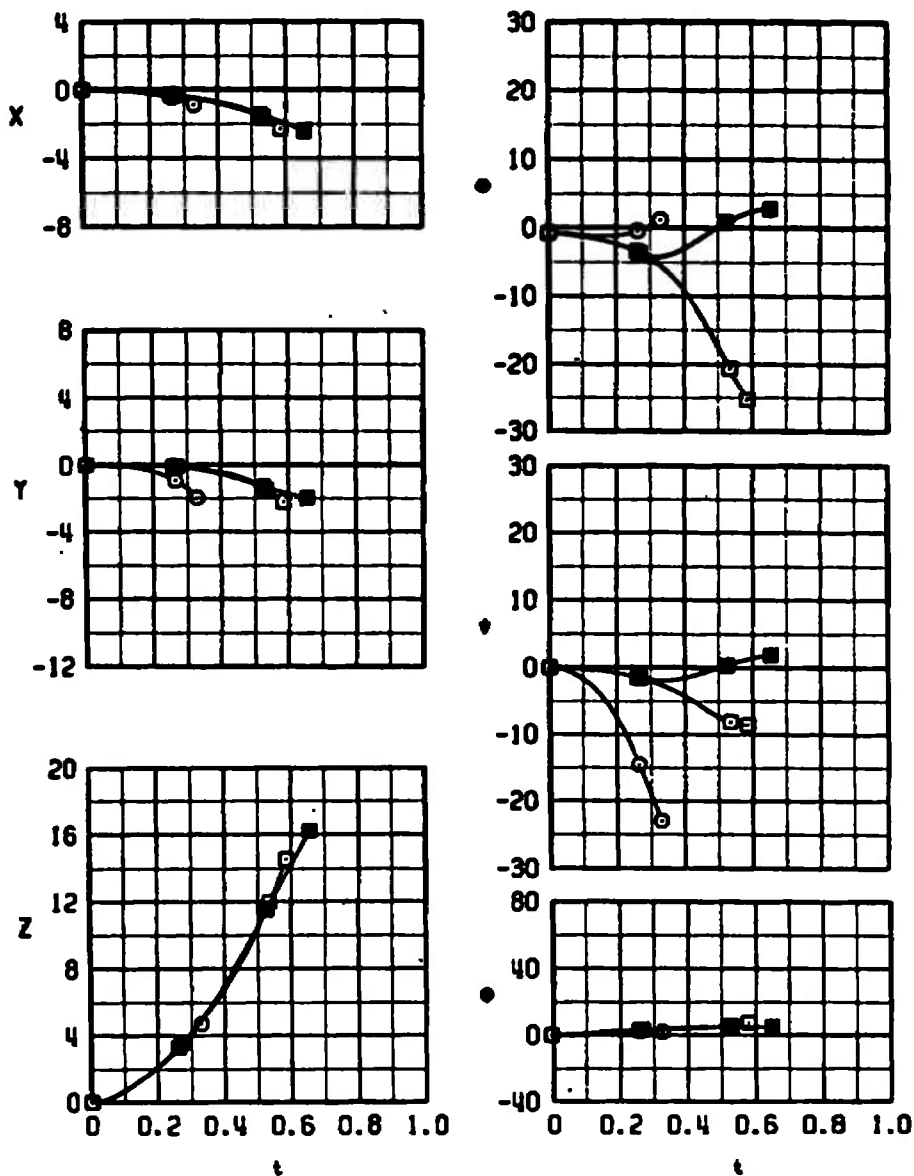
Figure 24. MK-84 trajectory comparisons for the F-4C with 370- and 600-gal fuel tanks, launch configurations 2 and 3.

SYMBOL	M_∞	α	CONFIG	ALTITUDE	DIVE	TIPS	TANK
○	0.90	10.0	3	40K	0	RETRACTED	600
□	0.90	10.0	2A	40K	0	↓	370
●	0.90	10.0	13	40K	0	EXTENDED	600
■	0.90	10.0	12A	40K	0	↓	370



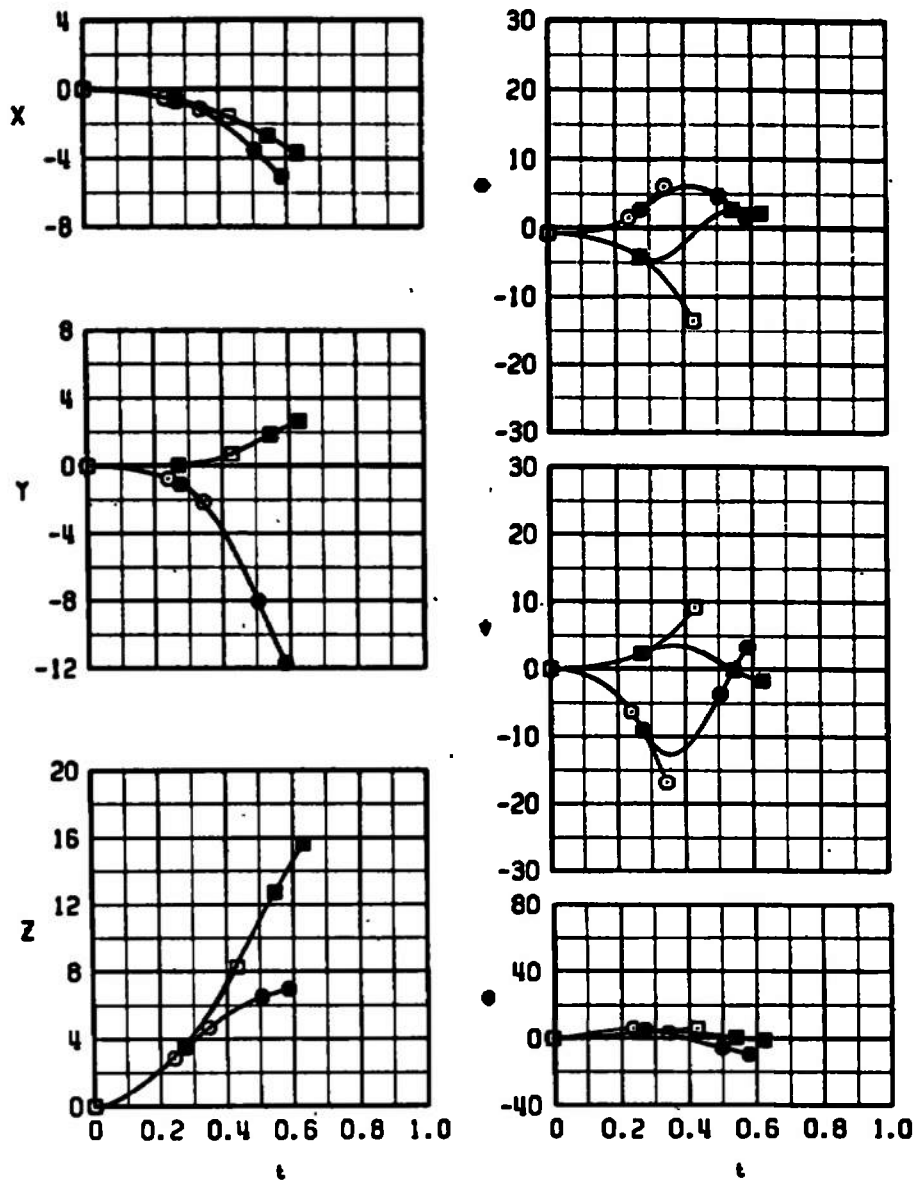
b. $M_\infty = 0.90$, $\alpha = 10$ deg
Figure 24. Continued.

SYMBOL	M_∞	α	CONFIG	ALTITUDE	DIVE	TIPS	TANK
○	0.95	0.2	3	20K	0	RETRACTED	600
□	0.95	0.2	2A	20K	0	↓	370
■	0.95	0.2	12A	20K	0	EXTENDED	370



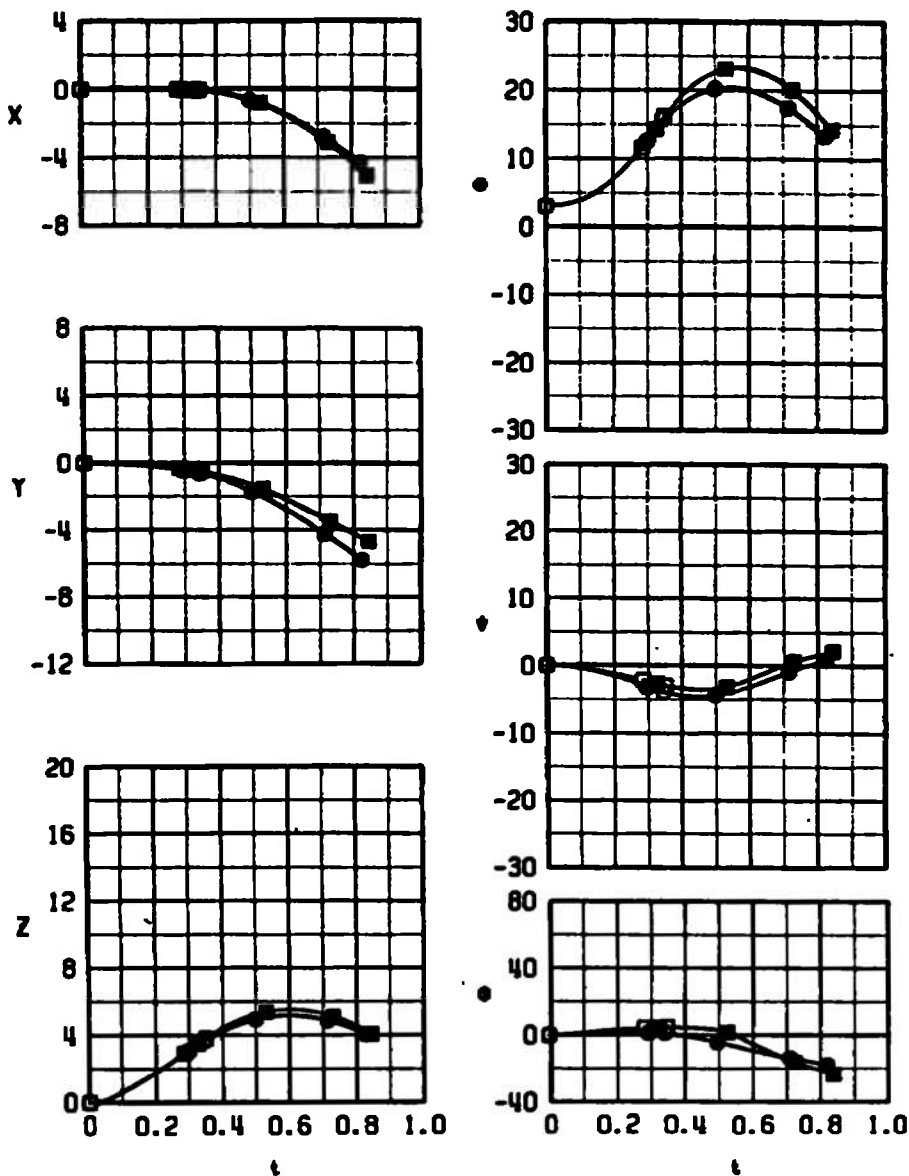
c. $M_\infty = 0.95$, $\alpha = 0.2$ deg
Figure 24. Continued.

SYMBOL	M_∞	α	CONFIG	ALTITUDE	DIVE	TIPS	TANK
○	1.05	0.2	3	20K	0	RETRACTED	600
□	1.05	0.2	2A	20K	0	↓	370
●	1.05	0.2	13	20K	0	EXTENDED	600
■	1.05	0.2	12A	20K	0	↓	370



d. $M_\infty = 1.05$, $\alpha = 0.2$ deg
Figure 24. Concluded.

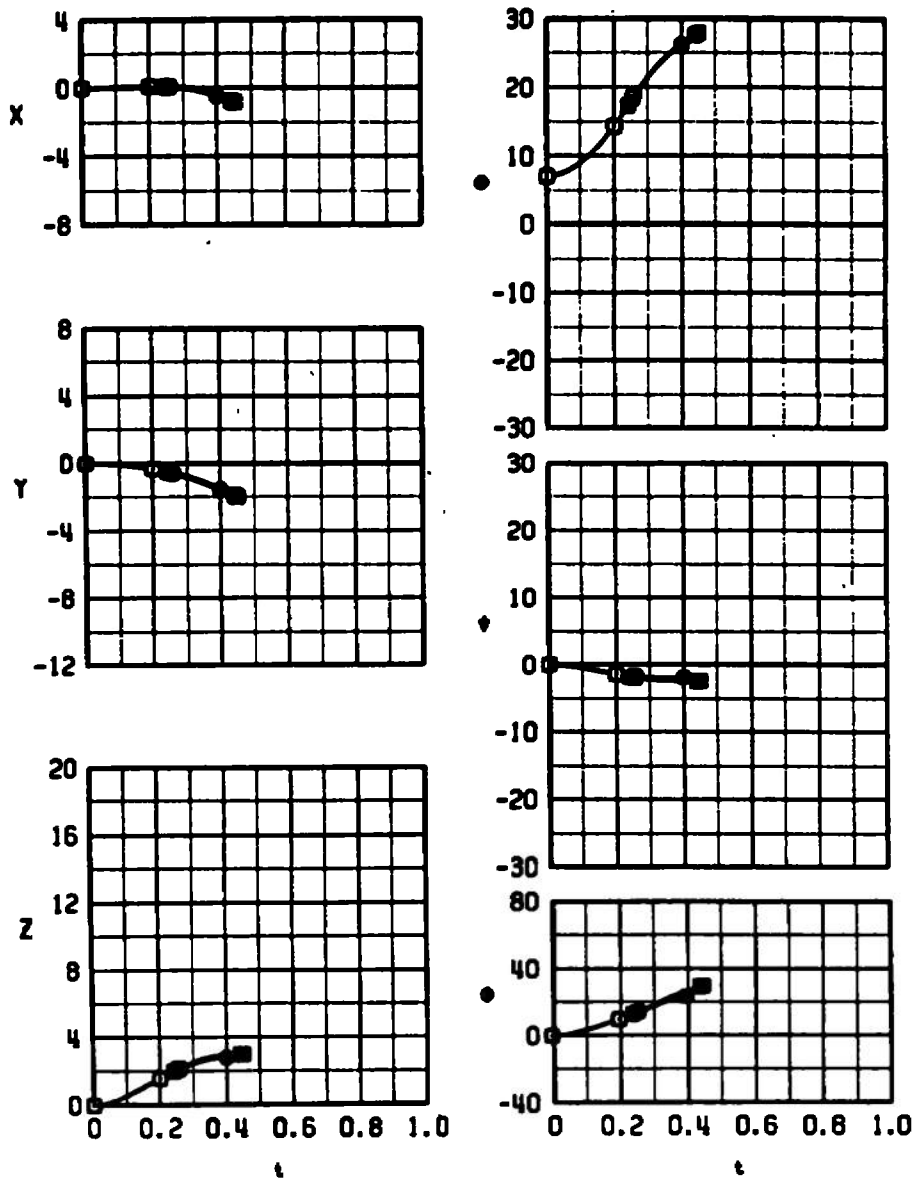
SYMBOL	M_0	α	CONFIG	ALTITUDE	DIVE	TIPS	ECM
○	0.65	4.0	5	20K	0	RETRACTED	ON
□	0.65	4.0	2A	20K	0	↓	OFF
●	0.65	4.0	15	20K	0	EXTENDED	ON
■	0.65	4.0	12A	20K	0	↓	OFF



a. $M_0 = 0.65$, $\alpha = 4$ deg

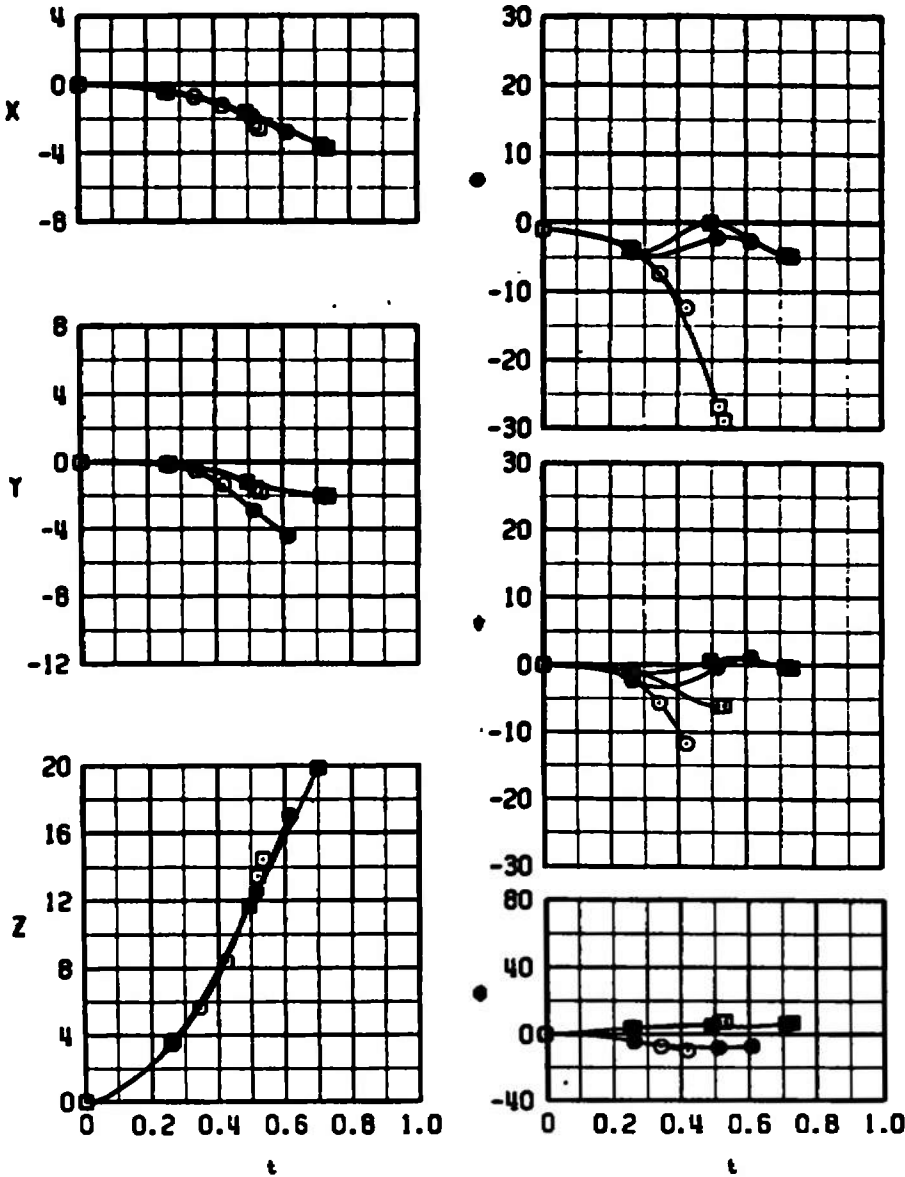
Figure 25. MK-84 trajectory comparisons for the F-4C with and without the ALQ-131 ECM pod, launch configurations 2 and 5.

SYMBOL	M_∞	α	CONFIG	ALTITUDE	DIVE	TIPS	ECM
○	0.65	8.0	5	20K	0	RETRACTED	ON
□	0.65	8.0	2A	20K	0	↓	OFF
●	0.65	8.0	15	20K	0	EXTENDED	ON
■	0.65	8.0	12A	20K	0	↓	OFF



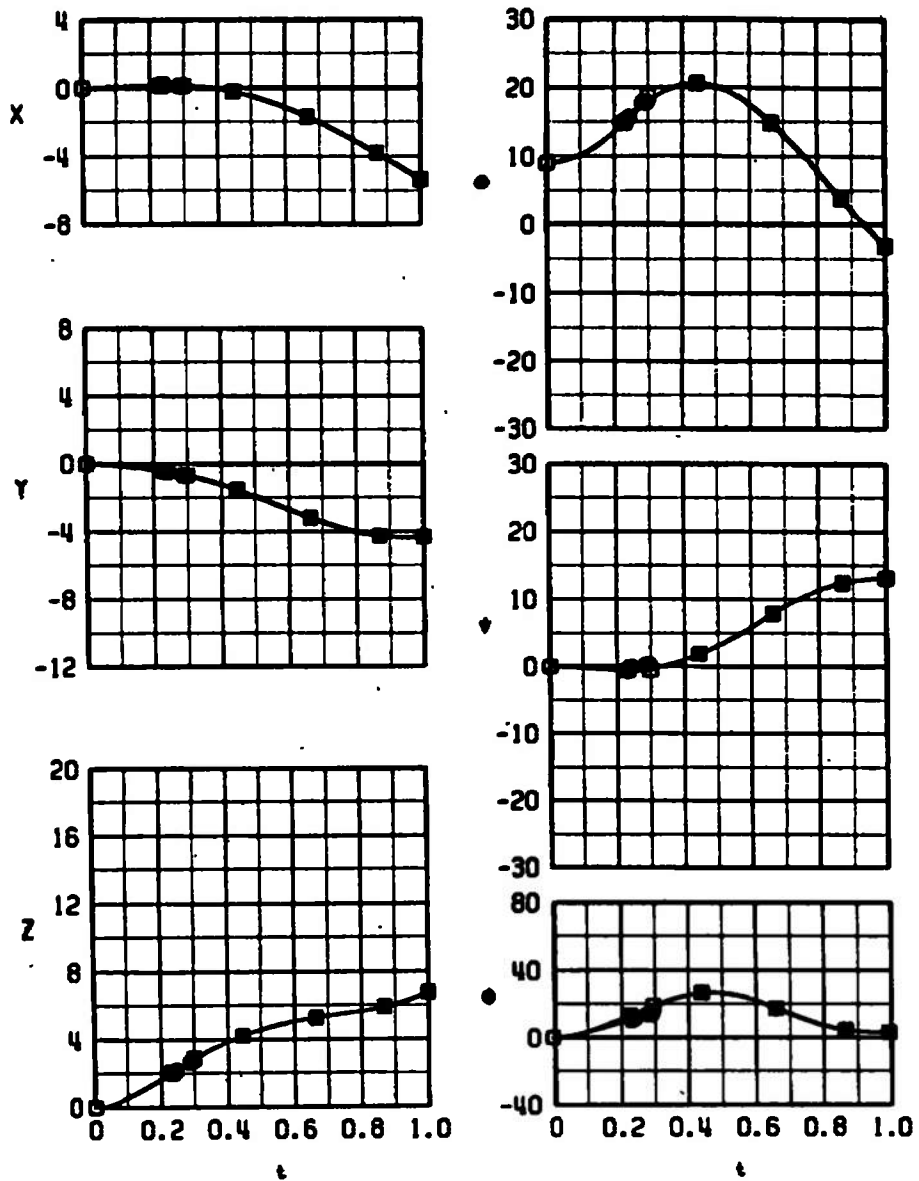
b. $M_\infty = 0.65$, $\alpha = 8$ deg
Figure 25. Continued.

SYMBOL	M_∞	α	CONFIG	ALTITUDE	DIVE	TIPS	ECM
○	0.90	0.0	5	5K	0	RETRACTED	ON
□	0.90	0.0	2A	5K	0	↓	OFF
●	0.90	0.0	15	5K	0	EXTENDED	ON
■	0.90	0.0	12A	5K	0	↓	OFF



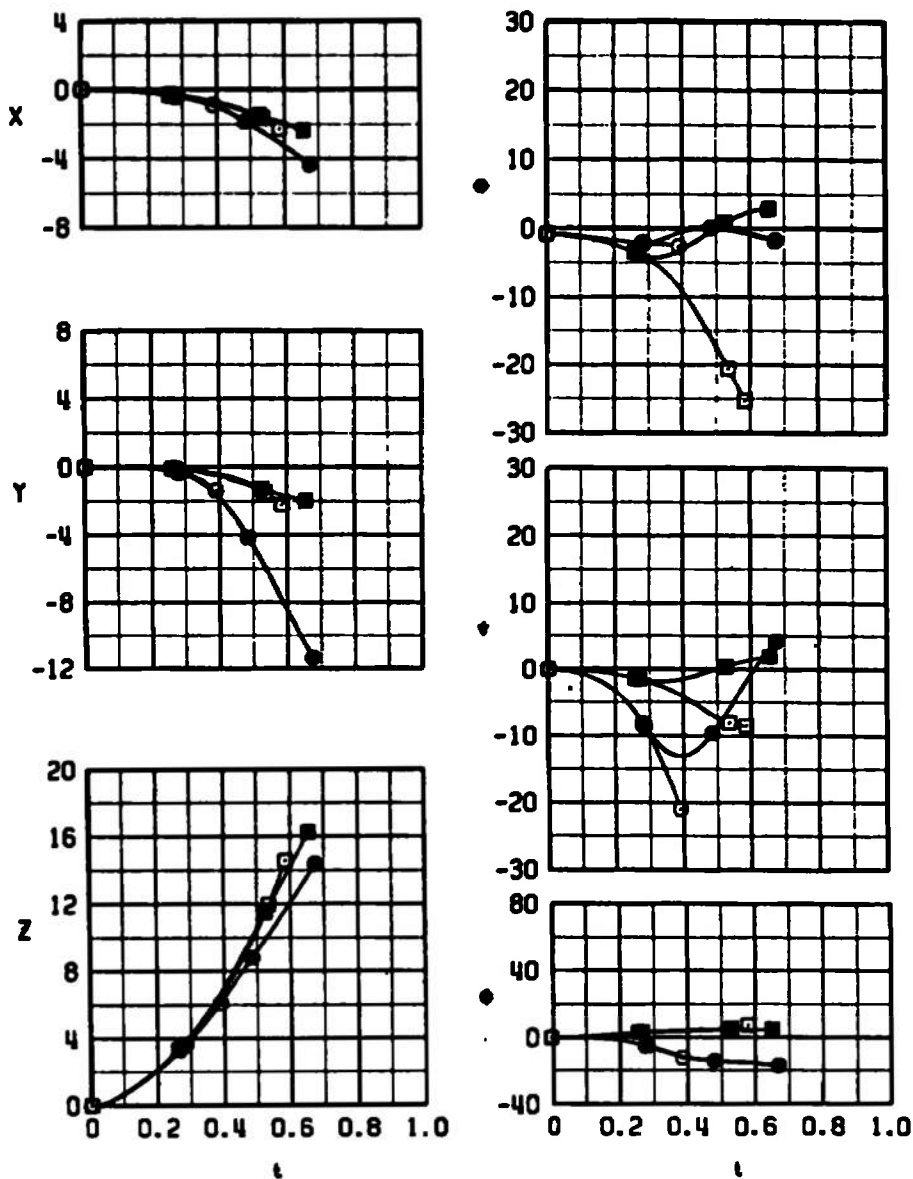
c. $M_\infty = 0.90, \alpha = 0$
Figure 25. Continued.

SYMBOL	M_∞	α	CONFIG	ALTITUDE	DIVE	TIPS	ECM
○	0.90	10.0	5	40K	0	RETRACTED	ON
□	0.90	10.0	2A	40K	0	↓	OFF
●	0.90	10.0	15	40K	0	EXTENDED	ON
■	0.90	10.0	12A	40K	0	↓	OFF



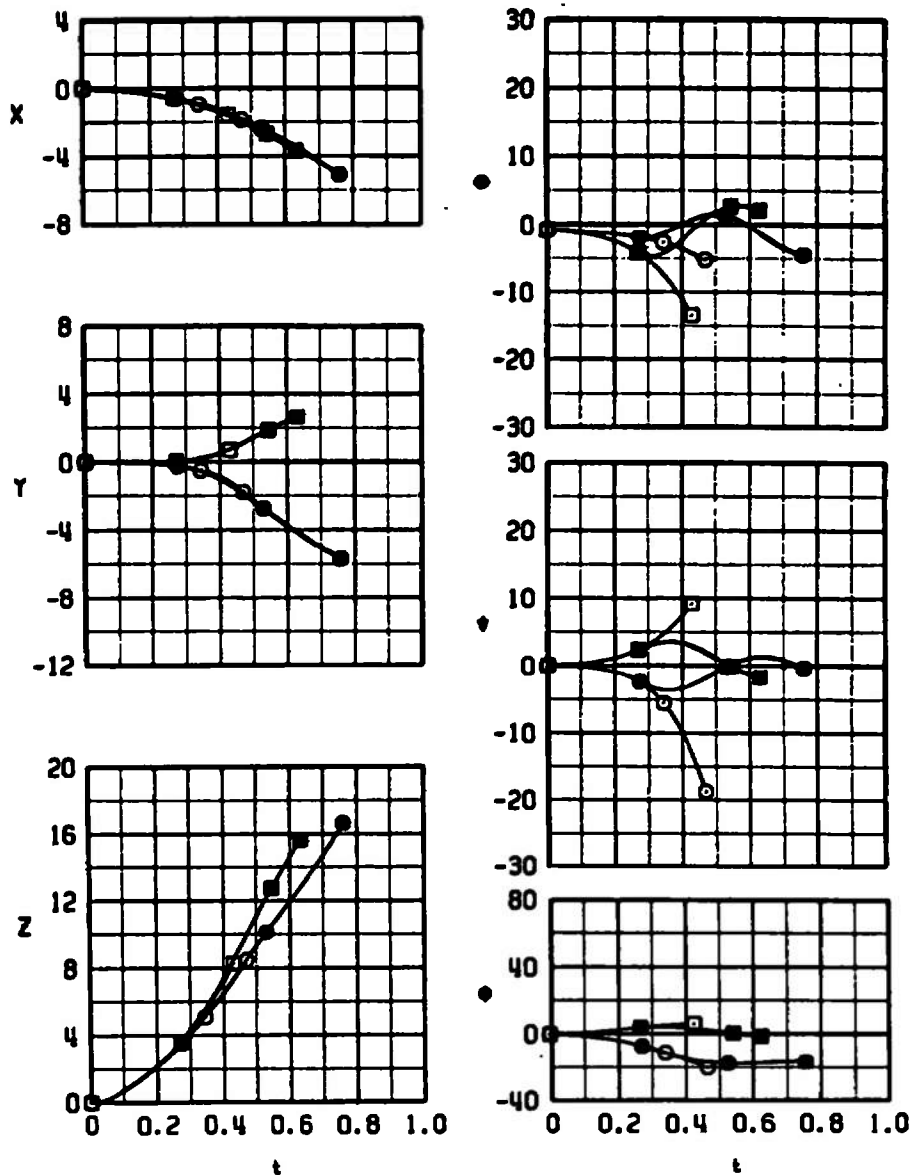
d. $M_\infty = 0.90, \alpha = 10^\circ$
Figure 25. Continued.

SYMBOL	M_∞	α	CONFIG	ALTITUDE	DIVE	TIPS	ECM
○	0.95	0.2	5	20K	0	RETRACTED	ON
□	0.95	0.2	2A	20K	0	↓	OFF
●	0.95	0.2	15	20K	0	EXTENDED	ON
■	0.95	0.2	12A	20K	0	↓	OFF



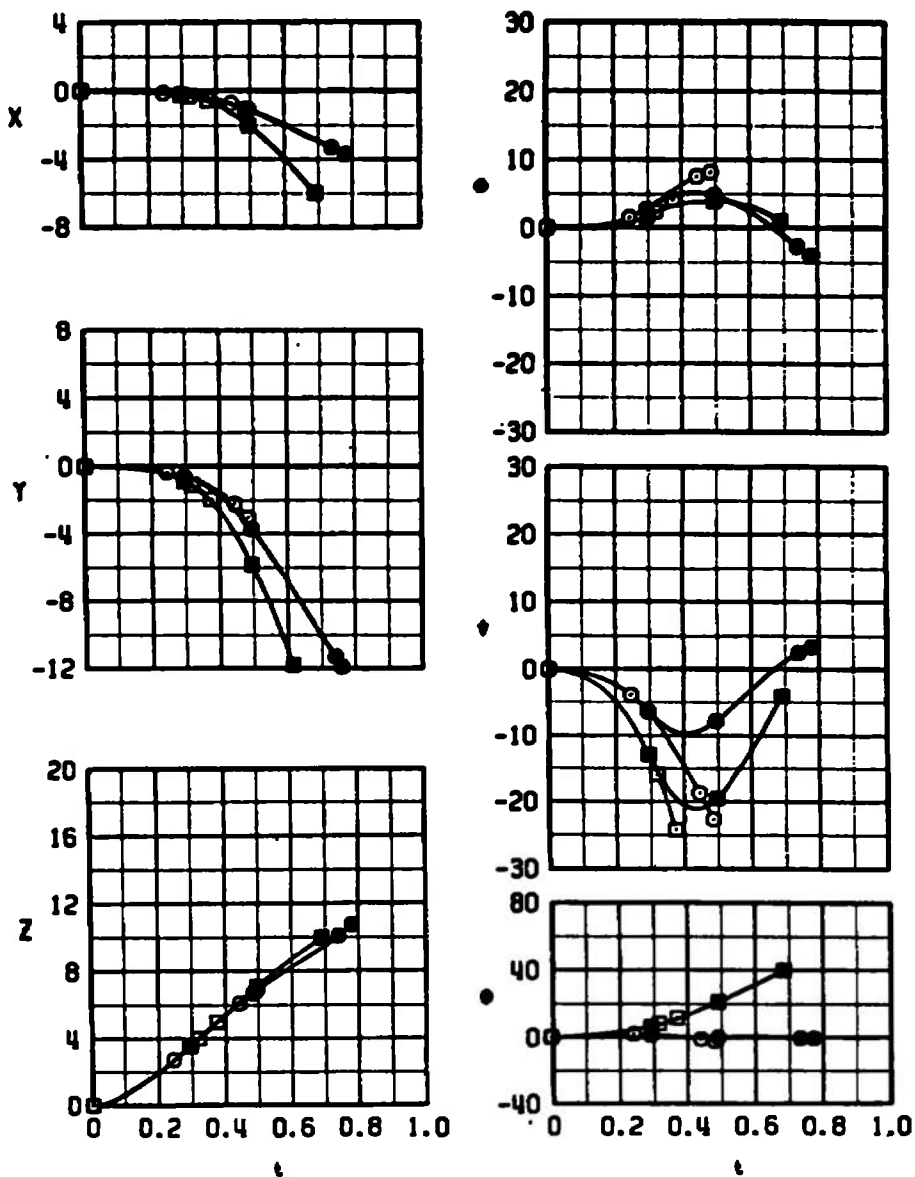
e. $M_\infty = 0.95$, $\alpha = 0.2$ deg
Figure 25. Continued.

SYMBOL	M_∞	α	CONFIG	ALTITUDE	DIVE	TIPS	ECM
○	1.05	0.2	5	20K	0	RETRACTED	ON
□	1.05	0.2	2A	20K	0	↓	OFF
●	1.05	0.2	15	20K	0	EXTENDED	ON
■	1.05	0.2	12A	20K	0	↓	OFF



f. $M_\infty = 1.05$, $\alpha = 0.2$ deg
Figure 25. Concluded.

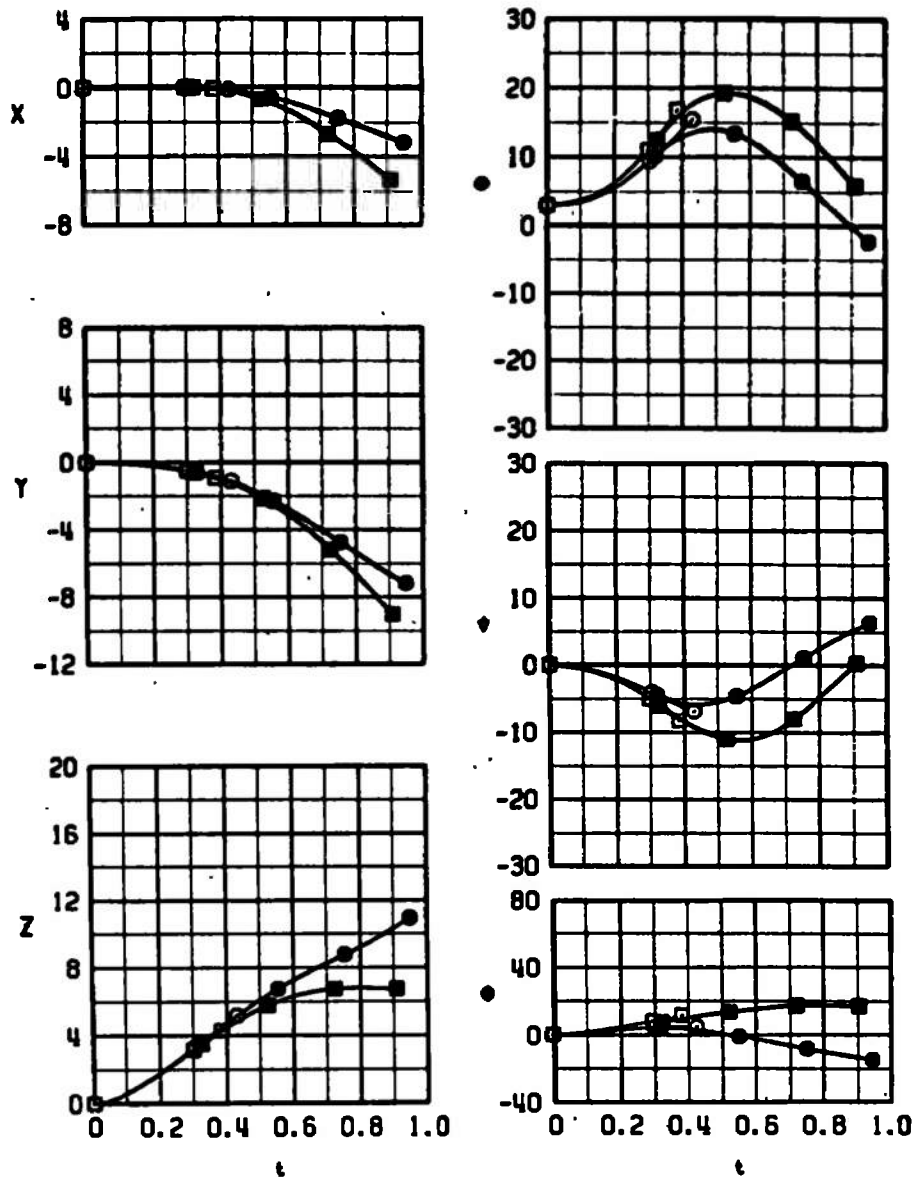
SYMBOL	M_∞	α	CONFIG	ALTITUDE	DIVE	TIPS	STORE
○	0.90	1.0	1	20K	0	RETRACTED	MK-84
□	0.90	1.0	6	20K	0	↓	SUU-54
●	0.90	1.0	11	20K	0	EXTENDED	MK-84
■	0.90	1.0	16	20K	0	↓	SUU-54



a. $M_\infty = 0.90$, $\alpha = 1$ deg

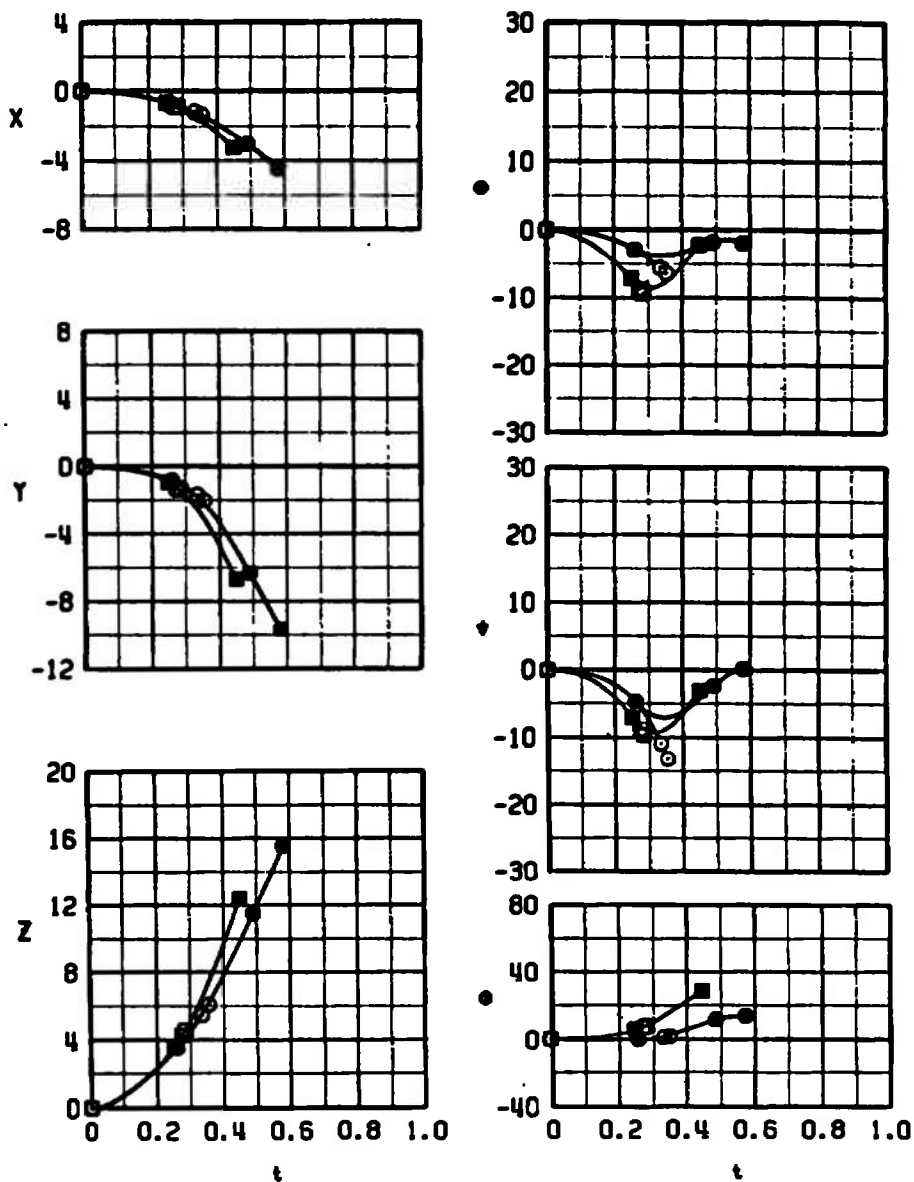
Figure 26. Comparison of the separation characteristics of the MK-84 and SUU-54 stores from the F-4C, launch configurations 1 and 6.

SYMBOL	M_∞	α	CONFIG	ALTITUDE	DIVE	TIPS	STORE
○	0.90	4.0	1	40K	0	RETRACTED	MK-84
□	0.90	4.0	6	40K	0	↓	SUU-54
●	0.90	4.0	11	40K	0	EXTENDED	MK-84
■	0.90	4.0	16	40K	0	↓	SUU-54



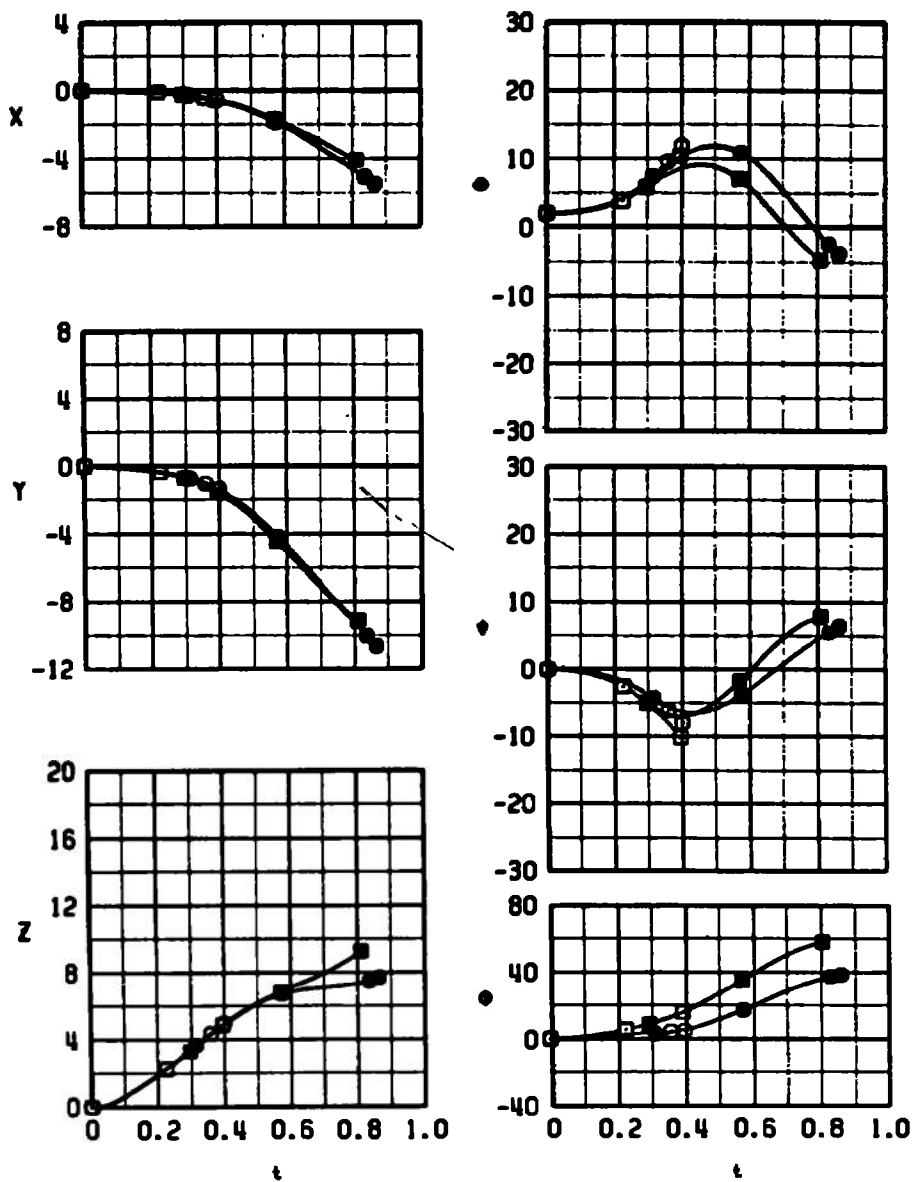
b. $M_\infty = 0.90$, $\alpha = 4^\circ$
Figure 26. Continued.

SYMBOL	M_∞	α	CONFIG	ALTITUDE	DIVE	TIPS	STORE
○	1.20	1.0	1	20K	0	RETRACTED	MK-84
□	1.20	1.0	6	20K	0	↓	SUU-54
●	1.20	1.0	11	20K	0	EXTENDED	MK-84
■	1.20	1.0	16	20K	0	↓	SUU-54



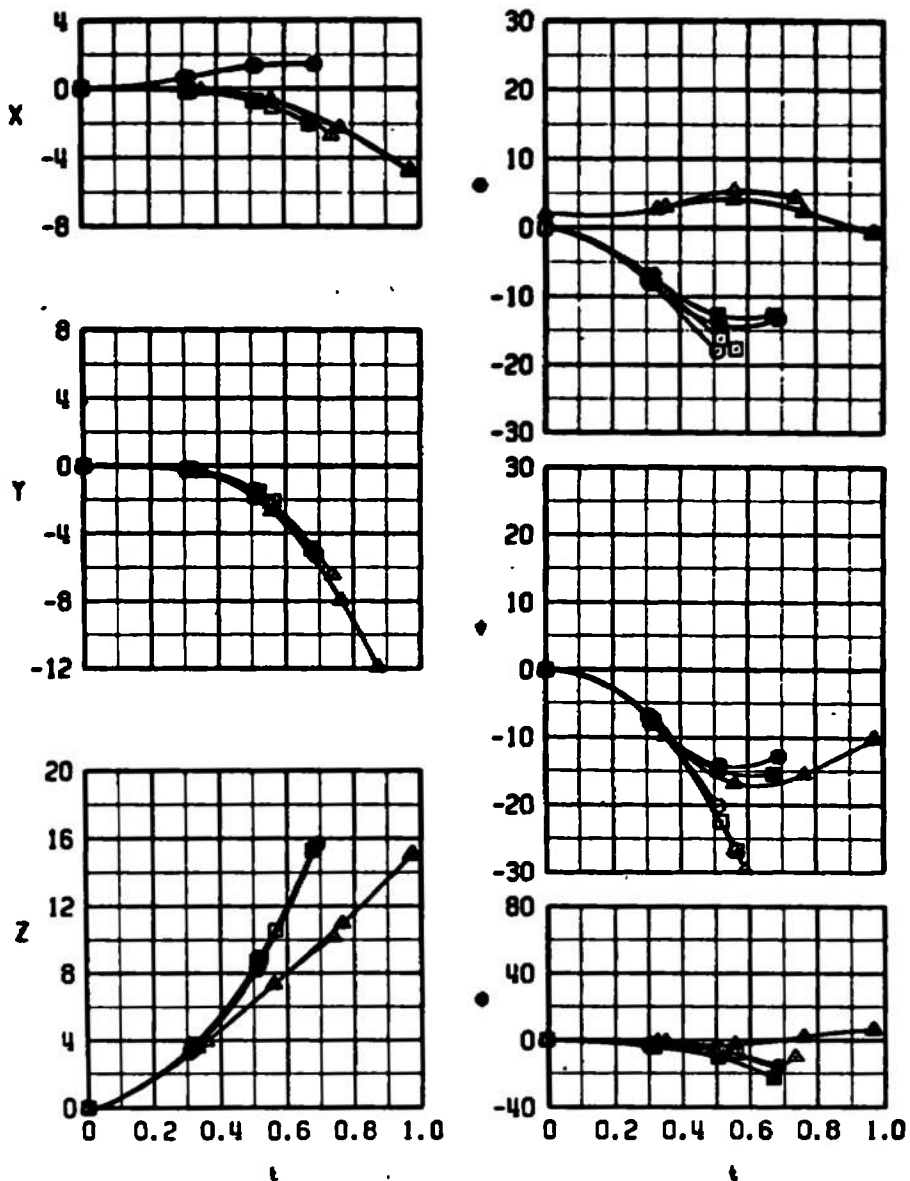
c. $M_\infty = 1.20$, $\alpha = 1$ deg
Figure 26. Continued.

SYMBOL	M_∞	α	CONFIG	ALTITUDE	DIVE	TIPS	STORE
○	1.20	3.0	1	40K	0	RETRACTED	MK-84
□	1.20	3.0	6	40K	0	↓	SUU-54
●	1.20	3.0	11	40K	0	EXTENDED	MK-84
■	1.20	3.0	16	40K	0	↓	SUU-54



d. $M_\infty = 1.20$, $\alpha = 3$ deg
Figure 26. Concluded.

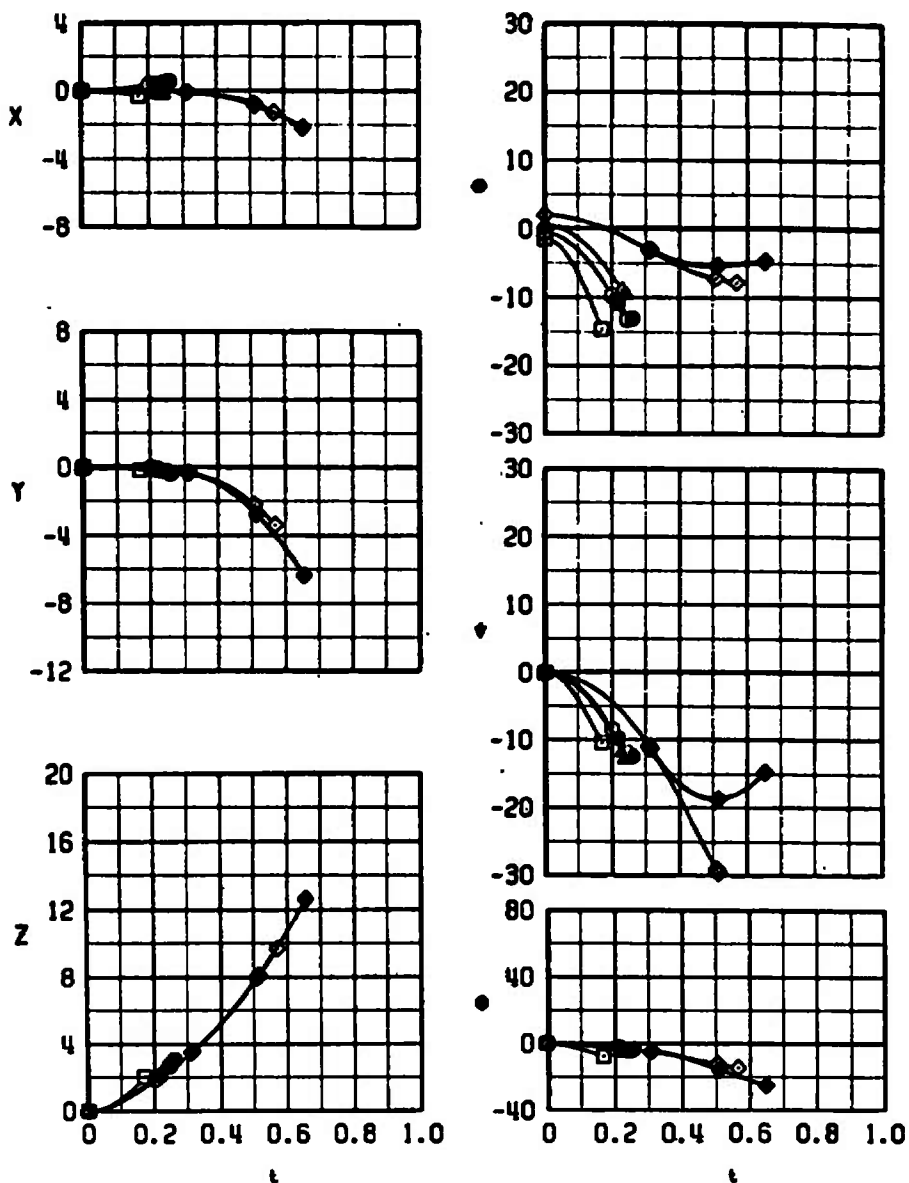
SYMBOL	M_∞	α	CONFIG	ALTITUDE	DIVE	TIPS
○	0.65	2.8	22	20K	30	RETRACTED
□	0.65	3.0	22	20K	0	↓
△	0.65	5.0	22	20K	0	EXTENDED
●	0.65	2.8	32	20K	30	↓
■	0.65	3.0	32	20K	0	EXTENDED
▲	0.65	5.0	32	20K	0	↓



a. $M_\infty = 0.65$

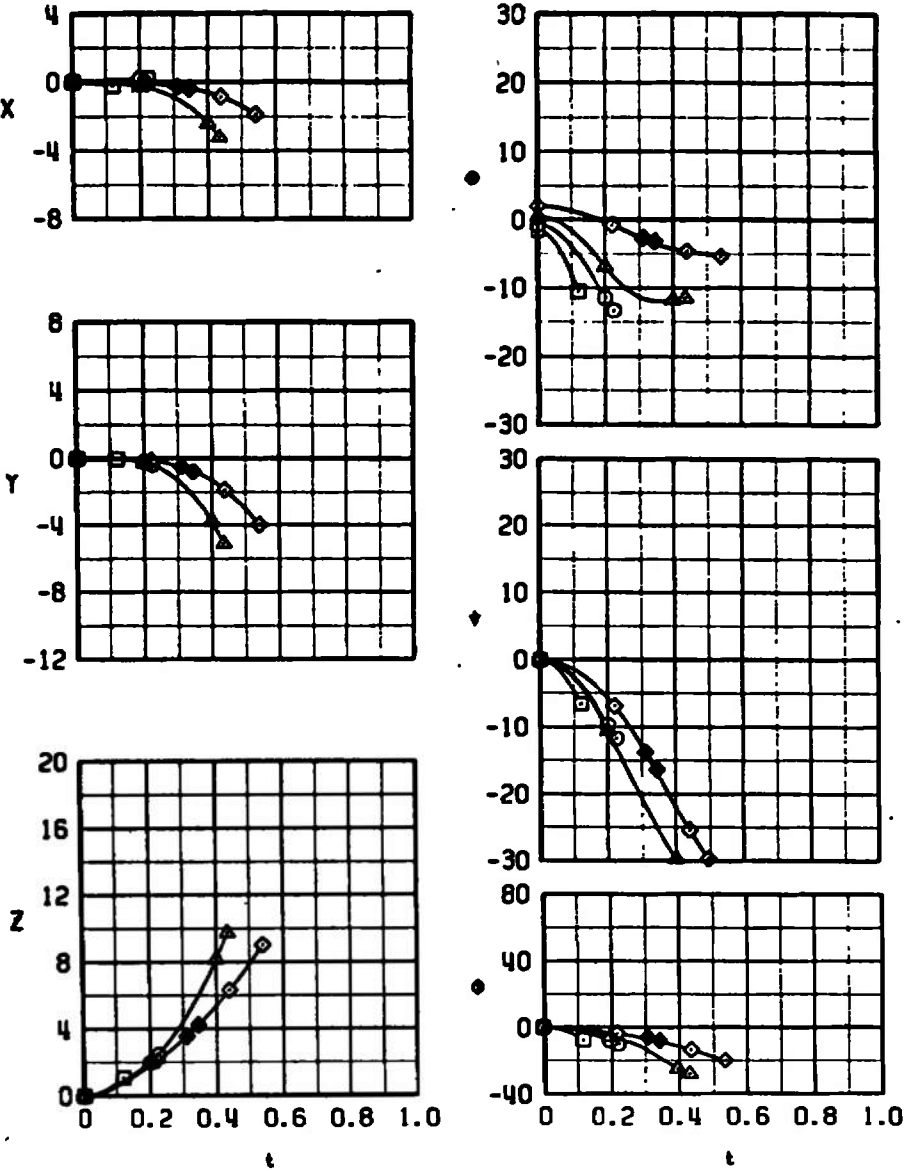
Figure 27. Separation characteristics of the MK-84 store from the A-7D left-wing center pylon with no adjacent stores.

SYMBOL	M_∞	α	CONFIG	ALTITUDE	DIVE	TIPS
○	0.90	2.3	22	20K	60	RETRACTED
□	0.90	1.5	22	5K	0	RETRACTED
△	0.90	3.5	22	20K	0	RETRACTED
◇	0.90	5.0	22	35K	0	RETRACTED
●	0.90	2.3	32	20K	60	EXTENDED
◆	0.90	5.0	32	35K	0	EXTENDED



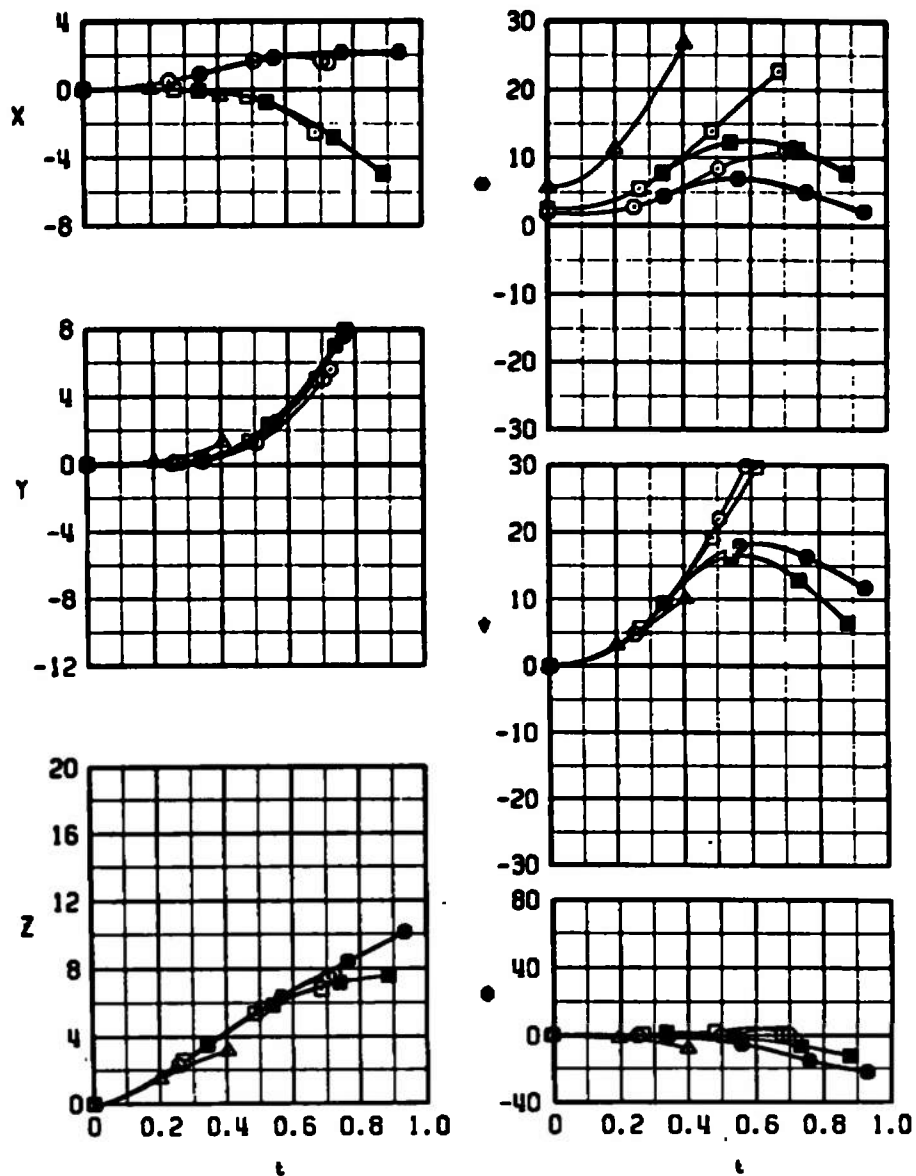
b. $M_\infty = 0.90$
Figure 27. Continued.

SYMBOL	M _∞	α	CONFIG	ALTITUDE	DIVE	TIPS
○	0.95	2.3	22	20K	60	RETRACTED
□	0.95	1.5	22	5K	0	RETRACTED
△	0.95	3.5	22	20K	0	RETRACTED
◇	0.95	5.0	22	35K	0	RETRACTED
◆	0.95	5.0	32	35K	0	EXTENDED



c. $M_{\infty} = 0.95$
Figure 27. Concluded.

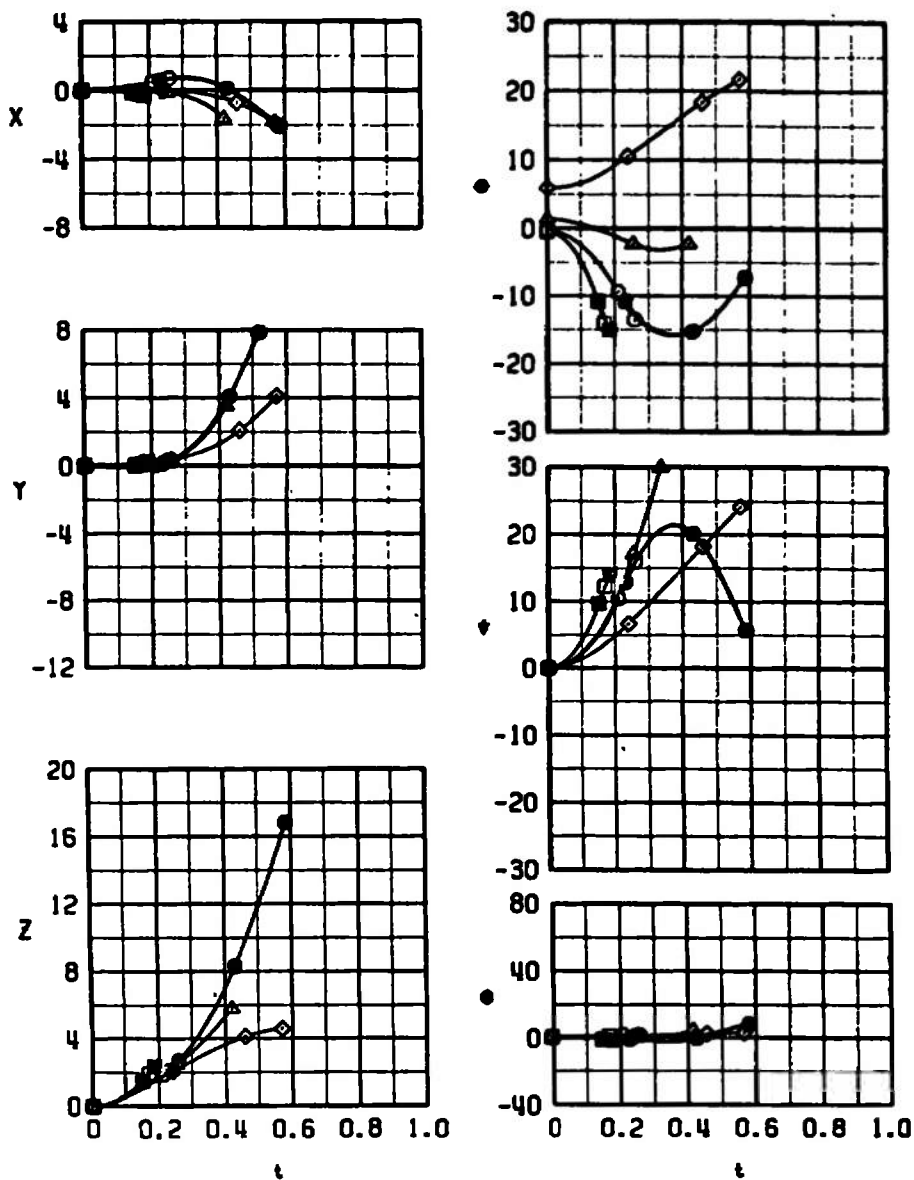
SYMBOL	M_∞	α	CONFIG	ALTITUDE	DIVE	TIPS
○	0.65	4.9	21	20K	30	RETRACTED
□	0.65	5.5	21	20K	0	↓
▲	0.65	8.7	21	20K	0	EXTENDED
●	0.65	4.9	31	20K	30	↓
■	0.65	5.5	31	20K	0	↓



a. $M_\infty = 0.65$

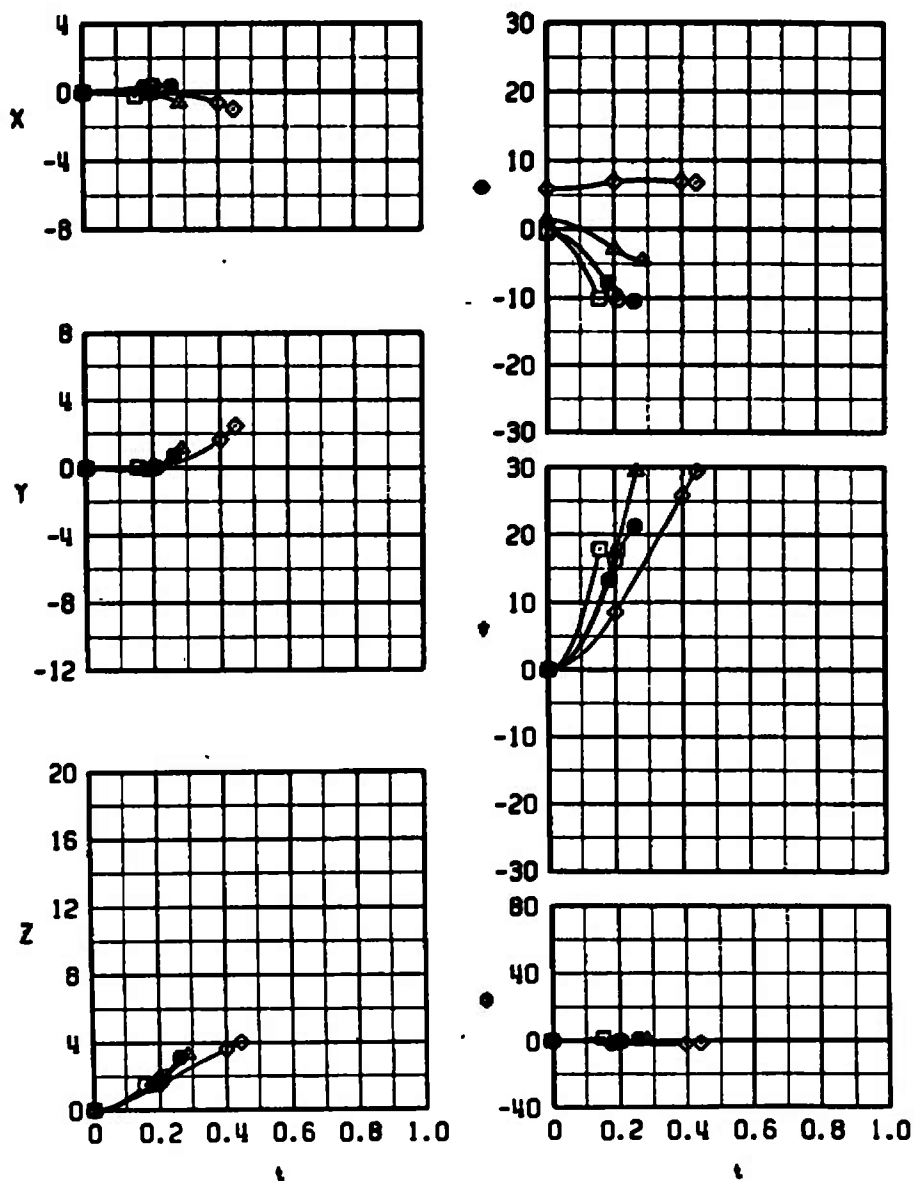
Figure 28. Separation characteristics of the MK-84 store from the A-7D right-wing outboard pylon, launch configuration 21.

SYMBOL	M_∞	α	CONFIG	ALTITUDE	DIVE	TIPS
○	0.90	3.3	21	20K	60	RETRACTED
□	0.90	2.5	21	5K	0	RETRACTED
△	0.90	4.4	21	20K	0	RETRACTED
◇	0.90	8.9	21	35K	0	RETRACTED
●	0.90	3.3	31	20K	60	EXTENDED
■	0.90	2.5	31	5K	0	EXTENDED



b. $M_\infty = 0.90$
Figure 28. Continued.

SYMBOL	M_∞	α	CONFIG	ALTITUDE	DIVE	TIPS
○	0.95	3.3	21	20K	60	RETRACTED
□	0.95	2.5	21	5K	0	RETRACTED
△	0.95	4.4	21	20K	0	RETRACTED
◇	0.95	8.9	21	35K	0	RETRACTED
●	0.95	3.3	31	20K	60	EXTENDED



c. $M_\infty = 0.95$
Figure 28. Concluded.

Table 1. Wind Tunnel Test Conditions

M_∞	p_t , psfa	T_t , °R	p_∞ , psfa	q_∞ , psfa	V_∞ , ft/sec	$Re_\infty \times 10^{-6}$, ft ⁻¹
0.65	1200	550	900	270	720	2.0
0.80	1100	550	720	320	860	2.1
0.90	900	560	530	300	970	1.8
0.95	900	560	500	320	1010	1.8
1.05	1000	560	500	390	1100	2.1
1.20	1100	560	450	460	1230	2.3
1.60	800	560	190	340	1510	1.6

Table 2. Test Summary

Store	Tips	ϕ , deg	α_S , deg	M_∞							Type Data
				0.65	0.80	0.90	0.95	1.05	1.20	1.60	
MK-84(w)(a)	Retracted, Extended	0, 22.5	-4 to 16	x	x	x	x	x	x		Store Free-Stream Aerodynamic ↓
MK-84 (w)	1 Tip Extended	90, 112.5	-4 to 16	x	x	x	x	x	x		
MK-84, SUU-54	Retracted, Extended	0, 22.5	-4 to 44(b)	x	x	x	x	x	x	x	
MK-84	1 Tip Extended	0, 90	-4 to 44(b)	x	x	x	x	x	x		

Config.	α , deg	β , deg	ϕ , deg	Z_P	M_∞							Type Data
					0.65	0.80	0.90	0.95	1.05	1.20	1.60	
18	-2 to 16	0, 4, 9	0	0	x		x			x		Store Aerodynamic in Parent Aircraft Flow- Field ↓
19	-2 to 16	4, 9	0	0	x		x			x		
1w, 11w(a)	0, 2, 4, 6	0	0	0 to 20(c)	x	x	x	x	x	x		
2w, 12w	0, 2, 4, 6	0	0	0 to 20(c)	x		x			x		
10w	0, 2, 4, 6	0	90	0 to 20(c)	x	x	x		x	x		
24w, 34w	1, 2, 4, 6, 8	0	0	0 to 20(c)	x		x	x		x		

Notes: (a) "w" denotes wedge-shaped fins and strakes on MK-84.

(b) Max-Min α_S not reached at some Mach numbers because of balance limitations.

(c) Max Z_P not reached at some α 's because of tunnel physical limitations.

Table 2. Continued

Config.	α , deg	β , deg	X_P	Z_P	M_∞							Type Data
					0.65	0.80	0.90	0.95	1.05	1.20	1.60	
41	-2, 0, 2, 4, 6, 8	0	0, -8.33	0 to 20(c)	x		x			x		F-4C Flow Field
41	12	0	0, -8.33	0 to 20(c)	x		x					↓
41	16	0	0, -8.33	0 to 20(c)	x							
42	-2, 0, 2, 4, 6, 8	0	0, -8.33	0 to 20(c)			x					
43	-2, 0, 2, 4, 6, 8	0	0, -8.33	0 to 20(c)	x	x	x	x	x	x		
43	12	0	0, -8.33	0 to 20(c)	x	x	x	x				
43	16	0	0, -8.33	0 to 20(c)	x	x						
44, 47	-2, 0, 10, 14	0	0, -4.17, -8.33	0	x		x			x		
45	-2, 0, 10, 14	9	0.83, -6.37 -11.35	0	x		x			x		↓
54	0	0	0, -8.33	0 to 20(c)	x	x	x	x				
54	2, 4, 6, 8	0	0, -8.33	0 to 20(c)	x	x		x				
54	12, 16	0	0, -8.33	0 to 20(c)	x							
57, 58	-2, 0, 12, 16	9	0, -4.17, -8.33	0	x		x	x				

Note: (c) Max Z_P not reached at some α 's because of tunnel physical limitations.

Table 2. Continued

Config.	M ₀							Type Data
	0.65	0.80	0.90	0.95	1.05	1.20	1.60	
1, 11	20K(d), 1.0(e) 20K, 4.0 25K, 4.8	S. L., -0.6 S. L., 1.0	5K, -1.0 20K, 1.0 40K, 4.0	20K, -0.4 20K, -0.6(45)(f)	20K, -0.4 20K, -0.6(45)	20K, -0.4 20K, 1.0 40K, 3.0	35K, 0 35K, 1.0	Trajectory (F-4C)
1w, 2w, 10w(a)	5K, 2.0 25K, 6.0		5K, 0 40K, 4.0			5K, 0 40K, 2.0		
2, 12	20K, 4.0 20K, 8.0 25K, 4.8	S. L., 1.0 S. L., 1.6(i)	5K, 0 20K, 3.0(i) 40K, 10.0	20K, 0.2 20K, 0(45)	20K, 0.2 20K, 0(45)			
3, 13			5K, 0 20K, 3.0 40K, 10.0	20K, 0.2(i) 20K, 0(45)(i)	20K, 0.2 20K, 0(45)			
4, 14			5K, -1.0 20K, 1.0 40K, 4.0	20K, -0.4 20K, -0.6(45)	20K, -0.4 20K, -0.6(45)	20K, -0.4 20K, 1.0 40K, 3.0	35K, 0 35K, 1.0	
5, 15	20K, 4.0 20K, 8.0		5K, 0 20K, 3.0(i) 40K, 10.0	20K, 0.2 20K, 0(45)	20K, 0.2 20K, 0(45)			
6, 16			5K, -1.0 20K, 1.0 40K, 4.0			20K, -0.4 20K, 1.0 40K, 3.0	35K, 0 35K, 1.0	
7, 17			5K, 0 20K, 3.0 40K, 10.0	20K, 0.2	20K, 0.2			
8, 9	20K, 4.0 20K, 8.0		5K, 0 40K, 10		20K, 0.2 20K, 0(45)			
10	20K, 1.0 20K, 4.0		5K, -1.0 40K, 4.0			20K, 1.0 40K, 3.0		

- Notes: (a) "w" denotes wedge-shaped fins and strakes on MK-84.
 (d) Simulated altitude of trajectory.
 (e) Parent aircraft angle of attack.
 (f) Simulated aircraft dive angle, deg (zero unless noted by number in parentheses).
 (i) Tips-extended configuration not tested at this condition.

Table 2. Concluded

Config.	M_∞						Type Data
	0.65	0.80	0.90	0.95	1.05	1.20	1.60
22, 32	20K(d), 3.0(e) 20K, 5.0 20K, 2.8(30)(f)		5K, 1.5(i) 20K, 3.5(i) 35K, 5.0 20K, 2.3(60)	5K, 1.5(i) 20K, 3.5(i) 35K, 5.0 20K, 2.3(60)(i)			Trajectory (A-7D)
21, 31	20K, 5.5 20K, 8.7(i) 20K, 4.9(30)		5K, 2.5 20K, 4.4(i) 35K, 8.9(i) 20K, 3.3(60)	5K, 2.5(i) 20K, 4.4(i) 35K, 8.9(i) 20K, 3.3(60)			
23, 33			5K, 1.5(i) 20K, 3.5 35K, 5.0 20K, 2.3(60)(i)				
24 w(a)	5K, 4.0 25K, 8.0		5K, 3.0 35K, 5.0	5K, 2.0 35K, 4.0			

- Notes: (a) "w" denotes wedge-shaped fins and strakes on MK-84.
 (d) Simulated altitude of trajectory, ft.
 (e) Parent aircraft angle of attack, deg.
 (f) Simulated aircraft dive angle, deg (zero unless noted by number in parentheses).
 (i) Time-extended configuration not tested at this condition.

Table 3. F-4C Load Configurations

Configuration	Left-Wing Outboard Pylon	Left-Wing Inboard Pylon	Forward Left-Missile- Well Pylon	Centerline Pylon	Forward Right-Missile- Well Pylon	Right-Wing Inboard Pylon	Right-Wing Outboard Pylon
1,1w ^(a)	Clean ^(b)	MK-84 Tips Retracted (Metric)	Clean	Clean	Clean	Empty ^(c)	370-gal Fuel Tank
2,2w		Empty		Clean		MK-84 Tips Retracted (Metric)	370-gal Fuel Tank
3		MK-84 Tips Retracted (Metric)		600-gal Fuel Tank		Empty	Clean
4,4w				Data Link Pod			
5	370-gal Fuel Tank		ALQ-131 Terminal Threat Pod	Clean			
6	Clean	SUU-54 Tips Retracted (Metric)	Clean				370-gal Fuel Tank
7		Empty				SUU-54 Tips Retracted (Metric)	
8						MK-84 1 Tip Extended $\phi = 0$ (Metric)	
9,9w						MK-84 1 Tip Extended $\phi = 90$ (Metric)	
10		MK-84 1 Tip Extended $\phi = 0$ (Metric)				Empty	
10w		MK-84 1 Tip Extended $\phi = 90$ (Metric)				Empty	

Notes: (a) "w" denotes wedge-shaped fins and strakes on MK-84.
 (b) Clean denotes pylon removed.
 (c) Empty denotes no store on pylon.

Table 3. Concluded

Configuration	Left-Wing Outboard Pylon	Left-Wing Inboard Pylon	Forward Left-Missile- Well Pylon	Centerline Pylon	Forward Right-Missile- Well Pylon	Right Wing Inboard Pylon	Right-Wing Outboard Pylon
11,11w	Clean	MK-84 Tips Extended (Metric)	Clean	Clean	Clean	Empty	370-gal Fuel Tank
12,12w		Empty		Clean		MK-84 Tips Extended (Metric)	370-gal Fuel Tank
13		MK-84 Tips Extended (Metric)		600-gal Fuel Tank		Empty	Clean
14				Data Link Pod			
15	370-gal Fuel Tank		ALQ-131 Terminal Threat Pod	Clean			
16	Clean	SUU-54 Tips Extended (Metric)	Clean				370-gal Fuel Tank
17		Empty				SUU-54 Tips Extended (Metric)	370-gal Fuel Tank
18		MK-84 Tips Retracted (Metric)				Empty	Clean
19		Empty				MK-84 Tips Retracted (Metric)	Clean
41		Empty				Conical Probe Survey	370-gal Fuel Tank
42		Conical Probe Survey		Data Link Pod		MK-84 Tips Retracted (Dummy)	Clean
43				Clean		Empty	370-gal Fuel Tank
44				Clean			Clean
45		Empty		Conical Probe Survey			
47		Empty		Clean		Conical Probe Survey	

Table 4. A-7D Load Configurations

Configuration	Left-Wing Outboard Pylon	Left-Wing Center Pylon	Left-Wing Inboard Pylon	Right-Wing Inboard Pylon	Right-Wing Center Pylon	Right-Wing Outboard Pylon
21	Empty (a)	Empty	Empty	300-gal Fuel Tank	Empty	MK-84 Tips Retracted (Metric)
22		MK-84 Tips Retracted (Metric)				Empty
23		Empty		Data Link Pod		MK-84 Tips Retracted (Metric)
24w(b)		MK-84 Tips Retracted (Dummy)		Empty	MK-84 Tips Retracted (Metric)	Empty
31		Empty		300-gal Fuel Tank	Empty	MK-84 Tips Extended (Metric)
32		MK-84 Tips Extended (Metric)				Empty
33		Empty		Data Link Pod		MK-84 Tips Extended (Metric)
34w		MK-84 Tips Retracted (Dummy)		Empty	MK-84 Tips Extended (Metric)	Empty
54			300-gal Fuel Tank		Conical Probe Survey	
57		Empty	Empty			
58		Conical Probe Survey			Empty	

Notes: (a) Empty denotes no store on pylon.

(b) "w" denotes wedge-shaped fins and strakes on MK-84.

Table 5. Full-Scale Store Parameters Used in Trajectory Calculations

Sym	Parameter	Store				
		MK-84 (w) (a) Tips Retracted and 1 Tip Extended	MK-84 Tips Retracted and 1 Tip Extended	MK-84 Tips Extended	SUU-54 Tips Retracted	SUU-54 Tips Extended
S	Store Reference Area, ft ²	1.766	1.766	1.766	1.766	1.766
b	Store Reference Width, ft	1.500	1.500	1.500	1.500	1.500
I _{xx}	Moment of Inertia, slug-ft ²	39.0	45.7	50.6	51.5	57.0
I _{yy}	Moment of Inertia, slug-ft ²	638.3	699.0	702.1	696.4	699.8
I _{zz}	Moment of Inertia, slug-ft ²	638.3	698.7	702.2	694.4	697.8
C _{m_q}	Pitch-Damping Derivative, per radian	-736	-763	-979	-718	-950
C _{n_r}	Yaw-Damping Derivative, per radian	-736	-763	-979	-718	-950
C _{l_p}	Roll-Damping Derivative, per radian	-52	-51	-177	-47	-177
X _{cg}	Center-of-Gravity Location from Nose, ft	7.25	7.19	7.19	7.49	7.49
Z _{cg}	Center-of-Gravity Location above Centerline, ft	0	0	0	0.05	0.05
m	Mass, slug	77.97	80.32	80.32	83.72	83.72
F _{Z1}	Forward Ejector Force, lb	4060	4060	4060	4060	4060
F _{Z2}	Aft Ejector Force, lb	4060	4060	4060	4060	4060
X _{L1}	Forward Ejector Piston Location, ft	0.998	0.940	0.940	0.865	0.865
X _{L2}	Aft Ejector Piston Location, ft	-0.668	-0.727	-0.727	-0.802	-0.802
Z _E	Ejector Stroke Length, ft	0.375	0.375	0.375	0.375	0.375

Note: (a) "w" denotes wedge-shaped fins and strakes on MK-84.

Table 6. Adjustments to the Pitching-Moment and Yawing-Moment Coefficients for Trajectory Calculations

Store	Sym	Value at M_∞						
		0.65	0.80	0.90	0.95	1.05	1.20	1.60
MK-84(w) (a) Tips Retracted and 1 Tip Extended	ΔX_{cg}	0	0	0	0	0	0	0
	C_{m_0}	↓	↓	↓	↓	↓	↓	↓
	C_{n_0}	↓	↓	↓	↓	↓	↓	↓
MK-84 Tips Retracted and 1 Tip Extended	ΔX_{cg}	0	0	0	0	0	0	-0.070
	C_{m_0}	0.27	0.18	0.25	0.31	0.40	0.06	-0.01
	C_{n_0}	-0.15	-0.11	-0.08	-0.19	-0.20	-0.09	-0.25
MK-84 Tips Extended	ΔX_{cg}	0	0	0	0.105	0.150	0	0
	C_{m_0}	0.13	0.12	-0.22	0.01	0.11	-0.44	0.06
	C_{n_0}	-0.10	-0.04	0.02	-0.07	-0.10	-0.19	-0.12
SUU-54 Tips Retracted	ΔX_{cg}	-0.138	-0.153	-0.250	-0.250	-0.305	-0.110	-0.255
	C_{m_0}	0.26	0.21	0.18	0.30	0.46	0.16	-0.09
	C_{n_0}	0.02	-0.02	-0.17	-0.11	-0.08	-0.10	-0.05
SUU-54 Tips Extended	ΔX_{cg}	0	0	0	0	0.055	0	-0.110
	C_{m_0}	0.13	0.16	0.03	0.05	0.36	-0.13	0.31
	C_{n_0}	0.06	0.08	-0.06	-0.02	-0.05	0.05	-0.02

Note: "w" denotes wedge-shaped fins and strakes on MK-84.

NOMENCLATURE

BL	Aircraft buttock line from plane of symmetry, in., model scale
b	Store reference dimension, ft, full scale
C_A	Store measured axial-force coefficient, axial force/ $q_\infty S$
C_l	Store rolling-moment coefficient, rolling moment/ $q_\infty S b$
C_{l_p}	Store roll-damping derivative, $dC_l/d(pb/2V_\infty)$
C_m	Store pitching-moment coefficient, referenced to the store cg, pitching moment/ $q_\infty S b$
C_{m_0}	Store pitching-moment coefficient correction, difference in measured pitching-moment coefficients for 0.25-scale and 0.05-scale models at $\alpha_s = 0$
C_{m_q}	Store pitch-damping derivative, $dC_m/d(qb/2V_\infty)$
C_{m_α}	Store pitching-moment coefficient derivative, $\partial C_m/\partial \alpha_s$, per degree
C_N	Store normal-force coefficient, normal force/ $q_\infty S$
C_{N_α}	Store normal-force coefficient derivative, $\partial C_N/\partial \alpha_s$, per degree
C_n	Store yawing-moment coefficient, referenced to the store cg, yawing-moment/ $q_\infty S b$
C_{n_0}	Store yawing-moment coefficient correction, difference in measured yawing-moment coefficients for 0.25-scale and 0.05-scale models at $\alpha_s = 0$
C_{n_r}	Store yaw-damping derivative, $dC_n/d(rb/2V_\infty)$
C_Y	Store side-force coefficient, side force/ $q_\infty S$
FS	Aircraft fuselage station, in., model scale
F_{Z_1}	Forward ejector force, lb
F_{Z_2}	Aft ejector force, lb
I_{xx}	Full-scale moment of inertia about the store X_B axis, slug-ft ²

I_{yy}	Full-scale moment of inertia about the store Y_B axis, slug-ft ²
I_{zz}	Full-scale moment of inertia about the store Z_B axis, slug-ft ²
M_∞	Free-stream Mach number
\bar{m}	Full-scale store mass, slugs
p	Store angular velocity about the X_B axis, radians/sec
p_t	Free-stream total pressure, psfa
p_∞	Free-stream static pressure, psfa
q	Store angular velocity about the Y_B axis, radians/sec
q_∞	Free-stream dynamic pressure, psf
Re_∞	Free-stream unit Reynolds number, per ft
r	Store angular velocity about the Z_B axis, radians/sec
S	Store reference area, ft ² , full scale
T_t	Free-stream total temperature, °R
t	Real trajectory time from initiation of trajectory, sec
V_L	Local velocity vector, ft/sec (see Fig. 13)
V_X	Component of local velocity along probe X_P axis, ft/sec (see Fig. 13)
V_{XY}	Component of local velocity in probe X_P - Y_P plane, ft/sec (see Fig. 13)
V_{XZ}	Component of local velocity in probe X_P - Z_P plane, ft/sec (see Fig. 13)
V_Y	Component of local velocity along probe Y_P axis, ft/sec (see Fig. 13)
V_Z	Component of local velocity along probe Z_P axis, ft/sec (see Fig. 13)
V_∞	Free-stream velocity, ft/sec
WL	Aircraft waterline from reference horizontal plane, in., model scale
X	Separation distance of the store cg parallel to the flight axis system X_F direction, ft, full scale measured from the prelaunch position

X_{cg}	Full-scale cg location, ft from nose of store
ΔX_{cg}	Store moment reference correction factor, in., model scale, positive for forward movement
X_{L1}	Forward ejector location relative to the store cg, positive forward of store cg, ft, full scale
X_{L2}	Aft ejector piston location relative to the store cg, positive forward of store cg, ft, full scale
Y	Separation distance of the store cg parallel to the flight axis system Y_F direction, ft, full scale measured from the prelaunch position
Z	Separation distance of the store cg parallel to the flight-axis system Z_F direction, ft, full scale measured from the prelaunch position
Z_{cg}	Full-scale cg location, ft, above centerline of store
Z_E	Ejector stroke, ft
α	Parent-aircraft model angle of attack relative to the free-stream velocity vector, deg
α_s	Store model angle of attack relative to the free-stream velocity vector, deg
α_{XY}	Angle between V_{XY} and V_X , deg (see Fig. 13)
α_{XZ}	Angle between V_{XZ} and V_X , deg (see Fig. 13)
β	Parent-aircraft model sideslip angle relative to the free-stream velocity vector, deg
γ	Simulated parent-aircraft dive angle; angle between the flight direction and the earth horizontal, deg, positive for decreasing altitude
θ	Angle between the store longitudinal axis and its projection in the X_F - Y_F plane, positive when store nose is raised as seen by the pilot, deg
ϕ	Angle between the projection of the store lateral axis in the Y_F - Z_F plane and the Y_F axis, positive for clockwise rotation when looking upstream, deg
ψ	Angle between the projection of the store longitudinal axis in the X_F - Y_F plane and the X_F axis, positive when the store nose is to the right as seen by the pilot, deg

FLIGHT-AXIS SYSTEM COORDINATES

Directions

X_F	Parallel to the free-stream wind vector, positive direction is forward as seen by the pilot
Y_F	Perpendicular to the X_F and Z_F directions, positive direction is to the right as seen by the pilot
Z_F	In the aircraft plane of symmetry, perpendicular to the free-stream wind vector, positive direction is downward

The flight-axis system origin is coincident with the aircraft cg and remains fixed with respect to the parent aircraft during store separation. The X_F , Y_F , and Z_F coordinate axes do not rotate with respect to the initial flight direction and attitude.

STORE BODY-AXIS SYSTEM COORDINATES

Directions

X_B	Parallel to the store longitudinal axis, positive direction is upstream in the prelaunch position
Y_B	Perpendicular to the store longitudinal axis, and parallel to the flight-axis system X_F - Y_F plane when the store is at zero roll angle, positive direction is to the right looking upstream when the store is at zero yaw and roll angles
Z_B	Perpendicular to both the X_B and Y_B axes, positive direction is downward as seen by the pilot when the store is at zero pitch and roll angles.

The store body-axis system origin is coincident with the store cg and moves with the store during separation from the parent airplane. The X_B , Y_B , and Z_B coordinate axes rotate with the store in pitch, yaw, and roll so that mass moments of inertia about the three axes are not time-varying quantities.

PYLON-AXIS SYSTEM COORDINATES

Directions

X_p	Parallel to the store (or probe) longitudinal axis in the prelaunch carriage position, positive direction is forward as seen by the pilot
-------	---

- Y_p Perpendicular to the X_p axis and parallel to the flight-axis system X_F-Y_F plane, positive direction is to the right as seen by the pilot
- Z_p Perpendicular to both the X_p and Y_p axes, positive direction is downward

For the aerodynamic loads test phase, the pylon-axis system origin is coincident with the store cg in the prelaunch carriage position. For the flow-field test phase, the pylon-axis system origin (see Fig. 13) is defined as follows:

a. Wing pylons (F-4C and A-7D)

Point in space 1.15 in. (model scale) aft of the store nose and on the store centerline of the MK-84 store in the pylon-carriage position.

b. Centerline (F-4C)

Point in space at the store nose and on the store centerline of the data link pod in the centerline carriage position.

The axes are rotated with respect to the flight-axis system by the prelaunch yaw and pitch angles of the store or probe. Both the origin and the direction of the coordinate axes remain fixed with respect to the flight-axis system throughout the trajectory.